AN ABSTRACT OF THE THESIS OF

Jeffrey D. Goby for the degree of Master of Science in Chemical Engineering presented on December 4, 2009.

Title: Experimental Approach for the Determination of Lignin Modification by Manganese Peroxidase

Abstract approved: _____

Christine J. Kelly

Degradation of lignin to simpler compounds is desirable for removing residual lignin during paper manufacture and accessing biomass carbohydrates for biofuel production, among other purposes. Lignin transformation using enzymes found in white rot fungi, some of nature's most efficient lignin-degrading organisms, offers a more environmentally benign, selective, and possibly less costly alternative to purely thermochemical means. One type of enzyme used by white rot fungi to degrade lignin *in vivo* is manganese peroxidase (MnP), which has been successfully purified from the native fungi and produced recombinantly in high yields. To facilitate investigation of lignin transformation by recombinant manganese peroxidase (rMnP), reaction systems were developed and assays refined to detect lignin transformation products. The systems were tested with different solid lignin substrates and sets of components that affect the ability of rMnP to degrade the solid substrate. In several experiments, the dye methylene blue was used as an rMnP substrate and lignin surrogate to rapidly determine the oxidative capacity of rMnP systems containing different short chain organic acids (malonate or oxalate), fatty acids (oleic, linoleic, or linolenic acids), and iron reducing agents (3,4-dihydroxyphenyl acetic acid, vanillic acid, wheat straw extracts). The dye was also used to determine the effect of a Fenton pretreatment on the ability of a subsequent rMnP treatment to degrade a substrate.

Two solid wheat straw lignin substrates were used in the reaction system tests: acid insoluble lignin (AIL) and lignin remaining after dilute acid pretreatment, and cellulase saccharification and desorption (mild acid lignin, MAL). Degradation of AIL was undetected in an rMnP system containing malonate and hydrogen peroxide at several concentrations, but a colored high molecular weight (>10 kDa) Mn(III)-malonate complex was generated in the system with 0.1 mM hydrogen peroxide. Degradation of MAL or improved glucose yield due to synergy between

cellulases and rMnP were also not definitively detected in a system containing rMnP, cellulases, and linoleic acid. On the other hand, rMnP-induced cellulase inhibition did appear to occur.

The rMnP systems containing an emulsified polyunsaturated fatty acid (linoleic acid or linolenic acid) were more effective at degrading methylene blue dye than rMnP systems containing malonate or oxalate in place of the fatty acid. This was likely due to formation of reactive lipid peroxyl radicals which oxidized the dye by hydrogen or electron abstraction. Addition of malonate, oxalate, or iron reducing agent to the rMnP system with emulsified linoleic acid resulted in variable dye degradation. Each iron reducing agent inhibited degradation, oxalate had no effect, and malonate drastically increased the degradation rate. It is likely that malonate increased the degradation rate because it promoted rMnP production of Mn(III) chelates. Degradation in this rMnP system depended on the presence of rMnP and manganese, but occurred more slowly without exogenous hydrogen peroxide. Degradation of malonate or lipid peroxyl radicals appears to provide the peroxides necessary for rMnP turnover when no hydrogen peroxide is added.

Dye degradation also occurred in the presence of Fenton's reagent (Fe(III) and hydrogen peroxide) and an iron reducing agent (3,4-dihydroxyphenyl acetic acid (DOPAC), vanillic acid, or wheat straw extracts). The degradation mechanism likely involved hydroxyl radical attack of the chromophore when DOPAC or vanillic acid were used, but additional mechanisms may have occurred with wheat straw extracts. Each iron reducing agent inhibited dye degradation during subsequent treatment with an rMnP system containing malonate or emulsified linoleic acid. Unoxidized iron reducing agent remaining in the reaction mixture after the Fenton treatment could have acted as a competitive substrate for rMnP oxidation, radical scavenger, or manganese chelator.

The presence of sodium malonate buffer (pH 4.5) and glycerin appeared to help maintain rMnP activity in aqueous solution over time. Also, when rMnP was combined with malonate, the presence of manganese prevented activity loss from hydrogen peroxide.

Future work should use solid lignin substrates in the rMnP systems which best degraded methylene blue to learn if the extent of solid substrate degradation correlates with the extent of dye degradation. If so, the dye may serve as an accurate surrogate for testing the ability of an rMnP system to degrade a solid lignin substrate, and more complicated fungal enzymatic system can be rapidly screened for their ability to degrade lignin.

©Copyright by Jeffrey D. Goby

December 4, 2009

All Rights Reserved

Experimental Approach for the Determination of Lignin Modification by Manganese Peroxidase

by
Jeffrey D. Goby

A THESIS

submitted to

Oregon State University

in partial fulfillment of
the requirements for the
degree of

Master of Science

Presented December 4, 2009
Commencement June 2010

Master of Science thesis of Jeffrey D. Goby presented on December 4, 2009.

APPROVED:

Major Professor, representing Chemical Engineering

Head of the School of Chemical, Biological, and Environmental Engineering

---

Dean of the Graduate School

I understand that my thesis will become part of the permanent collection of Oregon State University libraries. My signature below authorizes release of my thesis to any reader upon request.

Jeffrey D. Goby, Author

ACKNOWLEDGEMENTS

The author expresses sincere appreciation to his advisors, Christine Kelly and Michael Penner, and the numerous graduate students, friends, and family who guided and supported this research.

TABLE OF CONTENTS

Page

1 INTRODUCTION 1

1.1 Background 1

1.2 Hypotheses and objectives 2

1.3 Structure of thesis 3

2 LITERATURE REVIEW 5

2.1 Biomass 5

2.2 Potential benefits of enzymatic transformation of lignin 9

2.3 White rot fungi and lignin modifying enzymes 11

2.4 Pretreating biomass for biofuel production 20

3 FENTON AND rMnP DEGRADATION OF METHYLENE BLUE 24

3.1 Background 24

3.2 MnP function and the Fenton reaction 25

3.3 Hypotheses of the methylene blue experiments 38

3.4 Materials and Methods 39

3.5 Results and Discussion 43

4 PREPARATION OF SOLID rMnP SUBSTRATES 88

4.1 Introduction 88

4.2 Processing and milling of wheat straw 89

4.3 Particle size distribution of wheat straw 89

4.4 Preparation of severely acid treated substrate (acid insoluble lignin) 93

4.5 Preparation of mild acid treated substrate (saccharified pretreated wheat straw) 94

4.6 Chemical composition of biomass samples 103

TABLE OF CONTENTS (Continued)

Page

5 DEVELOPMENT OF LIGNIN TRANSFORMATION SYSTEMS AND ASSAYS FOR REACTION COMPONENTS 109

5.1 Lignin transformation system 1 (severe acid pretreated lignin with malonate/rMnP enzyme system) 109

5.2 Lignin transformation system 2 (mild acid pretreated lignin with linoleic acid/rMnP system and cellulases) 110

5.3 Assays for reaction components (descriptions and results) 112

6 CONCLUSIONS AND FUTURE WORK 149

6.1 Conclusions 149

6.2 Future work 153

BIBLIOGRAPHY 156

LIST OF FIGURES

Figure		Page
Figure 1-1:	Schematic showing approach to testing hypotheses.	3
Figure 2-1:	Illustration of wood tissue structure showing the relationship of contiguous cells (left), cutaway view of the cell wall layers (center), and a depiction of the relationship of the lignin, hemicelluloses, and cellulose in the secondary wall.	5
Figure 2-2:	Basic phenylpropanoid structural units of lignin.	7
Figure 2-3:	Model of spruce lignin (Adler 1977).	8
Figure 2-4:	Phenolic hydroxyl group in a phenolic lignin unit, and benzylic hydrogen in a non-phenolic lignin unit.	9
Figure 2-5:	Cell wall erosion of a conifer tracheid cell by a non-selective white rot fungus.	12
Figure 2-6:	Sections from intact wood trachaeid cells (1), and trachaeid cells decayed by *C. subvermispora* for two (2) and four weeks (3-6) after fixation with glutaraldehyde and staining with uranyl acetate (ML=middle lamella, S_1, S_2, S_3=secondary wall layers, H=hypha) (Blanchette, Krueger, et al. 1997).	15
Figure 2-7:	Schematic showing the ligninolytic systems of white rot fungi: lignin peroxidase, manganese peroxidase, and laccase.	17
Figure 2-8:	Manganese binding site in MnP	19
Figure 3-1:	Molecular structure of methylene blue (Sigma-Aldrich 2009).	24
Figure 3-2:	Catalytic cycle of MnP (Harazono, Watanabe and Nakamura 2003).	26
Figure 3-3:	Mn(III) substrates and oxidation products (Hofrichter 2002)	27
Figure 3-4:	Degradation of phenolic lignin units by MnP-induced hydrogen abstraction (adapted from (Hofrichter 2002)).	28
Figure 3-5:	Route for the conversion of phenolic lignin to carbon dioxide (Hofrichter 2002).	29
Figure 3-6:	Proposed route for the oxidation of non-phenolic lignin model dimer (I) by lipid peroxide via abstraction of the benzylic hydrogen (Bao, et al. 1994).	31
Figure 3-7:	Reactions of hydroxyl radical with lignin (Hammel, Kapich, et al. 2002).	34

LIST OF FIGURES (Continued)

Figure		Page
Figure 3-8:	Molecular structure of catechol, *o*-benzoquinone, *p*-benzoquinone, vanillic acid, and DOPAC.	37
Figure 3-9:	Fe(III) reduction by catechols to an *o*-benzoquinone, then to a dicarboxylic acid.	37
Figure 3-10:	Absorbance spectrum of methylene blue (10.0 mM) in distilled water.	44
Figure 3-11:	Broad range absorbance of methylene blue (665 nm) in distilled water versus concentration.	45
Figure 3-12:	Linear range absorbance of methylene blue (665 nm) in distilled water versus concentration.	45
Figure 3-13:	Absorbance spectrum of wheat straw extracts at 10% (v/v) concentration.	46
Figure 3-14:	Broad range absorbance of the ferrozine assay 15 minutes after addition of wheat straw extract samples.	47
Figure 3-15:	Linear range absorbance of the ferrozine assay 15 minutes after addition of wheat straw extract samples.	47
Figure 3-16:	Ferrozine assay absorbance (562 nm) over time of vanillic acid, DOPAC, and wheat straw extracts samples.	48
Figure 3-17:	Iron reducing activity, FeRA (µmole Fe(II) per mg dry weight) versus time for the three iron reducing agents.	49
Figure 3-18:	Initial FeRA of iron reducing agents (IRAs): vanillic acid (0.63±0.04), DOPAC (5.8±0.2), wheat straw extracts (0.067±0.001).	50
Figure 3-19:	Test for Fenton degradation of methylene blue.	53
Figure 3-20:	Spectral changes in methylene blue over time under Fenton treatment with wheat straw extracts.	54
Figure 3-21:	Spectral changes in methylene blue over time under Fenton treatment with DOPAC.	55
Figure 3-22:	Oxidation of phenanthrene to diphenic acid and the proposed oxidized product of methylene blue.	56

LIST OF FIGURES (Continued)

Figure — Page

Figure 3-23: The effect of iron reducing agent (IRA) concentration on methylene blue absorbance over time. 57

Figure 3-24: Short time-scale decrease in methylene blue absorbance under Fenton conditions with several iron reducing agent (IRA) concentrations..... 58

Figure 3-25: Long time-scale decrease in methylene blue absorbance under Fenton conditions with several iron reducing agent (IRA) concentrations..... 59

Figure 3-26: Molecular structure of oleic, linoleic, and linolenic acids (Ege 1989). 60

Figure 3-27: Screening of redox mediators for rMnP-induced degradation of methylene blue: absorbance over time. 61

Figure 3-28: Screening of redox mediators for rMnP-induced degradation of methylene blue: overall decrease in absorbance. 62

Figure 3-29: Positions of allylic and *bis*-allylic hydrogens of linoleic acid, and mechanism of *bis*-allylic hydrogen abstraction initiated by Mn(III). 63

Figure 3-30: Screening for constituents that increase the rate of methylene blue degradation by linoleic acid/Tween 20/rMnP: absorbance over time..... 66

Figure 3-31: Screening for constituents that increase the rate of methylene blue degradation by linoleic acid/Tween 20/rMnP: overall decrease in absorbance. 67

Figure 3-32: Screening for constituents that increase the rate of methylene blue degradation by linolenic acid/Tween 20/rMnP: absorbance over time..... 68

Figure 3-33: Screening for constituents that increase the rate of methylene blue degradation by linolenic acid/Tween 20/rMnP: overall decrease in absorbance. 69

Figure 3-34: Effect of removing components from the linoleic acid/Tween 20/malonate/rMnP system (base case) on the degradation of methylene blue: absorbance over time. 70

Figure 3-35: Effect of removing components from the linoleic acid/Tween 20/malonate/rMnP (base case) system on the degradation of methylene blue: overall decrease in absorbance. 71

LIST OF FIGURES (Continued)

Figure		Page
Figure 3-36:	Part 1 of mechanism of formation of lipid peroxyl radical and lipid hydroperoxides from linoleic acid by Mn(III).	72
Figure 3-37:	Part 2 of mechanism of formation of lipid peroxyl radical and lipid hydroperoxides from linoleic acid by Mn(III).	73
Figure 3-38:	Formation of hydroperoxy acetic acid (3) and hydrogen peroxide (9) from malonate degradation (Hofrichter, Ziegenhagen, et al. 1998).	75
Figure 3-39:	Effect of replacing the rMnP, hydrogen peroxide, and Mn(II) in the linoleic acid/Tween 20/malonate/rMnP system with Mn(III) acetate.	77
Figure 3-40:	Influence of organic acids on oxygen consumption in a lipid peroxidation system consisting of linoleic acid, Tween 20, MnP, $MnSO_4$, and hydrogen peroxide (Kapich, Steffen, et al. 2005).	79
Figure 3-41:	Blank absorbance of several reaction mixtures over time.	81
Figure 3-42:	Combined wheat straw extracts Fenton and malonate/rMnP treatment for degrading methylene blue.	83
Figure 3-43:	Combined DOPAC Fenton and malonate/rMnP treatments for degrading methylene blue.	84
Figure 3-44:	Combined DOPAC Fenton and linoleic acid/Tween 20/malonate/rMnP treatments for degrading methylene blue.	85
Figure 3-45:	Decrease in methylene blue absorbance during malonate/rMnP and linoleic acid/Tween 20/malonate/rMnP degradation with different concentrations of the iron reducing agents (IRA) wheat straw extracts and DOPAC.	86
Figure 4-1:	Percent weight by size fraction and sifting time for sifted milled wheat straw.	90
Figure 4-2:	Total mass of sieved particles over time expressed as a percentage of initial sample weight.	91
Figure 4-3:	Comparison of particle size distribution between original sifted and re-sifted milled wheat straw.	92
Figure 4-4:	Particle size distribution of two milled wheat straw samples.	93

LIST OF FIGURES (Continued)

Figure		Page
Figure 4-5:	Temperature profile of interior of pretreatment tube.	95
Figure 4-6:	Glucose concentration versus time in saccharification supernatant of pretreated wheat straw and controls.	98
Figure 4-7:	Glucose concentration versus time in the saccharification supernatant of wheat straw that had already been saccharified and the cellulases desorbed.	102
Figure 4-8:	Percent ash (as-received basis) in milled wheat straw by mesh size fraction.	106
Figure 4-9:	% nitrogen (w/w) of wheat straw samples by processing step.	108
Figure 5-1:	Molecular structure of commercially available alkali lignin (Sigma-Aldrich 2009).	113
Figure 5-2:	Absorbance spectrum of commercially available alkali lignin (27.5 mg/L).	113
Figure 5-3:	Absorbance spectra of 0.1 mM hydrogen peroxide treatments of lignin transformation system 1.	114
Figure 5-4:	All reaction components except acid insoluble lignin are necessary to reproduce the spectrum.	115
Figure 5-5:	Mixture of Mn(III) acetate and malonate formed the spectrum characteristic of the supernatant from lignin transformation system 1 (60% concentration).	116
Figure 5-6:	Addition of the reducing agent sodium sulfide resulted in removal of nearly all of the absorbance.	117
Figure 5-7:	Spectra of reaction supernatants before centrifugal filtration.	118
Figure 5-8:	Spectra of filtered reaction supernatants (retentate and filtrate).	118
Figure 5-9:	Time course spectra of base case of experiment using lignin transformation system 2.	119
Figure 5-10:	Folin assay absorbance with variation of development time for the assay completed with 5 minutes incubation and 20% sodium carbonate.	124
Figure 5-11:	Folin assay absorbance with variation of incubation time and sodium carbonate solution.	125

LIST OF FIGURES (Continued)

Figure		Page
Figure 5-12:	Effect of eliminating hydrogen peroxide and active rMnP from Folin assay sample.	126
Figure 5-13:	Effect of eliminating hydrogen peroxide and active rMnP from Folin assay sample in the presence of gallic acid.	126
Figure 5-14:	Gallic acid standard curve for the Folin total phenol assay.	127
Figure 5-15:	Folin assay absorbance of supernatant and solids of active and inactive rMnP treatments with 0.1 mM hydrogen peroxide in the lignin transformation system 1.	129
Figure 5-16:	Difference between the final and initial phenolics concentrations in supernatant samples from lignin transformation system 2.	130
Figure 5-17:	Nitrosation of a phenolic unit in lignin followed by deprotonation and tautomerization to a colored quinone mono-oxime.	131
Figure 5-18:	Standard curve for the Pearl-Benson phenolics assay using alkali lignin as standard compound.	134
Figure 5-19:	Net absorbance of supernatant and solids.	135
Figure 5-20:	Reaction sequence for the glucose oxidase/horseradish peroxidase (GOP) assay for glucose.	136
Figure 5-21:	Glucose concentration over time in supernatant of base case.	138
Figure 5-22:	Glucose concentration over time in supernatant of "no rMnP" treatment.	139
Figure 5-23:	Glucose concentration over time in supernatant of "no cellulases at second enzyme addition" treatment.	140
Figure 5-24:	Oxidation of 2,6-dimethoxyphenol to the colored 2,2',6,6'-tetramethoxydibenzo-1,1'-diquinone by MnP (Wariishi, Valli and Gold 1992).	141
Figure 5-25:	Corrected absorbance vs. concentration of rMnP standards.	144
Figure 5-26:	rMnP activities of mixtures with one extra component after ~28 hours.	145

LIST OF FIGURES (Continued)

Figure | Page

Figure 5-27: rMnP activities of mixtures with two or more extra components after ~28 hours. 146

Figure 5-28: rMnP activity time course for the base case treatment of the experiment using lignin degradation system 2. 147

Figure 5-29: rMnP activity time course for the "no cellulases at the second enzyme addition" treatment of the experiment using lignin degradation system 2. 148

LIST OF TABLES

Table		Page
Table 2-1:	Mass percent lignin in several biomass types.	6
Table 2-2:	Type and frequency of interunit linkages in softwood and hardwood lignins (number of linkages per one hundred 9-carbon units).	8
Table 3-1:	Concentrations of DOPAC and wheat straw extracts used in the Fenton phase of sequential degradation of methylene blue by Fenton and rMnP treatments.	42
Table 4-1:	Comparison of particle size distribution of two milled wheat straw samples.	93
Table 4-2:	Composition of milled wheat straw (WS), dilute acid pretreated WS, and dilute acid pretreated/saccharified WS.	99
Table 4-3:	Yield of pretreated, saccharified, and desorbed substrate by step and by mass of initial amount of milled wheat straw.	102
Table 5-1:	Concentrations of dilute acid pretreated lignin substrate used in lignin transformation system 2.	111

EXPERIMENTAL APPROACH FOR THE DETERMINATION OF LIGNIN MODIFICATION BY MANGANESE PEROXIDASE

1 INTRODUCTION

1.1 Background

Few organisms can efficiently degrade lignin, a major component of plants and the one most recalcitrant to degradation. Exceptions are the white rot fungi which secrete lignin-degrading enzymes such as manganese peroxidase (MnP), lignin peroxidase (LiP), versatile lignin peroxidase, and laccase to alter or degrade lignin and gain access to the other components of biomass needed for fungal metabolism (Kirk and Cullen 1998). Since white rot fungi possess the unique ability to efficiently degrade lignin, they provide the essential service of recycling lignin carbon in natural ecosystems.

Since the discovery of the enzymes responsible for lignin degradation by white rot fungi, researchers have studied their mechanisms, factors which affect the rate at which they degrade lignin, and the breadth of possible substrates. The broad motivation for the research has been to understand how biomass is degraded in the natural environment. This knowledge of the natural process hopefully will help develop cost effective and environmentally benign processes to remove lignin from biomass to access the remaining cellulose and hemicellulose sugars for ethanol production (Lee 1997), remove lignin during paper manufacture (Kirk and Cullen 1998), improve the digestibility of livestock forages (Sharma, et al. 2007), degrade recalcitrant environmental pollutants like polychlorinated biphenyls and dioxins (Reddy 1995), and lower concentrations of dyes and phenolic compounds in wastewater (Knapp, Newby and Reece 1995).

The majority of the research on MnP transformation of substrates has used soluble artificial lignin-like substrates (Hofrichter 2002) instead of solid *natural* lignin, and MnP derived from native fungi instead of recombinant organisms. The focus on artificial soluble lignin analogs has led to a deficit of knowledge surrounding how MnP degrades solid natural lignin. This is unfortunate since solid natural lignin is the relevant substrate for most of the applications mentioned above. The use of native MnP from fungi instead of recombinant MnP from other organisms is also unfortunate since recombinant MnP is likely to be the major source of the enzyme for any future industrial processes due to the higher yield and ease of cultivation (Jiang,

et al. 2008); (Singh and Chen 2008). There may also be functional differences between recombinant and native MnPs that should be considered when designing industrial processes.

The research presented in this thesis is meant to reduce the knowledge gap surrounding recombinant MnP (rMnP) transformation of solid natural lignin by (1) developing a reaction system and assays for determining the ability of an rMnP system (rMnP, other enzymes, buffer, redox mediators, pH, etc.) to degrade solid lignin substrate, and (2) testing the ability of several rMnP systems to actually degrade the lignin substrate. The lignin remaining after dilute or severe acid pretreatment of wheat straw were the chosen rMnP substrates since rMnP may find application in the biofuel industry where acid pretreatment of feedstocks is likely.

1.2 Hypotheses and objectives

Two experiments were completed testing the ability of rMnP systems to degrade solid lignin substrate, and several other experiments were completed using the dye methylene blue as a substrate and lignin analog. The central hypotheses of the experiments with either substrate were (1) an rMnP system containing a polyunsaturated fatty acid will best degrade the substrate, and the extend of degradation will increase with increasing unsaturation of the fatty acid; and (2) if the rMnP system does not contain a polyunsaturated fatty acid, then it will significantly degrade the substrate only if it is first chemically altered with a hydroxyl radical (·OH) generating system such as Fenton's reagent (Fe(III), hydrogen peroxide) with an iron reducing agent. The degree to which the rMnP system will degrade the substrate will increase with increasing severity of the hydroxyl radical treatment as varied by concentration of iron reducing agent.

Several tasks had to be completed to test these hypotheses:

1. Prepare and characterize two solid lignin substrates from wheat straw that represent the lignin remaining after mild or severe acid pretreatment. Substrates representing the lignin remaining after the two extremes of acid pretreatment were chosen since the reactivity of an rMnP system towards them would then represent the complete range of rMnP reactivity towards lignin in wheat straw that had undergone any severity of acid pretreatment.
2. Develop a system for reacting rMnP with the solid lignin substrate (reaction vessel, mixing conditions, pH, temperature, volume, etc.) that adequately mixes the solid and

aqueous phases, prevents evaporation, controls temperature, and maintains sterile conditions.

3. Develop assays to test for the concentration of soluble lignin degradation products (e.g. phenolics, an expected degradation product), and assays to detect changes to the solid substrate.
4. Develop a system for reacting rMnP with methylene blue that allows consistent timing between addition of reagents and absorbance measurements. This consistency is critical for meaningful comparisons between treatments and replicates.

The tasks related to experiments using solid lignin substrates are shown schematically in Figure 1-1.

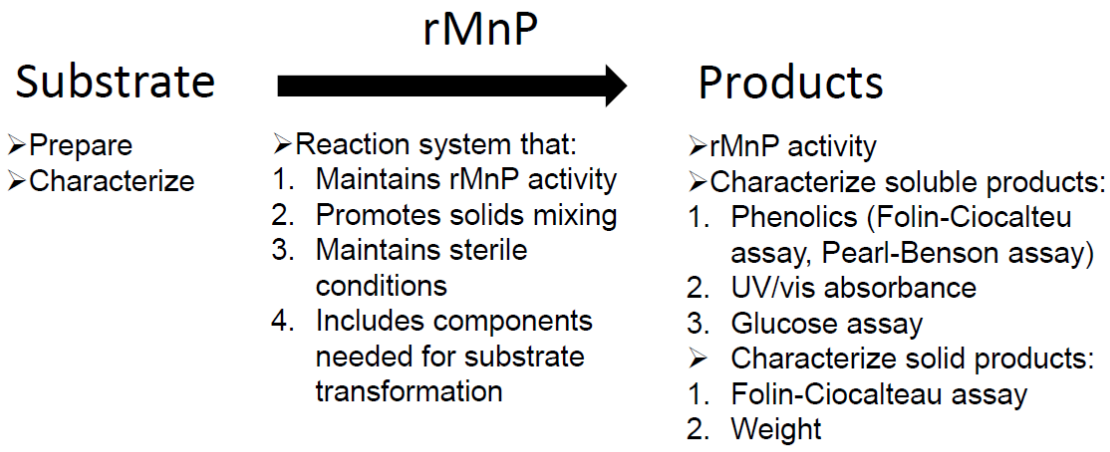

Figure 1-1: Schematic showing approach to testing hypotheses.

1.3 Structure of thesis

Following this chapter with a general introduction and experimental hypotheses, this thesis contains the following chapters:

1. A literature review describing the structure of lignin, the potential benefits of the enzymatic degradation of lignin, white rot fungi, and biomass pretreatment methods (especially acid pretreatment);

2. Experiments determining the effects of rMnP system components (e.g. short chain organic acids, fatty acids, iron reducing agents) on methylene blue degradation;
3. Preparation and characterization of the solid lignin rMnP substrates;
4. Development and testing of the reaction systems for degrading solid lignin substrates, including assays used to determine rMnP activity, glucose, and phenolics; and
5. Research conclusions and suggested future work.

2 LITERATURE REVIEW

2.1 Biomass

2.1.1 General structure

Woody biomass consists primarily of spindle-shaped cells (Figure 2-1). The walls of these cells are made mostly of three structural polymers (cellulose (~45% by mass), hemicelluloses (25-30%), and lignin (19-35%)), and adjacent cells are held together by lignin in middle lamella (M.L.) (Kirk and Cullen 1998); (Sarkanen and Ludwig 1971); (Pettersen 1984). Besides these three main structural polymers, other constituents of biomass include free sugars, lipids, and minerals. During plant growth, the primary cell wall (P) forms first and secondary cell walls (S1-S3) form later around a central cavity called the lumen.

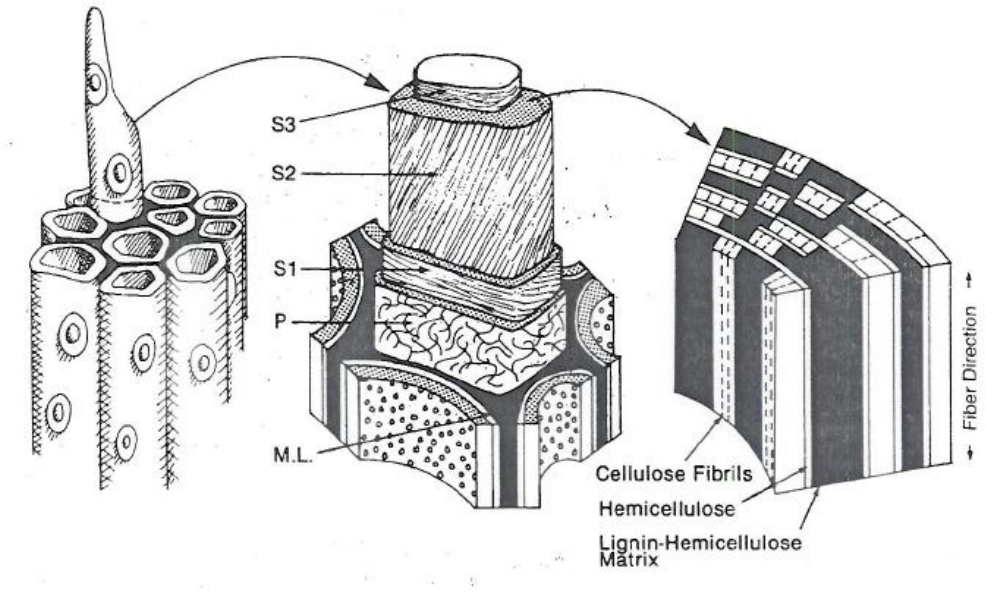

Figure 2-1: Illustration of wood tissue structure showing the relationship of contiguous cells (left), cutaway view of the cell wall layers (center), and a depiction of the relationship of the lignin, hemicelluloses, and cellulose in the secondary wall. The diameter of each cell is ~25 µm (Kirk and Cullen 1998).

The three structural polymers of biomass are chemically distinct. Lignin is a branched polymer of substituted phenylpropane units jointed by carbon-carbon and ether bonds. Hemicelluloses are polysaccharides with a backbone consisting of β-1,4-linked xylose or mannose units. The

hemicellulose polymer molecules are short in length (about 150-200 sugar monomers) and have side groups consisting of sugars, sugar acids, and acetyl esters. Like hemicelluloses, cellulose is also a polysaccharide linked by β-1,4-glycosidic bonds, but it is made solely of anhydrocellobiose units. About 40 individual cellulose polymer molecules bound by van der Waals forces and hydrogen bonding form an individual microfibril with a crystalline structure (Kirk and Cullen 1998). These microfibrils are arranged in layers in the plane of the cell wall and are embedded within the hemicelluloses and lignin. It has been proposed that hemicelluloses coat the microfibrils and are hydrogen bonded to them, and the lignin is linked to the hemicellulose coating (Goring 1977), but recent evidence implies that the hemicelluloses may be more intimately bonded within the cellulose microfibrils (Atalla 1995). The stability of the occasional linkages between lignin and some hemicelluloses units (arabinose, xylose, and galactose) has been cited as the source of the difficulty in removing residual lignin during the final steps of the alkaline pulping process (Erickson, Goring and Lindgren 1980); (Koshijima, Watanabe and Yaku 1989); (Minor 1986).

2.1.2 Lignin function and structure

Lignin in cell walls and the middle lamellae confers rigidity to plant stems and allows them to withstand the forces of wind and gravity. Lignin also aids water transport through stems, and constitutes a protective barrier against pests, microbial attack, and herbivores (Glasser, Northey and Schultz 2000); (Mosier, et al. 2005); (Hofrichter 2002); (Hatfield and Fukushima 2005). The mass percent of lignin in plants depends on the plant type (Table 2-1).

Table 2-1: Mass percent lignin in several biomass types.

Biomass type	**Percent lignin by mass**	**Source**
normal softwood	24-33	(Sarkanen and Ludwig 1971)
normal temperate zone hardwood	19-28	(Sarkanen and Ludwig 1971)
tropical hardwood	26-35	(Pettersen 1984)
nonwoody fiber sources	11-27	(Bagby, et al. 1971)

On a molecular level, lignin is an amorphous polyphenolic material formed when three types of cinnamyl alcohols (sinapyl, coniferyl, and *p*-coumaryl alcohols) (Figure 2-2) polymerize by a radical coupling reaction mediated by laccase and/or peroxidase enzymes (Fengel 1989). The sinapyl, coniferyl, and *p*-coumaryl alcohols are denoted syringyl, guaiacyl, and *p*-hydroxyphenyl propanoid units once incorporated into the lignin polymer (Figure 2-2). The resulting three-dimensional networked lignin polymer lacks the regularity found in other natural polymers such as cellulose, starch, and proteins (Dence and Lin 1992). This irregularity and the types of bonds linking the phenylpropanoid units are responsible for its resistance to enzymatic hydrolysis (Hofrichter 2002).

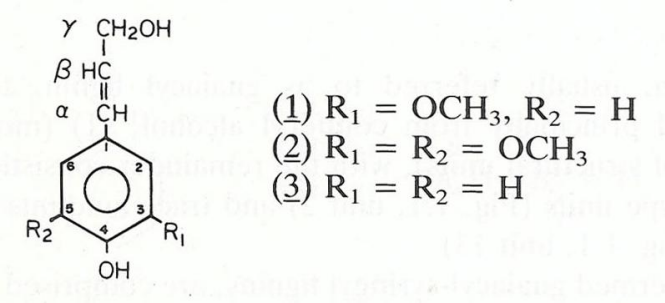

Figure 2-2: Basic phenylpropanoid structural units of lignin. (1) Coniferyl alcohol (guaiacyl unit in lignin polymer), (2) sinapyl alcohol (syringyl unit in lignin polymer), (3) *p*-coumaryl alcohol or *p*-hydroxyphenyl alcohol (*p*-hydroxyphenyl unit in lignin polymer) (Dence and Lin 1992).

Different types of biomass contain different proportions of the three phenylpropanoid monomers. Softwood mainly consists of guaiacyl units (>95% of units) with the remainder mostly *p*-hydroxylphenyl units with a trace of syringyl units. Hardwood and grass lignins consist mostly of guaiacyl and syringyl units, but unlike hardwood lignin, grass contains small amounts of *p*-hydroxylphenyl units.

The phenylpropanoid units in lignin are linked by carbon-carbon and ether bonds mostly to two other units, but occasional linkages to three units gives rise to the networked structure of lignin. The type and frequency of common linkages are listed in Table 2-2 and shown in Figure 2-3.

Table 2-2: Type and frequency of interunit linkages in softwood and hardwood lignins (number of linkages per one hundred 9-carbon units).

Linkage	**Percent in softwood (spruce) lignin** (Erickson, Larsson and Miksche 1973)	**Percent in hardwood (beech) lignin** (Nimz 1974)	**Structural units in Figure 2-3**
β-O-4	49-51	65	1/2, 4/5, 6/7, 7/8, 13/14
α-O-4	6-8		3/13, 15/16, 3/4
β-5	9-15	6	3/4
β-1	2	15	8/9
5-5	9.5	2.3	5/6, 11/12
4-O-5	3.5	1.5	8/10
β-β	2	5.5	10/11

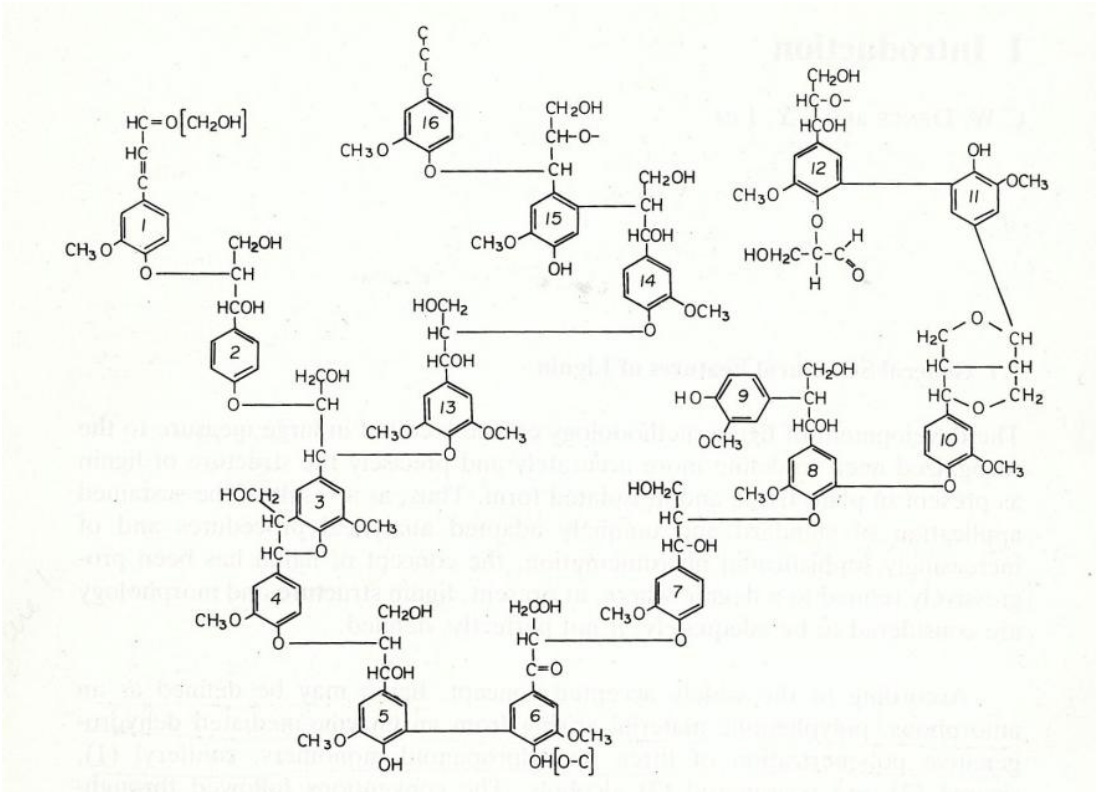

Figure 2-3: Model of spruce lignin (Adler 1977).

The phenolic hydroxyl groups and benzylic hydrogens of the phenylpropanoid units most determine the reactivity of the lignin polymer (Figure 2-4) (Hofrichter 2002). Lignin units containing phenolic hydroxyl groups are termed phenolic lignin, and units containing no phenolic hydroxyl groups are non-phenolic lignin. The phenolic lignin is easily degraded since a suitable oxidant can readily abstract the hydrogen from the phenolic hydroxyl group. Non-phenolic lignin is more difficult to degrade since degradation must be initiated by either abstraction of a benzylic hydrogen or an electron from the aromatic ring, both more difficult than abstraction of a hydrogen from a phenolic hydroxyl group. Oxidants that effectively degrade lignin must be strong enough to oxidize non-phenolic lignin since the majority of lignin units are non-phenolic (80-90%) (Kawai, Nakagawa and Ohashi 2002).

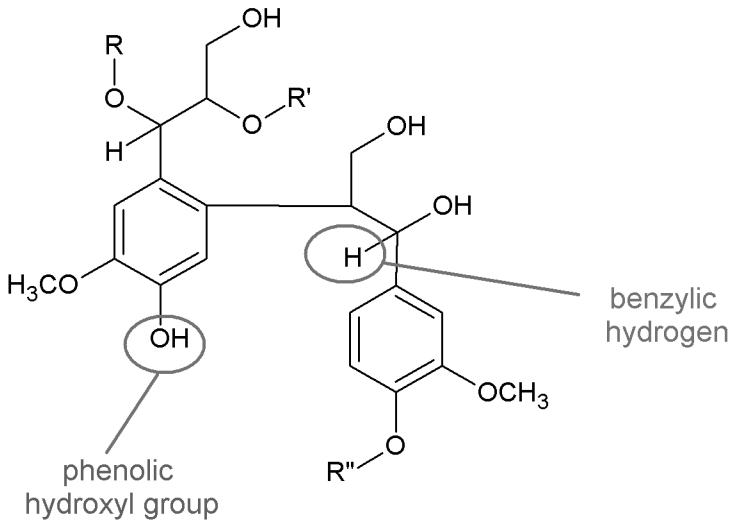

Figure 2-4: Phenolic hydroxyl group in a phenolic lignin unit, and benzylic hydrogen in a non-phenolic lignin unit.

2.2 Potential benefits of enzymatic transformation of lignin

Potential benefits of enzymatic transformation of lignin include (1) removal of residual lignin that may inhibit saccharification of cellulose to glucose and therefore efficient conversion of biomass to ethanol, (2) removal of lignin during paper manufacture, (3) improved digestibility of livestock feed.

2.2.1 Enzymatic transformation of lignin in bioethanol production

Lignin remains in biomass even after pretreatment (section 2.4), and the removal of this lignin may improve enzymatic saccharification of the remaining cellulose to glucose (Chen and Dixon 2007). Greater glucose yields per unit mass of biomass would result in greater ethanol yields when the sugars are fermented, thus enzymatically degrading remaining lignin offers a potential way to improve ethanol yields.

Improved saccharification through lignin removal may occur by (1) eliminating steric hindrance that prevents saccharification by cellulase enzymes, microbes, or chemical processes, and (2) preventing nonspecific adsorption and deactivation of cellulase enzymes onto lignin. An example of either of these phenomena is demonstrated by a study that showed that glucose yields from enzymatic saccharification of filter paper (consisting almost completely of cellulose) were reduced by 10-20% when the filter paper underwent high temperature dilute acid pretreatment with corn stover rind. Pretreatment of the corn stover rind resulted in the formation of semispherical droplets attached to rind cell walls and fine spherical droplets (50 nm to 2 um) in bulk solution. The bulk solution droplets adhered to the filter paper and reduced the enzymatic conversion of the filter paper to cellulose. The droplets may be lignin that has melted, extruded from the corn stover cell walls, and coalesced. There was found a direct relationship between the exposed surface area of the adhered droplets and the reduction in enzymatic saccharification, but it was not determined if the relationship was due to blockage of cellulase access to cellulose, increased nonspecific binding of cellulases to the droplets, or some other phenomenon (Selig, Viamajala, et al. 2007).

Another study showed that cellulases can adsorb preferentially onto lignin, but apparently adsorption occurs to a degree large enough to affect cellulase hydrolysis only when the lignin remaining is from severe acid pretreatment (Meunier-Goddik and Penner 1999).

2.2.2 Enzymatic transformation of lignin in paper manufacture

The cellulose fibers in the woody feedstocks used in paper manufacture must first be removed from the other constituents in the feedstock and separated before they can be laid down on screens to form paper sheets. This process of breaking down the feedstocks into separate cellulose fibers is called pulping. The resulting fibers have a tan or gray color due to the presence of

residual lignin, and bleaching of these fibers to remove remaining lignin must occur to produce white paper products and to prevent yellowing of paper over time.

Before applying traditional pulping methods, some lignin and hemicellulose can be removed from feedstocks by treatment with certain fungal species or isolated fungal enzymes. This process is called biopulping and it has been shown to reduce energy requirements during traditional pulping processes with the simultaneous improvement of fiber quality. Improved brightness also can occur depending on the traditional pulping method used (Messner and Srebotnik 1994). The improved brightness obtained is an example of biobleaching. The biobleaching process can involve treating pulp, instead of feedstock, with certain fungal species or enzymes, and can lead to reduced energy or chemical requirements (Jain, et al. 2007). Since the traditional method of bleaching involves using chlorine-based chemicals, fungal or enzymatic pretreatments can reduce the production of toxic organochlorine compounds and their release into the environment through paper mill effluent. Using fungi or enzymes to aide bleaching relies on two general strategies: degrading hemicellulose with xylanases which increases the extractability of lignin from kraft pulps during the subsequent traditional bleaching sequence, and directly degrading lignin with enzymes and mediators (Carlsson 2002).

2.2.3 Improved digestibility of livestock feed

The lignin present in forage cell walls reduces the digestibility of the forage cellulose by ruminant livestock such as cattle. Some researchers have proposed using fungi or isolated fungal enzymes to partially disrupt the lignin structure in forages such as grasses and straw, and thereby improve their digestibility (Sharma, et al. 2007). Biological treatment of forages may be preferred over physical or chemical means because it is lignin-specific, produces minimal harmful byproducts, and requires little energy.

2.3 White rot fungi and lignin modifying enzymes

2.3.1 Biology and action upon biomass

White rot fungi are in the Eumycota (true fungi) division, Basidiomycotina subdivision, Hymenomycetes class, and Holobasidiomycetidae subclass. This subclass contains nearly all of the wood decaying fungi and also the mycorrhizal, litter, and decomposer fungi (Burdsall 1998). White rot fungi and the related litter-degrading fungi are currently the only known organisms that

can mineralize lignin, i.e. oxidize lignin to carbon dioxide. As such, these fungi may be nature's only organisms for recycling lignaceous carbon (Kirk and Cullen 1998). Due to their unique ability to degrade lignin, several white rot fungi have been targeted for industrial applications: *Phanerochaete chrysosporium* (one of the best studied), *Ceriporiopsis subvermispora*, *Trametes versicolor*, and *Phanerochaete sordida* (Kirk and Cullen 1998). The term "white rot" derives from the white bleached appearance of infested biomass. The bleached appearance is due to the presence of mostly light colored cellulose after the darker colored lignin is degraded by the infesting fungus (Pointing 2001).

As do most fungi, white rot fungi exist mainly as hyphae which are branched threads 1-2 μm in diameter that grow from the tip and originate from spores or nearby fungal colonies (Kirk and Cullen 1998). The hyphae penetrate into the lumens of wood cells, lie along the wood cell wall, and secrete several enzymes and metabolites that degrade the cell wall (Figure 2-5). The sugars and other components that result from degradation are then assimilated by the hyphae and metabolized.

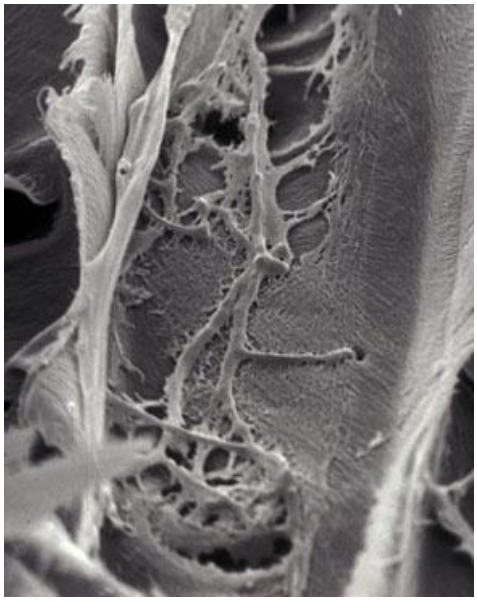

Figure 2-5: Cell wall erosion of a conifer tracheid cell by a non-selective white rot fungus. Branched hyphae are seen along the cell wall, and one hypha has penetrated the cell wall into the next cell with a bore hole. The hyphae and the adjacent cell wall are covered by a polysaccharide matrix produced by the hyphae (Blanchette 2006).

The white rot fungi are often classified according to whether they simultaneously degrade cellulose, hemicellulose, and lignin (non-selective fungi) (Figure 2-5), or whether they delignify, i.e. remove lignin and hemicellulose, before degrading cellulose (selective fungi). Non-selective white rot fungi form erosion troughs beneath the hyphae and the cell walls gradually thin, often nonuniformly, with holes appearing between cells. In contrast, when degraded by selective fungi, the cell walls maintain their structure during the delignification stage. Different fungal species, and strains within a species, vary in which decay pattern is used. Even a single fungus may simultaneously degrade all three cell wall components in one part of a plant and only delignify in another part. The factors that are responsible for the decay pattern are not yet understood, but such an understanding would be useful for using white rot fungi to delignify substrates in industrial processes (Kirk and Cullen 1998).

The molecular details of how selective white rot fungi delignify cell walls have become clearer in recent decades. An example of a study clarifying the mechanism was done by Blanchette et al. (1997) where wood chips were incubated for 2-8 weeks with and without the white rot fungus *C. subvermispora*. The wood chips were then fixed with glutaraldehyde, stained with uranyl acetate, and sectioned. The untreated wood did not reveal electron dense staining within the secondary walls (Figure 2-6 [1]). But after only 2 weeks of incubation, electron dense zones were present in the secondary walls of cells into which fungal hyphae had penetrated (Figure 2-6 [2]), indicating increased secondary wall permeability. The extent of cell wall staining increased with longer fungal incubation. In some cells, the electron dense zone was present only near a hypha (Figure 2-6 [3]) while in others it was present along the entire circumference of the secondary wall even though only one or two hyphae were present in the lumen (Figure 2-6 [4]). In these cases, an extracellular polysaccharide sheath around the hyphae and along the cell wall may have facilitated the diffusion of enzymes and metabolites secreted by the hyphae to distant locations (Nicole, et al. 1995). Some cells showed a dark zone of stain deep within the secondary wall that may be the advancing front of cell wall alteration (Figure 2-6 [5]). Decreases in the UV absorbance of the secondary walls and middle lamellae were observed during the early stages of fungal decay, indicating changes to phenolics in those regions. The middle lamellae are relatively distant from the hyphae in the cell lumens, so changes to the middle lamellae indicate how rapidly lignin degradation occurs during degradation by selective white rot fungi.

Proteins of several molecular weights (insulin, 5.7 kDa, myoglobin 17.6 kDa, and ovalbumin 44.3 kDa) were infiltrated into the undecayed and decayed wood, the proteins were then immunogold labeled, and the wood sections viewed with electron microscopy. The outer portion of the secondary wall became permeable to insulin after only two weeks of incubation, then to myoglobin after four weeks, and ovalbumin after eight weeks when extensive cell wall degradation had occurred. None of the proteins were isolated within the cell walls of the untreated wood, thus indicating that fungal treatment was responsible for the increased porosity of the secondary cell wall. Moreover, the insulin penetrated into roughly the same portion of the secondary cell wall as was stained with uranyl acetate.

The enzymes responsible for lignin degradation by white rot fungi have a molecular weight similar to that of ovalbumin, thus apparently the lignin within the secondary cell wall was extensively degraded even before lignin-degrading enzymes could contact the lignin substrate. This result suggests that only low molecular mass agents capable of diffusing into the cell wall are responsible for the early stages of degradation by selective white rot fungi.

As mentioned earlier, non-selective fungi cause thinning and erosion of cell walls, not just increased porosity. Thus, their mechanism of degrading cell walls may be more by direct action of extracellular enzymes on proximal cell wall polymers rather than by generating oxidizing agents capable of diffusing into the cell wall and oxidizing polymers distant from the enzymes.

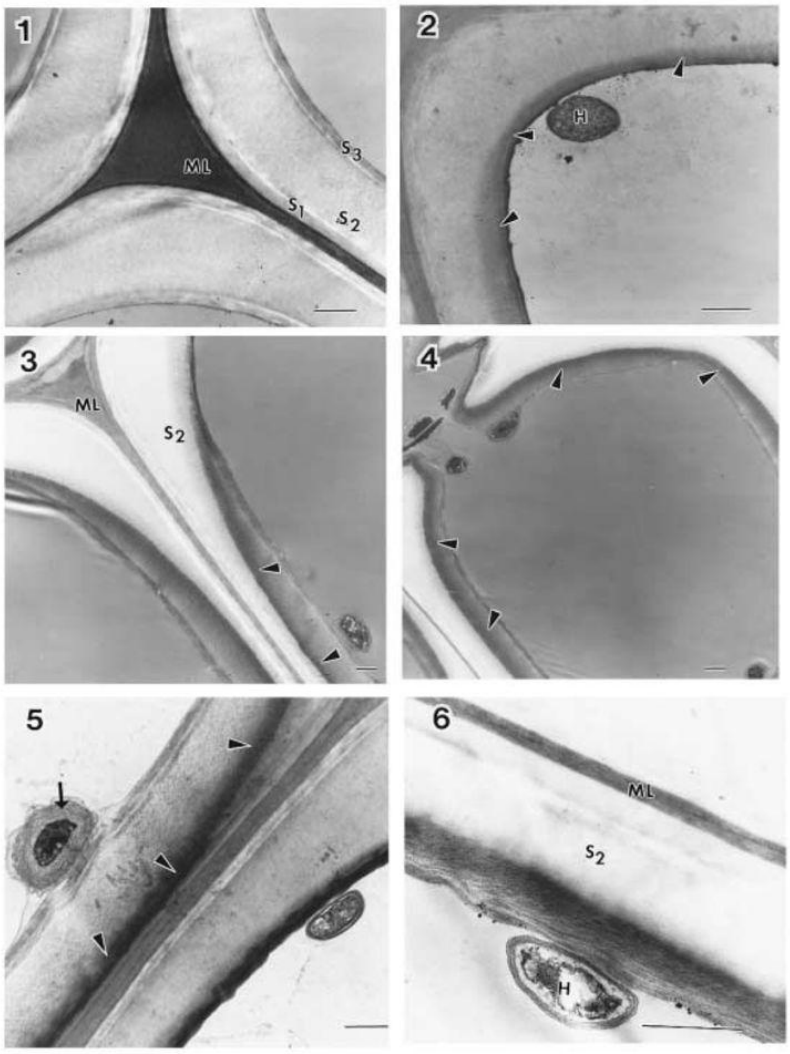

Figure 2-6: Sections from intact wood trachaeid cells (1), and trachaeid cells decayed by *C. subvermispora* for two (2) and four weeks (3-6) after fixation with glutaraldehyde and staining with uranyl acetate (ML=middle lamella, S_1, S_2, S_3=secondary wall layers, H=hypha) (Blanchette, Krueger, et al. 1997).

2.3.2 Extracellularly secreted enzymes

The hyphae of white rot fungi secrete several metabolites, cellulases, hemicellulases, and lignin-degrading enzymes (mostly lignin peroxidase (LiP), manganese peroxidase (MnP), and laccase) to degrade biomass (Blanchette, Abad, et al. 1991). All the lignin-degrading enzymes are glycosylated and have acidic pIs and pH optima (Kirk and Cullen 1998) and they are often

secreted under conditions where nitrogen, carbohydrate, or sulfur is limited (Keyser, Kirk and Zeikus 1978); (Jeffries, Choi and Kirk 1981); (Kirk and Farrell 1987). The enzymes and metabolites that degrade lignin must act extracellularly because the lignin polymer is too large to be transported across a hyphal cellular membrane and degraded intracellularly. The enzymes must also act oxidatively rather than hydrolytically since the lignin polymer must be degraded by breaking carbon-carbon and ether bonds. Lastly, due to the stereoirregularity of the lignin polymer, the enzymes must be more nonspecific than enzymes degrading cellulose or hemicelluloses. Some white rot fungi produce all three lignin-degrading enzymes, while others produce only two, or even one.

There is evidence that all three lignin-degrading enzymes use low molecular weight redox mediators to oxidize lignin. In this process, the enzyme first oxidizes the redox mediator (which can be a metal or organic compound) to an oxidized metal, reactive radical, or charged species, which then diffuses to and oxidizes the lignin substrate thereby producing lignin free radicals. These lignin free radicals can then undergo a variety of reactions resulting in the cleavage of the lignin polymer (Kirk and Cullen 1998). The relatively stable redox mediators may in fact be the uncharacterized low molecular weight diffusible agents previously discussed that are responsible for the degradation inside biomass cell walls before lignin-degrading enzymes can penetrate into those cell walls.

Likely candidates for the responsible mediators are several reactive oxygen species often encountered in biological systems such as peroxyl radicals (ROO·), hydroxyl radicals (·OH), and hydroperoxyl radicals (·OOH) (Hammel, Kapich, et al. 2002). Other possibilities include alkoxyl radicals (RO·) and alkyl radicals (R·) (both possibly derived from peroxyl radical degradation), singlet oxygen, hypochlorous acid, and peroxynitrite (Halliwell and Gutteridge 1999). Nonenzymatic routes may produce some of these species and complement the enzymatic system’s ability of degrade lignin or other biomass constituents.

2.3.2.1 Lignin peroxidase (LiP)

The enzyme LiP is similar in function to other peroxidases such as the well-studied horseradish peroxidase. As such it undergoes the typical peroxidase cycle where hydrogen peroxide oxidizes the enzyme to produce a two-electron deficient form called Compound I. The enzyme is reduced back to a one-electron deficient state called Compound II by completing a one-electron oxidation

of a substrate, then to its native state by completing another one-electron substrate oxidation. It contains one ferric protoporphyrin IX heme per enzyme molecule, has a molecular weight of ~40 kDa, and is a more powerful oxidant than typical peroxidases (Kirk and Cullen 1998). Its greater reduction potential allows it to oxidize the more recalcitrant non-phenolic lignin units.

Oxidation of lignin structures by LiP starts with the abstraction of an electron from an aromatic ring to form a radical cation (Figure 2-7). The radical cation can then react to form numerous products (Kirk and Farrell 1987).

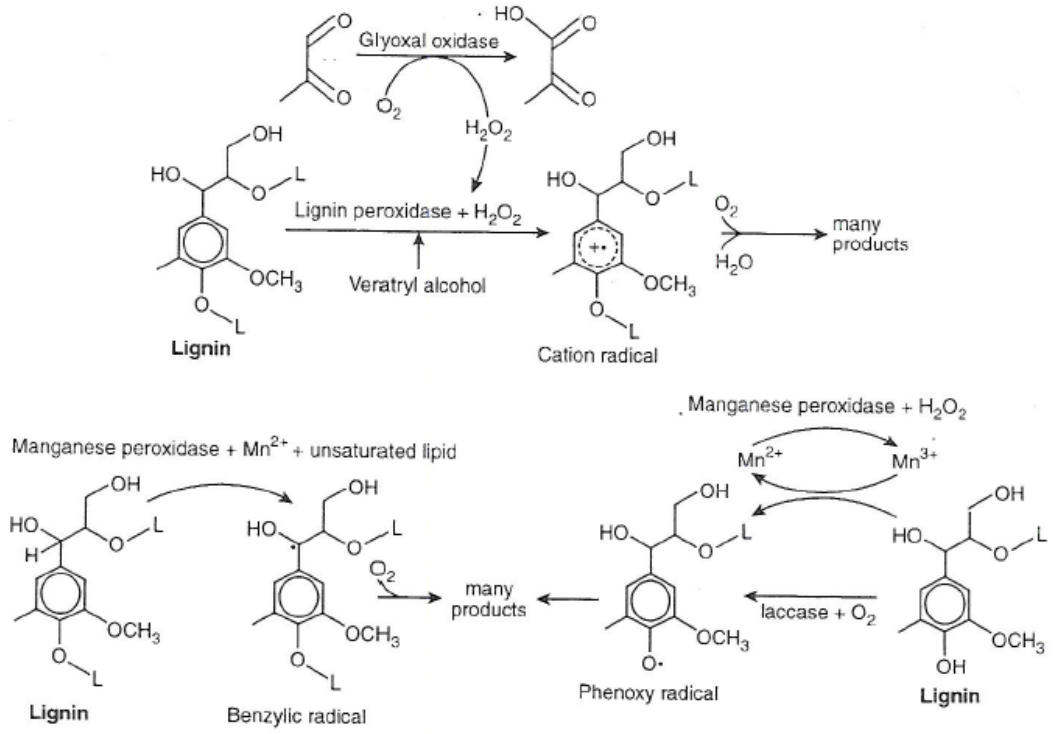

Figure 2-7: Schematic showing the ligninolytic systems of white rot fungi: lignin peroxidase, manganese peroxidase, and laccase. The hydrogen peroxide for oxidation of the peroxidases is produced in some fungi by glyoxal oxidase (Kirk and Cullen 1998).

Oxidation of lignin by LiP without mediation or with mediation at short distances from the enzyme would be the mode of degradation in non-selective fungal degradation where enzymes only need come into contact with the lignin at the lumen surface. But in selective degradation, redox mediation would be required since LiP is too large to penetrate the cell wall. Veratryl

alcohol, a secreted secondary metabolite of *P. chrysosporium*, has been proposed as a potential mediator since LiP can oxidize it to a cation radical and it has been shown to oxidize synthetic lignin *in vitro* (Hammel and Moen 1991). On the other hand, it is doubtful that veratryl alcohol serves as a redox mediator *in vivo* since the lifetime of the cation radical of veratryl alcohol is likely too short for it to diffuse from the site of generation at the cell wall surface into the cell wall interior (Khindaria, Grover and Aust 1995).

2.3.2.2 Manganese peroxidase (MnP)

As a peroxidase, MnP is also similar in function to horseradish peroxidase, but the enzyme prefers manganese over organic compounds as substrate. Certain organic substrates can reduce compound II to the native state, but the reaction is slow (Urzúa, Larrondo, et al. 1995). Production of Mn(III) by MnP is enhanced by bidentate organic acid chelators such as glycolate, oxalate, and malonate because either these chelators stabilize the release of Mn(III) from the enzyme (Kishi, et al. 1994); (Wariishi, Valli and Gold 1992) or they stabilize manganese binding by replacing the two water molecules in the manganese binding site (Sundaramoorthy, et al. 1997).

The resulting chelated Mn(III) most likely mediates oxidation of only phenolic lignin substrates since it is a weak oxidant. The resulting phenoxyl radicals can then react and result in lignin depolymerization. If the chelated Mn(III) first oxidizes fungal metabolites, such as organic acids or unsaturated lipids, the resulting oxyradicals are stronger oxidants than chelated Mn(III) and can oxidize the more recalcitrant non-phenolic lignin substrates through abstraction of benzylic hydrogens, for example (Figure 2-7).

MnP is larger than LiP (50-60 kDa), but like LiP also contains one ferric protoporphyrin IX heme per enzyme molecule (Leisola, et al. 1987). Five disulfide-bridging elements and two Ca(II) ions maintain the active site structure (Sutherland, et al. 2000) which consists of a heme propionate, three acidic amino acid ligands (Asp-179, Glu-35, Glu-39), and two water molecules (Figure 2-8) (Sundaramoorthy, et al. 1997).

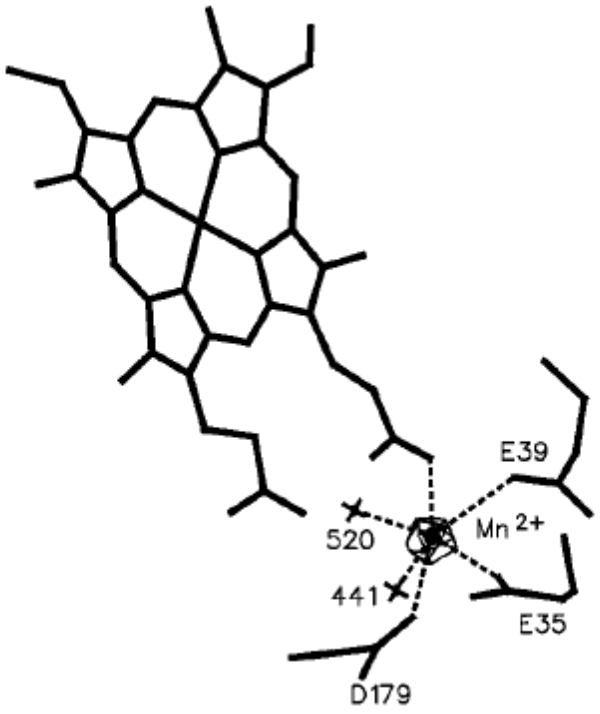

Figure 2-8: Manganese binding site in MnP. The manganese ligands are the three amino acids Asp-179, Glu-35, Glu-39, and two water oxygens labeled "520" and "441" (Sundaramoorthy, et al. 1997).

2.3.2.3 Laccases

Laccases are blue copper oxidases that, like MnP, promote the one-electron oxidation of phenolic lignin units to phenoxyl radicals leading to lignin depolymerization (Figure 2-7). Certain substrates (ABTS or 3-hydroxyanthranilate) can serve as redox mediators and allow laccases to oxidize non-phenolic lignin as well. Laccases catalyze four consecutive one-electron oxidations and then reduce molecular oxygen to water. The reduction of oxygen brings the enzyme back to the native state. The laccases of white rot fungi studied thus far are 60-80 kDa, and most white rot fungi produce them (Kirk and Cullen 1998).

2.3.2.4 Hydrogen peroxide generating enzymes

Both LiP and MnP require a peroxide to oxidize them to Compound I which can then catalyze substrate oxidation. The source of hydrogen peroxide *in vivo* may be any of several enzymes also secreted extracellularly. One possibility is glyoxal oxidase that transfers electrons from small

aldehydes (such as glyoxal and methylglyoxal, both extracellular metabolites of *P. chrysosporium*) to molecular oxygen, thereby producing hydrogen peroxide. Another possibility is aryl alcohol oxidase which transfers electrons from benzyl alcohols to molecular oxygen. A third possibility is a sugar oxidase called pyranose oxidase which transfers electrons from monosaccharides to molecular oxygen. This enzyme has been considered a likely source of hydrogen peroxide since it has been found in the polysaccharide matrix that covers the hyphae and lumen cell walls during fungal degradation (Kirk and Cullen 1998). Other enzymes that may generate hydrogen peroxide and serve other roles in the fungal system are cellobiose dehydrogenase, glucose oxidase (Nutt, et al. 1997), and an unknown substance 1-5 kDa in size (Tanaka, Itakura and Enoki 1999); (Tanaka, Itakura and Enoki 1999).

2.4 Pretreating biomass for biofuel production

Biomass is an enormous source of organic polymers that can be converted to fuels and chemicals. In particular, the cellulose and hemicellulose polysaccharide components can be converted to ethanol or other fuels through a process involving pretreatment, enzymatic hydrolysis of polysaccharides, fermentation, and product separation/purification (Mosier, et al. 2005). Ideally, pretreatment facilitates the subsequent enzymatic hydrolysis of polysaccharides by removing the other biomass components that encapsulate the polysaccharides, disrupting cellulose crystallinity, and reducing the size of the biomass elements. The pretreatment step, which can alter biomass both physically and chemically, is currently necessary to sufficiently reduce the cost of fuel production to compete with petroleum based fuels.

Treating biomass with whole fungal cultures or isolated fungal enzymes to remove lignin can occur before or after pretreatment, like in biopulping and biobleaching operations (Section 2.2.2). The end goal of such a treatment is to facilitate the conversion of the polysaccharides into fermentable sugars by improving the speed or yield of enzymatic hydrolysis of polysaccharides, or reducing the amount of chemicals or time necessary for the pretreatment step. Reducing the time or chemicals necessary for pretreatment may have the extra benefit of reducing levels of undesirable pretreatment products such as furfural.

An effective pretreatment has several qualities: avoids the need to reduce the biomass particle size beforehand, conserves the hemicellulose sugars, maximizes glucose yield from cellulose, converts the lignin into a form useful for other purposes, prevents formation of byproducts

(furfural, hydroxymethyl furfural, acetic acid) that inhibit subsequent fermentation, and minimizes energy use and costs (Council 1999). The current methods that best approach these goals are steam explosion, liquid hot water, dilute acid, lime, and ammonia pretreatments (Mosier, et al. 2005).

2.4.1 Steam explosion

In steam explosion, biomass is placed in a large vessel and high-pressure steam is applied for a few minutes to promote hemicellulose hydrolysis. Steam and the vessel contents are then discharged from the vessel to flash cool and explosively decompress the biomass. The flash cooling quickly terminates chemical reactions and the explosive decompression breaks apart the structure of the biomass to slightly enhance the enzymatic accessibility of the cellulose (Brownell, Yu and Saddler 1986). Most of the improved accessibility to the cellulose after steam explosion is due to the hydrolytic removal of the hemicellulose from around the cellulose microfibrils (Mosier, et al. 2005).

2.4.2 Liquid hot water

Liquid hot water involves subjecting the biomass to high temperature water (200-230 ºC) for up to 15 minutes, obviously under pressure to maintain the water in the liquid state at these temperatures. The process is alternately called hydrothermolysis, aqueous or steam/aqueous fractionation, uncatalyzed solvolysis, or aquasolv. The pH decreases and the dielectric constant increases as water is heated to such high temperatures (e.g. water has a pH of 5.0 at 200 °C) (Weil, et al. 1998). The low pH hydrolyzes hemiacetal bonds and ether linkages (Antal 1996), and the high dielectric constant promotes the dissolution of the hemicellulose and lignin. The process dissolves 4-22% of the cellulose, 35-60% of the lignin, and all the hemicellulose (Mosier, et al. 2005). The benefits of this approach are: (1) neutralization and conditioning is unnecessary since acid is not used, (2) size reduction is unnecessary since the biomass pieces break apart in the water, and (3) the process results in highly digestible cellulose and high yields of sugars from hemicellulose.

2.4.3 Dilute acid

Dilute acid pretreatments (~0.5-1.0%), usually at high temperature (160-220 ºC) for seconds to minutes, tend to hydrolyze and solubilize most of the hemicellulose and some of the lignin but

leave most of the cellulose. The remaining cellulose is made more susceptible to enzymatic hydrolysis by removal of the hemicellulose and lignin (Selig, Vinzant, et al. 2009); (Yang and Wyman 2004)**;** (Gray, Lishan and Emptage 2006). The addition of acid generally improves the hydrolysis of hemicellulose to monomeric sugars compared to the liquid hot water pretreatment method where acid is not used (Wyman, Dale, et al. 2005). One study varying temperature, time, and acid concentration found that 83-100% of the hemicellulose and 26-53% of the lignin was solubilized. Of the cellulose remaining after pretreatment, 90% was enzymatically hydrolyzed (Torget, et al. 1996).

A benefit of the process is that acid is less expensive than chemicals needed for other pretreatment processes. Drawbacks include the formation of compounds that inhibit subsequent fermentation such as furfural (Gray, Lishan and Emptage 2006), the need for costly construction materials to avoid acidic corrosion, necessary neutralization of the hydrolysate before fermentation, disposal of neutralization salts, need for particle size reduction, slower enzymatic hydrolysis of cellulose compared to other pretreatment methods, and non-productive binding of enzymes to remaining lignin (Wyman 1999)**;** (Ooshima, Burns and Converse 1990)**;** (Hsu 1996). The most widely used and studied acid is sulfuric acid, but nitric, hydrochloric, and phosphoric acids have also been tested (Mosier, et al. 2005).

2.4.4 Alkaline

Alkaline pretreatments use lower temperatures and pressures than other methods and are similar to the Kraft paper pulping process (Mosier, et al. 2005). They tend to remove the lignin from the cell walls of substrates, leave the hemicellulose and cellulose, and improve the enzymatic digestibility of cellulose. Drawbacks are that some of the alkali is converted to salts that cannot be recovered or are incorporated in the biomass; the alkaline chemicals are expensive; ferulate and acetate can remain in the hydrolysate, both of which can inhibit fermenting organisms (Gray, Lishan and Emptage 2006) (Wyman, Dale, et al. 2005); and the failure to remove hemicellulose may be a disadvantage since hemicellulose may occlude cellulose and prevent its hydrolysis even more than lignin (Selig, Vinzant, et al. 2009). Lime and hydroxide salts have been studied as the source of alkalinity.

2.4.5 Ammonia

The ammonia fiber/freeze explosion (AFEX) pretreatment results in high rates of enzymatic cellulose hydrolysis and gives nearly theoretical glucose yields (Mosier, et al. 2005). The method works well with herbaceous and agricultural residues like corn stover, but is not as well suited for hardwoods or softwoods. The ammonia reacts mostly with the lignin component, but also with some hemicellulose, by cleaving the bonds between lignin units and between lignin and hemicellulose. It also disrupts cellulose crystallinity. The ammonia and its recovery increase the cost of the process, but the overall process cost is more favorable when considering the high sugar yields achieved and the low levels of compounds formed that inhibit fermentation.

3 FENTON AND rMnP DEGRADATION OF METHYLENE BLUE

3.1 Background

In experiments reported in Chapter 5, severe and mild acid pretreated lignins were used as solid substrates for degradation by recombinant manganese peroxidase (rMnP). The two experiments did not definitively detect rMnP-induced substrate degradation through measurement of substrate weight loss, the evolution of phenolic compounds into solution, or interpretable differences in HPLC chromatograms of the reaction supernatant. Enzymatic degradation was not detected due to one or more deficiencies in the enzyme system use and the analyses performed on the remaining solids and reaction supernatant. Two of the more important deficiencies were not knowing if the enzyme system used had sufficient oxidative power to degrade the solid substrate, and not treating the substrates with a chemical oxidation step that may be necessary for rMnP to subsequently degrade the substrate. The chemical oxidation step could consist of adding the necessary constituents to promote generation of hydroxyl radicals via the Fenton reaction (discussed below). Such a chemical oxidation step may be necessary because white rot fungi may use the process to help degrade biomass (Aguiar, Brazil de Souza-Cruz and Ferraz 2006).

To better understand the oxidative power of various enzyme systems and the effect of performing a Fenton treatment on the ability of rMnP to subsequently degrade a substrate, the water soluble phenothiazinium dye methylene blue was used as a lignin surrogate (Figure 3-1).

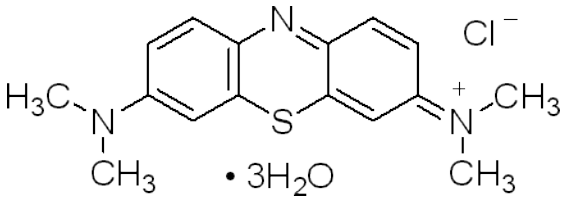

Figure 3-1: Molecular structure of methylene blue (Sigma-Aldrich 2009).

Methylene blue was chosen because previous studies have used it as a substrate for oxidative enzymes (Arantes and Milagres 2007); (Ferreira-Leitão, Andrade de Carvalho and Bon 2007), it is moderately difficult to oxidize with an oxidation potential of 507-516 mV (Wardman 1989) making degradation indicative of an oxidative enzymatic system, its degradation is simple to monitor by measuring its peak absorbance at ~665 nm, and its peak absorbance is distant from the UV absorbance wavelengths of MnP (406-420 nm) (Wariishi, Dunford, et al. 1989) and aromatic

compounds (260-290 nm) that can be added to the reaction system to help degrade methylene blue.

3.2 MnP function and the Fenton reaction

3.2.1 MnP function

Before discussing the hypotheses of the experiments performed with methylene blue, it is important to review the details of MnP function and the role of Fenton chemistry in white rot fungi. In short, MnP catalyzes the redox reaction between manganese and hydrogen peroxide (H_2O_2) or an organic peroxide (ROOH). The catalyzed reaction oxidizes divalent Mn(II) to trivalent Mn(III) with reduction of hydrogen peroxide (H_2O_2) or an organic peroxide (ROOH) to water or ROH. The Mn(III) in turn oxidizes organic substrates (Figure 3-2) (Glenn, Akileswaran and Gold 1986). Since manganese is ubiquitous in soil and biomass, the enzyme does not easily face manganese limitations (Hofrichter 2002).

The cycle begins with hydrogen peroxide (H_2O_2) or an organic peroxide (ROOH) binding to the native ferric (Fe(III)) enzyme. Cleavage of the peroxide oxygen-oxygen bond transfers two electrons from the enzyme to the peroxide molecule: one from the Fe(III) and another from the set of π electrons in the porphyrin ring (Dunford 1982). The reaction results in one molecule of water or ROH and the 2-electron deficient enzyme called Compound I (MnPI). Comparison of the spectral characteristics of MnPI with those of two other peroxidase enzymes (horseradish peroxidase and LiP) suggests that the iron in MnPI is in the [Fe^{4+}=O] state with the oxygen from the peroxide (Wariishi, Akileswaran and Gold 1988). The first reduction of the enzyme from MnPI to MnPII occurs by transfer of an electron from a substrate to the porphyrin ring, and the second reduction by transfer of an electron from the substrate to the Fe^{4+}=O structure. One molecule of water is released during the second reduction when the oxygen of the Fe^{4+}=O combines with two protons from solution. A variety of organic substrates can reduce MnPI to MnPII, and MnPII back to its native ferric state, but reduction from MnPII to its native state by organic compounds is very slow or nonexistent. Hence, manganese is the preferred substrate for reducing the enzyme from MnPII to its native state. The cause may be that entry of a larger organic substrate into the MnP active site for oxidation by the Fe^{4+}=O moiety is sterically hindered, but not for oxidation by the porphyrin ring during the MnPI-to-MnPII reduction

(Wariishi, Akileswaran and Gold 1988); (Wariishi, Dunford, et al. 1989)(Urzúa, Larrondo, et al. 1995).

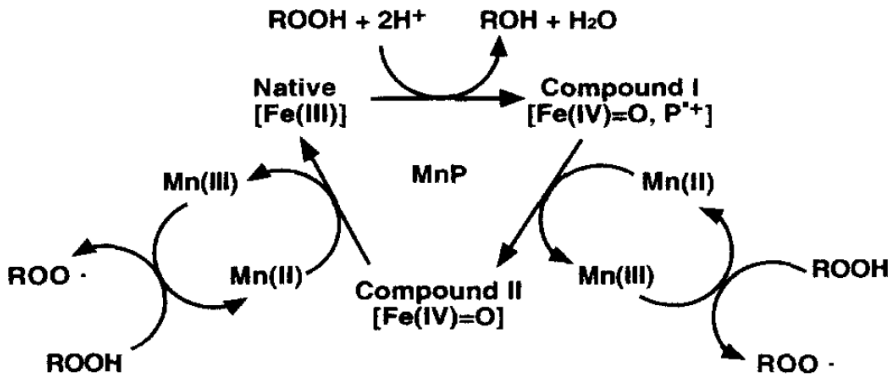

Figure 3-2: Catalytic cycle of MnP (Harazono, Watanabe and Nakamura 2003).

The overall reactions catalyzed by MnP between manganese and hydrogen peroxide or an organic peroxide are given in Equations 3-1 and 3-2. Note that two moles of Mn(III) are produced for every mole of peroxide consumed:

$$H_2O_2 + 2Mn^{2+} + 2H^+ \rightarrow 2H_2O + 2Mn^{3+} \qquad \text{Equation 3-1}$$

$$HOOR + 2Mn^{2+} + 2H^+ \rightarrow H_2O + HOR + 2Mn^{3+} \qquad \text{Equation 3-2}$$

The efficiency of Mn(III) production by MnP appears to depend on the type of manganese chelator present (e.g. oxalate promotes more enzyme turnover than lactate). This effect may be due to differences in the ability of an organic chelator to facilitate release of Mn(III) from the enzyme and stabilize the resulting chelate in solution (Kishi, et al. 1994); (Wariishi, Valli and Gold 1992). It could also be due to the chelator replacing the two water molecules inside the manganese binding site, and thereby changing the thermodynamics of manganese binding, oxidation, and release (Sundaramoorthy, et al. 1997).

3.2.2 Redox mediators

The chelated Mn(III) can serve as a redox mediator, whereby the Mn(III) diffuses to the ultimate substrate, oxidizes it, and then the resulting Mn(II) returns to the enzyme to be oxidized again to Mn(III). This redox mediation process thus allows the oxidative capacity of the enzyme to diffuse

to substrates distant from the enzyme. Even though Mn(III) chelated with malonate or oxalate has a high redox potential of 0.9-1.2 V (Waters and Littler 1965); (Demmer, et al. 1980), it is still only capable of oxidizing relatively easily oxidized substrates. The two fundamental reactions that can occur between the chelated Mn(III) and a substrate are hydrogen abstraction from various substrates (Equation 3-3) and electron abstraction from an aromatic substrate (Equation 3-4):

$$Mn^{3+} + RH \rightarrow Mn^{2+} + R\cdot + H^{+} \qquad \text{Equation 3-3}$$

$$Mn^{3+} + Ar \rightarrow Mn^{2+} + Ar\cdot^{+} \qquad \text{Equation 3-4}$$

Electron abstraction from an aromatic structure by chelated Mn(III) occurs only with the easily oxidized electron rich non-phenolic aromatic substrates such as tetramethoxybenzene or anthracene (Figure 3-3) (Popp and Kirk 1991); (Sack, Hofrichter and Fritsche 1997).

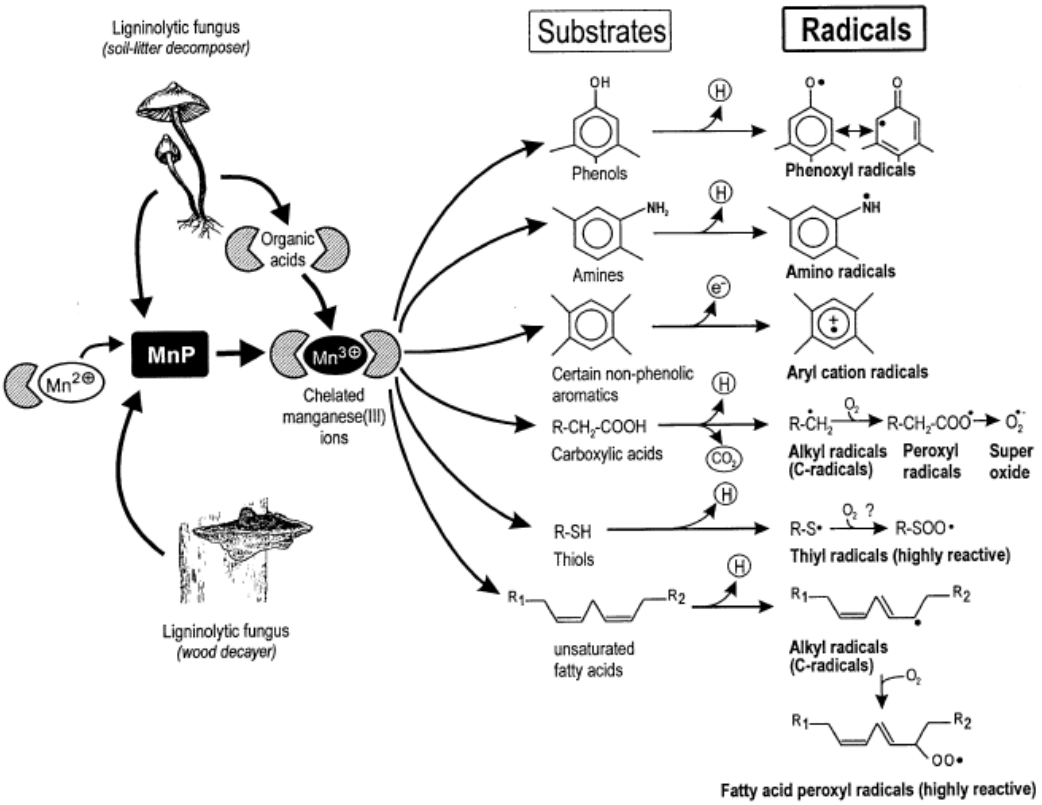

Figure 3-3: Mn(III) substrates and oxidation products (Hofrichter 2002).

Hydrogen abstraction by chelated Mn(III) also occurs only on more easily oxidized substrates. The hydrogen abstraction can occur on a hydrogen from a hydroxyl or amino group substituent of an aromatic ring, allylic or *bis*-allylic hydrogens on unsaturated fatty acids (Figure 3-3), or a hydrogen on a carbon adjacent to a hydroxyl or ether group (O'Neal and Benson 1973), all of which result in a radical stabilized by delocalization. Hydrogen abstraction from a hydroxyl group substituent an aromatic ring is the initial step in the oxidation of phenolic lignin units. The resulting resonance stabilized phenoxyl radical can then undergo several reactions to give different end products (Figure 3-4).

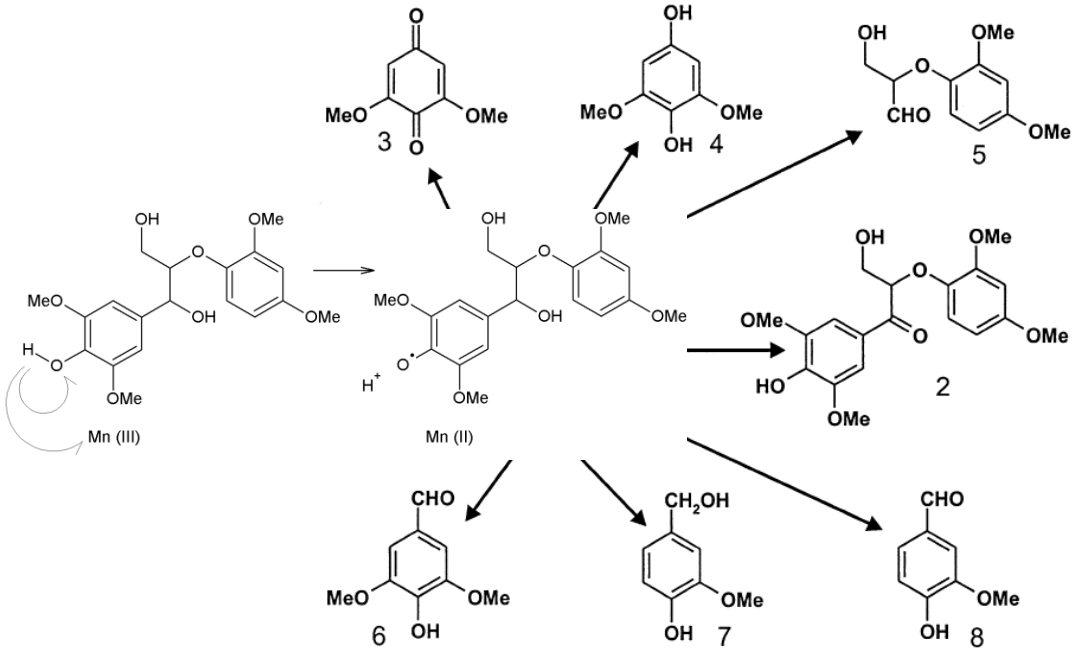

Figure 3-4: Degradation of phenolic lignin units by MnP-induced hydrogen abstraction (adapted from (Hofrichter 2002)).

Figure 3-3 shows that after hydrogen abstraction from the carbon adjacent to the carboxyl group of a carboxylic acid, the resulting alkyl radical ($RCH^{\bullet}COOH$) can undergo further reactions, including loss of a carboxyl group as CO_2 to form another alkyl radical ($RCH_2^{\bullet}$) and addition of oxygen. Addition of oxygen to the alkyl radical results in the peroxyl radical ($RCH_2COO^{\bullet}$) which is a potent oxidizing agent. The peroxyl radicals can further oxidize to a carbonyl-containing compound with the simultaneous reduction of molecular oxygen to form superoxide ($OO^{\bullet-}$).

The superoxide formed from oxidation off carboxylic acids secreted by white rot fungi may aide in the *in vivo* mineralization of phenolic lignin units to carbon dioxide. The basis of the process is the addition of superoxide to the carbon-centered radical formed after hydrogen abstraction of the phenolic lignin. The resulting unstable ether peroxide undergoes ring fission and subsequent loss of carbon dioxide (Figure 3-5) (Hofrichter 2002).

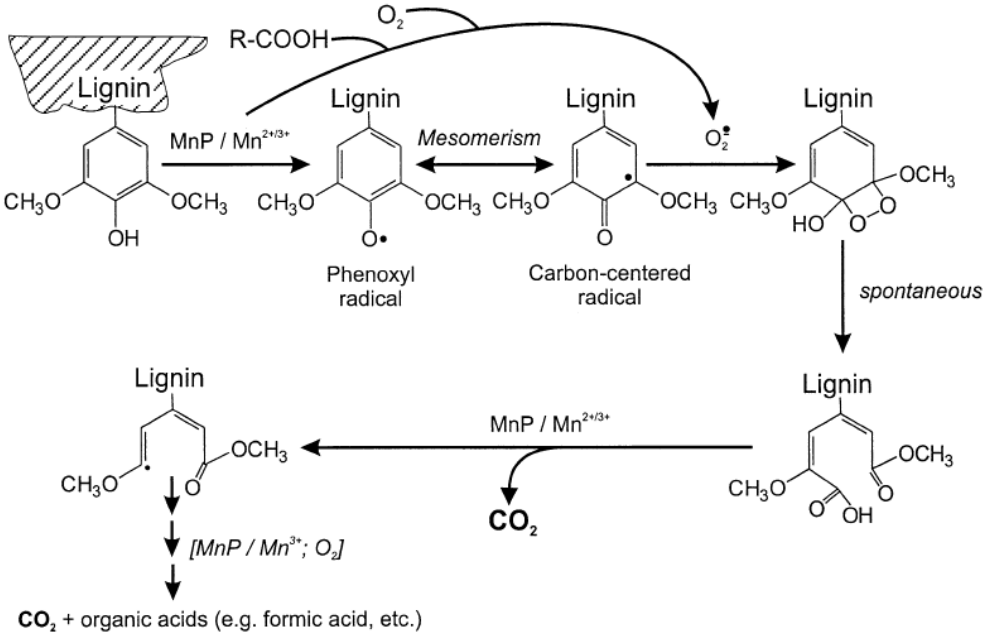

Figure 3-5: Route for the conversion of phenolic lignin to carbon dioxide (Hofrichter 2002).

Peroxyl radicals and superoxide, upon hydrogen abstraction of another molecule, are reduced to organic peroxide (RCH_2COOH) or hydrogen peroxide (HOOH), respectively, and are thought to be a source of peroxide that can oxidize MnP to Compound I *in vivo* or *in vitro* (e.g. (Wariishi, Akileswaran and Gold 1988)). The carboxylic acid precursors of the organic peroxides that may oxidize MnP to Compound I *in vivo* are the shorter chain organic acids secreted by whit rot fungi such as malonate and oxalate. These organic acids also chelate Mn(III) and promote enzymatic Mn(III) production (Urzúa, Kersten and Vicuna 1998); (Hofrichter, Ziegenhagen, et al. 1998). Besides carboxylic acid oxidation, other *in vivo* sources of hydrogen peroxide are production by glyoxal oxidase, aryl alcohol oxidase, pyranose oxidase (Kirk and Cullen 1998), cellobiose

dehydrogenase, glucose oxidase (Nutt, et al. 1997), and an unidentified glycopeptides 1-5 kDa in size (Tanaka, Itakura and Enoki 1999).

Chelates of Mn(III) can oxidize phenolic lignin units but not the non-phenolic units (Popp and Kirk 1991). This limitation would not pose a barrier to degrading non-phenolic lignin in fungi that secrete LiP since the LiP enzyme is highly oxidative and can degrade the more recalcitrant non-phenolic lignin units. Nevertheless, white rot fungi which produce MnP but not the highly oxidative LiP still are able to substantially degrade lignin (Paice, et al. 1993). This has prompted the search for more powerful redox mediators than Mn(III) chelates that can be generated in a fungal system secreting only MnP.

As seen in Figure 3-3, hydrogen abstraction can occur on the acidic hydrogen of a thiol group (Wariishi, Valli and Renganathan, et al. 1989) or the allylic or *bis*-allylic hydrogens of a polyunsaturated fatty acid. The resulting fatty acid radical can undergo oxygen addition, forming a peroxyl radical. Both the thiyl and peroxyl radicals have a higher reduction potential than chelates of Mn(III). Since white rot fungi do not secrete thiols extracellularly, the search for the more powerful redox mediators has centered on lipid peroxyl radicals.

Lipid peroxyl radicals are believed to be involved in degradation of biomass by white rot fungi due to five lines of evidence: (1) an MnP/lipid system is capable of degrading a non-phenolic lignin model dimer via peroxyl radical abstraction of the benzylic hydrogen (Figure 3-6) (Bao, et al. 1994), (2) unsaturated fatty acids have been detected in the natural MnP system and these fatty acids decrease in concentration with the simultaneous rise in the concentration of organic hydroperoxides (Enoki, et al. 1999), (3) the products generated by MnP/lipid degradation of a lignin model compound are similar to products formed with authentic peroxyl radical generating systems (Kapich, Jensen and Hammel 1999), (4) peroxyl radicals have half lives in the range of seconds, are effective hydrogen abstracting agents, and are small enough to enter wood cell wall pores (Bao, et al. 1994), (5) the related lipid hydroperoxides (ROOH) formed from hydrogen abstraction by a peroxyl radical ($ROO\cdot + HR \rightarrow ROOH + \cdot R$) can chelate with Mn(III), diffuse into wood cell wall pores due to their relative stability, and convert back to peroxyl radicals by Mn(III) oxidation (Equation 3-5), thus generating peroxyl radicals *in situ* deep within wood cell walls.

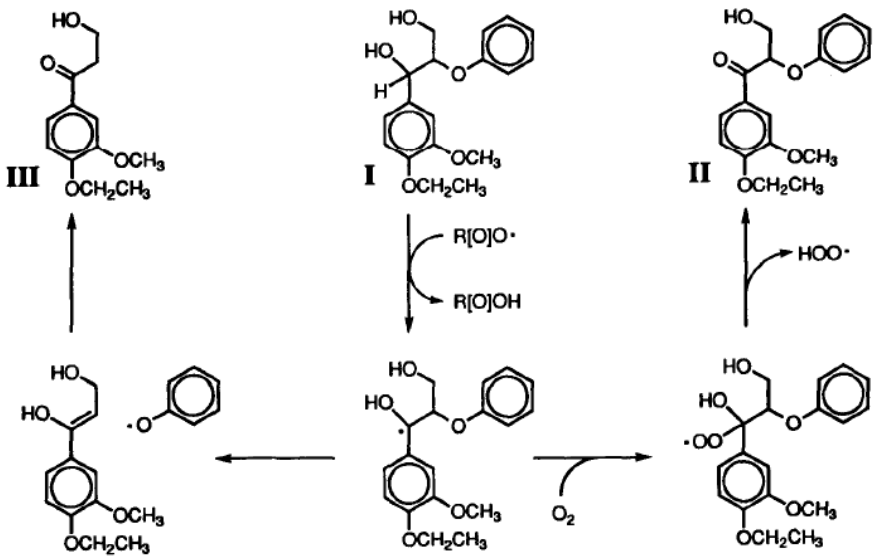

Figure 3-6: Proposed route for the oxidation of non-phenolic lignin model dimer (I) by lipid peroxide via abstraction of the benzylic hydrogen (Bao, et al. 1994).

A higher pH environment inside the cell wall compared to near the hyphae may be the driving force for the production of the peroxyl radicals inside the cell wall. Lignin oxidation distant from the site of enzyme secretion near hyphae is observed in fungal degradation of wood (Figure 2-6), and diffusible organic peroxides can explain this observation.

$$Mn^{3+} + ROOH \rightleftarrows Mn^{2+} + ROO\cdot + H^{+} \qquad \text{Equation 3-5}$$

The Mn(III) chelates and peroxyl radicals are only a few of the redox mediators generated by the MnP system. Other species such as alkoxyl radicals ($RO^{\bullet}$) and alkyl radicals ($R^{\bullet}$) (Watanabe, Katayama, et al. 2000), and all the species produced by the reactions between these species and carboxylic acids or substrate, can serve as redox mediators that vary in size, hydrophobicity, and reduction potential. This variety makes redox mediation an effective strategy among white rot fungi for degrading the highly heterogeneous solid lignocellulose that is often too dense for enzyme penetration.

3.2.3 Recombinant MnP

Most studies of MnP function have used MnP isolated from cultures of white rot fungi, but the experiments presented herein were completed using an MnP produced recombinantly (rMnP) by

cultivation of the yeast *Pichia pastoris* in high cell density fed-batch cultivations. A gene encoding MnP (*mnp1*) from the white rot fungus *P. chrysosporium* was cloned into a protease deficient strain of the yeast so that during cultivation the yeast secretes rMnP. The secreted MnP then was concentrated from 2,500 U/L in the bioreactor culture to 30,000 U/L in 0.1 M potassium phosphate buffer with a combination of centrifugation, acetone precipitation, dialysis, and freeze drying (Jiang, et al. 2008). The high activity freeze-dried concentrate was the source of the rMnP used in the experiments reported here.

3.2.4 Other processes for degrading non-phenolic lignin

Other enzymatic or purely chemical systems operating in parallel to the MnP system have been proposed to explain the ability of certain MnP-producing white rot fungi to degrade non-phenolic lignin when those fungi do not produce LiP to help oxidize the non-phenolic units. Several of the proposals involve the production of hydroxyl radicals ($^{\bullet}OH$) by a Fenton reaction (explained below) because hydroxyl radical generation by the Fenton reaction has already been observed in brown rot fungi for degrading polysaccharides (Goodell 2003); (Jensen, et al. 2001) and the hydroxyl radical is a more powerful oxidant than the peroxyl radical and one of the most powerful oxidants that can exist in aqueous solution (Buettner 1993).

If hydroxyl radicals produced by the Fenton system are involved in white rot decay, they should be produced at a distance from the hyphae to prevent oxidative damage to the fungus, and within the biomass cell walls rather than on the surface to effectively degrade cell wall components (Hammel, Kapich, et al. 2002). The hydroxyl radical must be generated within the cell wall because its half life is 10^{-9} s and it will react within five to ten molecular diameters of potential reactants (Cadenas 1995).

The Fenton reaction is shown in Equation 3-6. Before soluble ferrous iron (Fe(II)) is available for the Fenton reaction, ferric iron (Fe(III)), the predominant form of iron in aerobic environments, must be reduced. In a system with no other components capable of reducing iron, ferric iron reduction occurs slowly by reaction with hydrogen peroxide (Equation 3-7). If there are no other reagents in the system that can react with Fe(II) before it reacts with hydrogen peroxide, then the net reaction is the iron catalyzed decomposition of hydrogen peroxide (Equation 3-8) (Walling and Goosen 1973).

$$H_2O_2 + Fe^{2+} \rightarrow Fe^{3+} + HO\cdot + HO^- \qquad \text{Equation 3-6}$$

$$Fe^{3+} + H_2O_2 \rightarrow Fe^{2+} + HOO\cdot + H^+ \qquad \text{Equation 3-7}$$

$$\text{net reaction: } 2H_2O_2 \rightarrow HOO\cdot + HO\cdot + H_2O \qquad \text{Equation 3-8}$$

It should be noted that Cu(II) and Cu(I) can also perform the same function as Fe(III) and Fe(II), respectively, in promoting Fenton chemistry (Arantes and Milagres 2007), and the coordination of the involved metal affects the reaction rate (Ueda, Saito and Ozawa 1996); (Watanabe, Koller and Messner 1998). It should also be noted that an organic peroxide can replace the hydrogen peroxide, in which case the reactions are:

$$ROOH + Fe^{2+} \rightarrow Fe^{3+} + RO\cdot + HO^- \qquad \text{Equation 3-9}$$

$$Fe^{3+} + ROOH \rightarrow Fe^{2+} + ROO\cdot + H^+ \qquad \text{Equation 3-10}$$

$$\text{net reaction: } 2ROOH \rightarrow ROO\cdot + RO\cdot + H_2O \qquad \text{Equation 3-11}$$

Mn(III) has been shown to replace Fe(III) in the formation of a peroxyl radical ($ROO^{\bullet}$) from a lipid peroxide (ROOH) (Equation 3-10), but Mn(II) has not been shown to promote the cleavage of a lipid peroxide to an alkoxyl radical ($RO^{\bullet}$) (Equation 3-9) (Watanabe, Katayama, et al. 2000).

The hydroxyl radical quickly completes a one-electron oxidation of almost all organics by abstracting a hydrogen atom from aliphatic compounds (Equation 3-12) or adding as an electrophile to aromatics such as lignin (Figure 3-7).

$$R - CH_2 - R' + HO\cdot \rightarrow R - CH\cdot - R' + H_2O \qquad \text{Equation 3-12}$$

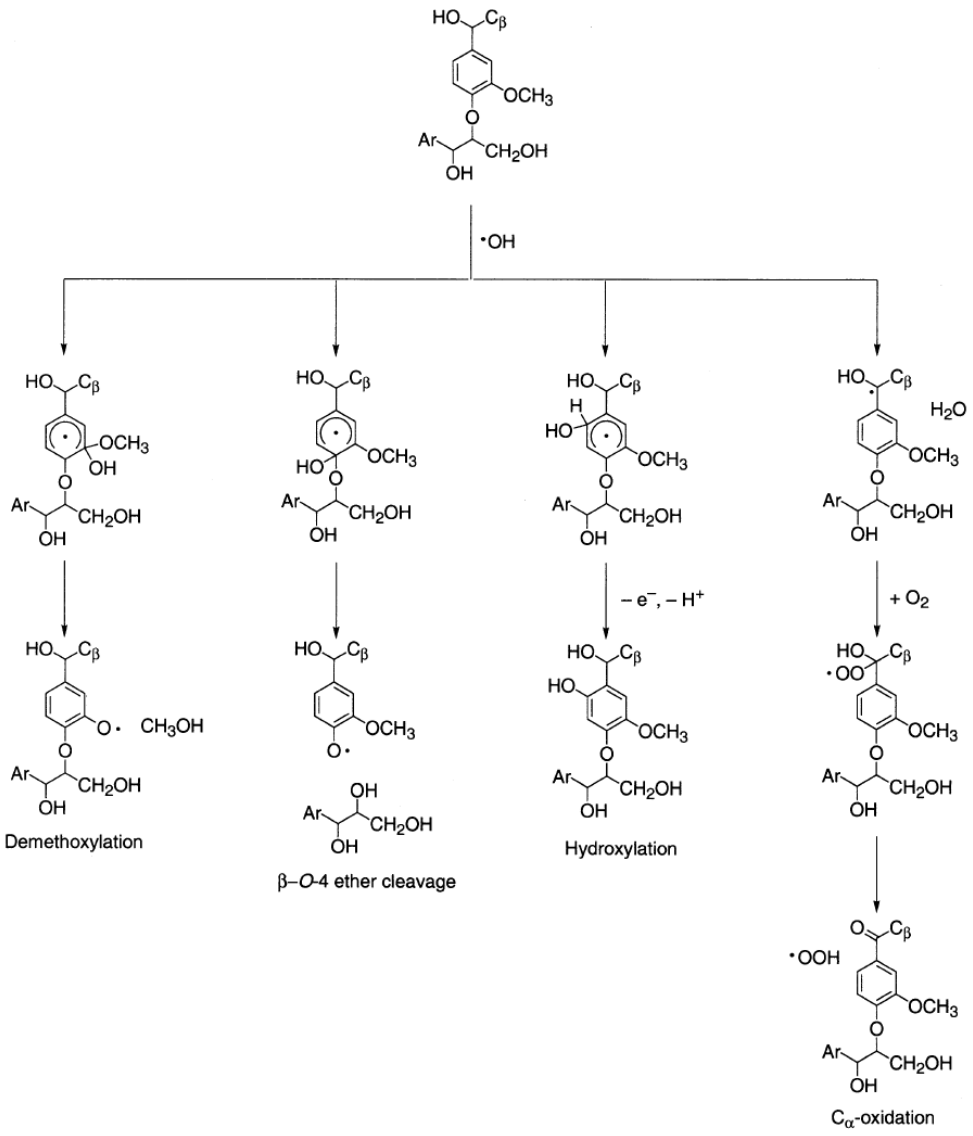

Figure 3-7: Reactions of hydroxyl radical with lignin (Hammel, Kapich, et al. 2002).

If the hydroxyl radical abstracts a hydrogen from an unsaturated lipid, it may facilitate the formation of peroxyl radicals (Elissetche, et al. 2006). If the hydroxyl radical adds as an electrophile to the aromatic ring of non-phenolic lignin, the lignin is converted to a phenolic form which is more easily oxidized than non-phenolic lignin by MnP-generated redox mediators (Mn(III) and peroxyl radicals).

3.2.4.1 Cellobiose dehydrogenase generation of hydroxyl radicals

One proposal for the generation of hydroxyl radicals *in vivo* by white rot fungi involves the enzyme cellobiose dehydrogenase generating the Fe(II) and hydrogen peroxide necessary for the Fenton reaction (Kremer and Wood 1992); (Nutt, et al. 1997); (Hildén, et al. 2000). The white rot fungus *P. chrysosporium* secretes cellobiose dehydrogenase under cellulolytic conditions when the lignin-degrading enzymes are not secreted, but also possibly simultaneously with the lignin-degrading enzymes. Thus, cellobiose dehydrogenase may play a role in both selective and non-selective lignin degradation.

Cellobiose dehydrogenase produces hydrogen peroxide by oxidizing cellobiose and transferring those electrons to molecular oxygen (i.e. reduces molecular oxygen) thereby producing hydrogen peroxide. Cellobiose dehydrogenase can also form ferrous iron (Fe(II)) by transferring electrons to ferric iron (Fe(III)) as an alternative to oxygen as the electron acceptor. The presence of hydrogen peroxide and Fe(II) would permit the generation of hydroxyl radicals via the Fenton reaction, and thereby convert non-phenolic lignin to phenolic lignin by reactions shown in Figure 3-7. The hydrogen peroxide for the Fenton reaction does not have to come from cellobiose dehydrogenase because several other oxidases secreted by white rot fungi can also produce it (e.g. glyoxal oxidase, aryl alcohol oxidase, pyranose oxidase, glucose oxidase).

Evidence for cellobiose dehydrogenase eliciting the Fenton reaction was found when the non-phenolic lignin model compound veratryl glycol was made more susceptible to oxidation by MnP when it was first treated with cellobiose dehydrogenase (Hildén, et al. 2000). The proposed mechanism is demethoxylation of the veratryl glycol to a phenol alcohol which could then be more easily oxidized by the MnP system than the original veratryl glycol.

Besides generating hydroxyl radicals, cellobiose dehydrogenase may also work with MnP *in vivo* by transferring electrons from cellobiose to solid MnO_2 present in biomass, thereby producing the Mn(II) needed for MnP function (Roy, et al. 1994). Along these same lines, oxalate secreted by fungal systems may also reduce MnO_2 to Mn(II), and in the process may generate species capable of oxidizing lignin structures (Lequart, et al. 1998).

3.2.4.2 Generation of hydroxyl radicals by an unidentified glycoprotein

Another system observed in *T. versicolor* and *P. chrysosporium* is similar to the cellobiose dehydrogenase system, but a smaller unidentified low molecular weight (1-5 kDa) compound appears to catalyze reduction of oxygen to hydrogen peroxide, and Fe(III) bound within the compound to Fe(II). Through association of the produced hydrogen peroxide and reduced iron, the unidentified compound catalyzes the production of hydroxyl radicals. The compound contains by weight ~18% protein, ~20% carbohydrate, and ~0.28% Fe(II) (Tanaka, Itakura and Enoki 1999).

3.2.4.3 Hydroxyl radical production by chelator-mediated Fenton reaction

Yet another proposal delineates a purely non-enzymatic route for the production of hydroxyl radicals during fungal degradation of biomass. Extracts of pine wood were found to have iron reducing capacity (Aguiar, Brazil de Souza-Cruz and Ferraz 2006), primarily due to the presence of catechols and catechol-like compounds. Catechols, such as DOPAC in Figure 3-8 are ortho configured diphenolics; catechols-like compounds, such as vanillic acid, possess a methoxyl group in place of one of the hydroxyl groups (DOPAC was found in the iron reducing fraction of cultures of the brown rot fungus *Gloeophyllum trabeum*) (Goodell, Jellison, et al. 1997).

During the initial phase of fungal degradation, secretion of oxalate would chelate Fe(III) already present in biomass (Harazono, Kondo and Sakai 1996) and make it available for reduction by the catechols compounds present in pine or other biomass, thereby making Fe(II) available for the Fenton reaction (Ahmad 1995). A possible mechanism for iron reduction is shown in Figure 3-9. Not shown in the Figure is the possible reduction of molecular oxygen during removal of the second electron from the catechol, with the consequent production of a superoxide anion and a quinone. Dismutation of two superoxide anions with addition of two protons would form hydrogen peroxide which, when combined with the reduced iron, would produce hydroxyl radicals inside the cell wall. Also not shown is the possibility that the quinone is reduced back to a catechol by the fungus or superoxide anion to complete a quinone redox cycle, which can continue to occur and produce more Fe(II) (Goodell, Jellison, et al. 1997).

This route to generating hydroxyl radicals is called “chelator-mediated Fenton reaction” since catechols are iron chelators and promote the Fenton reaction by speeding reduction of Fe(III) to

Fe(II) beyond the rate attainable by simple hydrogen peroxide reduction of Fe(III) as occurs in the pure Fenton reaction where chelators are not present (Equation 3-7).

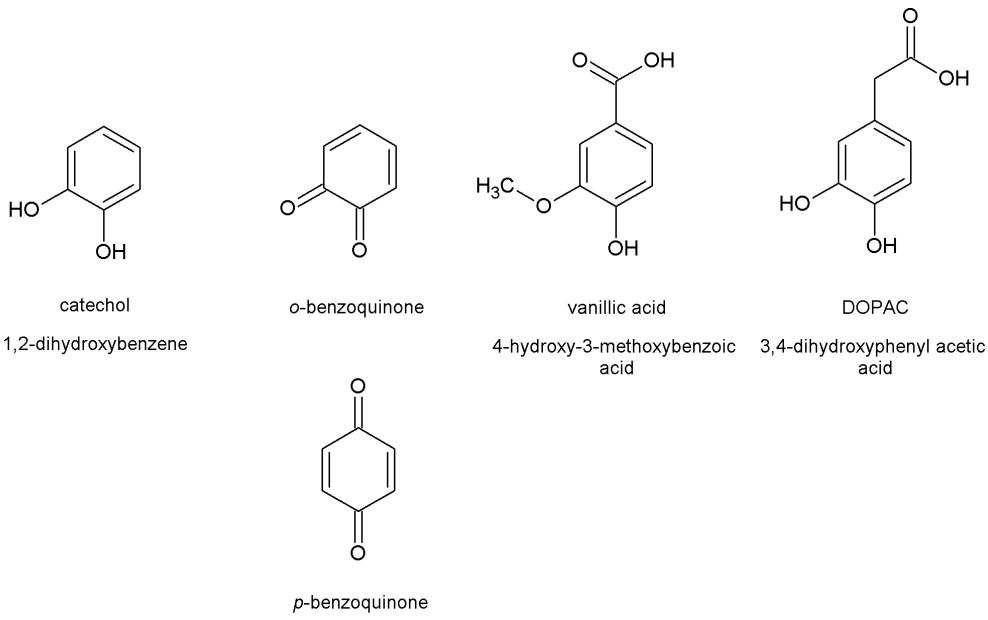

Figure 3-8: Molecular structure of catechol, *o*-benzoquinone, *p*-benzoquinone, vanillic acid, and DOPAC.

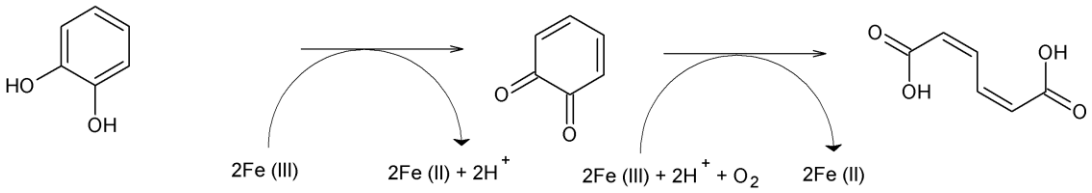

Figure 3-9: Fe(III) reduction by catechols to an *o*-benzoquinone, then to a dicarboxylic acid.

The iron reducing compounds in the extracts may eventually become chemically modified and will no longer reduce iron (see dicarboxylic acid product of catechols oxidation in Figure 3-9), but white rot fungi have been shown to secrete iron reducing compounds, and the process of lignin depolymerization itself generates catechols. Catechols are formed during lignin degradation since most of the aromatic lignin degradation products have ortho hydroxyl groups or an ortho hydroxyl and methoxyl group pair (Chen and Chang 1985). Both the secreted iron reducing compounds and the catechols produced by lignin degradation could continue to confer

high iron reducing ability to the system after iron reducing extractives become chemically modified (Goodell, Jellison, et al. 1997).

3.3 Hypotheses of the methylene blue experiments

Now that a review of MnP function and Fenton chemistry is complete, the hypotheses of the experiments using methylene blue as substrate can be stated. The first hypothesis is that an rMnP system will degrade the dye significantly only if the rMnP system contains a polyunsaturated fatty acid. The hypothesis comes from a study showing that MnP requires a polyunsaturated lipid to oxidize phenanthrene, a polycyclic aromatic similar in structure to methylene blue (Moen and Hammel 1994). In other words, the Mn(III) complexes that form between Mn(III) and carboxylic acids, such as Mn(III) malonate or Mn(III) acetate, will be insufficiently oxidative to directly degrade the dye. Instead, the Mn(III) chelate must first oxidize a polyunsaturated fatty acid to a radical species reactive enough to oxidize the dye.

Another part of this hypothesis is that the degree to which the rMnP system degrades the dye will increase with increasing unsaturation of the fatty acid. This part of the hypothesis is based on the theoretical expectation that greater unsaturation will lead to more rapid formation and higher concentrations of peroxyl radicals (ROO·) via peroxidation of the unsaturated fatty acids. The more rapid formation and concentrations would be due to the greater abundance among more unsaturated fatty acids of labile *bis*-allylic hydrogens which must be abstracted to form the peroxyl radicals that are thought to be the predominant agent of lignin degradation by white rot fungi (Kapich, Jensen and Hammel 1999).

The phenanthrene oxidant in the Moen and Hammel (1994) study showing phenanthrene oxidation in an MnP system may have been a lipid peroxyl radical (Kapich, Jensen and Hammel 1999). The alkoxyl radical (RO·), a product of peroxyl radical transformation, was an unlikely oxidant of phenanthrene because it undergoes rapid intramolecular epoxidation or β-scission. The hydroperoxyl radical (HOO·), also a product of peroxyl radical transformation, was also a possible oxidant since it is about as reactive as the peroxyl radical, but scavenging of hydroperoxyl radicals by Mn(II) present in an MnP-based system would reduce its availability.

The second hypothesis of the methylene blue experiments was that without an unsaturated fatty acid, the rMnP system could significantly degrade the dye only if it was partially degraded

beforehand with hydroxyl radicals generated by a chelator-mediated Fenton reaction. Also, the rMnP system could degrade the Fenton pretreated dye with increasing ease with increasing severity of Fenton pretreatment. This second hypothesis comes from one study which reported that significant MnP-based degradation of the dye azure B occurred only after previous treatment with Fenton's reagent (Fenton's reagent is Fe(III) and hydrogen peroxide) and the low molecular weight compounds (<5 kDa) isolated from white rot fungi culture media (Arantes and Milagres 2007) possessing iron reducing activity. Since catechols, but not proteins, were found in the culture media, it was proposed that the iron reducing activity was due to the catechols. The dye azure B used in Arantes and Milagres (2007) study is similar to methylene blue but with a methyl group missing from one of the tertiary amines.

Chemical agents, instead of enzymatic agents such as cellobiose dehydrogenase were chosen as the iron reducing agents in the studies presented here due to ease of handling. The chemical agents chose were two catecholate compounds, 3,4-dihydroxyphenyl acetic acid (DOPAC) and vanillic acid (Figure 3-8), and wheat straw extracts. DOPAC was chosen because it previously has been shown to facilitate oxidation of azure B, presumably by reducing Fe(III) to Fe(II) and thereby promoting the Fenton reaction (Arantes and Milagres 2007). Vanillic acid was chosen because, unlike DOPAC which possesses two ortho hydroxyl groups, vanillic acid possesses only one hydroxyl group oriented ortho with a methoxyl group. The methoxyl group was expected to reduce the iron reducing capacity of vanillic acid relative to DOPAC (Aguiar, Brazil de Souza-Cruz and Ferraz 2006), thus vanillic acid is a comparison against any effect due to DOPAC. Wheat straw extracts were chosen as the third iron reducing agent because a previous study reported that biomass extracts contain high iron reducing activity (Aguiar, Brazil de Souza-Cruz and Ferraz 2006) and the extracts may also contain compounds that facilitate rMnP degradation of methylene blue (Hofrichter, Lundell and Hatakka 2001).

3.4 Materials and Methods

3.4.1 Preparation of wheat straw extracts

Under sterile conditions, 14.0 g of milled wheat straw and 700 mL HPLC grade water (Mallinckrodt 6795-10) were placed into an autoclaved Erlenmeyer flask. The flask was sealed with a rubber stopper sterilized with ethanol and orbitally shaken at 170 rpm for 2 hours at 40 °C. The slurry was filtered through a Whatman GF-D glass fiber filter to remove solids from the

filtrate. The filtrate was then passed through a 0.2 µm sterile filter (Nalgene surfactant free cellulose acetate) that had been pre-rinsed with ~250 mL of HPLC grade water to remove any contaminants. The wheat straw extracts were kept frozen until use.

Solids in the wheat straw extracts (mg solids/mL extracts) was determined in triplicate by adding 5000 µL to a pre-weighed aluminum tray, drying at 105 °C for 4.2 hours, and weighing.

3.4.2 Measurement of iron reducing activity (FeRA) with the ferrozine assay

The assay for FeRA was adapted from Arantes and Milagres (2007), and is based on the formation of the stable magenta colored ferrozine-Fe(II) complex. Into a semi-micro cuvette was added, in order, sodium acetate buffer (400 µL of a 50 mM solution, pH 4.8), ferrozine solution (200 µL of a 1% w/v solution), freshly prepared Fe(III) (as $FeCl_3 \cdot 6H_2O$, 25 µL of a 20 mM solution), distilled water, and the sample (375 µL combined distilled water and sample volume) to make a total assay volume of 1000 µL. Absorbance was recorded at 562 nm at various times after sample addition to determine the kinetics of ferrozine-Fe(II) formation, and the absorbance at 3 minutes was used to determine the initial rate of ferrozine-Fe(II) formation. This initial rate was chosen as the measure of FeRA. The absorbance due to the assay reagents was determined by assaying a distilled water sample. The assay absorbance due to reagents was subtracted from the assay absorbance. The resulting net absorbance was then converted to moles Fe(II) formed per minute per mg dry iron reducing agent by using the extinction coefficient ε=27,900 $M^{-1} \cdot cm^{-1}$, and dividing by three minutes and the dry mass of iron reducing agent added to the assay volume. The FeRA of the wheat straw extracts was calculated using a wheat straw extracts dry weight of 1.69±0.04 mg/mL determined as in Section 3.4.1.

3.4.3 Fenton treatments

All reactions were completed at room temperature in triplicate in polystyrene cuvettes. Reaction mixtures for the Fenton degradation of methylene blue were mixed by first adding to the cuvettes methylene blue (4.0 mM, J.T. Baker Q475-03), sodium acetate buffer (50 mM, pH 4.8), and enough distilled water to bring the final reaction volume to 1000 µL upon addition of the remaining components. Then, in order, were added the iron reducing agent (3,4-dihydroxyphenyl acetic acid (DOPAC, Sigma 850217), vanillic acid (Fluka 94770), or wheat straw extracts,

concentrations listed by experiment in Results and Discussion), freshly prepared Fe(III) (0.1 mM as $FeCl_3 \cdot 6H_2O$), and freshly prepared hydrogen peroxide (0.1 mM). The final volume of each reaction mixture was 1000 µL. The elapsed reaction time began upon addition of hydrogen peroxide and the first absorbance reading was taken 15 seconds afterwards unless stated otherwise. All absorbance readings were at 665 nm, the peak absorbance of methylene blue. When indicated, one replicate of a blank of each treatment was run alongside the treatment, where the blank consisted of all components of the treatment except methylene blue solution which was replaced with distilled water. The absorbance of the blank was measured at 665 nm at the same times as the treatment. The blank allowed the determination of the absorbance of reagents, and therefore removal of their absorbance from the absorbance of the treatments. The resulting net absorbance was due just to changes in methylene blue absorbance at 665 nm.

3.4.4 rMnP treatments

All reactions were completed at room temperature in triplicate in polystyrene cuvettes. Reaction components were mixed by first adding to the cuvettes methylene blue (4.0 mM, J.T. Baker product Q475-03), sodium acetate buffer (50 mM, pH 4.8), and enough distilled water to bring the final reaction volume to 1000 µL. Sets of components that had been pre-mixed were then added. The first set contained the desired short chain organic acid (sodium malonate or sodium oxalate, each at 30 mM and pH 4.8), the desired fatty acid (oleic acid [Sigma O1008], linoleic acid [Sigma L1376], or linolenic acid [Acros 302820010], 2.0 mM each), Tween 20 (Calbiochem 655205, 0.2% w/w), and iron reducing agent (3,4-dihydroxyphenyl acetic acid (DOPAC) [Sigma 850217], vanillic acid [Fluka 94770], or wheat straw extracts, concentration shown by experiment in Results and Discussion). A fatty acid or Tween 20 was added individually to some mixtures, and as a fatty acid/Tween 20 emulsion to other mixtures. Fatty acid/Tween 20 emulsions were freshly prepared and thoroughly mixed on a vortex mixer unless stated otherwise. The second set added to the cuvettes contained Mn(II) (as $MnSO_4$, 0.5 mM) and rMnP (0.1 U/mL). The rMnP was either active or inactive, and inactivated to a measured activity of 0 U/mL by autoclaving at 121 °C for ≥20 minutes. The third added component was freshly prepared Fe(III) (0.1 mM as $FeCl_3 \cdot 6H_2O$), and the fourth was freshly prepared hydrogen peroxide (0.1 mM). The elapsed reaction time began upon addition of hydrogen peroxide and the first absorbance reading was taken 15 seconds afterwards.

3.4.5 Mn(III) treatments

The treatments containing Mn(III) acetate were conducted like the rMnP treatments except that 0.5 mM Mn(III) (as a suspension of Mn(III) acetate in distilled water) was added in place of Mn(II), rMnP, and H_2O_2. The elapsed reaction time began upon addition of the Mn(III) acetate suspension.

3.4.6 Combined Fenton and rMnP treatments

Sequential degradation of methylene blue with a Fenton treatment followed by an rMnP treatment was performed. The Fenton phase was completed as described previously except:

1. The methylene blue concentration was 5.7 mM instead of 4.0 mM so that the methylene blue concentration would be 4.0 mM upon addition of the reagents necessary to start the rMnP phase.
2. The total reaction volume was 700 µL instead of 1000 µL
3. The iron reducing agents (DOPAC or wheat straw extracts) were added at four concentrations each (none, low, medium, high) (Table 3-1).
4. The Fenton phase was conducted for ~3.5 hours.

Table 3-1: Concentrations of DOPAC and wheat straw extracts used in the Fenton phase of sequential degradation of methylene blue by Fenton and rMnP treatments.

Iron reducing agent type (unit)	**low**	**medium**	**high**
DOPAC initial FeRA (nmole Fe (II) per minute)	3.4	10	31
DOPAC concentration (nM)	5.0	15	45
WS extracts initial FeRA (nmole Fe (II) per minute)	3.3	10	30
WS extracts concentration (mg/mL)	0.07	0.21	0.64

Upon completion of the Fenton phase, the rMnP phase began. The rMnP phase was based on either a malonate/rMnP system or a linoleic acid/Tween 20/malonate/rMnP system. After the Fenton phase, the total reaction volume was 700 µL and the sodium acetate buffer concentration was 50 mM. In preparation for the rMnP phase, first were added to the cuvettes enough additional sodium acetate buffer (pH 4.8) to maintain the 50 mM concentration, and enough distilled water to bring the final reaction volume to 1000 µL after addition of subsequent components (with a final reaction volume of 1000 µL, the 5.7 mM methylene blue concentration during the Fenton phase diluted to a 4.0 mM concentration). Sets of components that had been pre-mixed were then

added. The first set consisted of sodium malonate (30 mM), or malonate/linoleic acid/Tween 20 emulsion (30 mM malonate/2.0 mM linoleic acid/0.2% w/w Tween 20). The second set consisted of Mn(II) (as $MnSO_4$, 0.5 mM) and rMnP (0.1 U/mL). The rMnP was either active or inactive, and inactivated to a measured activity of 0 U/mL by autoclaving at 121 °C for ≥20 minutes. The third added component was freshly prepared hydrogen peroxide (0.1 mM). The elapsed reaction time began upon addition of hydrogen peroxide and the first absorbance reading was taken 15 seconds afterwards. One replicate of a blank of each treatment was run alongside the treatment. The blank consisted of all components of the treatment except the methylene blue which was replaced with distilled water. The blank allowed determination of the absorbance of reagents, and therefore determination of the absorbance of the methylene blue only by subtracting reagent absorbance from the treatment absorbance. The rMnP phase was run for ~17 hours.

3.5 Results and Discussion

3.5.1 Absorbance spectra of methylene blue and wheat straw extracts

3.5.1.1 Methylene blue

The absorbance spectrum of methylene blue in distilled water was obtained to find an optimal wavelength at which to monitor its degradation (Figure 3-10). The absorbance maxima occurred at 246, 292, and 666 nm, with 666 nm the absolute maximum. The absorbance from 664 nm to 666 nm was nearly identical. The dye was monitored at 665 nm during the experiments to maximize sensitivity to absorbance changes.

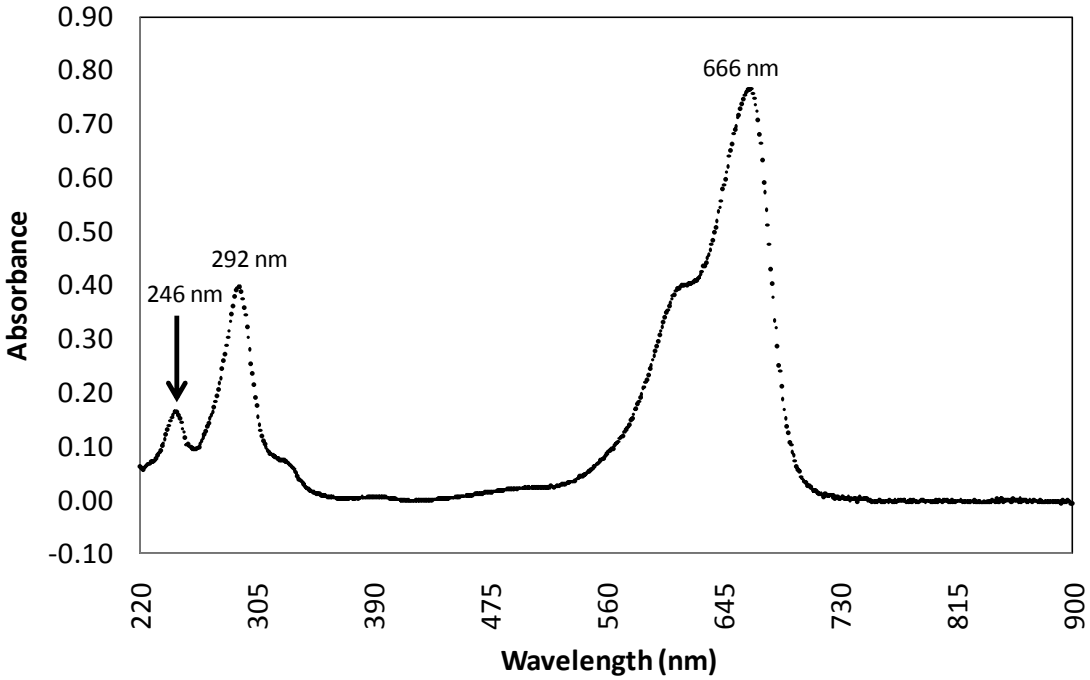

Figure 3-10: Absorbance spectrum of methylene blue (10.0 mM) in distilled water.

To infer methylene blue concentration from absorbance values, the absorbance linear range was determined. The absorbance curve showed linearity in the range 0-0.36 (0-4 mM) (Figure 3-11 and Figure 3-12).

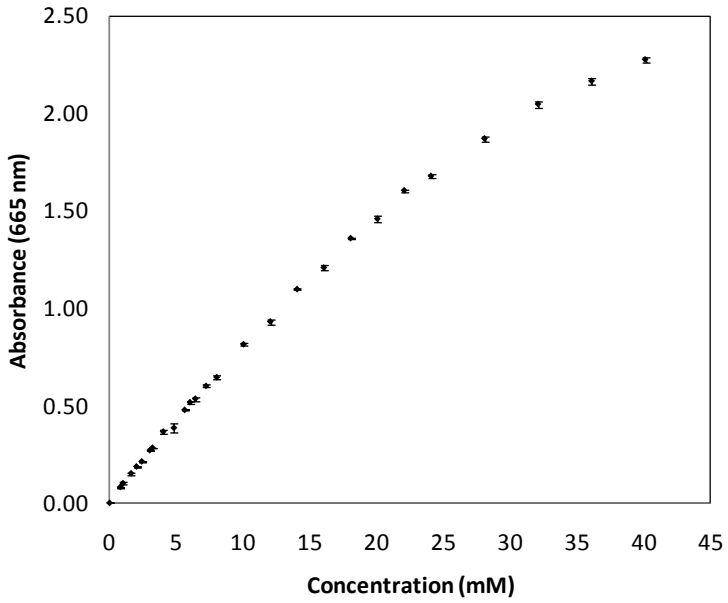

Figure 3-11: Broad range absorbance of methylene blue (665 nm) in distilled water versus concentration. The error bars are ±1 standard deviation of absorbance measurements of triplicate dilutions.

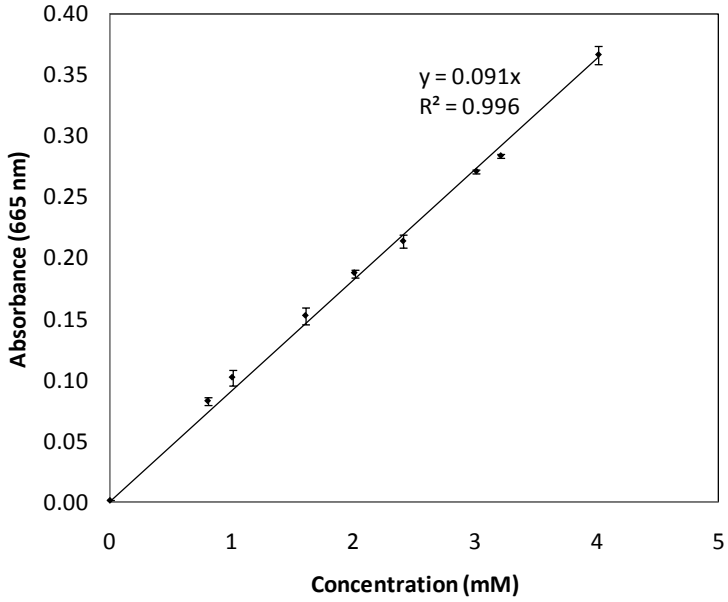

Figure 3-12: Linear range absorbance of methylene blue (665 nm) in distilled water versus concentration. The error bars are ±1 standard deviation of absorbance measurements of triplicate dilutions.

3.5.1.2 Wheat straw extracts

The absorbance spectrum of the wheat straw extracts (10% v/v solution) was obtained to see if the extracts could contain aromatic compounds (one absorbance maximum of aromatics is at 260-290 nm (Silverstein, Bassler and Morrill 1991)). The absorbance was also determined to verify that the absorbance would not significantly interfere with the absorbance of methylene blue at 665 nm (Figure 3-13). The nominal absorbance at 280 nm shows that aromatics may be present, and the minimal absorbance at 665 nm indicates that wheat straw extracts would not significantly interfere with methylene blue absorbance at 665 nm.

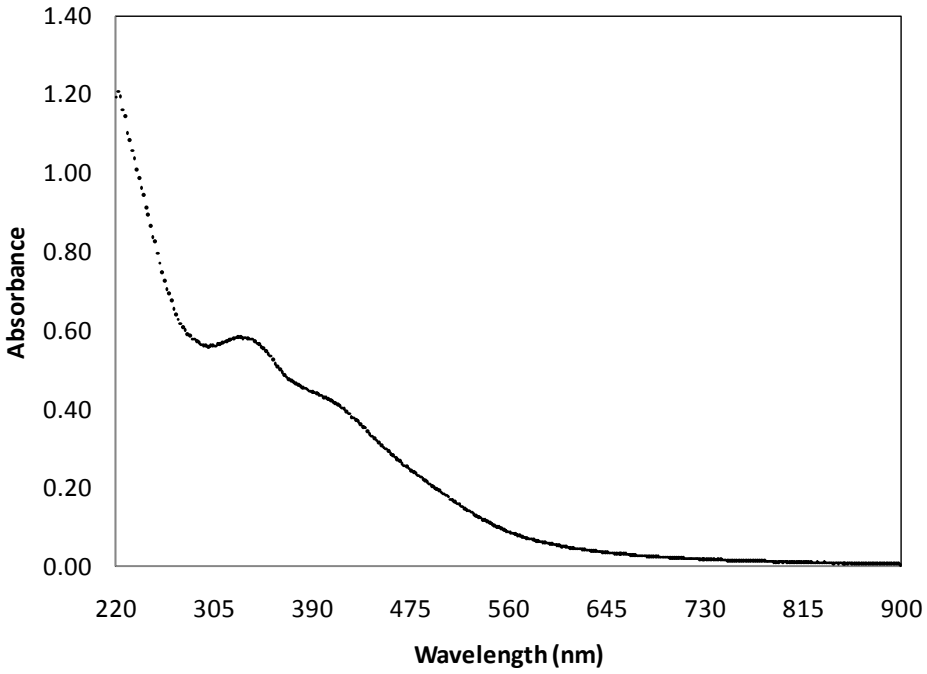

Figure 3-13: Absorbance spectrum of wheat straw extracts at 10% (v/v) concentration.

3.5.2 Development of the ferrozine assay for iron reducing activity (FeRA) measurement

The ferrozine assay was completed on wheat straw extracts at several concentrations to find the linear absorbance range of the ferrozine-Fe(II) complex at 562 nm. The absorbance was measured 15 minutes after addition of the wheat straw extracts samples to the assay mixture. The absorbance curve demonstrated linearity in the range 0 to 0.55 (0 to 5% v/v wheat straw extracts) (Figure 3-14 and Figure 3-15).

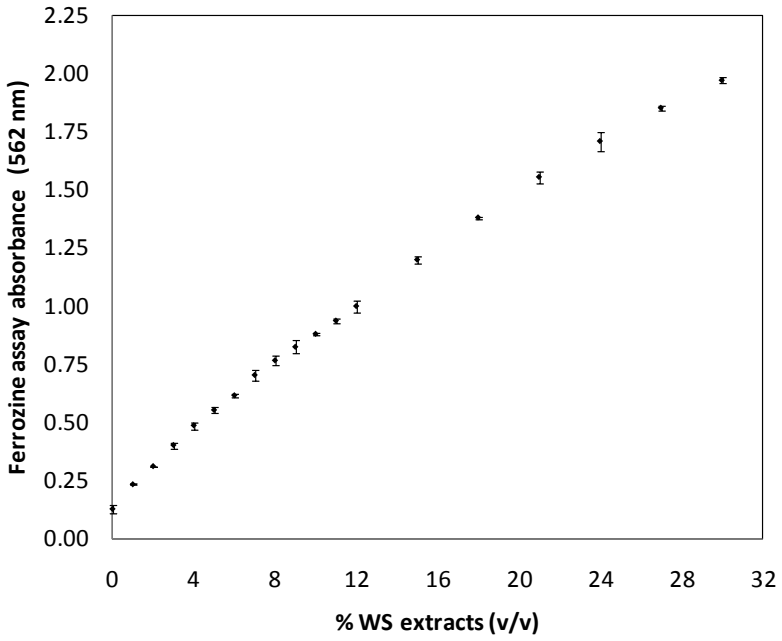

Figure 3-14: Broad range absorbance of the ferrozine assay 15 minutes after addition of wheat straw extract samples. Absorbance values are uncorrected for reagent absorbance. Error bars are ±1 standard deviation of triplicate assays completed simultaneously.

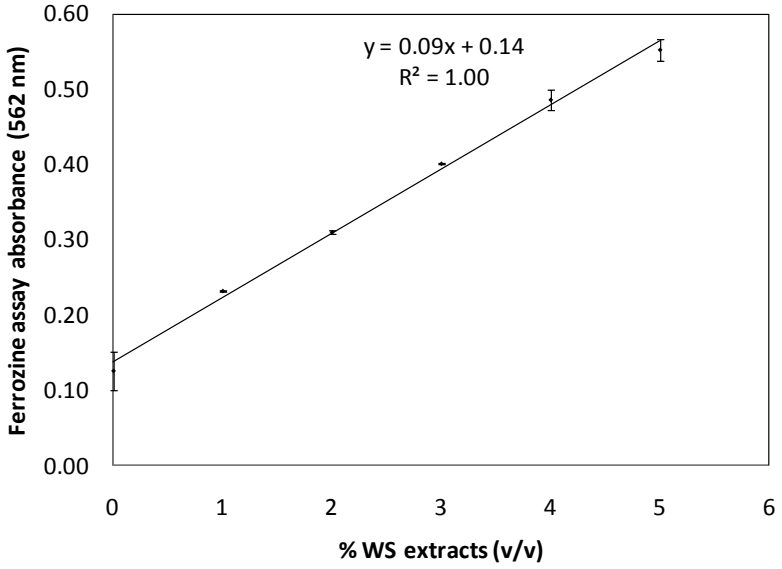

Figure 3-15: Linear range absorbance of the ferrozine assay 15 minutes after addition of wheat straw extract samples. Absorbance values are uncorrected for reagent absorbance. Error bars are ±1 standard deviation of triplicate assays completed simultaneously.

The ferrozine assay absorbance (562 nm) was measured over time after addition of wheat straw extracts, DOPAC, vanillic acid, and distilled water to inspect the kinetics of ferrozine-Fe(II) complex formation. The samples were diluted to stay within the linear absorbance range of 0-0.55. The results are shown in Figure 3-16 where the absorbance values of the DOPAC, vanillic acid, and wheat straw extracts samples have been corrected for reagent absorbance by subtracting the absorbance of the distilled water sample (also shown) from the absorbance values of the samples containing DOPAC, vanillic acid, or wheat straw extracts.

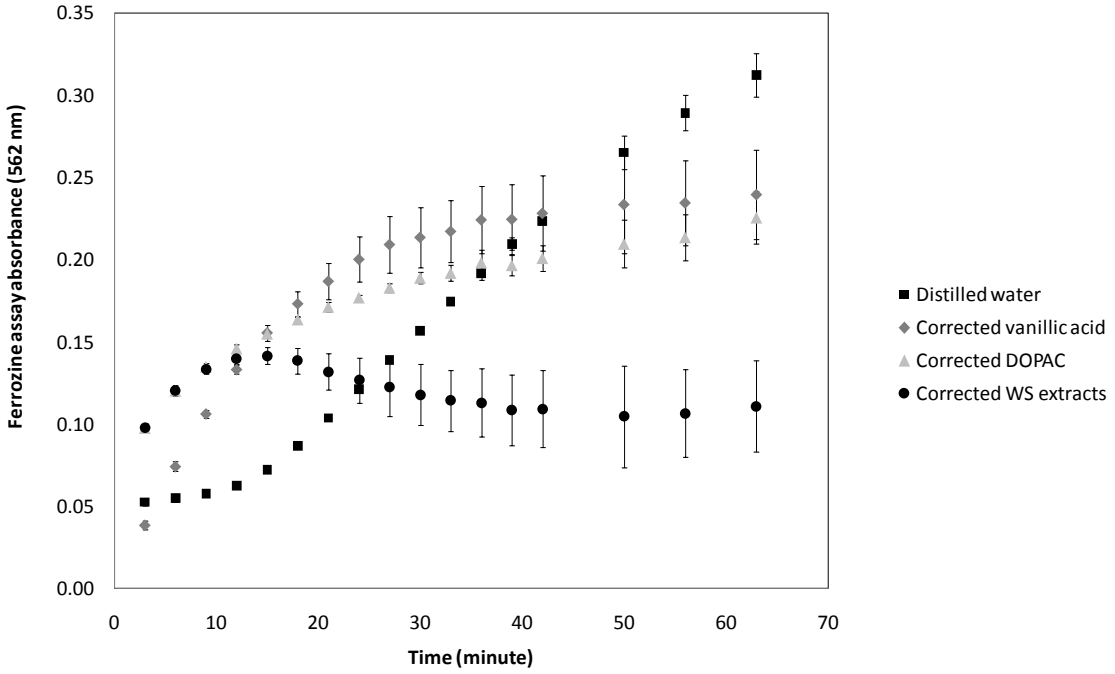

Figure 3-16: Ferrozine assay absorbance (562 nm) over time of vanillic acid, DOPAC, and wheat straw extracts samples. The absorbance values of all three samples are corrected for reagent absorbance, shown as the distilled water sample. Error bars are ±1 standard deviation of triplicate assays completed simultaneously.

Conversion of the assay absorbance values to iron reducing activity (FeRA), in units of μmole Fe(II) per mg iron reducing agent (dry weight) is shown in Figure 3-17.

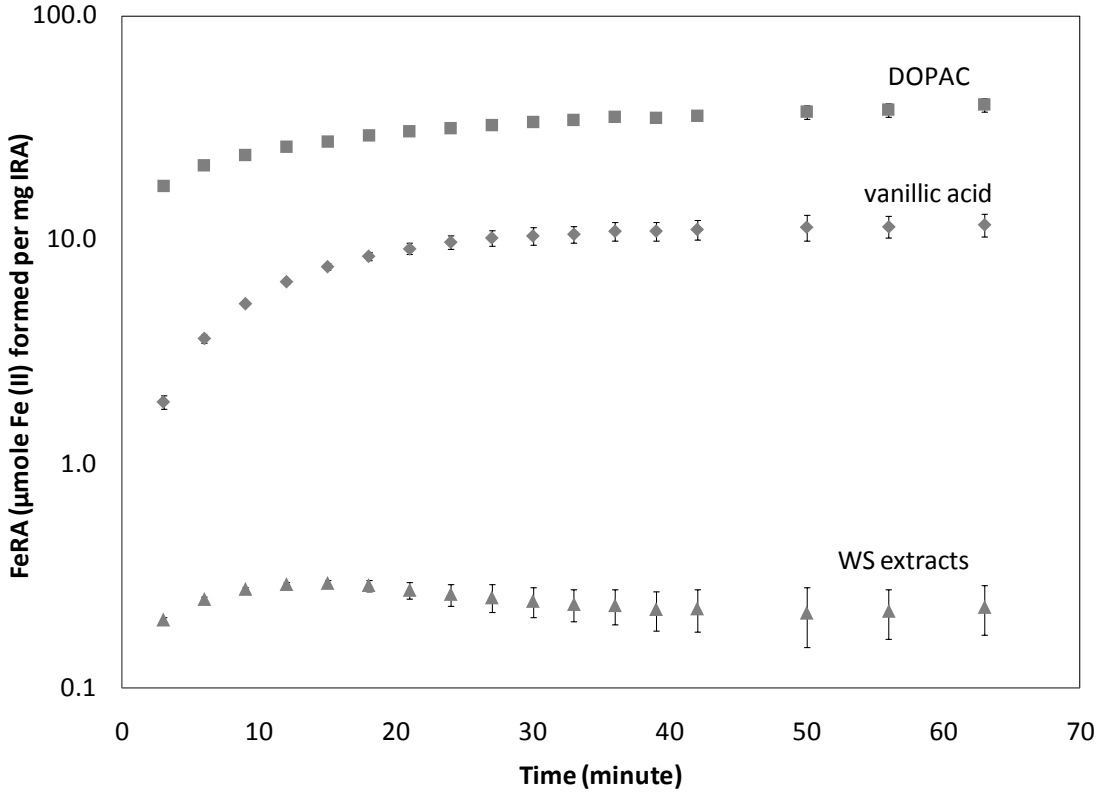

Figure 3-17: Iron reducing activity, FeRA (µmole Fe(II) per mg dry weight) versus time for the three iron reducing agents. Error bars are ±1 standard deviation of triplicate assays completed simultaneously.

One way to quantify iron reducing activity is to choose a time at which the formation of the ferrozine-Fe(II) complex is reasonably complete, and then determine at that time the moles Fe(II) formed per unit weight iron reducing agent. Another way is to determine the initial rate of Fe(II) formation and express the iron reducing activity in terms of moles Fe(II) formed per unit time per unit weight iron reducing agent. The latter method has been chosen here because it has lower uncertainty as indicated by the smaller error in the early measurements of iron reducing activity (Figure 3-17). The latter method also circumvents the difficulty of interpreting the assay absorbance values of wheat straw extracts which peaked at ~15 minutes then decreased for unknown reasons. The resulting values are average rates of Fe(II) formation during the first three minutes (Figure 3-18).

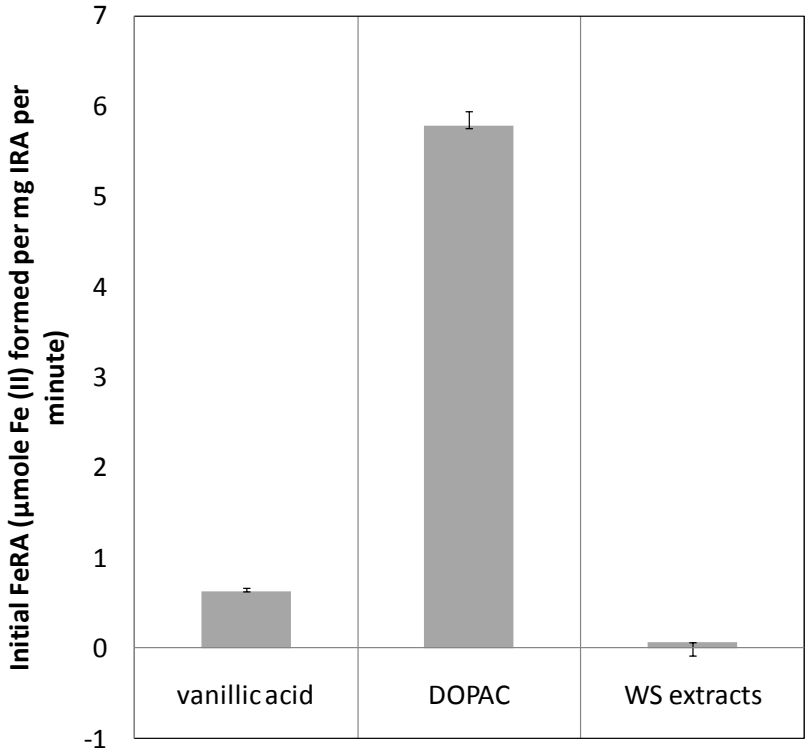

Figure 3-18: Initial FeRA of iron reducing agents (IRAs): vanillic acid (0.63±0.04), DOPAC (5.8±0.2), wheat straw extracts (0.067±0.001).

A previous study (Arantes and Milagres 2006) found that the initial FeRA of DOPAC was 12 µmole Fe(II)/L at the three minute mark with a 20 µmole/L DOPAC concentration. Converting this value gives 1.2 µmole Fe(II) per mg DOPAC per minute which is comparable to the 5.8 µmole Fe(II) per mg DOPAC per minute value found here. Regarding the wheat straw extracts, a previous study (Aguiar, Brazil de Souza-Cruz and Ferraz 2006) found that the FeRA of a solution containing the extracts of *Pinus taeda* wood chips after 90 days of extraction in a sterile bioreactor was 0.29 mmole Fe(II) per liter extracts solution per minute when measured at three minutes of the ferrozine assay. Conversion of the initial FeRA of wheat straw extracts found here results in the comparable value of 0.11 mmole Fe(II) per liter extracts solution per minute.

The amounts of Fe(II) formed per mg vanillic acid and DOPAC after 63 minutes of the ferrozine assay were 11.7 and 40.1 µmole, respectively. These amounts translate to 2.0 and 6.8 µmole Fe(II) per µmole IRA, both nonstoichiometric values. Nonstoichiometric values have been observed previously (Arantes and Milagres 2006). The 2.0 µmole Fe(II) per µmole vanillic acid

nonstoichiometric value indicates that vanillic acid may oxidize only to a quinone-like product (Figure 3-9) since reduction of two moles of Fe(III) results in a quinone, while the 6.8 µmole Fe(II) per µmole DOPAC value indicates that DOPAC may convert to a product even more oxidized that the dicarboxylic acid shown in Figure 3-9 since the dicarboxylic acid forms with the reduction of four moles of Fe(III).

3.5.3 Detecting Fenton chemistry in the degradation of methylene blue

The effect on methylene blue degradation of removing Fe(III) and H_2O_2 from a mixture of Fe(III), H_2O_2, and iron reducing agent was studied to verify the presence of Fenton-based degradation. Fenton-based degradation should not occur in the absence of either Fe(III) or H_2O_2.

The reaction components were added according to the standard method in the Materials and Methods section except that the Fe(III), H_2O_2, and iron reducing agent were pre-mixed and added simultaneously instead of separately to the methylene blue/sodium acetate buffer/distilled water mixture already in the cuvettes. A problem with this addition method is that the three pre-mixed components could have time to react and the H_2O_2 concentration decrease before addition to the methylene blue, thereby possibly decreasing the extent or nature of dye degradation. Other differences with the standard method include using 1.0 mM instead of 0.1 mM H_2O_2, and using wheat straw extracts made by extracting wheat straw in sterile-filtered distilled water for 4.6 days instead of HPLC grade water for two hours. After extraction, the solids were removed from the filtrate and the filtrate sterile filtered as described in the standard method. Residual Fe(III) in the distilled water used in the extraction could have increased the Fe(III) concentration. And even though the wheat straw extracts were sterile filtered before use, the long extraction time makes possible contamination of the wheat straw extracts solution with compounds secreted during microbial growth since those secreted compounds can pass through the 0.2 µm sterile filter. The iron reducing agent concentrations used in the experiment were (FeRA in nmole Fe(II) per min, concentration in mM or mg/mL): vanillic acid (11, 0.1 mM), DOPAC (97, 0.1 mM), and wheat straw extracts (~60, 0.39 mg/mL). No blanks were run alongside the treatments to correct for reagent absorbance.

The results (Figure 3-19) show generally more degradation when Fe(III), hydrogen peroxide, and iron reducing agent were present than when Fe(III) or H_2O_2 or both were missing. This is evidence of Fenton degradation with all three iron reducing agents. Some of the degradation

observed in the treatments without Fe(III) may still be due to Fenton chemistry since there may have been some residual iron present in the distilled water that was not removed by distillation. Some of the degradation in the treatments without hydrogen peroxide could also be due to Fenton chemistry because phenolic compounds have been found to undergo autoxidation to produce hydrogen peroxide (Pueyo and Ariza 1993). Since iron reducing agents are present in the wheat straw extracts, and some iron in the wheat straw would have inevitably partitioned into the aqueous phase during extraction, some of the degradation observed in the extracts mixtures without Fe(III), hydrogen peroxide, or both is likely due to Fenton chemistry. This is especially applicable to the treatments without any added Fe(III) or hydrogen peroxide, but the results of this experiment do not rule out the possibility of other degradation mechanisms occurring in the wheat straw extracts treatments.

A treatment containing Fe(III) and hydrogen peroxide but no iron reducing agent (see "base case" column of Figure 3-19) showed slight degradation, indicating that a simple treatment with Fenton's reagent (Fe(III) and hydrogen peroxide) does not significantly degrade the dye. A different experiment which ran several replicates of the same treatment (i.e. with Fe(III), hydrogen peroxide, and no iron reducing agent) resulted in essentially no dye degradation (see section 3.5.5 below). The low or absent degradation without an iron reducing agent demonstrates the importance of an iron reducing agent in promoting dye degradation, most likely by hydroxyl radicals generated by the Fenton reaction.

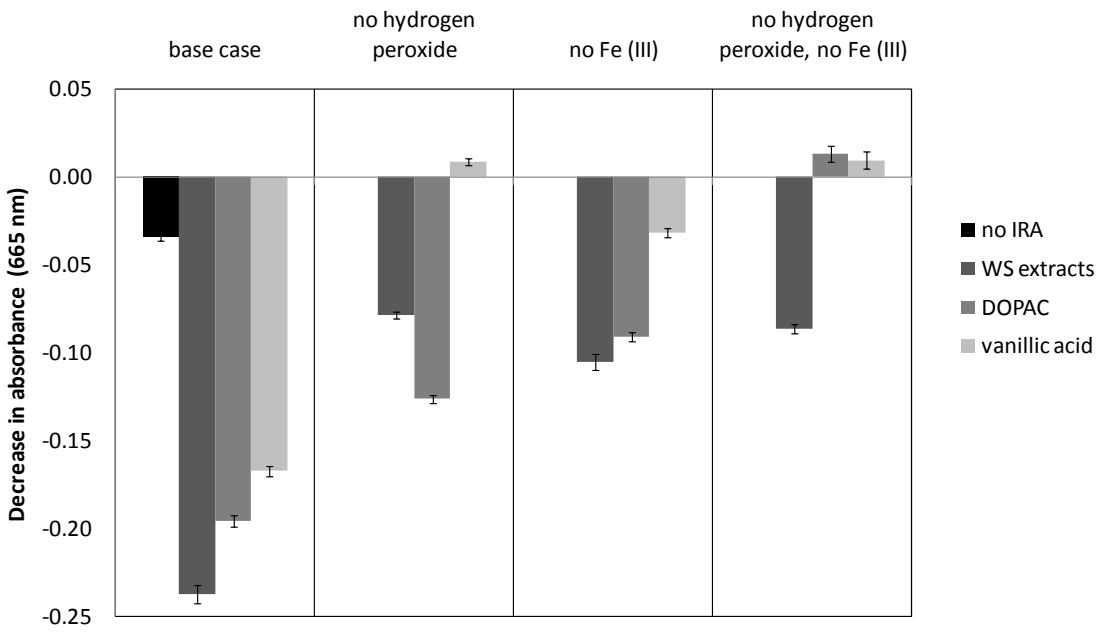

Figure 3-19: Test for Fenton degradation of methylene blue. The graph shows the decrease in methylene blue absorbance 16.9 hours after addition of Fe(III), H_2O_2, and iron reducing agent (IRA), or subset thereof. The decrease in absorbance is measured relative to the absorbance, 15 seconds after addition, of a mixture containing all constituents mentioned above except an IRA. Absorbance values are not corrected for reagent absorbance. Error bars are ±1 standard deviation of triplicate experiments completed simultaneously.

3.5.4 Spectral changes in methylene blue with Fenton treatment

Methylene blue degradation by the enzyme horseradish peroxidase results in successive demethylation of the amine groups (Ferreira-Leitão, Godinho da Silva and Bon 2003). Removal of one methyl group results in the formation of the dye azure B, two methyl groups (azure A), three (azure C), and four (thionin). Each dye has a peak absorbance wavelength progressively shorter than 665 nm (StainsFile 2009). Thus the question arises whether the decrease in dye absorbance at 665 nm observed in the experiment reported previously is simply a shift in the maximum absorbance to shorter wavelengths and is due only to demethylation, or whether the decrease in absorbance is due to an overall decrease in the absorbance and due to chromophore degradation. To answer this question, the degradation of methylene blue was observed over time with spectral scans from 300 nm to 900 nm (5 nm increments) under Fenton conditions.

The reaction components were added according to the standard method in the Materials and Methods section except that the addition of Fe(III) marked the start of the reaction, and the concentration of each component was 95% of the listed value. The iron reducing agent concentrations were: DOPAC (92 nmole Fe(II) per min, 0.095 mM), and wheat straw extracts (~60 nmole Fe(II) per min, 0.37 mg/mL). No blanks were run alongside the treatments to correct for reagent absorbance.

Time courses of the spectra (Figure 3-20 and Figure 3-21) show that the entire peak centered at ~665 nm decreased in intensity, indicating degradation of methylene blue chromophore. With wheat straw extracts (Figure 3-20) there was no shift in the wavelength of maximum absorbance, while with DOPAC (Figure 3-21) there was a slight shift to shorter wavelengths as the reaction progressed. The shift to shorter wavelengths may indicate demethylation, but no further tests were performed to determine the nature of this chemical change.

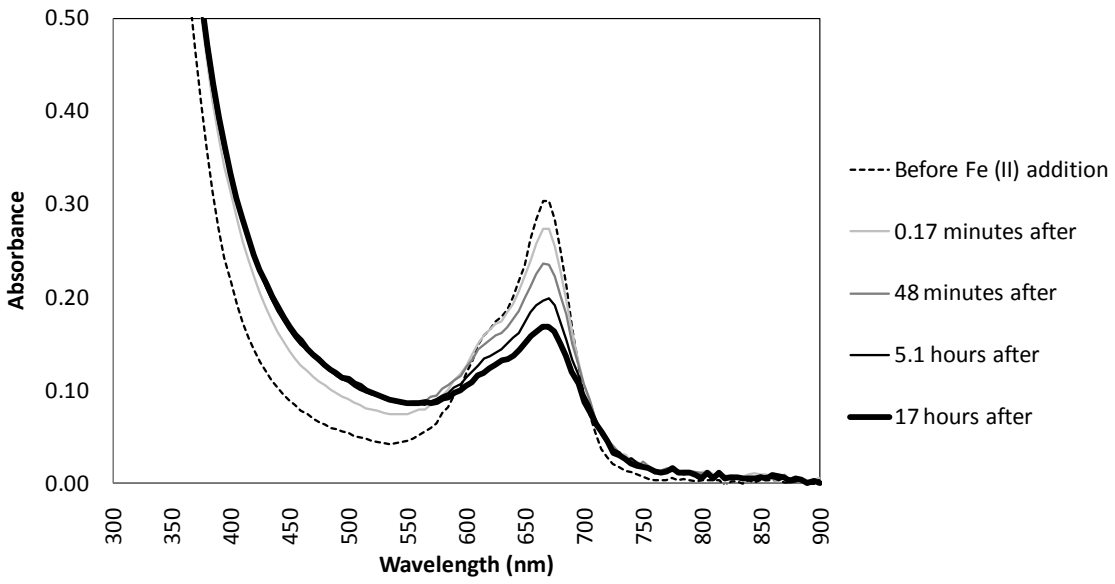

Figure 3-20: Spectral changes in methylene blue over time under Fenton treatment with wheat straw extracts. The wavelength of peak absorbance (~665 nm) does not shift noticeably to higher or lower wavelengths.

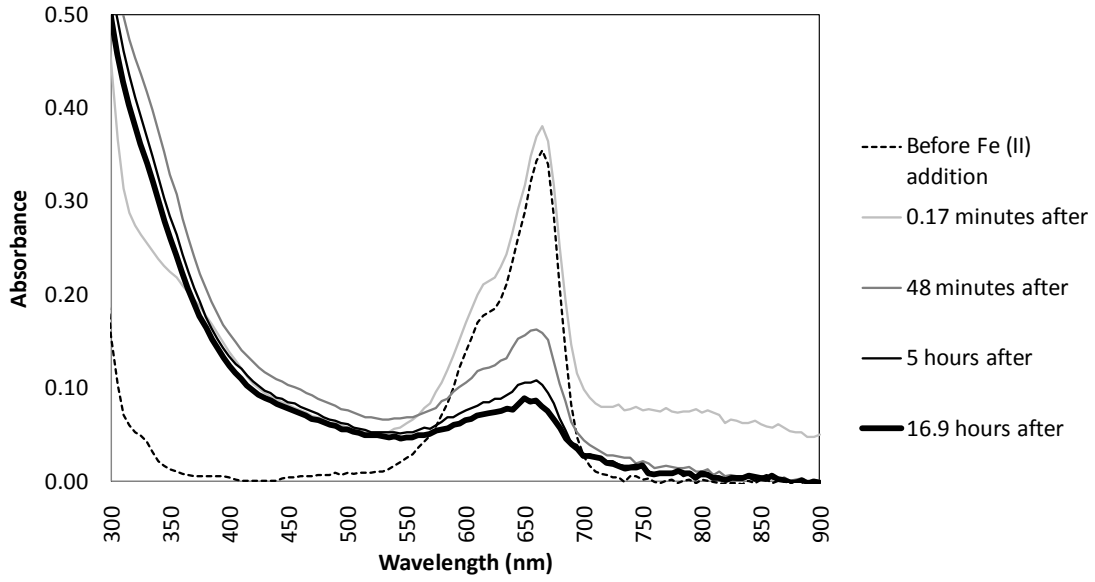

Figure 3-21: Spectral changes in methylene blue over time under Fenton treatment with DOPAC. The wavelength of peak absorbance (~665 nm) shifts slightly with time to shorter wavelengths.

Phenanthrene degradation by a lipid/MnP was previously observed (Moen and Hammel 1994), and the mechanism is thought to involve hydrogen or electron abstraction, followed by addition of molecular oxygen to form a quinone. The addition of another molecule of oxygen and cleavage then forms the dicarboxylic acid diphenic acid (Figure 3-22). Degradation of methylene blue by Fenton treatment is tentatively proposed to involve formation of the same carboxylic acid intermediate as for phenanthrene degradation, but the individual steps to this intermediate may be different given that a chelator-mediated Fenton treatment generates oxidants different than those generated in a lipid/MnP system. The carboxylic acid intermediate is proposed because it accounts for the destruction of the polycyclic conjugation responsible for the absorbance at 665 nm.

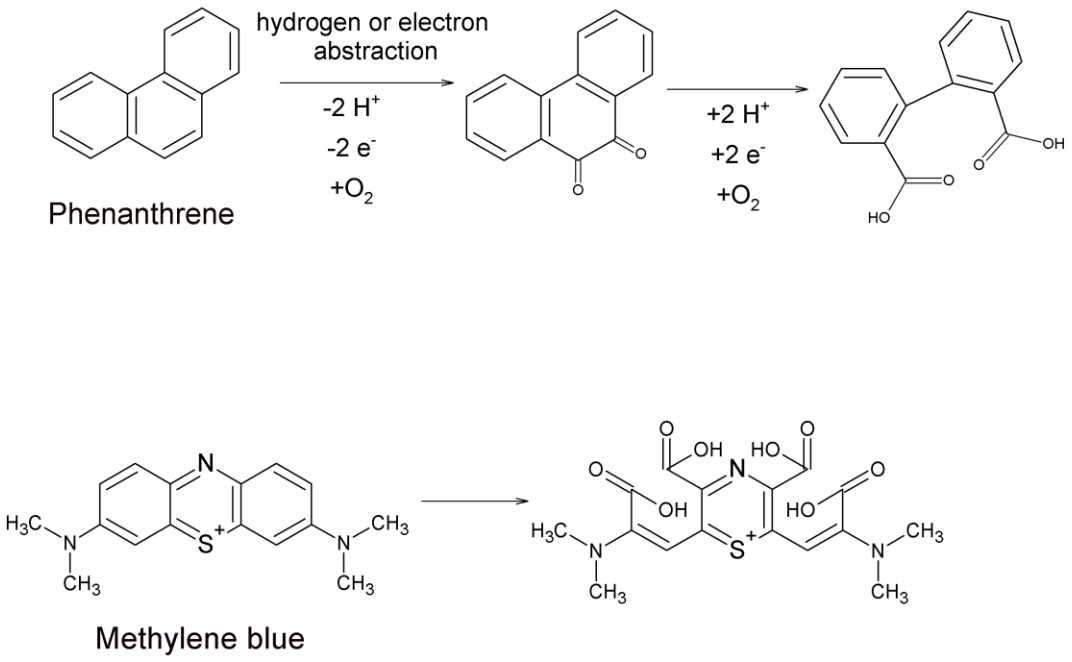

Figure 3-22: Oxidation of phenanthrene to diphenic acid and the proposed oxidized product of methylene blue.

3.5.5 Kinetics of Fenton degradation of methylene blue and the effect of iron reducing agent concentration

The kinetics of the reaction occurring between a Fenton system and methylene blue, and the effect of iron reducing agent type and concentration, also deserved study. Thus, three concentrations each of wheat straw extracts and DOPAC were used in a Fenton system, and the absorbance of the dye monitored over time. Vanillic acid was not studied since its effect was expected to be similar to that of DOPAC. The Fenton treatments were carried out according to the method of the Fenton phase of the combined Fenton and rMnP treatment discussed in the Materials and Methods section.

The dye degraded only in the presence of an iron reducing agent as seen by the negligible change in absorbance in the two treatments containing no iron reducing agent (Figure 3-23).

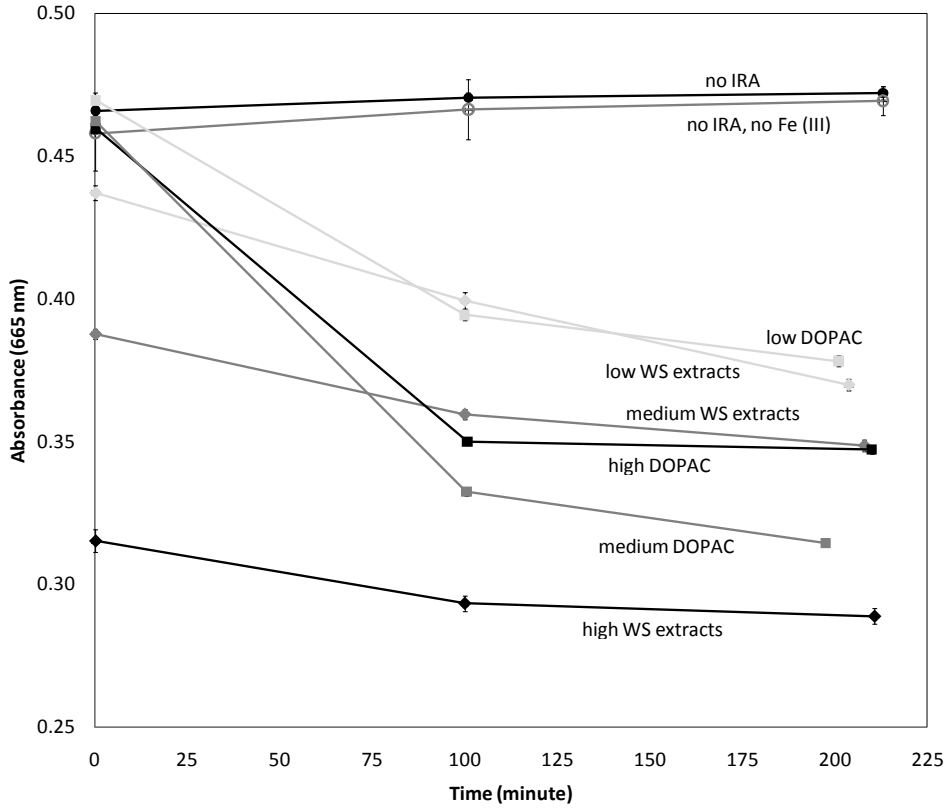

Figure 3-23: The effect of iron reducing agent (IRA) concentration on methylene blue absorbance over time. All absorbance values are corrected for reagent absorbance. Error bars are ±1 standard deviation of 6 experiments, except for the "high DOPAC" and "no IRA" treatments in which the standard deviation is of 12 experiments. The first absorbance values are 15 seconds after addition of hydrogen peroxide, and the initial concentration of methylene blue was the same in all treatments.

The absorbance decreased rapidly when wheat straw extracts were used but more slowly with DOPAC, as seen by the first absorbance values recorded 15 seconds after addition of hydrogen peroxide (Figure 3-24). The reason for the fast degradation with extracts may be that there is non-Fenton based degradation occurring in the treatments containing wheat straw extracts that does not depend on the generation of hydroxyl radicals.

Over the longer term (Figure 3-25), the absorbance of the DOPAC treatments neared the absorbance of the wheat straw extracts treatments. The quantity of the two iron reducing agents was nearly the same on an initial FeRA basis (Table 3-1), so similar long-term degradation may

be expected with the two iron reducing agents. On the other hand, the similar long-term degradation may be fortuitous given that non-Fenton based dye degradation likely occurred in the treatments containing wheat straw extracts.

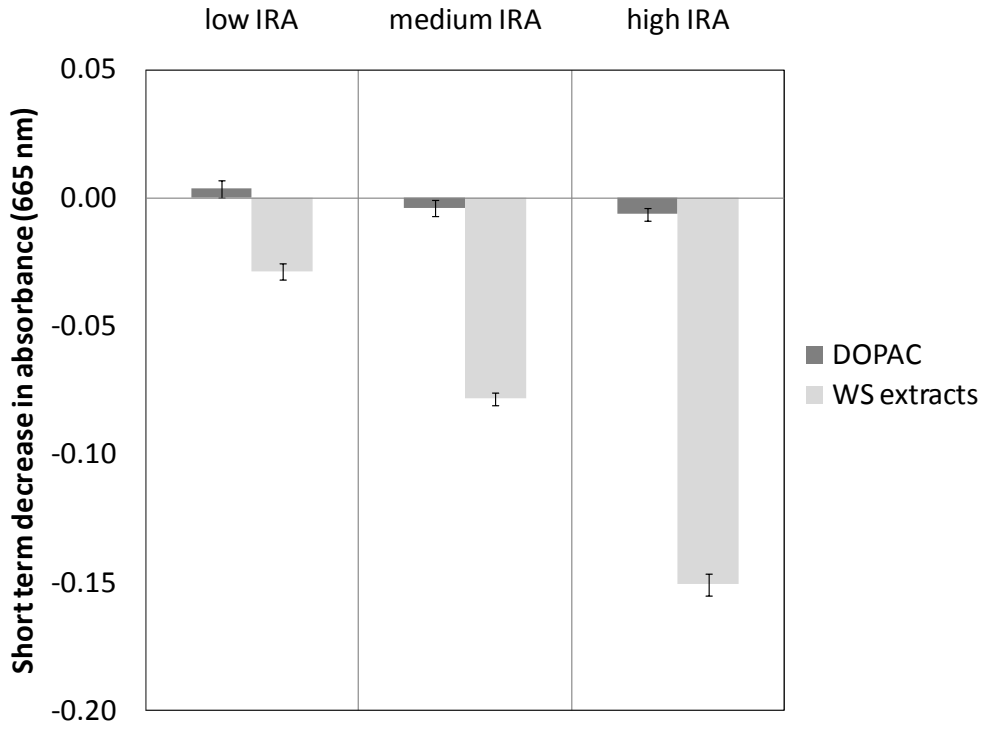

Figure 3-24: Short time-scale decrease in methylene blue absorbance under Fenton conditions with several iron reducing agent (IRA) concentrations. Each value shown is the decrease in absorbance 15 seconds after the addition of hydrogen peroxide relative to the 15 second absorbance of the "no IRA" mixture. All absorbance values are corrected for reagent absorbance. Error bars are ±1 standard deviation of 6 experiments completed simultaneously, except for the high DOPAC treatment in which the standard deviation is of 12 experiments completed simultaneously.

The long term absorbance decrease in the wheat straw extract treatments was directly related to wheat straw extract concentration but not for the DOPAC treatments because the absorbance of the treatment with the highest DOPAC concentration fell less than the treatment with a medium DOPAC concentration. A possible reason was that at the high DOPAC concentration, the DOPAC became a competitive substrate with the dye for the hydroxyl radicals generated during the Fenton reaction. In other words, hydroxyl radical oxidation of DOPAC would occur in

parallel with the dye, and thereby decrease the amount of hydroxyl radicals available to oxidize the dye and lower the iron reducing capacity of the system by degrading DOPAC.

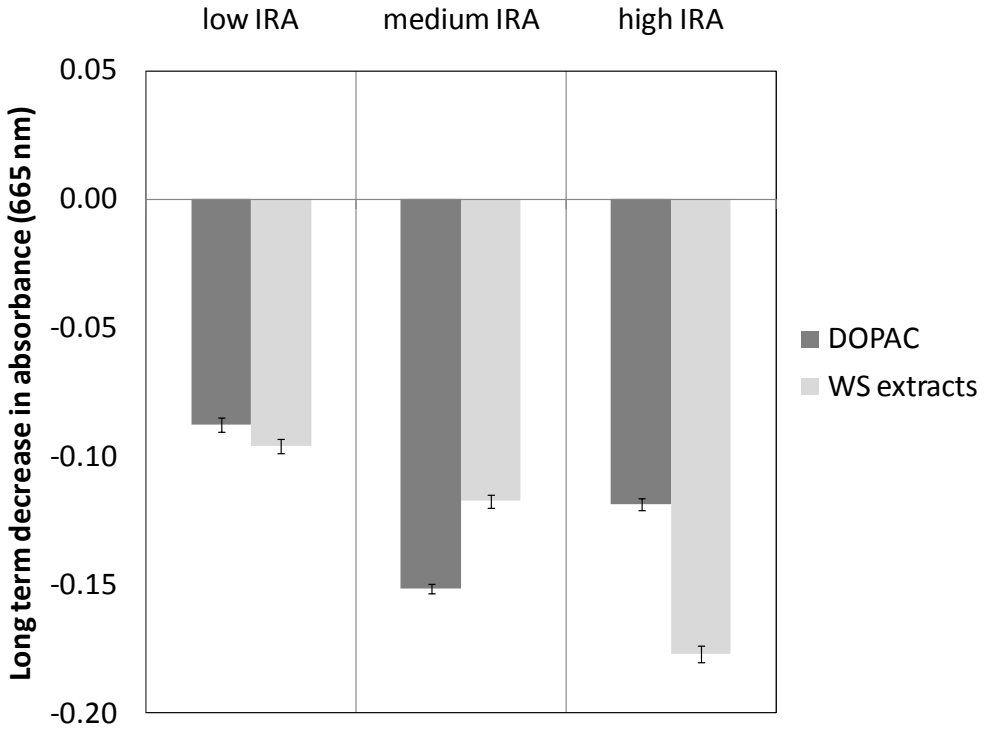

Figure 3-25: Long time-scale decrease in methylene blue absorbance under Fenton conditions with several iron reducing agent (IRA) concentrations. Each value shown is the decrease in absorbance ~3.5 hours after the addition of hydrogen peroxide relative to the 15 second absorbance of the "no IRA" treatment. All absorbance values are corrected for reagent absorbance. Error bars are ±1 standard deviation of 6 experiments completed simultaneously, except for the high DOPAC treatment in which the standard deviation is of 12 experiments completed simultaneously.

3.5.6 Screening rMnP systems for maximum methylene blue degradation

Of interest was finding a redox mediator system that allows rMnP to effectively degrade the dye. Thus, several treatments were applied to the dye and the absorbance monitored over time. The first experiment involved adding a short chain organic acid (malonate or oxalate), fatty acid (oleic, linoleic, or linolenic acid) (Figure 3-26), each emulsified in Tween 20, or Tween 20 by itself to the base case system consisting of rMnP, Mn(II), hydrogen peroxide, sodium acetate buffer, dye, and distilled water. The short chain organic acids malonate and oxalate were added

because it has been proposed that they facilitate enzyme turnover and production of Mn(III) (Kuan, Johnson and Tien 1993) and stabilization of the Mn(III) in solution (Wariishi, Akileswaran and Gold 1988). The three fatty acids were chosen since it has been observed that unsaturated fatty acids promote lignin degradation, probably through their transformation into reactive peroxyl radicals (Kapich, Jensen and Hammel 1999). The three fatty acids used differ in saturation level: oleic acid has one unsaturation, linoleic has two, and linolenic has three. Tween 20 was chosen as the surfactant for the fatty acids because it is a saturated surfactant, thus preventing its interference as a separate peroxidizable species, and a previous study used Tween 20 as the surfactant to study the peroxidation of linoleic acid (Kapich, Steffen, et al. 2005). Tween 20 alone with the rMnP system was examined to determine its effect on enzymatic degradation. No blanks were run alongside the treatments to correct for reagent absorbance. Since the measured absorbance values were uncorrected for reagent absorbance, the absorbance values of treatments with fatty acid emulsions were initially higher than treatments without fatty acid emulsions since the emulsions absorb at the monitored wavelength of 665 nm. The results are shown in Figure 3-27 and Figure 3-28.

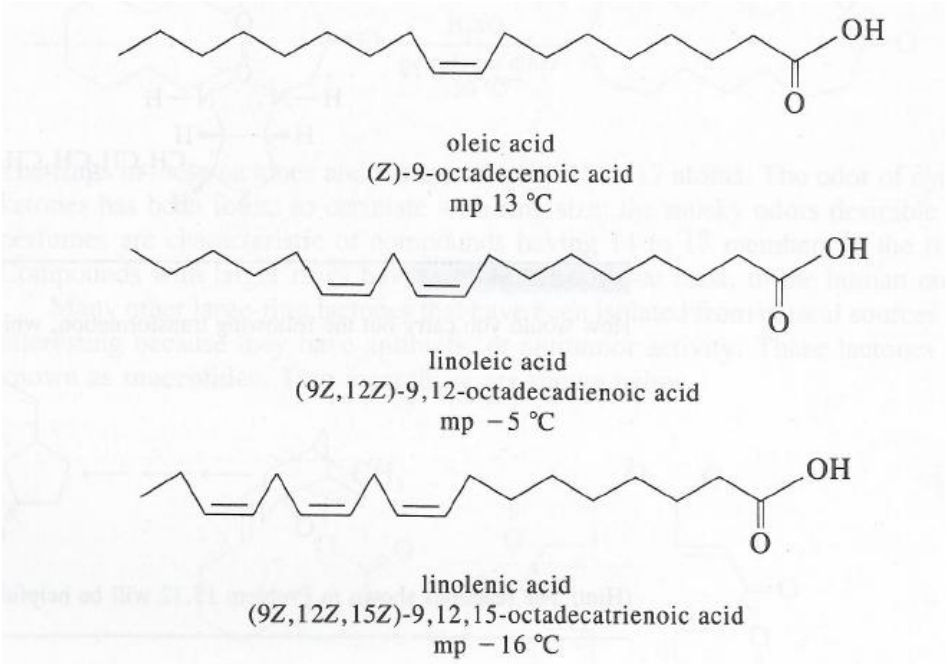

Figure 3-26: Molecular structure of oleic, linoleic, and linolenic acids (Ege 1989).

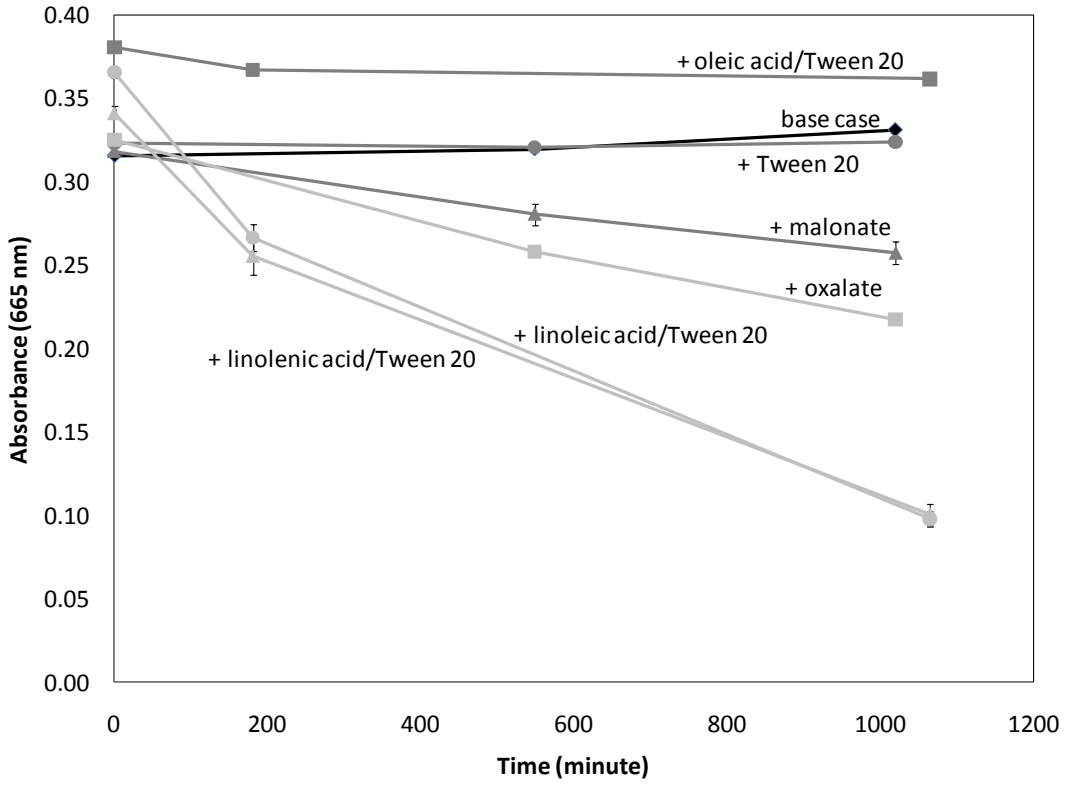

Figure 3-27: Screening of redox mediators for rMnP-induced degradation of methylene blue: absorbance over time. Absorbance values are uncorrected for reagent absorbance. Error bars are ±1 standard deviation of triplicate experiments completed simultaneously.

There was little overall change in absorbance in the base case, "+ Tween 20", and "+oleic acid/Tween 20" treatments, but substantial overall decrease in the "+malonate", "+ oxalate", "+linoleic acid/Tween 20", and "+linolenic acid/Tween 20" treatments. The "+malonate" and "+oxalate" treatments were similar in degradation rate and mildly degraded the dye, and the "+linoleic acid/Tween 20" and "+linolenic acid/Tween 20" treatments also were similar in rate but degraded the dye more completely.

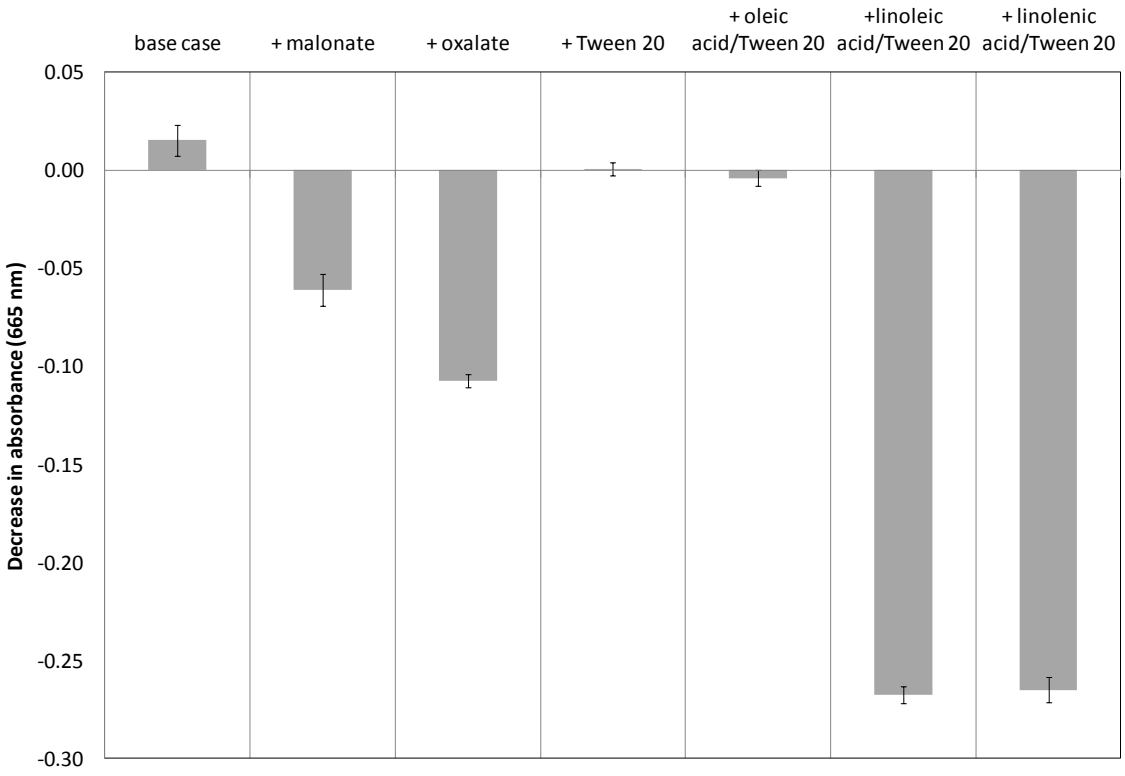

Figure 3-28: Screening of redox mediators for rMnP-induced degradation of methylene blue: overall decrease in absorbance. The graph shows the decrease in methylene blue absorbance 17 hours after addition of hydrogen peroxide relative to the absorbance 15 seconds after addition. Absorbance values are uncorrected for reagent absorbance. Error bars are ±1 standard deviation of triplicate experiments completed simultaneously.

It is believed that in MnP systems containing fatty acids, peroxyl radicals formed from the fatty acids are the chemical species most responsible for lignin degradation (Kapich, Jensen and Hammel 1999). Before a fatty acid is converted to a peroxyl radical, a hydrogen atom must first be abstracted from an allylic or *bis*-allylic position. Allylic hydrogens are attached to carbons on either side of one double bond or a series of double bonds, and *bis*-allylic hydrogens are attached to carbons in between two or more double bonds (Figure 3-26). Thus, oleic acid has only allylic hydrogens, and four of them, whereas linoleic acid has four allylic hydrogens and two *bis*-allylic hydrogens.

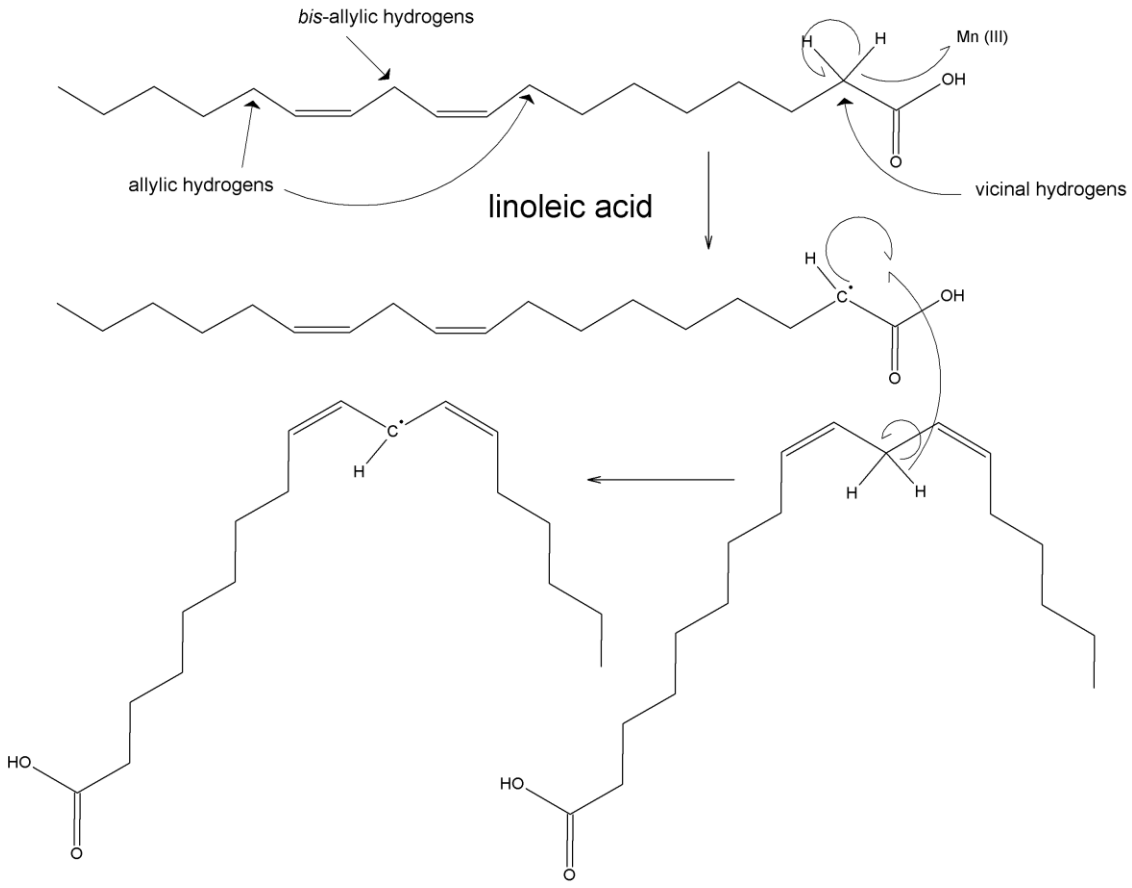

Figure 3-29: Positions of allylic and *bis*-allylic hydrogens of linoleic acid, and mechanism of *bis*-allylic hydrogen abstraction initiated by Mn(III).

The *bis*-allylic hydrogens are more labile than allylic hydrogens because the resulting radical is more delocalized with the removal of a *bis*-allylic hydrogen. Thus, among the three fatty acids studied here, hydrogen abstraction is theoretically least likely to occur to oleic acid, more likely to linoleic acid, and the most labile hydrogens belong to linolenic acid. Thus, on theoretical grounds, one would expect that the fatty acids would generate peroxyl radicals in the rate order of oleic<linoleic<linolenic, and the dye degradation rate would follow the same order. The results show that linoleic and linolenic acids degraded the dye more rapidly that oleic acid in agreement with theory, but the linoleic and linolenic acids degraded the dye almost equally in contrast to theory. Another study also contrasted with the theoretical prediction since the degradation of a lignin model compound was slower with linolenic acid than with linoleic acid (Kapich, Jensen and Hammel 1999).

The linoleic and linolenic acid systems of the previous experiment were the most potent dye degraders. To see if additional components could improve the degradation rate or extent, both of these systems were allowed to react with a select set of new components. In these experiments, the base cases were defined as the "+linoleic acid/Tween 20" and "+linolenic acid/Tween 20" treatments of the previous experiment. Thus, the base cases consisted of linoleic acid/Tween 20 emulsion or linolenic acid/Tween 20 emulsion, rMnP, Mn(II), hydrogen peroxide, sodium acetate buffer, dye, and distilled water. To each base case was added an iron reducing agent (vanillic acid, DOPAC, or wheat straw extracts), Fe(III), both DOPAC and Fe(III), or a short chain organic acid (oxalate or malonate). The components of the Fenton system were added individually and together to test their effect on the rMnP system. This knowledge was important later when anticipating the effect of Fenton components in an experiment involving sequential Fenton and rMnP treatment of the dye. Another reason why wheat straw extracts were added is because pine extracts have already been shown to promote the oxidation of a lignin model compound by MnP (Hofrichter, Lundell and Hatakka 2001). The increased oxidation may be due to peroxidizable fatty acids in the extracts (Gutiérrez, et al. 2002). Other components in biomass extracts other than fatty acids include waxes, sterols, sterol esters, resin acids, and phenolic compounds (Sun, Salisbury and Tomkinson 2003), and these compounds may also act as redox mediators or in other unknown ways to improve dye degradation. The organic acids oxalate and malonate were added to treatments to possibly combine the degradative capacities of an organic acid (malonate or oxalate) and a fatty acid that were observed in the experiment reported above.

The concentrations of vanillic acid and DOPAC added to the treatments were: vanillic acid (11 nmole Fe(II) per min, 0.10 mM), DOPAC (97 nmole Fe(II) per min, 0.10 mM). The concentration of wheat straw extracts added to the treatments was (26 nmole Fe(II) per min, 390 µg/mL). No blanks were run alongside of the treatments, so absorbance values are uncorrected for reagent absorbance. The results for linoleic acid are shown in Figure 3-30 and Figure 3-31, and for linolenic acid in Figure 3-32 and Figure 3-33.

The base case of Figure 3-30 (same data as the "+linoleic acid/Tween 20" treatment of Figure 3-27) is shown for comparison with the other treatments. Each iron reducing agent inhibited dye degradation compared to the base case. The cause may be that each iron reducing agent is a

competitive substrate for rMnP. In other words, rMnP oxidizes an iron reducing agent rather than the dye, thereby preventing some dye degradation.

Previous work has shown that certain phenolics can inhibit lipid peroxidation and degradation of a lignin model compound by MnP (Kapich, Galkin and Hatakka 2007). Benzoic acid derivatives with two ortho substituted hydroxyl groups (similar to DOPAC), or an ortho substituted methoxyl group and hydroxyl group (vanillic acid), or wheat straw extracts were most effective at inhibiting peroxidation and lignin model compound degradation, but the methoxyl group inhibited less. Surprisingly, substitutions of two ortho methoxyl groups, or one hydroxyl group, or no group on the benzoic acid structure did not substantially inhibit peroxidation or lignin model degradation. The benzoic acid derivatives may inhibit oxidation by serving as free radical scavengers or chelating the Mn(III) generated by MnP.

Of the degradation that did occur with iron reducing agents in the study presented here, the degradation extents agree in order of magnitude with the degradation extents of the "no Fe(III)" treatments in the study for detecting Fenton-based dye degradation (Figure 3-19): vanillic acid<DOPAC<wheat straw extracts. The similarity of order suggests that Fenton-based degradation is the only type of dye degradation occurring in these rMnP treatments with iron reducing agents.

A previous study found that the polyunsaturated lipid arachidonic acid was converted to a peroxyl radical by hydroxyl radical initiated hydrogen abstraction, where the hydroxyl radical was generated with a small amount of Fe(III) and hydrogen peroxide (Kapich, Jensen and Hammel 1999). In the "+ DOPAC + Fe(III)" treatment (Figure 3-30) the peroxyl radical of linoleic acid could have formed by the same process. But since negligible dye degradation occurred, the DOPAC likely inhibited peroxidation.

Addition of oxalate slightly decreased the initial rate of degradation but not the overall extent, and addition of Fe(III) had no effect. Surprisingly, the addition of malonate drastically increased the degradation rate and nearly completely degraded the dye (it should be noted that the increase in the absorbance of the "+malonate" treatment from ~200 minutes to ~1,100 minutes of reaction time was due to the formation of a suspension of fine white particulate of unknown identity).

In agreement with the degradation promotion by malonate observed here, a previous work has shown that relative to oxalate, malonate increased the ability of a system consisting of MnP and Tween 80 (an unsaturated non-ionic surfactant) to depolymerize milled pine wood, and there was greater degradation of the malonate than oxalate in the reaction mixture (Hofrichter, Lundell and Hatakka 2001). But contrary to the result found here, the addition of malonate in another study was found to inhibit degradation of a lignin model compound by an MnP/linoleic acid/Tween 20 system relative to no added chelator, presumably by reducing formation of lipid peroxyl radicals from linoleic acid (Kapich, Steffen, et al. 2005). The result of the milled pine wood study could be due to malonate supporting greater Mn(III) production by MnP, or either the extractives in the pine or the Tween 80 surfactant interacting with malonate in some way. It remains unknown why the results of the lignin model compound study would not have occurred in the study presented here on methylene blue degradation since the reaction conditions are similar. Further research is needed here.

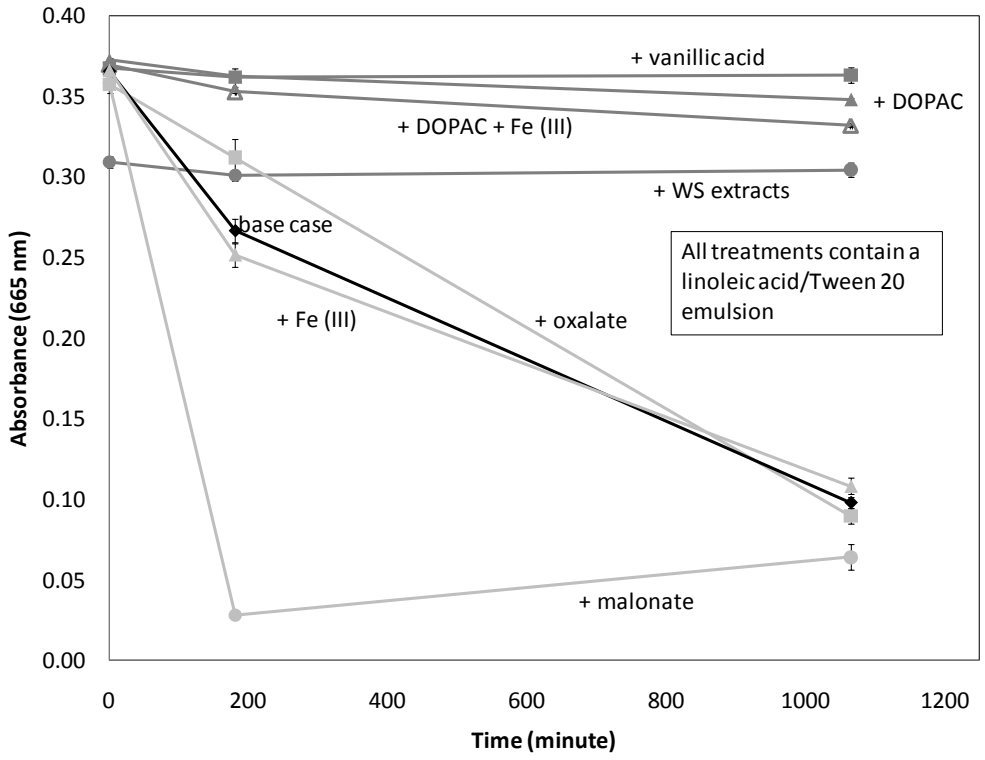

Figure 3-30: Screening for constituents that increase the rate of methylene blue degradation by linoleic acid/Tween 20/rMnP: absorbance over time. Absorbance values are uncorrected for reagent absorbance. Error bars are ±1 standard deviation of triplicate experiments completed simultaneously.

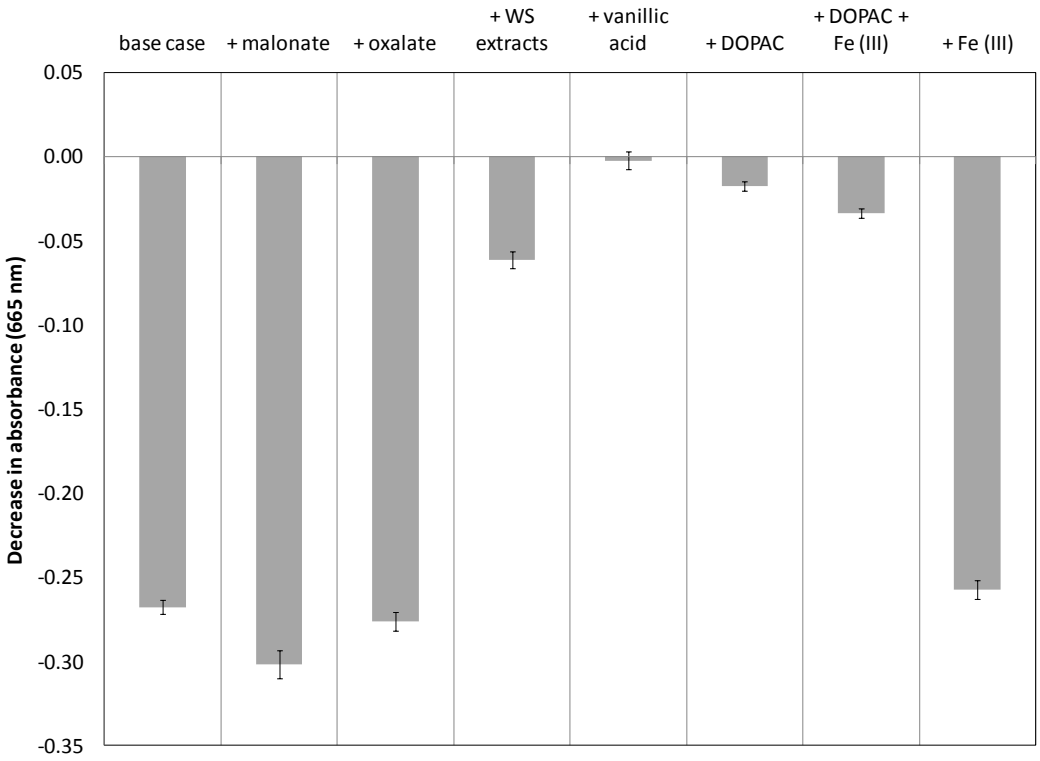

Figure 3-31: Screening for constituents that increase the rate of methylene blue degradation by linoleic acid/Tween 20/rMnP: overall decrease in absorbance. The graph shows the decrease in methylene blue absorbance 17.8 hours after addition of hydrogen peroxide relative to the absorbance of the base case 15 seconds after addition. Absorbance values are uncorrected for reagent absorbance. Error bars are ±1 standard deviation of triplicate experiments completed simultaneously.

The addition of the same set of reaction components to the linolenic acid base case gave results similar to the linoleic acid base case, except the dye absorbance did not decrease as rapidly with addition of oxalate or malonate (Figure 3-32 and Figure 3-33). The linolenic acid/Tween 20 emulsion used in this experiment had been previously frozen, and its turbidity was less initially than after thawing. The high turbidity is reflected in the high absorbance values of the treatments (~0.5 for the mixtures containing linolenic acid versus ~0.35 for the mixtures containing linoleic acid; compare Figure 3-30 and Figure 3-32). The slow loss of absorbance in the oxalate and malonate treatments may result only from the slow loss of fatty acid emulsion turbidity, or only dye degradation, or both. Dye degradation could be reduced due to the previously frozen emulsion affecting the kind or rate of interactions between the linolenic acid, enzyme, redox

mediators, and dye. In sum, the results do not permit confident conclusions about the effect of linolenic acid in the linolenic acid/Tween 20/rMnP system.

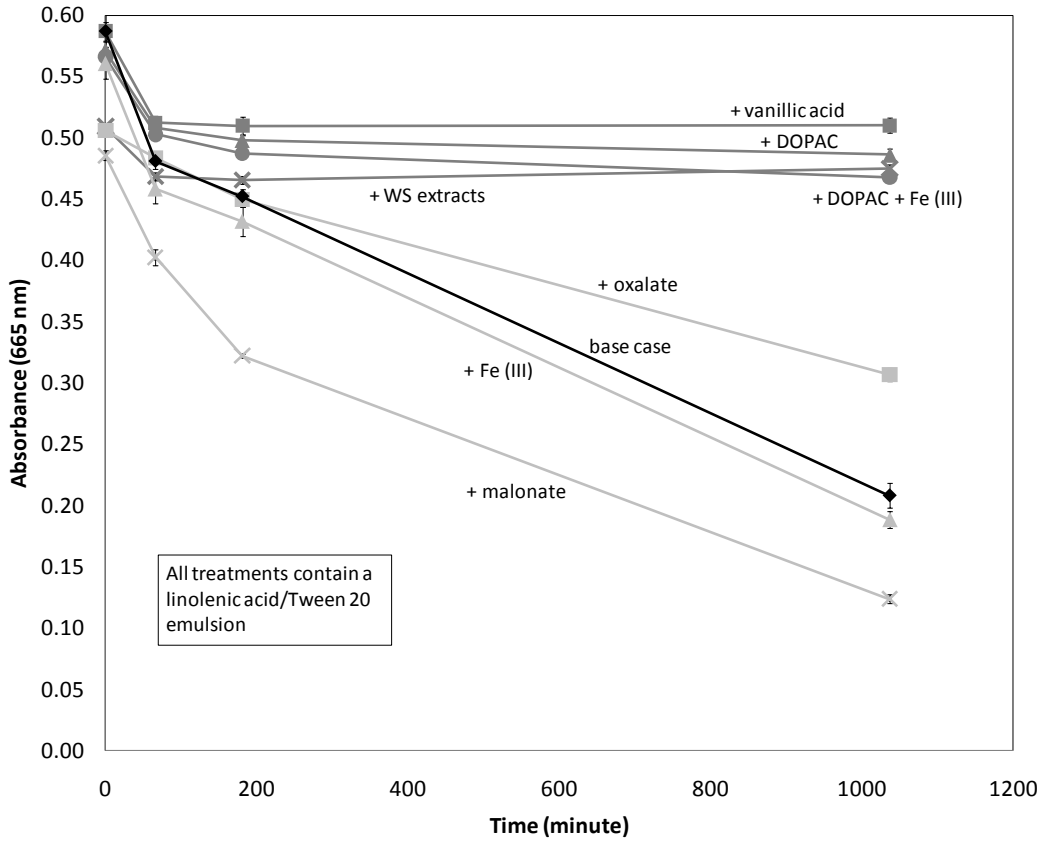

Figure 3-32: Screening for constituents that increase the rate of methylene blue degradation by linolenic acid/Tween 20/rMnP: absorbance over time. Absorbance values are uncorrected for reagent absorbance. Error bars are ±1 standard deviation of triplicate experiments completed simultaneously.

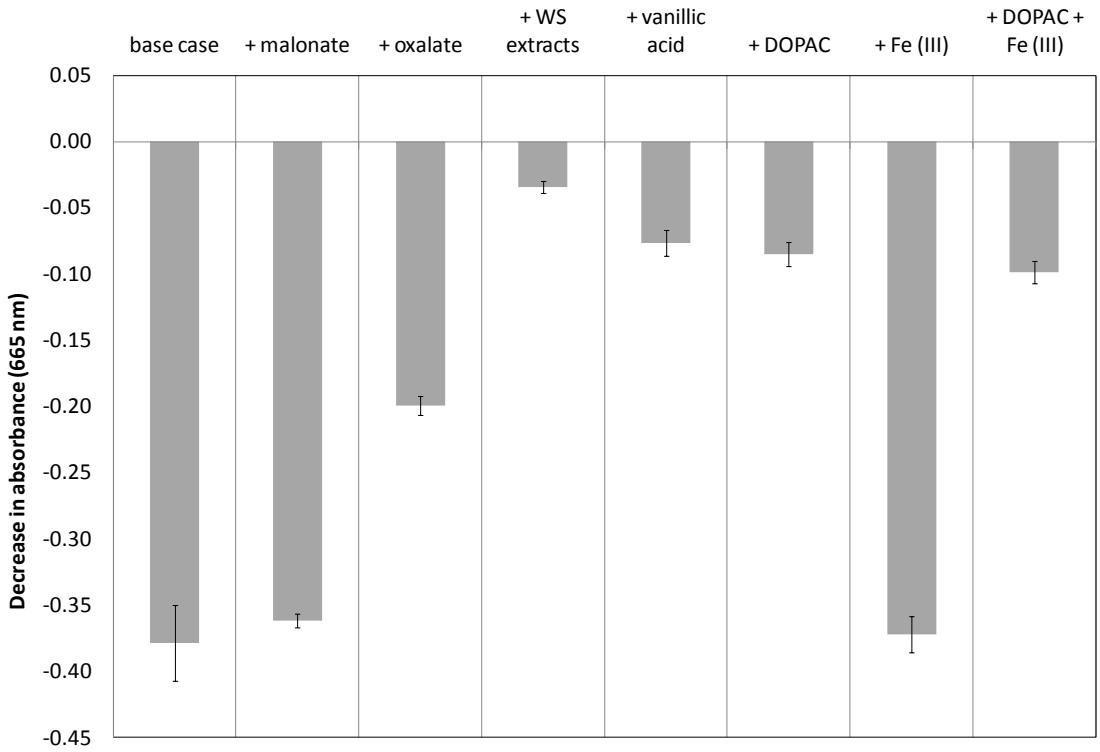

Figure 3-33: Screening for constituents that increase the rate of methylene blue degradation by linolenic acid/Tween 20/rMnP: overall decrease in absorbance. The graph shows the decrease in methylene blue absorbance 17.3 hours after addition of hydrogen peroxide relative to the absorbance 15 seconds after addition. Absorbance values are uncorrected for reagent absorbance. Error bars are ±1 standard deviation of triplicate experiments completed simultaneously.

3.5.7 Inferring the mechanism of methylene blue degradation by the linoleic acid/Tween 20/malonate/rMnP system

The rapid dye degradation by the linoleic acid/Tween 20/malonate/rMnP system led to a study in which individual reactions components were removed from the reaction system, replaced with distilled water, and absorbance monitored to help reveal the degradation mechanism. The base case in this study consisted of a linoleic acid/Tween 20 emulsion, malonate, rMnP, Mn(II), H_2O_2, acetate buffer, dye, and distilled water. The components removed included active rMnP, Mn(II), linoleic acid, Tween 20, H_2O_2, a combination of H_2O_2 and malonate, and acetate buffer.

Several important observations resulted from the experiment (Figure 3-34 and Figure 3-35). No degradation occurred with the inactive rMnP, and only limited degradation in the absence of Mn(II), thus indicating the importance of active rMnP and Mn(II) in dye degradation. Limited

degradation of other aromatic substrates in the absence of Mn(II) has been observed (Urzúa, Larrondo, et al. 1995), and may be due to the ability of the aromatic substrate to bind within the active site of the enzyme. The same process may have occurred here in the treatment without Mn(II).

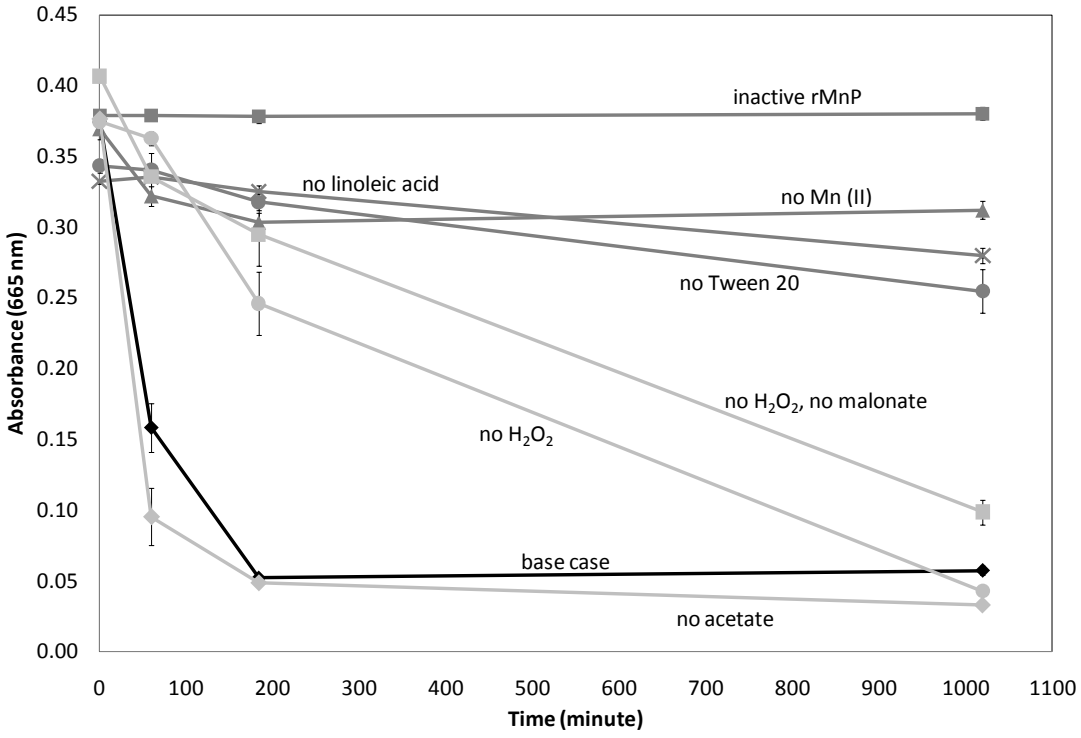

Figure 3-34: Effect of removing components from the linoleic acid/Tween 20/malonate/rMnP system (base case) on the degradation of methylene blue: absorbance over time. Absorbance values are uncorrected for reagent absorbance. Error bars are ±1 standard deviation of triplicate experiments completed simultaneously.

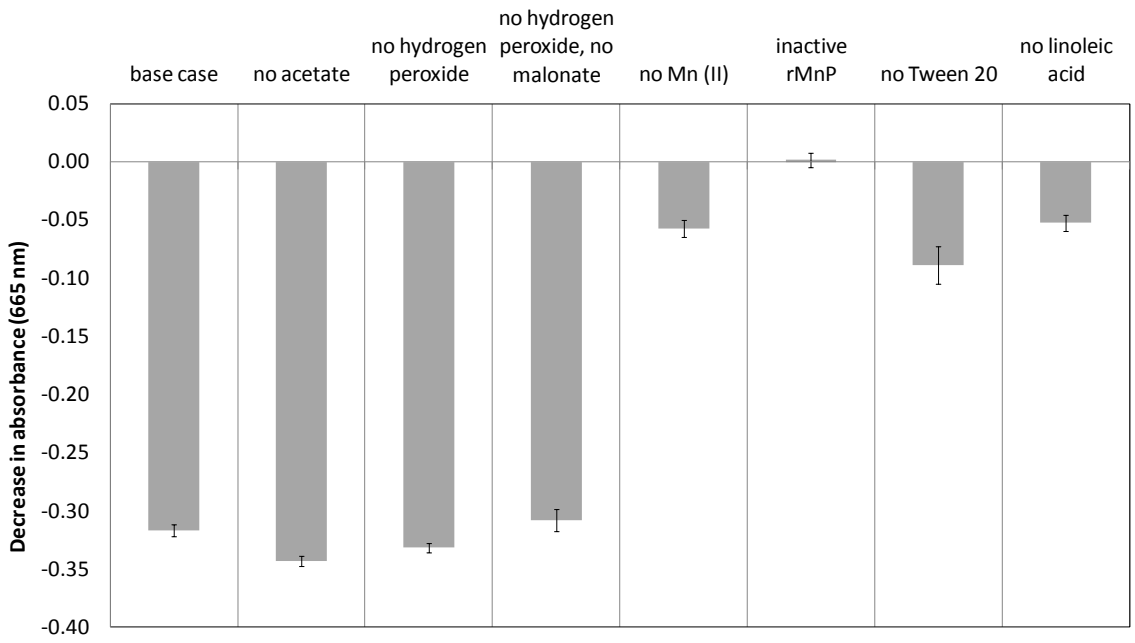

Figure 3-35: Effect of removing components from the linoleic acid/Tween 20/malonate/rMnP system (base case) on the degradation of methylene blue: overall decrease in absorbance. The graph shows the decrease in methylene blue absorbance (665 nm) 17 hours after addition of hydrogen peroxide relative to the absorbance 15 seconds after addition. Absorbance values are uncorrected for reagent absorbance. Error bars are ±1 standard deviation of triplicate experiments completed simultaneously.

Another observation is that the "no linoleic acid" treatment only mildly degraded the dye. This indicates the importance of linoleic acid in promoting dye degradation. Lipid peroxyl radicals are believed to be one of the agents primarily responsible for the degradation of lignin by MnP (Kapich, Jensen and Hammel 1999), so the linoleic acid present could have been converted to lipid peroxyl radicals which would then degrade the dye. The mechanism of peroxyl radical generation by Mn(III) is presented in Figure 3-36 and Figure 3-37 and proposed in Watanabe, Katayama, et al. (2000). The mechanism involves Mn(III) abstracting a hydrogen from the vicinal carbon of linoleic acid to form an alkyl radical. The alkyl radical could then abstract a labile *bis*-allylic hydrogen from another linoleic acid molecule. Addition of molecular oxygen to a stable conjugated resonance contributor results in the peroxyl radical of linoleic acid. Reduction by Mn(II) or hydrogen abstraction from the dye, another linoleic acid molecule, or another compound then results in the hydroperoxide of linoleic acid.

Direct abstraction of the *bis*-allylic hydrogen of linoleic acid by Mn(III) might be expected, but the Watanabe, Katayama, et al. (2000) study found that this did not occur; the hydrogen vicinal to the carboxyl group was abstracted instead. The effect may be due to the proximity of the vicinal hydrogens to the metallic center when the carboxyl group of linoleic acid coordinates around the Mn(III).

Hydrogen abstraction of the dye or another compound by the peroxyl radical of linoleic acid would result in the lipid peroxide (ROOH), as discussed. Organic peroxides can promote MnP turnover, and one may expect that the peroxide of linoleic acid would also, but the Watanabe et al. (2000) study found that the hydroperoxide of linoleic did not readily promote enzyme turnover in aqueous solution.

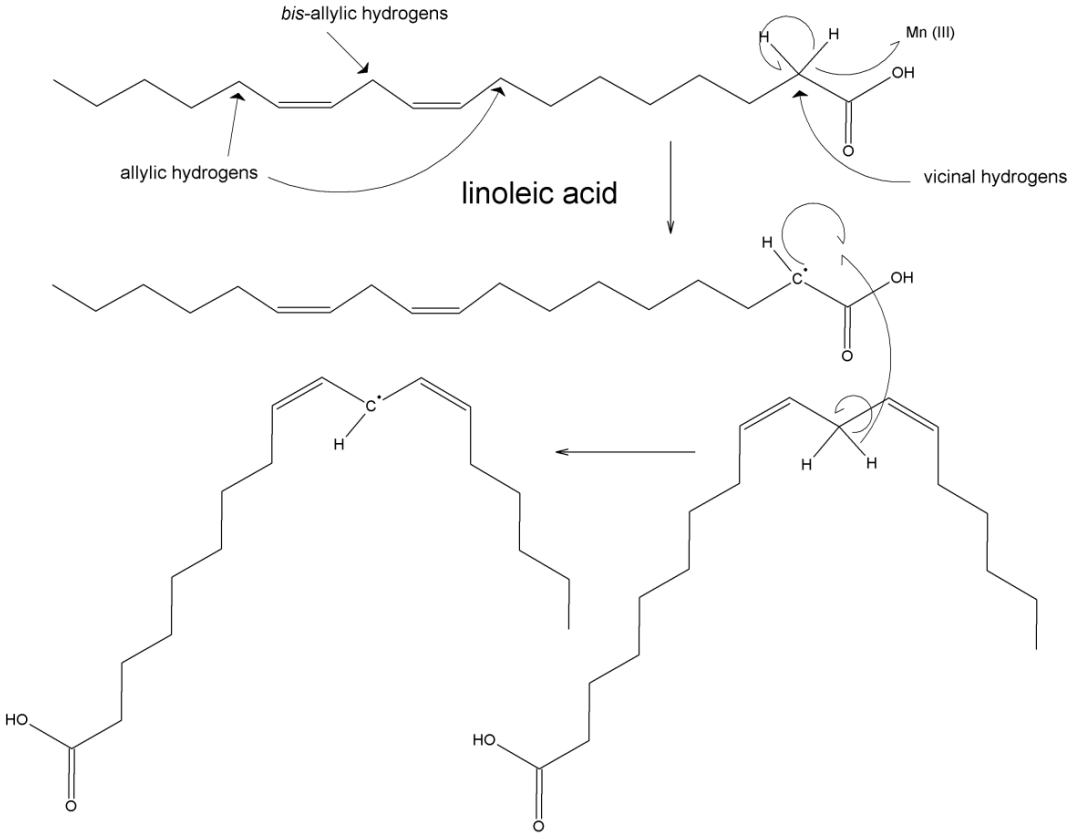

Figure 3-36: Part 1 of mechanism of formation of lipid peroxyl radical and lipid hydroperoxides from linoleic acid by Mn(III).

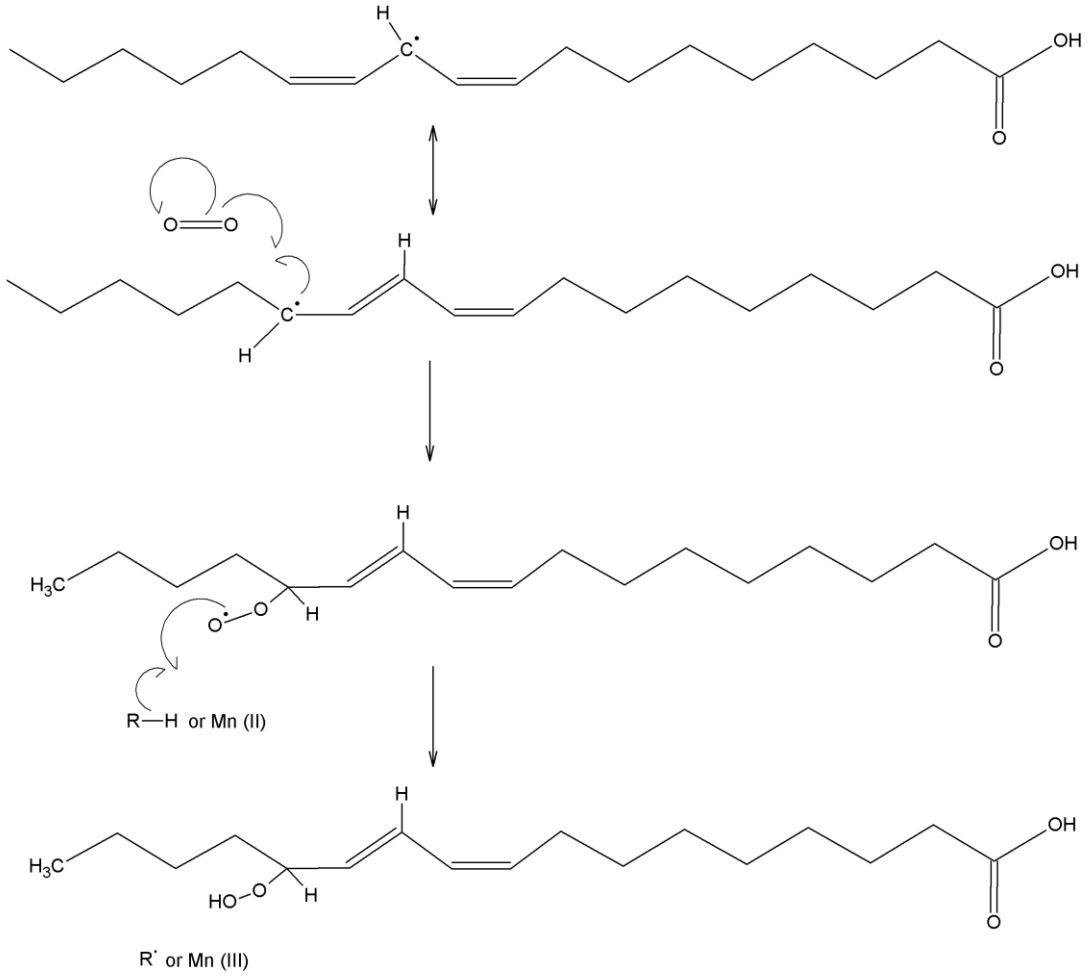

Figure 3-37: Part 2 of mechanism of formation of lipid peroxyl radical and lipid hydroperoxides from linoleic acid by Mn(III).

Interestingly, addition of linoleic acid emulsified without Tween 20 ("no Tween 20" treatment) was much less effective at degrading the dye than the linoleic acid emulsified with Tween 20 (base case). The greater dye degradation with the linoleic acid/Tween 20 emulsion may be due to the greater degree of peroxidation of linoleic acid that could occur. The greater peroxidation could occur because no linoleic acid remained phase-separated on the top of the reaction mixture (as was the case with the linoleic acid only treatment) or the average micelle size was smaller when emulsified with Tween 20. The lower turbidity of the linoleic acid emulsified with Tween 20 compared to without Tween 20 is evidence for a smaller micelle size (data not shown). The

smaller micelle size would increase the surface area over which Mn(III) chelates or other radical species could come into contact with linoleic acid and initiate peroxidation.

Another result of the study is that without the addition of exogenous H_2O_2 but in the presence of malonate (the "no H_2O_2" treatment), the degradation rate was slowed but the extent of degradation was similar to the treatment with added hydrogen peroxide (base case). Hydrogen peroxide or an organic peroxide is necessary for the MnP catalytic cycle, so what is the source of the peroxide? A previous study observed that an azo dye was degraded in the presence of MnP and malonate but without exogenous hydrogen peroxide (Harazono, Watanabe and Nakamura 2003). The authors hypothesized that autoxidation of a trace amount of Mn(II) to Mn(III) in the reaction mixture would initiate the degradation of malonate to the peroxides hydroperoxy acetic acid ($HOOCCH_2OOH$) and hydrogen peroxide (see equations [3] and [9] in Figure 3-38 for the mechanism of hydroperoxy acetic acid and hydrogen peroxide production, respectively). Since organic peroxides as well as hydrogen peroxide can oxidize MnP to Compound I, both of these peroxides could promote enzyme turnover and the production of more Mn(III). The produced Mn(III) would then initiate the degradation of more malonate and formation of more peroxides. Since two moles of Mn(III) are formed for every one mole of peroxide consumed, substantial concentrations of Mn(III) and peroxides would accumulate and allow the MnP system to function without an exogenous peroxide.

$$\text{COOH-CH}_2\text{-COOH} + \text{Mn(III)} \rightarrow \text{COOH-CH}_2^{\bullet} + \text{CO}_2 + \text{H}^+ + \text{Mn(II)} \quad (1)$$

$$\text{COOH-CH}_2^{\bullet} + \text{O}_2 \rightarrow \text{COOH-CH}_2\text{OO}^{\bullet} \quad (2)$$

$$\text{COOH-CH}_2\text{OO}^{\bullet} + \text{Mn(II)} + \text{H}^+ \rightarrow \text{COOH-CH}_2\text{OOH} + \text{Mn(III)} \quad (3)$$

$$\text{COOH-CH}_2\text{OOH} + 2\text{Mn(II)} \xrightarrow{\text{MnP}} \text{COOH-CHO} + \text{H}_2\text{O} + 2\text{Mn(III)} \quad (4)$$

$$\text{COOH-CH}_2\text{OO}^{\bullet} + \text{O}_2 \rightarrow \text{COOH-COOH} + \text{O}_2^{\bullet -} + \text{H}^+ \quad (5)$$

$$\text{COOH-CHO} + \text{Mn(III)} + \tfrac{1}{2}\text{O}_2 \rightarrow \text{HCOOH} + \text{CO}_2^{\bullet -} + \text{Mn(II)} \quad (6)$$

$$\text{COOH-COOH} + \text{Mn(III)} \rightarrow \text{CO}_2 + \text{CO}_2^{\bullet -} + \text{Mn(II)} \quad (7)$$

$$\text{CO}_2^{\bullet -} + \text{O}_2 \rightarrow \text{CO}_2 + \text{O}_2^{\bullet -} \quad (8)$$

$$\text{O}_2^{\bullet -} + \text{Mn(II)} + 2\text{H}^+ \rightarrow \text{H}_2\text{O}_2 + \text{Mn(III)} \quad (9)$$

$$\text{H}_2\text{O}_2 + \text{Mn(II)} \xrightarrow{\text{MnP}} \text{H}_2\text{O} + 2\text{Mn(III)} \quad (10)$$

Figure 3-38: Formation of hydroperoxy acetic acid (3) and hydrogen peroxide (9) from malonate degradation (Hofrichter, Ziegenhagen, et al. 1998).

The formation of multiple radicals species during malonate degradation by Mn(III) opens up the possibility that any of them could have helped form the peroxyl radical of linoleic acid which is likely responsible for some of the dye degradation. The radical species would have participated probably by abstracting directly the *bis*-allylic hydrogen from linoleic acid which leads to formation of the peroxyl radical. The radical species that may have participated include the alkyl radical of acetic acid ($CH_2^{\bullet}COOH$), hydroperoxyl acetic acid radical ($^{\bullet}OOCCH_2OOH$), hydroperoxyl radical ($^{\bullet}OOH$) derived from hydrogen abstraction by superoxide ($O_2^{\bullet -}$) or dismutation of superoxide. The format radical ($CO_2^{\bullet -}$) could have served a different role as reducing agent to form carbon dioxide.

These radical species could also have oxidized the dye by hydrogen or electron abstraction depending on their reduction potentials and half lives, and any radical species resulting from dye oxidation could also have become a hydrogen or electron abstracting agent. Over a series of radical chain reactions, the reduction potentials of the radical products would move towards lower values, as thermodynamics requires. Some carbon dioxide and water would form during the radical chain reactions, hence the term enzymatic combustion for degradation by lignin-degrading enzymes (Kirk and Farrell 1987). The chain reactions would terminate with radical-radical coupling, reduction or oxidation of metal species, or dismutation.

Another important result of the study was that the "no H_2O_2, no malonate" treatment containing no malonate also extensively degraded the dye. Without malonate, the routes proposed above for production of peroxides that could support enzyme turnover could not occur. As mentioned previously, the peroxide of linoleic acid also has not been shown to support enzyme turnover, so this is not a proven possibility. An explanation is that the reduction of molecular oxygen by degradation of peroxyl radicals (equation [5] of Figure 3-38 for example) would generate superoxide ($O_2^{\bullet -}$). Disproportionation of two superoxide anions, or reduction of superoxide by Mn(II) (equation [9] of Figure 3-38), would then produce hydrogen peroxide to support enzyme turnover (Watanabe, Katayama, et al. 2000).. This mechanism of supporting enzyme activity could also occur in the treatment with no hydrogen peroxide but with malonate (the "no H_2O_2" treatment).

Given that sodium acetate buffer was present in both the "no H_2O_2" and "no H_2O_2, no malonate" treatments, the hydroperoxyl acetic acid radical ($^{\bullet}OOCCH_2OOH$) could have formed through hydrogen abstraction of the vicinal hydrogen from acetate by Mn(III) or a peroxyl radical or other radical species, with subsequent addition of oxygen, instead of by malonate degradation. But this reaction is not expected to occur to a large extent since abstraction of a hydrogen from the electron poor vicinal carbon of acetate is thermodynamically undesirable.

To further elucidate the role of malonate and Mn(III) in dye degradation by the linoleic acid/Tween 20/malonate/rMnP system, absorbance over time of the base case of the previous experiment (base case shown in Figure 3-34) was compared against a treatment wherein a suspension of Mn(III) acetate was added in place of H_2O_2, Mn(II) sulfate, and rMnP. A similar treatment was also run where the Mn(III) acetate suspension was added in place of H_2O_2, Mn(II)

sulfate, rMnP, and malonate. In effect, the Mn(III) acetate replaced the enzymatic system for Mn(III) generation.

The results (Figure 3-39) show that the absorbance decreased similarly to the base case, thus providing further evidence that Mn(III) is involved in dye degradation. The "+ Mn(III)" treatment with malonate had a slightly higher degradation rate than the "+ Mn(III), no malonate" treatment. The enhanced degradation of the treatment with malonate may be due to two phenomena: (1) the malonate, as a manganese chelator, helped solubilize the Mn(III) after the insoluble Mn(III) acetate was added to the reaction mixture, or (2) the radical species generated by malonate degradation (most likely the hydroperoxyl acetic acid radical ($^{\bullet}OOCCH_2OOH$) or the hydroperoxyl radical ($^{\bullet}OOH$) since they are the most stable) contributed to dye degradation along with the peroxyl radical of linoleic acid.

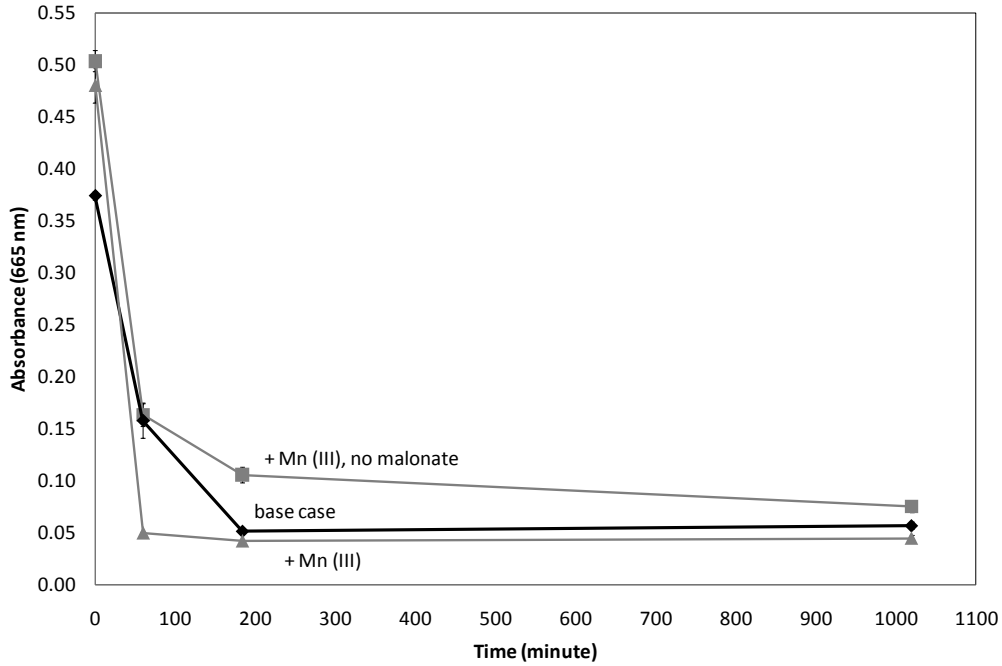

Figure 3-39: Effect of replacing the rMnP, hydrogen peroxide, and Mn(II) in the linoleic acid/Tween 20/malonate/rMnP system with Mn(III) acetate. For the base case, the time is from the addition of hydrogen peroxide. For the Mn(III) treatments, the time is from Mn(III) addition. Absorbance values are uncorrected for reagent absorbance. Error bars are ±1 standard deviation of triplicate experiments completed simultaneously.

If the second possibility was the predominant phenomenon, then the difference in degradation rates between the treatments with and without malonate roughly indicates the extra dye degrading ability of radicals derived from malonate degradation. Assuming the rate difference is due only to radicals from malonate degradation, then another process must be occurring to account for the dramatic increase in the rate of dye degradation observed when malonate was added to the linoleic acid/Tween 20/rMnP treatment (Figure 3-30). The faster rate with malonate may be due to the ability of malonate to chelate Mn(III) thereby facilitating its release from MnP and more rapid production by MnP (Wariishi, Valli and Gold 1992).

Dye degradation in the treatments without hydrogen peroxide, one with and the other without malonate, occurred at nearly the same rate (Figure 3-34). But based on the preceding argument that malonate enhances the ability of rMnP to produce chelated Mn(III), one would expect degradation in the treatment with malonate to occur more quickly. The explanation may be that the rate limiting step in the generation of the peroxyl radicals likely responsible for dye degradation may not be the release of Mn(III) from the enzyme but instead oxidation of enzyme from its native state to Compound I. This enzyme oxidation step may be slower because it depends on peroxides that are scarce because they are generated slowly *in situ* rather than added. Thus, the effect of malonate facilitating release and production of Mn(III) from the enzyme makes only a negligible difference in these two treatments. In comparison, the addition of malonate to the linoleic acid/Tween 20/rMnP base case of Figure 3-30 drastically increases the degradation rate because in these treatments the rate limiting step is the release of Mn(III) from the enzyme rather than enzyme turnover which occurs rapidly since there is abundant added hydrogen peroxide.

Another observation of the results in Figure 3-39 is that a Mn(III) concentration of only 0.5 mM degraded nearly all of the methylene blue (4.0 mM). This non-stoichiometric ratio is consistent with Mn(III) initiating a radical chain reaction between methylene blue molecules.

One last observation of the results in Figure 3-34 is that the rate of dye degradation without acetate buffer (“no acetate” treatment) appears slightly faster than with buffer (“base case” treatment). The explanation may be that acetate, as a ligand competing with malonate and linoleate for Mn(III), prevents the association of malonate or linoleate with Mn(III) and thereby

hinders their oxidation by Mn(III) to the precursors to the peroxyl radicals species likely responsible for dye degradation.

The same effect of one ligand competing with another ligand for coordination with Mn(III) may be responsible for the reduced oxygen consumption observed in Kapich et al. (2005) when different organic acids were added to a peroxidation system consisting linoleic acid/Tween 20, MnP, $MnSO_4$, and hydrogen peroxide (Figure 3-39). The Kapich et al. (2005) study found that the oxygen concentration quickly decreased when acetate was the only other organic acid present, but the presence of malonate or tartrate drastically reduced the rate of oxygen consumption. The effect can be explained by the fact that malonate and tartrate are bidentate ligands that bind tightly to Mn(III), thereby preventing association of the Mn(III) with the monodentate linoleic acid. Preventing formation of the Mn(III)-linoleic acid complex would prevent hydrogen abstraction and addition of oxygen to linoleic acid, thus reducing oxygen consumption. Comparatively, monodentate acetate does not bind as tightly and does not interfere as much with the association between linoleic acid and Mn(III).

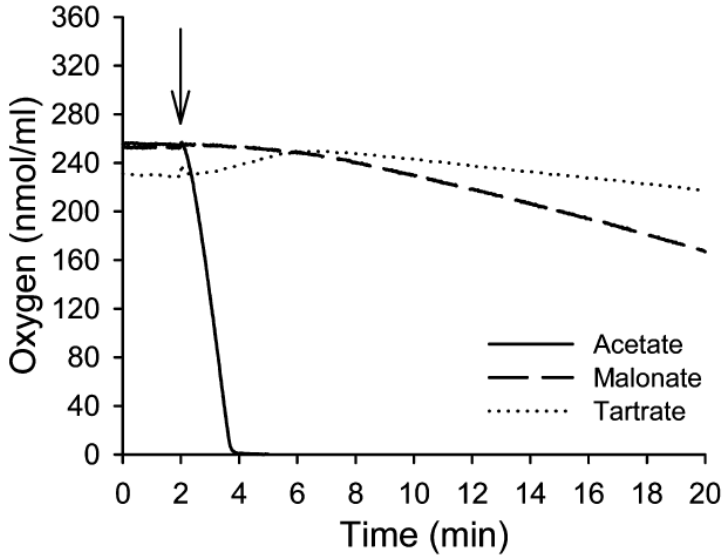

Figure 3-40: Influence of organic acids on oxygen consumption in a lipid peroxidation system consisting of linoleic acid, Tween 20, MnP, $MnSO_4$, and hydrogen peroxide (Kapich, Steffen, et al. 2005).

The above experiments answer the first hypothesis of the methylene blue experiments which was that an rMnP system would degrade the dye significantly only if the rMnP system contained a polyunsaturated fatty acid, and the degree of degradation would be greater with increasing unsaturation. The experiments have shown this to be true since the monounsaturated fatty acid, oleic acid, did not promote dye degradation, and oxalate and malonate only mildly encouraged dye degradation compared to the substantial degradation that occurred with the polyunsaturated fatty acid linoleic acid (Figure 3-27). The hypothesis was false in predicting that linolenic acid would promote more rapid degradation than linoleic acid; the actual result was that the rates were similar. These results do not allow prediction of what would occur with the same rMnP systems applied to solid lignin substrate.

3.5.8 Sequential Fenton and rMnP treatments of methylene blue

The next set of experiments tracked dye absorbance with sequential Fenton and rMnP treatments to test the second hypothesis, which was that substantial dye degradation will occur in an rMnP system missing unsaturated fatty acid only if the dye is first chemically altered by hydroxyl radicals generated by a Fenton treatment consisting of Fenton's reagent (Fe(III) and hydrogen peroxide) and an iron reducing agent. Another part of the hypothesis was that the lability of dye degradation would increase with increasing severity of the Fenton pretreatment as varied by iron reducing agent concentration.

The experiments involved performing the Fenton treatment with the two iron reducing agents DOPAC and wheat straw extracts, each at four concentrations—none, low, medium, and high—to test the effect of iron reducing agent type and concentration during the Fenton treatment on the ability of rMnP to degrade the dye during the rMnP treatment. The type of rMnP treatment chosen was the malonate/rMnP system which only mildly degraded the dye (Figure 3-27). The mild rMnP system was chosen so that any effect of Fenton treatment variation could be detected during the rMnP treatment whether that effect was degradation enhancement or inhibition. For each variation in Fenton treatment, the type of rMnP (active or inactive) was also varied to elucidate the effect of active enzyme on the dye. A limited set of treatments using only DOPAC at two levels (none and high) as the iron reducing agent and the linoleic acid/Tween 20/malonate/rMnP system was run to see if the effect of the iron reducing agent depended on the type of rMnP treatment.

The absorbance values shown in the results of these experiments were corrected in two ways. The first correction involved subtracting the absorbance of a blank reaction mixture containing all reaction components except methylene blue. The blank was run alongside each treatment and the absorbance measured at the same times as the treatment. To demonstrate the magnitude of blank absorbance, some examples are shown in Figure 3-41. Correcting for blank absorbance was most important for mixtures containing high DOPAC concentrations or lipid emulsions. The second correction involved reducing the original absorbance values recorded during the Fenton treatment proportionally to the dilution of methylene blue that occurred upon addition of the rMnP treatment components. This adjustment was made to eliminate changes in absorbance due only to dilution at the start of the rMnP treatment.

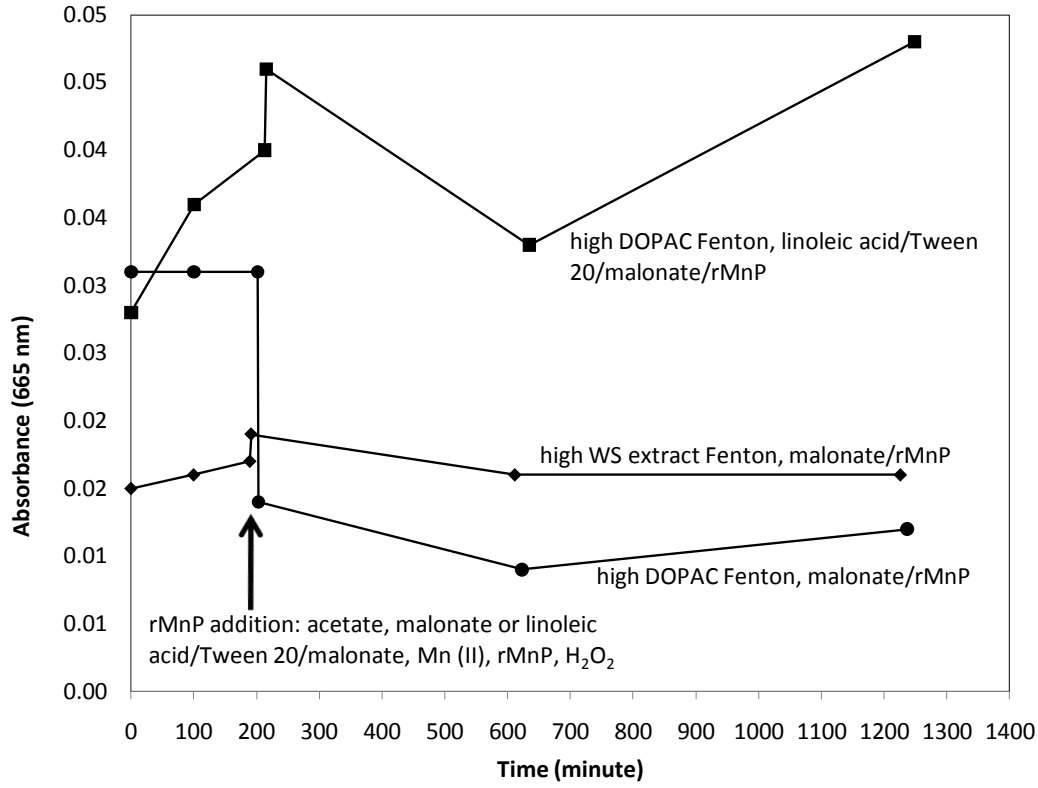

Figure 3-41: Blank absorbance of several reaction mixtures over time.

The effects of iron reducing agent type and concentration during the Fenton phase were already discussed in section 3.5.5. The effect of Fenton treatment on the rMnP degradation is discussed here.

Increasing wheat straw extracts concentrations during the Fenton treatment decreased the effectiveness of the malonate/rMnP treatment. This effect can be seen in Figure 3-42 by the diminished absorbance reduction during the rMnP phase with increasing extracts concentration. Some of the iron reducing agent in the extracts may remain unoxidized after the Fenton phase, thereby serving as a competitive substrate for enzymatic oxidation during the rMnP phase. The result is that remaining iron reducing agent is oxidized instead of the dye, thereby limiting dye degradation. The inhibition of rMnP dye degradation by wheat straw extracts is contrary to a study that found that pine extracts enhance degradation of a lignin model compound (Hofrichter, Lundell and Hatakka 2001) but consistent with a study showing that wheat straw extracts inhibited MnP-induced peroxidation of linoleic acid and degradation of a lignin model compound (Kapich, Galkin and Hatakka 2007). In the Kapich et a. (2007) study, the inhibition was purportedly due to catechol compounds serving as radical scavengers or manganese chelators.

Higher wheat straw extract concentrations during the Fenton treatment tended to cause the absorbance to increase as the rMnP treatment progressed when inactive enzyme was used. This observation cannot be explained readily, but one possibility is that a chemical species absorbing at 665 nm was generated by combining components remaining after Fenton treatment with the components added to initiate the rMnP treatment.

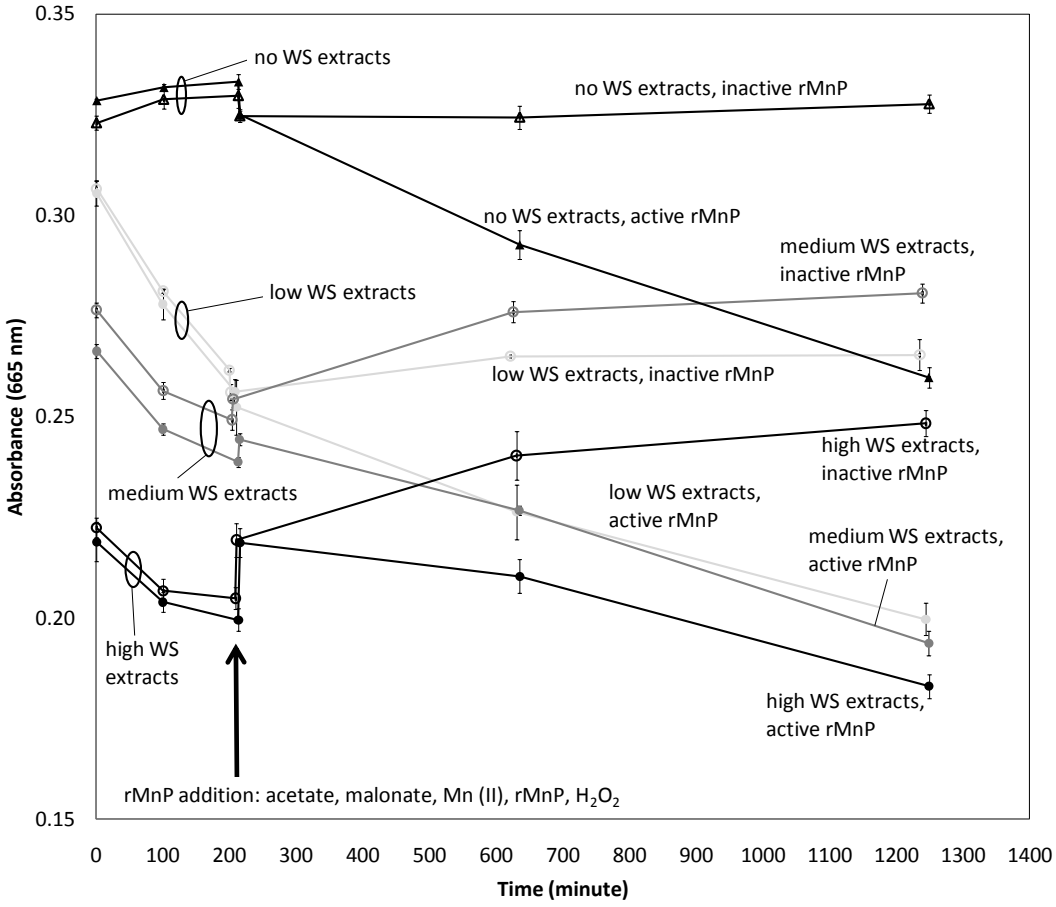

Figure 3-42: Combined wheat straw extracts Fenton and malonate/rMnP treatment for degrading methylene blue. Error bars are ±1 standard deviation of triplicate experiments completed simultaneously.

Increasing DOPAC concentration during the Fenton phase consistently decreased the effectiveness of degradation during the active rMnP phase (Figure 3-43). The explanation is the same as for wheat straw extracts. An interesting observation is the "high DOPAC, active rMnP" curve during the rMnP phase first increases in absorbance before decreasing. With the interpretation that unoxidized DOPAC serves as a competitive substrate for rMnP, the curve suggests that during the first part of the rMnP phase, active rMnP oxidized residual DOPAC while unknown processes occurred to increase the absorbance at 665 nm. Upon oxidizing a majority of the DOPAC about half through the rMnP phase, rMnP then began to oxidize the dye thus causing the absorbance at 665 nm to decrease.

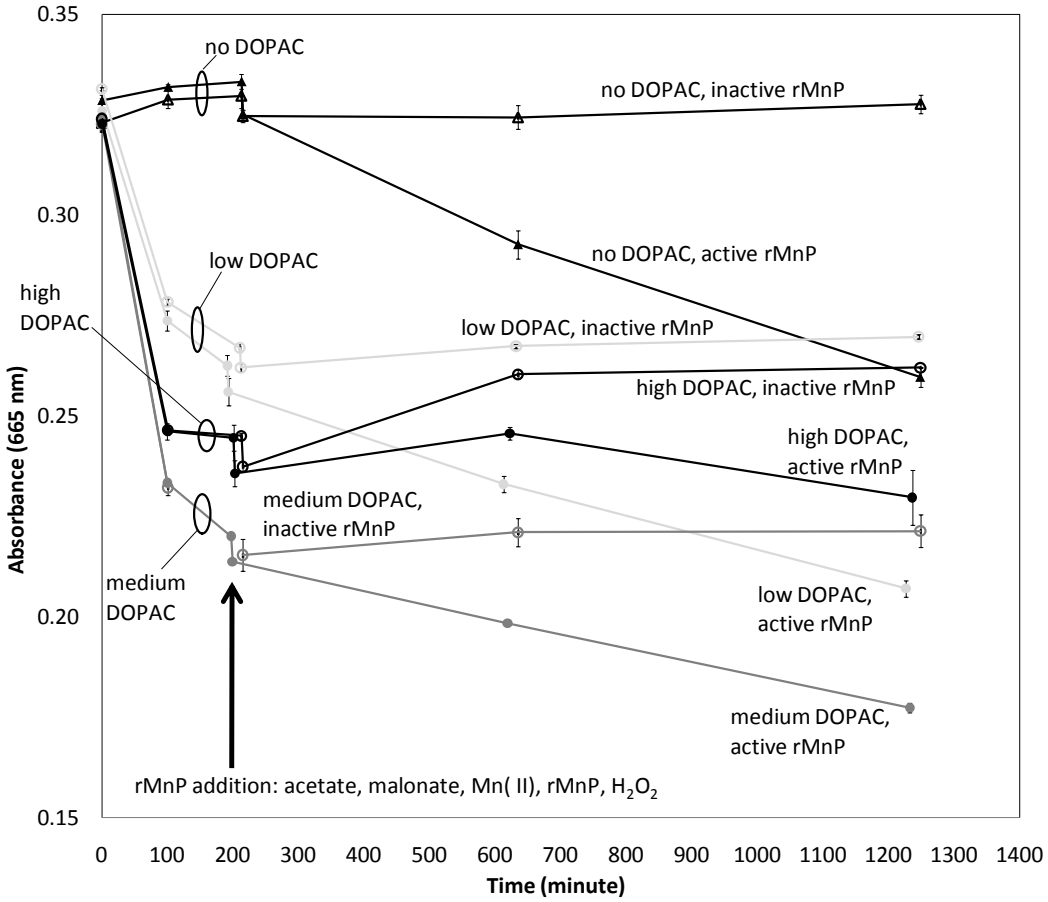

Figure 3-43: Combined DOPAC Fenton and malonate/rMnP treatments for degrading methylene blue. Error bars are ±1 standard deviation of triplicate experiments completed simultaneously.

The presence of DOPAC during the Fenton treatment also diminished degradation during the linoleic acid/Tween 20/malonate/rMnP treatment (Figure 3-44), just as in the malonate/rMnP system discussed above, although the percentage decrease was less than in the malonate/rMnP system (Figure 3-45). Thus, the more oxidative rMnP system was less affected by antioxidant DOPAC remaining after the Fenton treatment. The explanation for reduced rMnP degradation is the same as given previously.

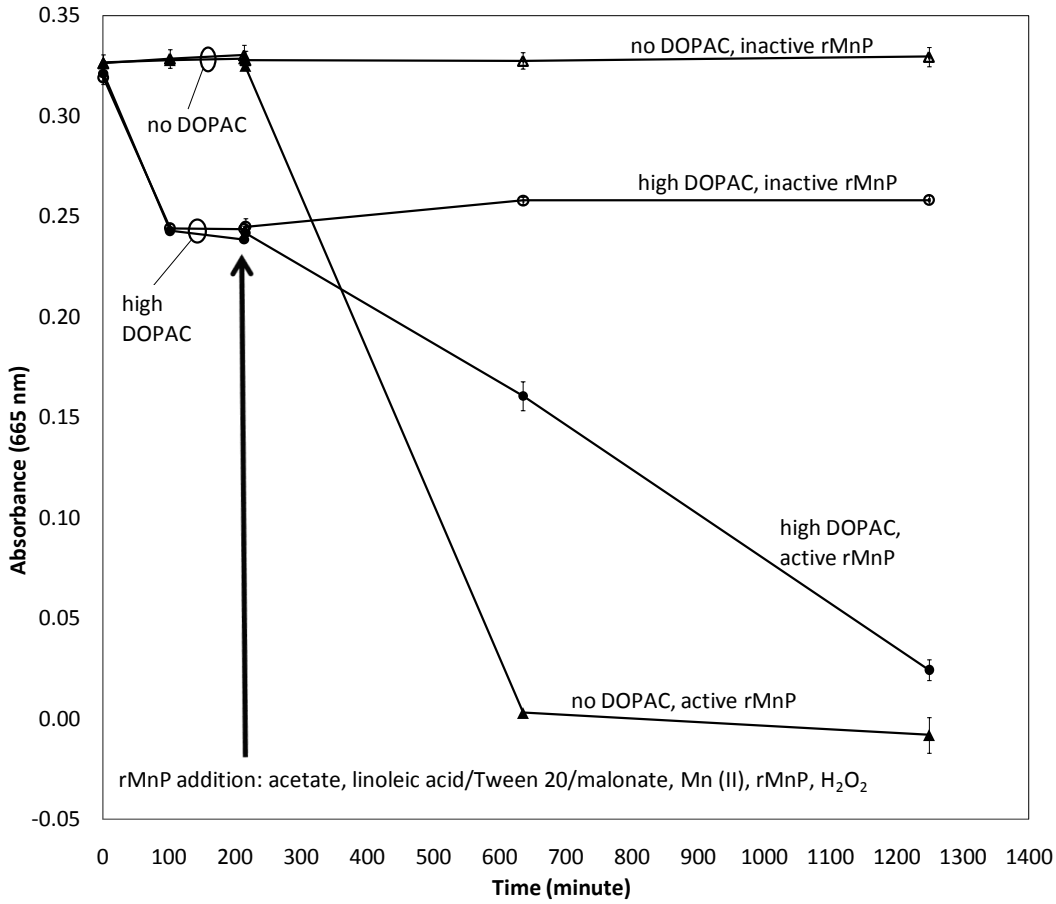

Figure 3-44: Combined DOPAC Fenton and linoleic acid/Tween 20/malonate/rMnP treatments for degrading methylene blue. Error bars are ±1 standard deviation of triplicate experiments completed simultaneously.

A summary of the overall dye degradation by iron reducing agent type and concentration is shown in Figure 3-45.

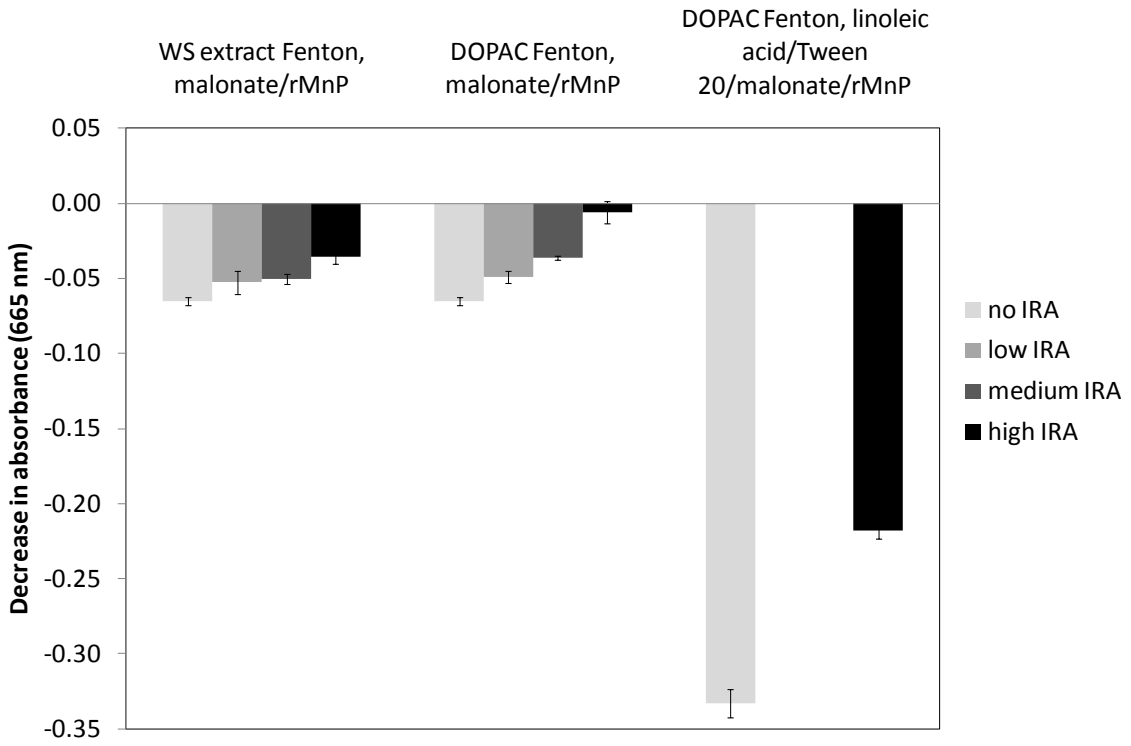

Figure 3-45: Decrease in methylene blue absorbance during malonate/rMnP and linoleic acid/Tween 20/malonate/rMnP degradation with different concentrations of the iron reducing agents (IRA) wheat straw extracts and DOPAC. The graph shows the decrease in absorbance from 15 seconds after hydrogen peroxide addition to the last absorbance reading at ~21 hours. All absorbance values are corrected for reagent absorbance. Error bars are ±1 standard deviation of triplicate experiments performed simultaneously.

The results of the study on combined Fenton and rMnP treatments neither prove nor disprove the second hypothesis, i.e. the results do not show that the malonate/rMnP system is capable of significantly degrading the dye only after a Fenton pretreatment, and they also do not show whether increasing the concentration of iron reducing agent affects the lability of the dye during rMnP degradation. The confounding factor lies in the likely possibility that unoxidized iron reducing agent remained after the Fenton treatment and was a competing substrate for the enzyme. Thus, it is possible that the dye was chemically altered during the Fenton phase and made more susceptible to oxidation during the rMnP phase, but it is impossible to know with certainty because the iron reducing agent served as a competitive substrate with the dye and therefore obscured any potential differences in the rMnP degradability of the dye. The results do now allow prediction of the result of the same treatment sequence (Fenton then rMnP) on a solid

lignin substrate, but the results do indicate that if iron reducing agents are used in a Fenton treatment of a solid substrate, they should be removed from the reaction solution and the solids washed before the rMnP treatment.

The results of the combined Fenton and rMnP treatments contrast to those of another study by Nadarajah et al. (2002) which found that Fenton pretreatment of the polycyclic aromatic compounds anthracene and benzo[a]pyrine before bacterial degradation of those compounds resulted in greater degradation than either treatment alone. Of course, the experiments presented here did not apply exactly the same kind of Fenton pretreatment in the Nadarajah et al. (2002) study to the methylene blue dye, nor did they employ bacterial treatments, but the results of the Nadarajah et al. (2002) study may provide valuable information about the direction of future research (Nadarajah, et al. 2002).

4 PREPARATION OF SOLID rMnP SUBSTRATES

4.1 Introduction

Lignin remaining after acid pretreatment (mild and severe) had to be made before the hypotheses related to solid substrates could be tested. Those hypotheses were stated in the Introduction and are equivalent to the hypotheses of the methylene blue experiments stated in Chapter 3.

Wheat straw was chosen as the substrate for rMnP transformation because it is an abundant agricultural product in the Pacific Northwest (Graf and Koehler 2000), it is more easily collected and transported to processing facilities than other materials, and the energy required to reduce it into particles small enough to serve as a biofuel feedstock is lower than other materials such as wood

Acid pretreatment of the wheat straw was chosen because it is one of the more likely pretreatment methods that may be employed in future biofuel industries (Mosier, et al. 2005). Severe and mild pretreatments were chosen to produce residual lignins that span the range of possible lignin types that would result from any degree of severity to the acid pretreatment. The severity of acid pretreatment can influence subsequent processing steps towards biofuel manufacture because the amount of nonspecific adsorption of cellulase enzymes onto lignin has previously been found to depend on whether the lignin had undergone mild or severe acid pretreatment (Meunier-Goddik and Penner 1999). The same phenomenon could occur with lignin transforming enzymes, thus emphasizing the importance of testing lignins produced under different conditions.

The acid insoluble lignin (Klason lignin) produced using the standard National Renewable Energy Laboratory (NREL) procedure for biomass composition analysis was chosen to represent the lignin after severe acid pretreatment. The material represents lignin after severe acid pretreatment because the determination of acid insoluble lignin involves hydrolysis of biomass with 72% (w/w) sulfuric acid for one hour, followed by hydrolysis by dilute sulfuric acid (3% w/w) in an autoclave for one hour. Nearly all extractives and sugars, and even some lignin (the acid soluble lignin component), are removed during the hydrolysis steps. The chemical structure of the remaining acid insoluble lignin is presumably severely altered from its original form.

The substrate chosen to represent dilute acid pretreatment involved treating wheat straw with 0.9 % (w/w) sulfuric acid at elevated temperature (~180 °C) for about one minute, then removing

the hemicellulose and cellulose by saccharification with a commercial cellulase mixture, and finally desorbing the cellulases from the substrate. The dilute concentration of sulfuric acid used, and the short duration of treatment, made the treatment extremely mild compared even to other mild pretreatments. During the mild treatment, only some extractives and hemicellulose sugars are removed, but more extractives, hemicellulose, and cellulose are removed by subsequent enzymatic saccharification. Substantial extractives, cellulose, and hemicellulose may remain in the biomass even after saccharification and desorption of the enzymes, so the end product is not pure lignin. The presence of remaining sugars and extractives is a drawback of using this substrate in a reaction with rMnP since the presence of those other components can complicate interpretation of results (e.g. rMnP could possibly adsorb to remaining cellulose and become inactive, thereby decreasing the active rMnP concentration in the reaction solution).

4.2 Processing and milling of wheat straw

Whole Stephens wheat plants were harvested from Hyslop Farm (Corvallis, Oregon) in 2004 and air dried for four years indoors at ~68 °F away from sunlight. Stem and leaves were collected from ~6 inches below the seed head to just above the first above-ground node without roots, the stems broken into pieces 4-8 inches long, and both the stems and leaves milled to pass a 2 mm screen (# 10 mesh) using a Thomas-Wiley knife mill model 4. The milled straw was thoroughly mixed and stored in four sealed jars at ~68 °F away from sunlight.

4.3 Particle size distribution of wheat straw

An Allen-Bradley sonic sifter (model L3P series A) was used to determine the particle size distribution of the milled wheat straw. From bottom to top, the sieve column consisted of weigh paper to collect the smallest particles, sieves #80, #60, #40, #30, #20, #10, and weigh paper to prevent particle loss from the #10 sieve upon which the sample was loaded. A 3.50 g quantity of milled wheat straw was placed on the #10 sieve and sieved with a vertical oscillating air column setting of 7 (out of 10) and a periodic vertical mechanical pulse amplitude of 5 (out of 10). The periodic vertical mechanical pulse was applied to the sieve column to break clustered particles formed by agglomeration.

To determine the amount of sifting time necessary to ensure a stable and accurate particle size distribution, the percent weight of each size fraction was measured over time (Figure 4-1).

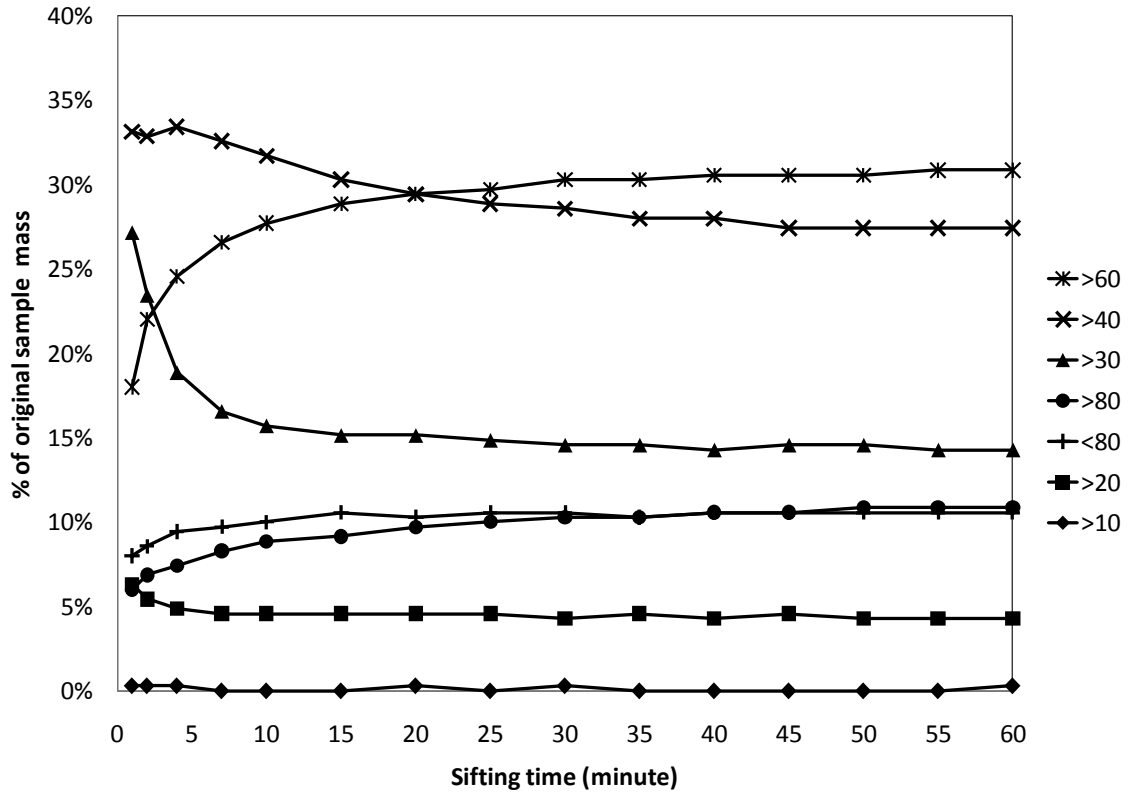

Figure 4-1: Percent weight by size fraction and sifting time for sifted milled wheat straw.

Figure 4-1 shows that 50 minutes of sifting was sufficient to reach a stable particle size distribution, but a few possible complications to using a 50 minute sieve test on milled wheat straw required verification.

One complication was that during the long sifting period, some particle sizes could have fallen from the sifting column more than other sizes, thereby biasing the resulting particle distribution. To show that mass loss was minimal during sifting, and therefore that no particular particle size was lost from the sieve column, the total weight of all particle sizes expressed as a percentage of the initial sample weight was plotted versus time (Figure 4-2). The result shows that negligible mass loss occurred during sifting.

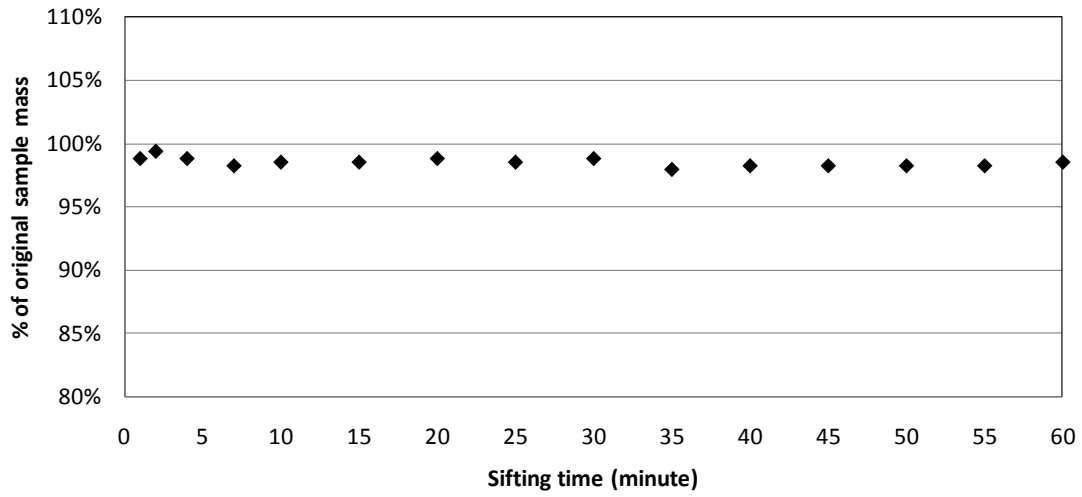

Figure 4-2: Total mass of sieved particles over time expressed as a percentage of initial sample weight.

Another complication was the possibility that a sifting duration of 50 minutes broke the milled straw particles into smaller particles, thereby biasing the results to smaller particle sizes. To test this hypothesis, all of the milled wheat straw available from the previous test was collected (3.49 g out of the original 3.50 g), placed again on the sieve column, and sieved for 4 minutes. The resulting 4-minute size distribution was compared against the original 4-minute size distribution (Figure 4-3).

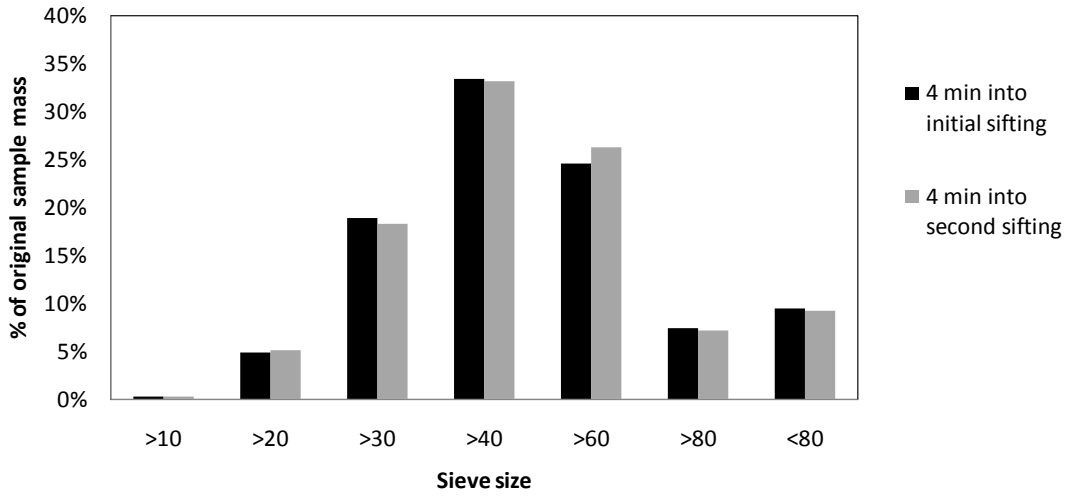

Figure 4-3: Comparison of particle size distribution between original sifted and re-sifted milled wheat straw.

The size distribution of the milled wheat straw was not substantially different after resifting, so it was assumed that particle size reduction did not occur during the extended sifting analysis.

Thus, the particle size distribution found during the initial 50 minute sifting was valid. For comparison, the size distribution of an independent second sample was determined after 50 minutes of sifting. The result of the second test is compared to the first test (Table 4-1 and Figure 4-4).

Table 4-1: Comparison of particle size distribution of two milled wheat straw samples.

	Percent of original sample mass by sieve fraction							
	>10	>20	>30	>40	>60	>80	<80	Total percent
sample 1	0.0%	4.3%	14.6%	27.4%	30.6%	10.9%	10.6%	98.3%
sample 2	0.0%	4.9%	15.7%	29.1%	30.9%	9.7%	8.0%	98.3%
Absolute difference	0.0%	0.6%	1.1%	1.7%	0.3%	1.1%	2.6%	0.0%
Mean	0.0%	4.6%	15.1%	28.3%	30.7%	10.3%	9.3%	98.3%

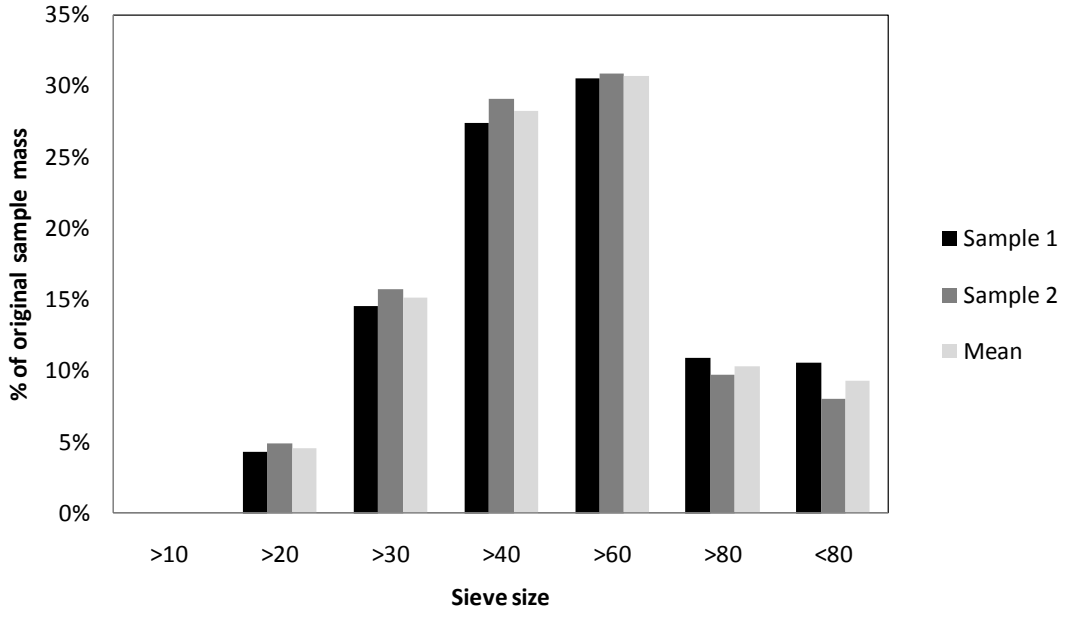

Figure 4-4: Particle size distribution of two milled wheat straw samples.

4.4 Preparation of severely acid treated substrate (acid insoluble lignin)

It was decided that the severely acid treated lignin substrate for rMnP would be the acid insoluble lignin resulting from compositional analysis of wheat straw using the standard methods of the National Renewable Energy Laboratory (Sluiter, Ruiz, et al. 2008); (A. Sluiter, B. Hames and r. Ruiz, et al. 2008).This substrate was chosen because it is simple to make and is well defined in composition.

Wheat straw was first extracted with distilled water for 24 hours, then with 95% (v/v) ethanol for 24 hours in a Soxhlet apparatus. The extracted wheat straw was then vacuum filtered with cellulose filter paper in a Buchner funnel, washed with ~100 mL of 95% (v/v) ethanol, and air

dried. The extracted air dried wheat straw was mixed with sulfuric acid in the ration of 1 g wheat straw per 10 mL 72% (w/w) sulfuric acid and incubated in a 30 °C water bath for one hour with occasional stirring. The solution was then transferred to an autoclave bottle, diluted with distilled water to a 4% (w/w) acid concentration, the bottle sealed, then autoclaved at 116 °C for 90 minutes. After cooling in the autoclave for 30 minutes, the bottle was removed and placed in ice. The solids in the hydrolysate were removed under vacuum with a medium porosity Gooch filter crucible, washed ≥3 times with ~10 mL distilled water, and air dried.

4.5 Preparation of mild acid treated substrate (saccharified pretreated wheat straw)

4.5.1 Pretreatment

Stainless steel pressure tubes (5/8" ID X 12" long) filled with a 5% (w/w) slurry of wheat straw in 0.9% (w/w) H_2SO_4 were placed in a basket and then inserted into 400 °C sand inside a Techne SBL-2D fluidized bath equipped with a Techne TC-8D temperature controller. The temperature of the slurry inside the tubes was estimated using a thermocouple sealed inside one of the pressure tubes containing an amount of water with the same thermal capacity as the slurry. When the temperature reached 180 °C, the basket containing the tubes was removed from the bath and placed on the floor for 1 minute. After 1 minute, the basket was placed inside a bucket of cold tap water for 30 seconds, then placed in a fresh bucket of cold tap water until the temperature no longer changed. The temperature of the tubes as indicated by the thermocouple is shown in Figure 4-5.

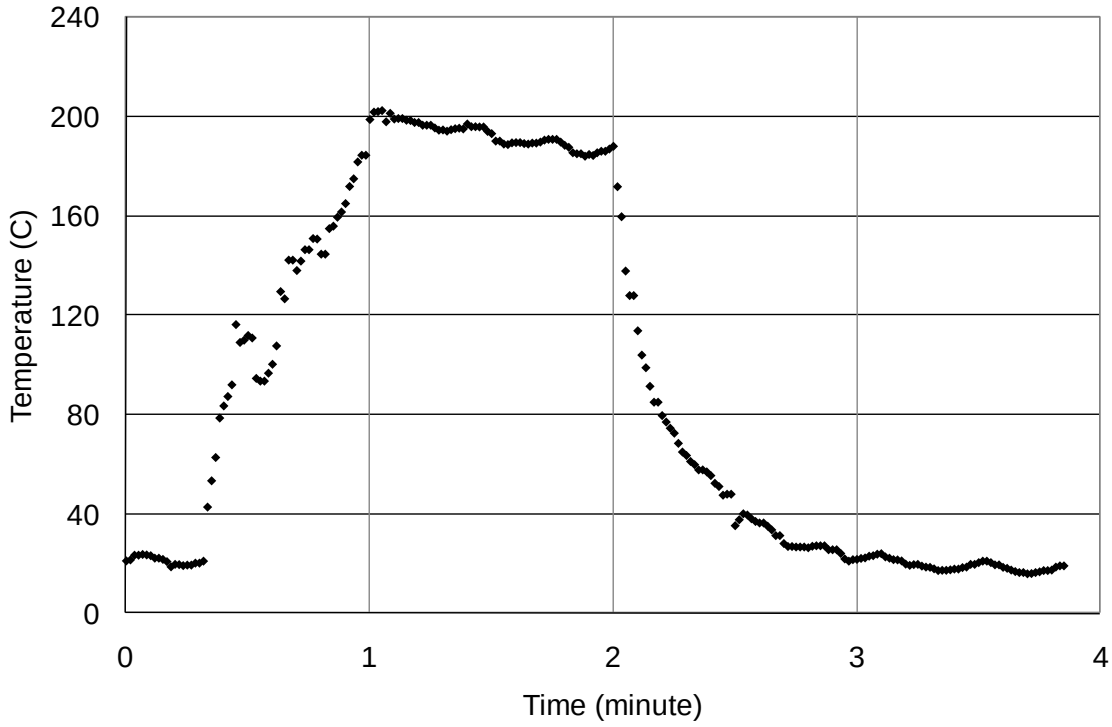

Figure 4-5: Temperature profile of interior of pretreatment tube.

After pretreatment, the slurry was vacuum filtered through a Fisher G8 glass fiber filter disc (2.5 µm pore size), and the solids washed until the filtrate pH was above 4.8. The 4.8 pH value was chosen in preparation for the next step which was enzymatic saccharification of the substrate in a solution buffered at pH 4.8. The solids were frozen moist and stored in freezer until saccharified with cellulase enzymes.

4.5.2 Enzymatic saccharification of pretreated wheat straw

It was desired to isolate the lignin remaining in the pretreated wheat straw by removing the polysaccharides without significantly altering the lignin chemical structure. To do so, the polysaccharides (cellulose and hemicellulose) remaining in the pretreated wheat straw had to be removed using a mild treatment. Enzymatic saccharification with cellulases was chosen since the low temperature of the saccharification process (50 °C) and the reaction medium (aqueous solution) would minimally alter the remaining lignin.

The enzymatic saccharification of the pretreated wheat straw was performed similarly to the standard NREL method (Selig, Weiss and Ji 2008). The saccharification was initiated by adding to an Erlenmeyer flask an amount of Accellerase 1000 (Genencor, lot 1600877126) equal to 44.5 FPU per gram cellulose to a solution containing 13.5 mg cellulose per mL (23.3 mg dry pretreated wheat straw per mL) and 50 mM sodium citrate buffered at pH 4.8. The cellulase activity of the Accellerase mixture was determined to be 60 FPU/mL using the standard NREL procedure (Adney and Baker 2008). The flask was stoppered and rotated at 170 rpm at 50 °C for 48 hours with periodic sampling of the slurry and the addition of more Accellerase at 24 hours at a dosage of 45.6 FPU per gram cellulose. Control flasks containing (1) pretreated wheat straw but no Accellerase, and (2) Accellerase but no pretreated wheat straw, were included for comparison of glucose production during the reaction.

It was necessary to measure the cellulose content of the remaining solids to know how much cellulose was removed enzymatically. It was also necessary to measure the nitrogen content to indicate the amount of cellulases remained adsorbed on the substrate. To accurately measure both the cellulose and nitrogen content, residual glucose and cellulases had to be washed from the solids. Maximum retention of solids during the washing process was desired to maximize yield, so centrifugal washing with distilled water was chosen, and eight washings were considered adequate to remove most free glucose and cellulases. Thus, the saccharified and control solids were washed with distilled water by centrifuging eight times in 50 mL polypropylene centrifuge tubes: each time the tubes were centrifuged at 2,020 rcf for 3-5 minutes, the supernatant removed, distilled water added, the contents shaken thoroughly, and the tube centrifuged again.

Some of the solids in the form of light brown particles did not pelletize during these washing steps and were therefore discarded along with the supernatant. To determine if the discarded particles could be removed from suspension, they were centrifuged at 16,100 rcf for 5 minutes in a microcentrifuge, upon which the particles pelletized. To determine the approximate size of the discarded particles, the supernatant was passed through filters of two different pore sizes. The particles passed through a 5 µm pore size woven nylon filter, but were retained on a 2.5 µm pore size Fisher G8 glass fiber filter, indicating the particles were between 2.5 and 5 µm in size.

The washed solids (saccharified and control) were filtered through a 0.45 µm polyetheresulfone membrane (Pall Supor), removed from the membrane, and frozen moist. The small pore membrane was used to prevent loss of smaller particles and to maximize yield.

4.5.3 Measuring glucose concentration in saccharification supernatant

The glucose concentration in the supernatant of all three treatments was measured over time to know when saccharification became limited. The glucose concentration in supernatant samples was determined using the glucose oxidase peroxidase assay (GOP) described in detail in Section 5.3.4. The results show that addition of more cellulase enzymes at 24 hours increased the glucose concentration, but that glucose levels remained relatively constant after ~40 hours (Figure 4-6). Both controls showed negligible glucose levels.

Saha, Iten, Cotta, & Wu (2005) found that pretreating wheat straw with 0.9% (w/w) sulfuric acid for 15 minutes at 180 °C followed by enzymatic saccharification for 72 hours yielded 375 mg glucose per g of dry wheat straw. The saccharification presented here yielded 220 mg glucose per g dry wheat straw. The lower value found here is understandable given that this value does not take into account the amount of glucose, if any, evolved during the dilute acid pretreatment, and the saccharification period used here was 48 hours instead of 72 hours.

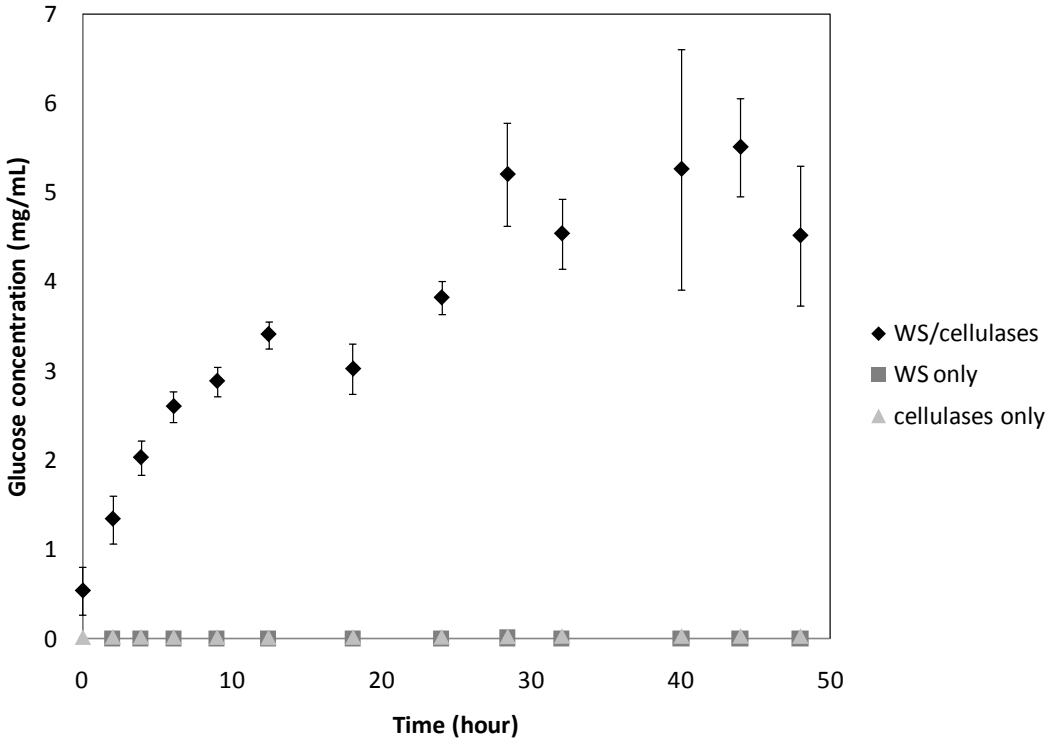

Figure 4-6: Glucose concentration versus time in saccharification supernatant of pretreated wheat straw and controls. WS=wheat straw. Error bars are ±1 standard deviation of triplicate glucose assays performed simultaneously.

The resulting solids still contained cellulose (glucan content in Table 4-2), but no further saccharification of cellulose was possible under the given reaction conditions, possibly because lignin sterically hindered further saccharification of cellulose or there was non-productive cellulase adsorption onto cellulose. The original intention of saccharification was to remove all cellulose and produce a pure lignin product upon which rMnP could act, but the residual cellulose in the substrate provided the unanticipated opportunity to see if rMnP action upon the substrate could affect the rate at which cellulases saccharify the remaining cellulose. The test would involve comparing glucose evolution in a treatment with both rMnP and cellulases to treatments containing only one of either enzyme. The enzyme rMnP could possibly affect cellulose saccharification by removing lignin that sterically hinders cellulase access to the cellulose in the substrate. Such an experiment was completed (Section 5.2). But before the substrate was suitable for the experiment, the potentially interfering adsorbed cellulases were desorbed (see next section).

Table 4-2: Composition of milled wheat straw (WS), dilute acid pretreated WS, and dilute acid pretreated/saccharified WS. All values are percent of mass of dry solids. Standard deviation values are of triplicate measurements completed simultaneously. HPLC=high performance liquid chromatography, GOP=glucose oxidase/horseradish peroxidase glucose assay, DW=distilled water.

Sample	Milled WS (trial 1)	Standard deviation	Milled WS (trial 2)	Standard deviation	Dilute acid pretreated WS	Standard deviation	Dilute acid pretreated/ saccharified WS (DW washed)	Standard deviation	Dilute acid pretreated/ saccharified WS (DW washed and desorbed)	Standard deviation	Note on values for Dilute acid pretreated/ saccharified WS (DW washed)
Total glycan	53.2%	4.3%	99.2%	NA	97.9%	2.4%					
Glucan (HPLC)	37.7%	2.8%	66.0%	NA	77.8%	2.2%					
Glucan (GOP)					58.3%	5.2%	67.1%	1.5%			
Glucan (subtracting supernatant GOP)							38.6%	NA			
Xylan (HPLC)	12.8%	2.7%	25.6%	NA	17.8%	0.7%					
Galactan (HPLC)	0.0%	0.0%	0.0%	NA	0.0%	0.0%					
Arabinan (HPLC)	2.7%	1.9%	6.6%	NA	2.2%	0.7%					
Mannan (HPLC)	0.0%	0.0%	1.0%	NA	0.1%	0.1%					
Ash	5.0%	0.3%	5.3%	0.2%	4.5%	0.2%	4.6%	0.1%			determined without prior extraction
Extractives	14.3%	2.0%	12.2%	1.4%	13.0%	4.4%					
Acid soluble lignin (240 nm)	2.6%	0.1%	3.3%	0.3%	2.3%	0.0%	3.1%	0.2%			determined without prior extraction
Acid insoluble lignin	13.7%	0.3%	14.4%	0.7%	15.1%	0.8%	28.5%	0.5%			determined without prior extraction
Total	88.8%	4.8%	134.5%	NA	132.7%	5.1%					
Nitrogen	0.2%	0.0%			0.2%	0.0%	12.3%	0.6%	3.1%	0.8%	

4.5.4 Cellulase desorption

Cellulase enzymes adsorbed to the saccharified wheat straw could potentially interfere sterically with rMnP transformation of the wheat straw. Thus, the enzyme was desorbed from the saccharified wheat straw with sodium dodecyl sulfate (SDS) similarly to the method of Hing, Ye, & Zhang (2007). A solution of 1.1% SDS (w/v) was mixed with the damp saccharified wheat straw in an Erlenmeyer flask in a ratio of 20 mL to 0.1 g dry solids, then orbitally mixed at 170 rpm at 40 °C for 4 hours. The temperature was kept at 40 °C instead of 80 °C as in Hing, Ye, & Zhang (2007) to minimize possible changes to the chemical structure of the substrate. The solids were transferred to 50 mL polypropylene centrifuge tubes, centrifuged at 2,130 rcf for 5 minutes, and the supernatant discarded. The solids were then washed three times with a 75% ethanol (v/v), each time by filling the tubes with the solution, shaking thoroughly, centrifuging at 7,700 rcf for 7 minutes, and decanting the supernatant. The solids were then washed six times with distilled water, each time by filling the tubes with distilled water, shaking thoroughly, centrifuging at 2,140 rcf for 5 minutes, and decanting the supernatant. The resulting solids were vacuum filtered over a 0.45 µm pore size polypropylene membrane (Sterlitech) and then stored frozen in moist form. The wheat straw from the saccharification control treatment that contained wheat straw but no cellulase enzymes was also processed similarly to serve as a baseline for subsequent nitrogen measurements.

4.5.5 Re-saccharification of pretreated wheat straw

It was initially hoped that the desorbed saccharified wheat straw could not be further saccharified with cellulase enzymes so that any glucose generated during the simultaneous treatment of the wheat straw with rMnP and cellulases would be due to synergy between the two enzyme types and not just cellulases acting upon remaining cellulose. Thus, saccharification of the solids was performed again by following a procedure similar to the standard NREL method (Selig, Weiss and Ji 2008). The saccharification was initiated by adding to a scintillation vial an amount of Accellerase 1000 (Genencor, lot 1600877126) equal to 37 FPU per gram cellulose to a solution containing 16.1 mg cellulose per mL (41.7 mg dry pretreated wheat straw per mL) and 50 mM sodium acetate buffered at pH 4.8. The cellulase activity of the Accellerase mixture was determined to be 60 FPU/mL using the standard NREL procedure (Adney and Baker 2008). The scintillation vial was capped and inversion rotated at 8 rpm at 50 °C for ~7 hours with periodic

sampling. Leakage of reaction liquid from the scintillation vial after ~7 hours of reaction time necessitated the transfer of the reaction slurry to a 15 mL polypropylene centrifuge tube and the addition of the same amounts of acetate buffer and Accellerase as were initially added. The reaction continued for another 17 hours with periodic sampling. A control treatment containing Accellerase but no pretreated wheat straw was included alongside the treatment containing Accellerase and wheat straw.

The glucose concentration in the reaction supernatant over time was determined with the GOP assay described in Section 5.3.4. The results, shown in Figure 4-7, show the lag in glucose generation at the 10 hr and 17 hr sampling times due to having added new reaction liquids at ~7 hours so that glucose had not had time to accumulate. But the 24 hr sampling point clearly indicates that the wheat straw that had already been saccharified and desorbed of cellulases was capable of further saccharification. Thus, any glucose generation during the experiment where the substrate was simultaneously exposed to cellulases and rMnP could not be attributed only to some form of synergy between the enzyme types, but could also be due just to the cellulases acting upon the substrate.

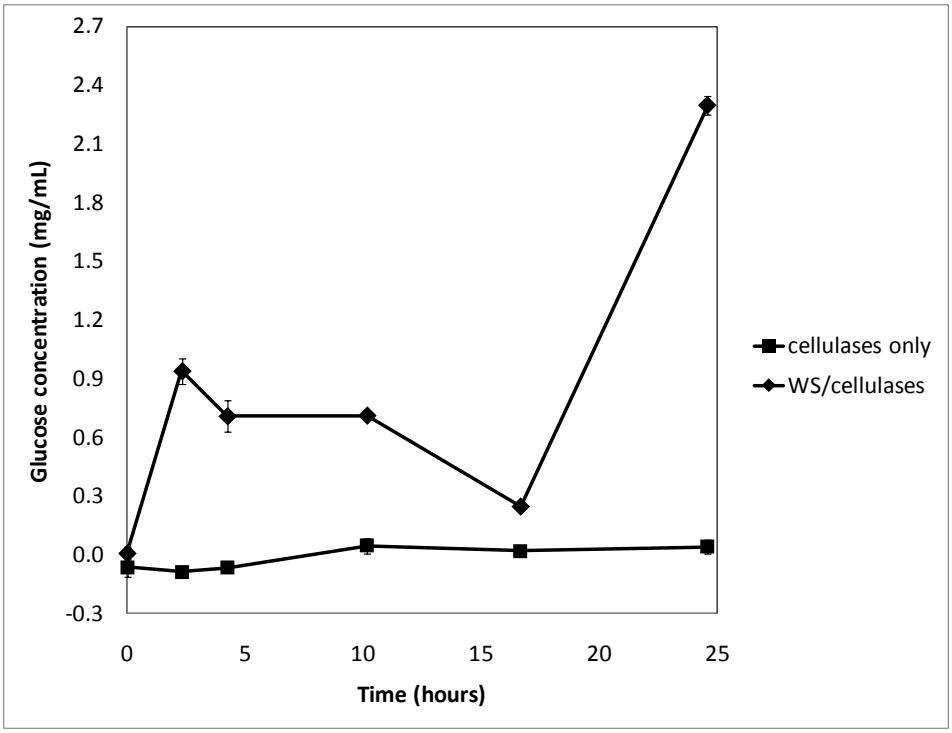

Figure 4-7: Glucose concentration versus time in the saccharification supernatant of wheat straw that had already been saccharified and the cellulases desorbed. WS=wheat straw. The error bars are ±1 standard deviation of triplicate glucose assays performed simultaneously.

4.5.6 Yield of mild acid treated substrate

Mass yields for each step in the production of mild acid treated wheat straw were recorded and are shown in Table 4-3 along with the overall yield based on the starting mass of milled wheat straw.

Table 4-3: Yield of pretreated, saccharified, and desorbed substrate by step and by mass of initial amount of milled wheat straw.

Step	**yield within step**	**yield after step as percent of starting mass of milled wheat straw**
dilute acid pretreatment	57.3%	57.3%
enzymatic saccharification	69.2%	39.7%
cellulase desorption	76.8%	30.5%

4.6 Chemical composition of biomass samples

4.6.1 Methods

4.6.1.1 Milled wheat straw

With minor variation the chemical composition of the milled wheat straw was determined according to the standard laboratory analytical procedures of the National Renewable Energy Laboratory (NREL) (Sluiter, Hames and Hyman, et al. 2008); (Sluiter, Ruiz, et al. 2008); (Hames, et al. 2008); (A. Sluiter, B. Hames and R. Ruiz, et al. 2008). To analyze for polysaccharide content of wheat straw using high performance liquid chromatography (HPLC), a Biorad Aminex HPX-87P column was heated to 80 °C, and an Agilent G1362A or Waters 410 refractive index detector was used. Polysaccharide composition values determined using HPLC are labeled as such in the summary of composition values (Table 4-2).

The substantive variation from the NREL procedures was that all particle sizes of the milled wheat straw were included in the chemical analysis instead of the NREL recommendation of using particles greater than 80 mesh (0.177 mm) and smaller than 20 mesh (0.841 mm) (Hames, et al. 2008). The absorbance at 240 nm and the extinction coefficient for bagasse (ε=25 L-g^{-1}-cm^{-1}) were used to determine acid soluble lignin because the resulting total lignin content more closely matches prior literature values.

4.6.1.2 Dilute acid pretreated wheat straw

The chemical composition of pretreated wheat straw was determined to know the effects of pretreatment, especially on lignin and xylose content. Its composition was determined in the same way as for milled wheat straw. The glucan (cellulose) content was determined also using the GOP assay to compare with HPLC values and to rapidly know the appropriate amount of cellulases to add for enzymatic saccharification. The glucose oxidase/horseradish peroxidase glucose (GOP) assay was performed on the $CaCO_3$ neutralized acid hydrolysate of extracted biomass samples, like the standard HPLC polysaccharide analysis in the NREL procedure. The assay was performed on the hydrolysate in microplates according to the GOP assay as described in detail in Section 5.3.4. Glucan composition values determined using the GOP assay are labeled as such in the summary of composition values (Table 4-2).

4.6.1.3 Saccharified pretreated wheat straw

The lignin, ash, and glucan content of the saccharified pretreated wheat straw were determined. The glucan (cellulose) content was important to know to what degree saccharification removed cellulose. The lignin and ash contents were determined like for the milled wheat straw except the samples were not extracted beforehand. The glucan content was determined using two methods. The first was using the GOP assay as was used to determine glucan of the pretreated wheat straw except the solids were dried at 44 °C instead of air dried before acid hydrolysis. The second method involved subtracting the end glucose concentration in the saccharification reaction supernatant, as determined with the GOP assay, from the cellulose content of the pretreated wheat straw before saccharification. The net glucan is the amount of cellulose remaining in the substrate after saccharification. Cellulose content measured using the subtractive method is labeled as "subtracting supernatant GOP".

4.6.1.4 Nitrogen content of biomass

The nitrogen content of all biomass samples was measured to indicate native protein content in the wheat straw and the degree to which cellulase enzymes remained adsorbed onto wheat straw after enzymatic saccharification. A Costech ECS 4010 CHNSO Analyzer was used in semi-micro mode to measure samples dried at 105 °C. Acetanilide or atropine was used as nitrogen standard. The instrument combusts a sample and separates the resulting combustion gases through a gas chromatography column to determine the amount of an element present in the sample.

4.6.1.5 Effect on biomass composition of analyzing all particle sizes

4.6.1.5.1 General discussion

It was mentioned previously that all particle sizes of the milled, pretreated, and saccharified wheat straw were included for compositional analysis. The alternative is to analyze only the -20/+80 size particles, as is recommended in the standard NREL protocol (Hames, et al. 2008). In the standard protocol, the weight fraction of a constituent (e.g. lignin) in the original unfractionated wheat straw is then determined by summing the weight fraction of the constituent in the -20/+80 size particles with the weight fraction in the -80 size particles adjusted by the difference in ash content between the two particle size classes. With this method, it is assumed that the chemical composition of the non-ash part of the two size classes is the same.

Correcting for the difference in ash content between the two size classes prevents over-estimation of a constituent, and completing compositional analyses on only the -20/+80 size particles limits bias in the carbohydrate and lignin content. Including -80 mesh particles may bias the carbohydrate content low due to excessive carbohydrate degradation in the small particles during acid hydrolysis, and including +20 mesh particles may also bias carbohydrate content low due to incomplete carbohydrate hydrolysis in the larger particles. If carbohydrates are excessively hydrolyzed, they become part of acid soluble lignin, and if not hydrolyzed, they become part of the acid insoluble lignin, both of which bias total lignin content high. Since the analyses reported herein were performed on all particle sizes, the values may contain low bias in the carbohydrate content and high bias in the lignin content.

The reason all particle sizes were analyzed was because analysis of the -20/+80 size particles of, for instance, the pretreated wheat straw, would not necessarily have indicated the chemical changes that occurred during pretreatment of the milled wheat straw since all milled wheat straw particles were subject to pretreatment. This fact demanded that all particle sizes of the pretreated wheat straw be analyzed, which then demanded that all particle sizes of the other biomass types (milled wheat straw, saccharified wheat straw) also be analyzed similarly so that comparisons could be made on an equal basis.

4.6.1.5.2 Ash composition versus particle size

It was believed early in the composition experiments that the composition of the wheat straw particles would vary by particle size. To know to what degree composition could vary, several size fractions were collected and tested for ash content in the hope of indicating potential differences in the contents of other biomass constituents by particle size, such as lignin, carbohydrates, etc. The results of the ash analysis by particle size show that smaller particles do contain more ash, but the NREL standard protocol assumes that all non-ash components are present in the same proportions for all particle sizes (Hames, et al. 2008). Also, there was not found any literature precedent disproving this claim. Thus, the ash results presented here are not necessarily indicative of differences in other biomass constituents by particle size. Nevertheless, the ash results may be useful for some future purpose, so they are presented here.

The milled wheat straw was sifted to mesh size fractions +20, -20/+60, -60/+80, and -80. Triplicate sets of these size fractions were then dried at 105 °C and ashed in crucibles. The results

show that the percent ash on a dry weight basis contained in the milled wheat straw is significantly higher in smaller milled wheat straw particles (-80 mesh fraction) than in larger particles (+20 mesh fraction) (Figure 4-8). This means that including the -80 fraction, as was done in the compositional analyses, biases the ash content high, and including the +20 fraction biases it low. Including both the +20 and -80 fractions biases the overall value high or low depending on the masses of the two fractions.

Greater proportions of ash have been found in leaves than in the nodes or internodes of wheat plants, suggesting that the smaller milled particles derive more from the leaves than from other parts (Antongiovanni and Sargentini 1991). The higher ash content of leaves means there is higher inorganic content (e.g. Ca, Mg, SiO_2) which may make leaves more brittle and likely to fracture into smaller particles when milled.

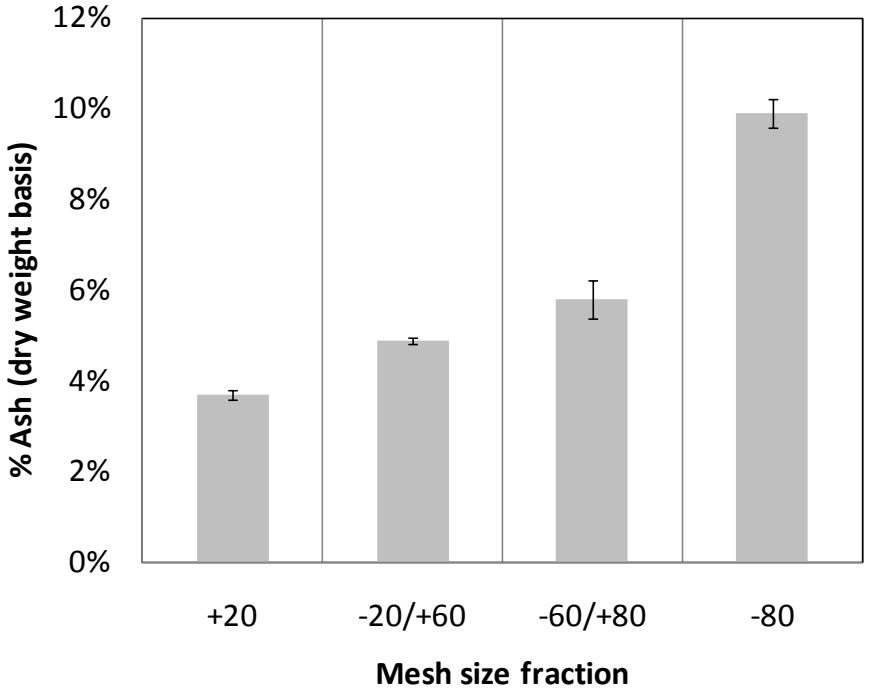

Figure 4-8: Percent ash (as-received basis) in milled wheat straw by mesh size fraction.

4.6.2 Compositional results

Keeping in mind that the lignin and carbohydrate composition of the biomass samples may be biased due to including all particle sizes in the analysis, the results of the compositional analyses are discussed below.

Trial 2 of the composition of milled wheat straw has dramatically higher sugar concentrations than trial 1. Most of this inaccuracy likely came from sugar concentration gradients that were present in the HPLC vials before HPLC analysis. The concentration gradients were present because the vials had previously undergone a freeze/thaw cycle and were not agitated before HPLC analysis. The same inaccuracies are present in the sugar composition of the dilute acid pretreated wheat straw because those samples were run together with the milled wheat straw samples on the HPLC.

The glucan content of the "Dilute acid pretreated/saccharified WS (DW washed)" as determined by the GOP method is substantially higher than the value determined by subtracting the supernatant glucose concentration from the initial cellulose present in the wheat straw before saccharification (i.e. the "subtracting supernatant GOP" value). This result is most likely due to the medium of the GOP glucose standards being of a different sulfuric acid concentration than the samples, and differences in calibration between the two precision balances that were used to measure masses of samples and sugar standards.

It is noteworthy that extracts in milled wheat straw (12.2±1.4%) were not significantly reduced during pretreatment (13.0±4.4%), but xylan content was significantly reduced (25.6% to 17.8±0.7%), as were arabinan (6.6% to 2.2±0.7%), mannan (1.0% to 0.1±0.1%), and acid soluble lignin (3.3±0.3% to 2.3±0.0%) (note that these sugar values are biased high, as explained above, but are nevertheless comparable since the values for milled wheat straw and pretreated wheat straw were determined simultaneously). The high remaining extracts after pretreatment of the wheat straw may indicate that the extracts level in the pretreated/saccharified/desorbed substrate also is high. If so, rMnP degradation of that substrate may be hindered since tests of rMnP degradation of methylene blue in the presence of wheat straw extracts inhibited dye degradation.

Saccharification of the pretreated wheat straw significantly reduced glucan if the glucan content of the saccharified solids is measured as the difference between initial glucan and glucan evolved

into solution during saccharification (58.3±5.2% to 38.6%). Saccharification also increased the relative amount of acid insoluble lignin (15.1±0.8% to 28.5±0.5%). The nitrogen content of the saccharified solids after thorough washing with distilled water was significantly larger (12.3±0.6%, w/w) than the saccharification control solids that were not exposed to cellulases (0.3±0.7%, data not shown in Table 4-2). The high nitrogen content was due to cellulases remaining adsorbed to the solids (Figure 4-9). Desorption of the cellulases with SDS removed some cellulases (from 12.3±0.6% to 3.1±0.8%), but not to the level of the control solids that underwent washing with SDS like the saccharified sample (0.9±1.3%, data not shown in Table 4-2).

The 0.2±0.0% nitrogen in the milled wheat straw was not altered significantly by pretreatment, since the pretreated solids also had a nitrogen content of 0.2%±0.0%.

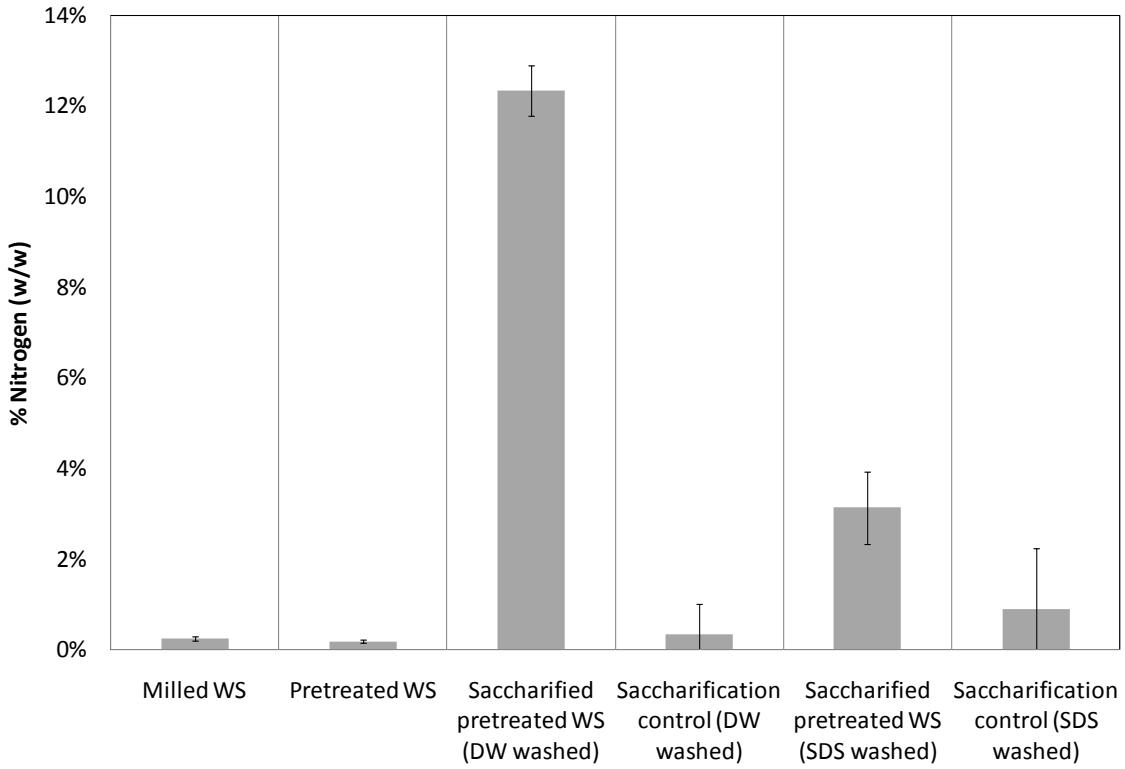

Figure 4-9: % nitrogen (w/w) of wheat straw samples by processing step. WS=wheat straw, DW=distilled water, SDS=sodium dodecyl sulfate. Error bars are ±1 standard deviation of triplicate assays.

5 DEVELOPMENT OF LIGNIN TRANSFORMATION SYSTEMS AND ASSAYS FOR REACTION COMPONENTS

Two systems for reacting rMnP with solid substrate were tested and are described below.

5.1 Lignin transformation system 1 (severe acid pretreated lignin with malonate/rMnP enzyme system)

The first lignin transformation system was used in an experiment that examined the effect of four concentrations of hydrogen peroxide and the activity (fully active or inactive) of a malonate mediated rMnP system (designated "malonate/rMnP") on the transformation of severe acid pretreated lignin. The substrate for this experiment was the acid insoluble lignin remaining after standard compositional analysis of wheat straw. There were four hydrogen peroxide levels, each with two rMnP activity levels (fully active or inactive), resulting in eight treatments, each run in triplicate.

The hypothesis of the experiment was that there would be a hydrogen peroxide concentration at which rMnP would significantly transform the acid insoluble lignin and the transformation could be detected by the evolution of soluble phenolics into solution or reduction in the weight of solids remaining in the reaction mixtures. Assays for phenolics in the reaction supernatants and solids were completed and are reported below.

To a 125 mL baffled Erlenmeyer flask was added, in order, acid insoluble wheat straw lignin (2 mg/mL), sodium malonate (50 mM, pH 4.5) and $MnSO_4$ (0.8 mM), and enough distilled water to bring the final reaction volume to 30 mL. Then either active or inactive rMnP (0.2 U/mL) was added to each treatment. The rMnP was inactivated by boiling or autoclaving until no activity was detected. Initial reaction samples were taken before initiating the reaction by adding hydrogen peroxide in four concentrations (1.0 mM, 0.1 mM, 0.01 mM, and 0 mM). The flasks were covered with aluminum foil and orbitally shaken at 150 rpm at 21.5 °C for 24 hours with sampling and hydrogen peroxide addition every three hours. Enough hydrogen peroxide was added to maintain the indicated concentration.

A problem with the orbital agitation of reaction mixtures was that the acid insoluble lignin adhered to the meniscus and was therefore mixed poorly with the liquid phase.

5.2 Lignin transformation system 2 (mild acid pretreated lignin with linoleic acid/rMnP system and cellulases)

The second lignin transformation system was used in an experiment that examined the effect of rMnP activity (fully active or inactive) in a linoleic acid mediated rMnP system (linoleic acid/rMnP), cellulase activity (fully active or inactive), and both, on mild acid pretreated lignin. This substrate was wheat straw that had previously undergone mild acid pretreatment, saccharification by cellulases, and desorption of the cellulases.

The hypotheses of the experiment were that rMnP would (1) transform some of the lignin, thereby evolving soluble phenolics into solution, and (2) increase the rate of cellulase-mediated saccharification by degrading lignin which may sterically hinder cellulase access to cellulose. The presence of more soluble phenolics in treatments with rMnP, and more glucose in cellulase treatments with rMnP than without, would indicate rMnP-induced lignin decomposition and improved access to cellulose. Assays for rMnP activity, pH, absorbance for lignin degradation products, and glucose and phenolics concentrations in the reaction supernatants over time were completed and are reported.

The reaction system involved mixing reaction solutions by inversion because the orbital shaking motion used in lignin transformation system 1 did not adequately mix solids with the liquid phase.

The treatments of the experiment were run in triplicate and were:

1. base case (active rMnP and active cellulases)
2. no cellulases (active rMnP and inactive cellulases)
3. no rMnP (inactive rMnP and active cellulases)
4. no cellulases, no rMnP (inactive rMnP and inactive cellulases)
5. no cellulases at second enzyme addition (active rMnP and active cellulases added initially, after 29 hours of reaction only active rMnP added)

The lignin substrate was added first to sterile 15 mL polypropylene centrifuge tubes. It was present at different concentrations in different reaction mixtures due to substrate shortage (Table 5-1). The cellulose composition of the substrate was previously measured as 38.6% (w/w).

Table 5-1: Concentrations of dilute acid pretreated lignin substrate used in lignin transformation system 2.

Treatment	base case	no cellulases	no rMnP	no cellulases, no rMnP	no cellulases at the second enzyme addition
Replicate	Dry solids concentration (mg/mL)				
1	11.2	11.3	11.3	7.7	4.1
2	11.3	11.2	11.2	6.3	3.7
3	11.2	11.3	11.3	2.8	7.8

To each reaction mixture was then added linoleic acid (3.0 mM, Sigma L1376) dissolved in acetone. The acetone was evaporated by heating to 40 °C for 27 minutes at 27.5 inches Hg vacuum.

Several additional components were added after the linoleic acid. All components except the enzymes were sterile filtered or made in autoclaved distilled water. Calcium, in the form of $CaCl_2$, was added to the reaction mixtures because calcium has been shown to improve the stability of rMnP (Yee 2009). The cellulases were as Accellerase 1000 (Genencor) and the aliquots added contained a ratio of solid and liquid representative of the ratio found in the commercial mixture. The rMnP was lyophilized product reconstituted in 100 mM sodium acetate buffered at pH 4.8. The reconstituted rMnP was centrifuged before the supernatant was added to reaction mixtures. The filter paper unit (FPU) activity of the cellulase mixture was determined using the standard NREL protocol (Adney and Baker 2008). The activity of rMnP was determined using the standard DMP activity assay (described below).The rMnP and cellulases were inactivated by autoclaving for 20 minutes. When inactive rMnP or inactive cellulases were added to a reaction mixture, the volume added of either was equal to the volume of active enzyme added. The addition of autoclaved enzyme solutions was to maintain equivalent protein concentrations in all reaction mixtures.

To the substrate and linoleic acid were added, in order, enough sterile distilled water to bring the final fluid reaction volume to 10 mL (not including volume of solid substrate), sodium acetate buffer (50 mM, pH 4.8), $CaCl_2$ (0.06 mM), and $MnSO_4$ (2.0 mM). The resulting mixtures were then brought to 35 °C in a water bath, and the following components added in order: hydrogen peroxide (0.9 mM), active or inactive cellulases (0.16 FPU/mL), and active or inactive rMnP

(1.05 U/mL). The addition of enzymes marked the start of reaction. Samples were taken ~20 minutes after addition of the enzymes. All sampling was performed by removing the tube cap, vigorously agitating the reaction mixture with nitrile-covered thumb over tube opening to suspend solids, then rapidly withdrawing with a sterile pipette tip a 1 mL sample to obtain a representative mixture of the solid and liquid phases. The samples were placed at -80 °C. After initial sampling, the reaction mixtures were rotated at 8 rpm at 35 °C for 48 hours. Every eight hours, the mixtures were placed in a water bath between 30 °C and 42 °C, samples withdrawn, and hydrogen peroxide added (0.1 mM). The water bath temperature varied due to poor temperature controllability. After 29 hours of reaction, an amount of rMnP, cellulases, or both were added to the mixtures in concentrations equal to the initial addition.

5.3 Assays for reaction components (descriptions and results)

5.3.1 UV/vis absorbance

5.3.1.1 Introduction

Absorbance measurement is a simple and rapid test to indicate sample composition and changes over time. Thus, the absorbance from 220 nm to 900 nm of samples of reaction supernatant was measured. Absorbance in the ultraviolet range (220-400 nm) was measured because phenolics, expected soluble products formed by enzymatic transformation of lignin (Reid, Abrams and Pepper 1982), absorb in that spectral region. Visible (400-900 nm) absorbance was also measured to characterize any colored products formed.

5.3.1.2 UV/vis absorbance methods

5.3.1.2.1 Standard method

Disposable plastic cuvettes designed for absorbance measurements in the 220-900 nm range were used in a Genesys 6 spectrophotometer (Thermo Electron Scientific Instrument Corporation). Absorbance measurements were made relative to distilled water. The absorbance spectrum of commercially available alkali lignin (Sigma 471003) was obtained to verify that soluble lignin absorbs in the ultraviolet region. Sodium sulfide (0.8 mM) was added to some samples to reduce the absorbance due to Mn(III) malonate complex.

5.3.1.3 UV/vis absorbance results and discussion

5.3.1.3.1 Alkali lignin

The absorbance of commercially available alkali lignin (Figure 5-1) confirms that most absorbance due to soluble lignin can occur in the ultraviolet range (Figure 5-2). Thus, soluble lignin evolved into solution from enzymatic degradation of lignin substrates may also absorb mostly in the ultraviolet range.

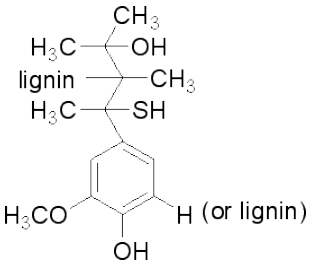

Figure 5-1: Molecular structure of commercially available alkali lignin (Sigma-Aldrich 2009).

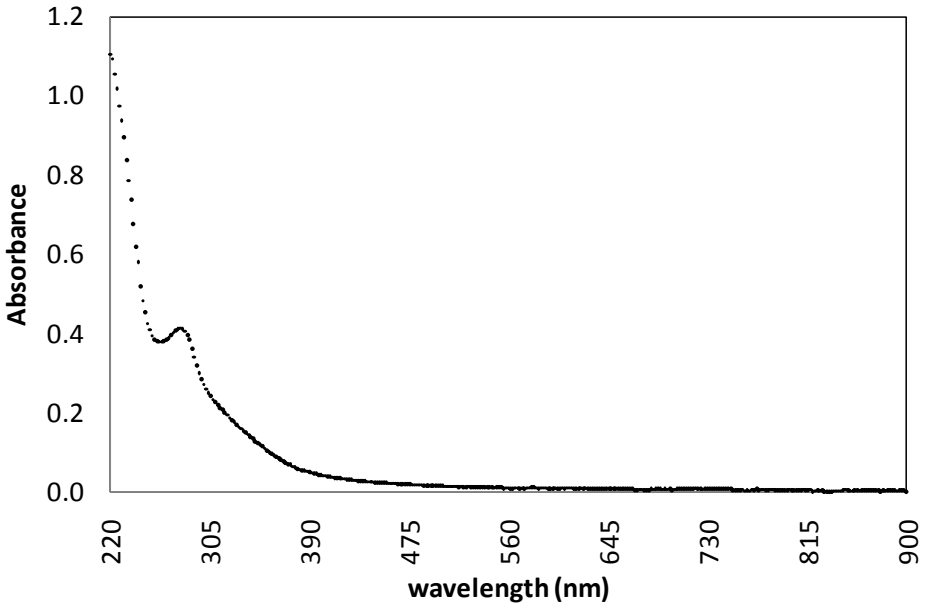

Figure 5-2: Absorbance spectrum of commercially available alkali lignin (27.5 mg/L).

5.3.1.3.2 Lignin transformation system 1

In the first lignin transformation system, the most substantial spectral difference was detected between treatments with active and inactive rMnP and a 0.1 mM hydrogen peroxide concentration (Figure 5-3).The difference was visible as a brown color in the treatment with active rMnP and no color with inactive rMnP. The absorbance peaks were at approximately 270 nm and 460 nm.

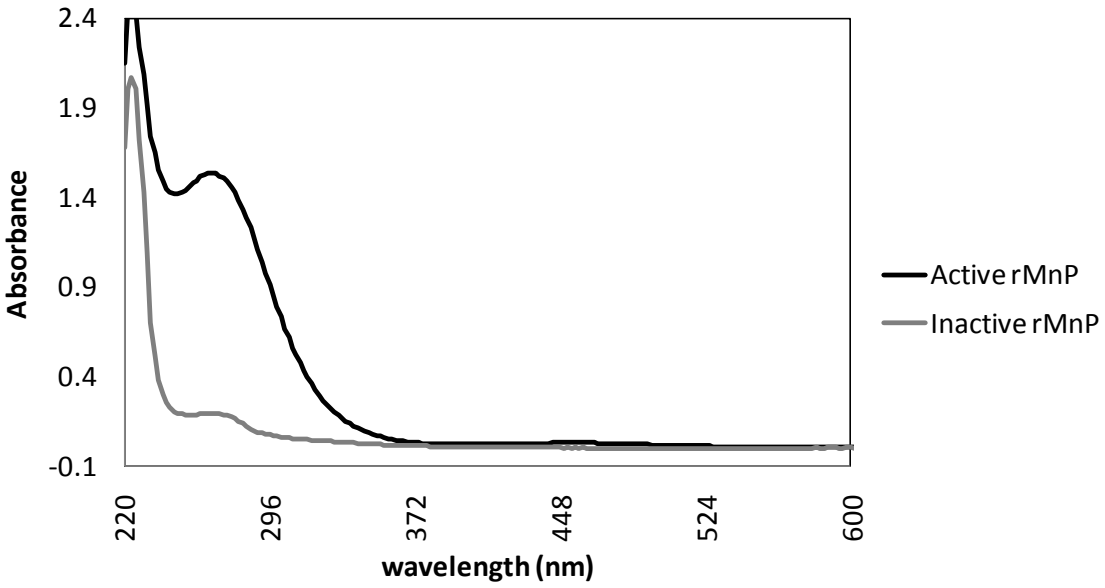

Figure 5-3: Absorbance spectra of 0.1 mM hydrogen peroxide treatments of lignin transformation system 1. Spectra are of 42% concentration supernatant samples after 24 hours of reaction time.

5.3.1.3.3 Identifying brown compound found in supernatant of lignin transformation system 1

To determine the cause of the spectral difference, a subtractive experiment was completed with treatments containing all reaction components, and subsets thereof, but none contained acid insoluble lignin. The base case was the treatment containing all reaction components (hydrogen peroxide, $MnSO_4$, malonate, and active or inactive rMnP). The results show that the spectral shape could be reproduced without acid insoluble lignin in a treatment containing all components. The absence of any one of these components resulted in loss of the characteristic peaks, thus the absorbance is due to formation of a new chemical species from the components.

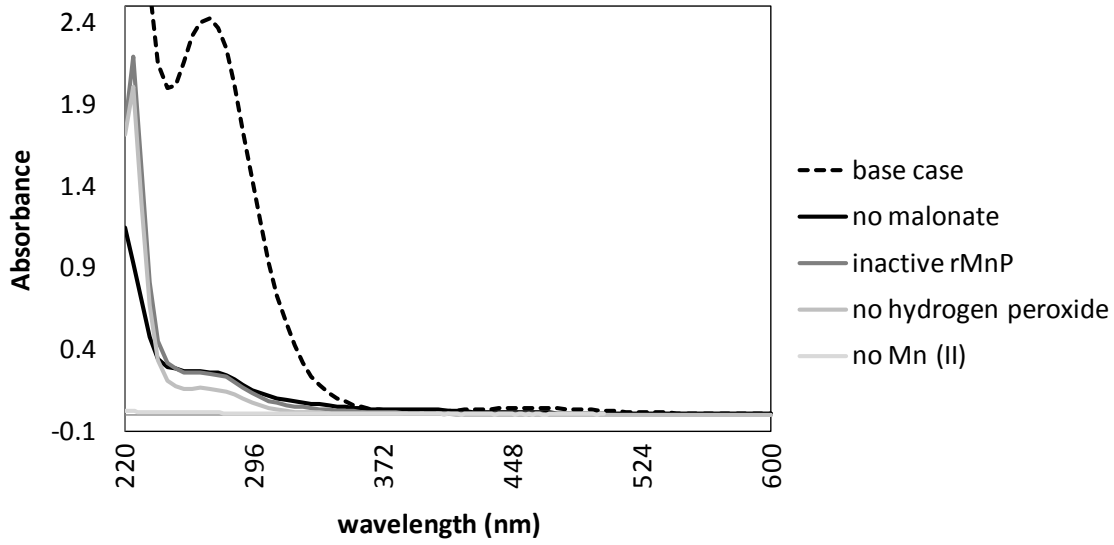

Figure 5-4: All reaction components except acid insoluble lignin are necessary to reproduce the spectrum. Spectra are of 100% concentration supernatant samples taken after 6 hours of reaction time.

To elucidate the identity of the chemical species formed, Mn(III) acetate was added to malonate (Figure 5-5). The mixture of Mn(III) acetate and malonate was equivalent to replacing the Mn(III) enzymatically generated with rMnP, Mn(II), and hydrogen peroxide with exogenous Mn(III). The result shows that the combination reproduces the spectrum, thus the species was likely a complex between Mn(III) and malonate that would have formed in the lignin transformation system after rMnP oxidized Mn(II) to Mn(III) which then complexed with available malonate. Further evidence of the species' identity comes from a previous study that monitored the concentration of the Mn(III)-malonate complex at 270 nm (ε_{270} = 11.59 mM^{-1} cm^{-1}) and 458 nm (ε_{458} = 1.93 mM^{-1} cm^{-1}) (Wariishi, Valli and Gold 1992). Thus, the absorbance spectra of supernatant samples from lignin transformation system 1 failed to show the presence of compounds from lignin transformation.

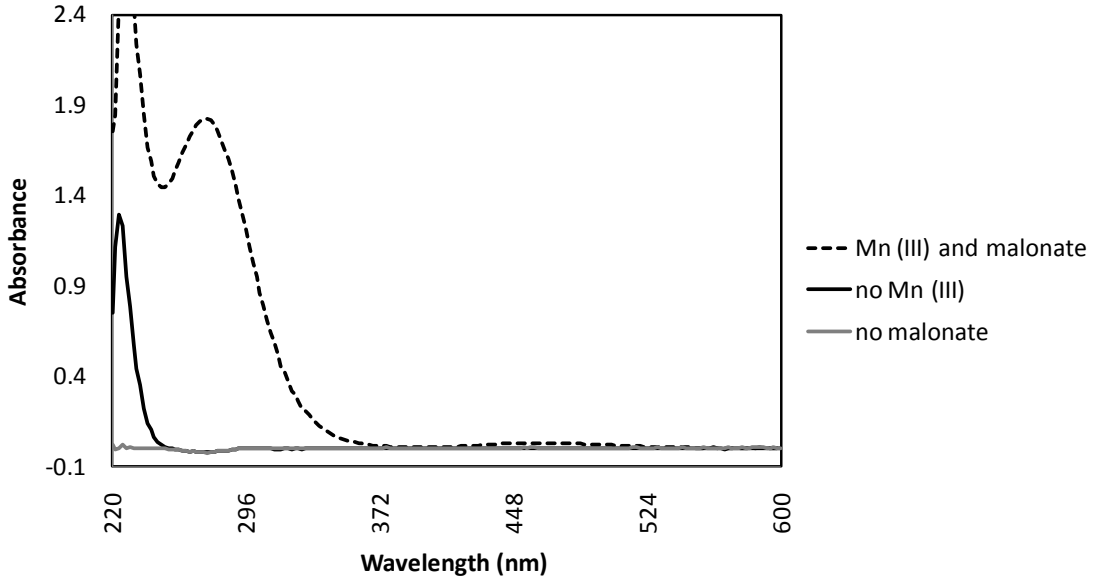

Figure 5-5: Mixture of Mn(III) acetate and malonate formed the spectrum characteristic of the supernatant from lignin transformation system 1 (60% concentration).

The 270 nm peak due to the Mn(III)-malonate complex may interfere substantially with peaks from phenolics that evolve into solution during lignin transformation, thus an attempt was made to decrease the absorbance by adding the mild reducing agent sodium sulfide (Na_2S). The reducing agent resulted in near complete removal of absorbance ~7 minutes after addition, with little change observed ~2.5 hours later (Figure 5-6). The resulting spectrum resembled the spectrum of the control in Figure 5-5 to which only malonate was added. Sodium sulfide is known to reduce nitro groups to amines, but is not expected to reduce the aromatic rings or carbonyl groups typically found in lignin structures (Encyclopedia of Reagents for Organic Synthesis 2006).

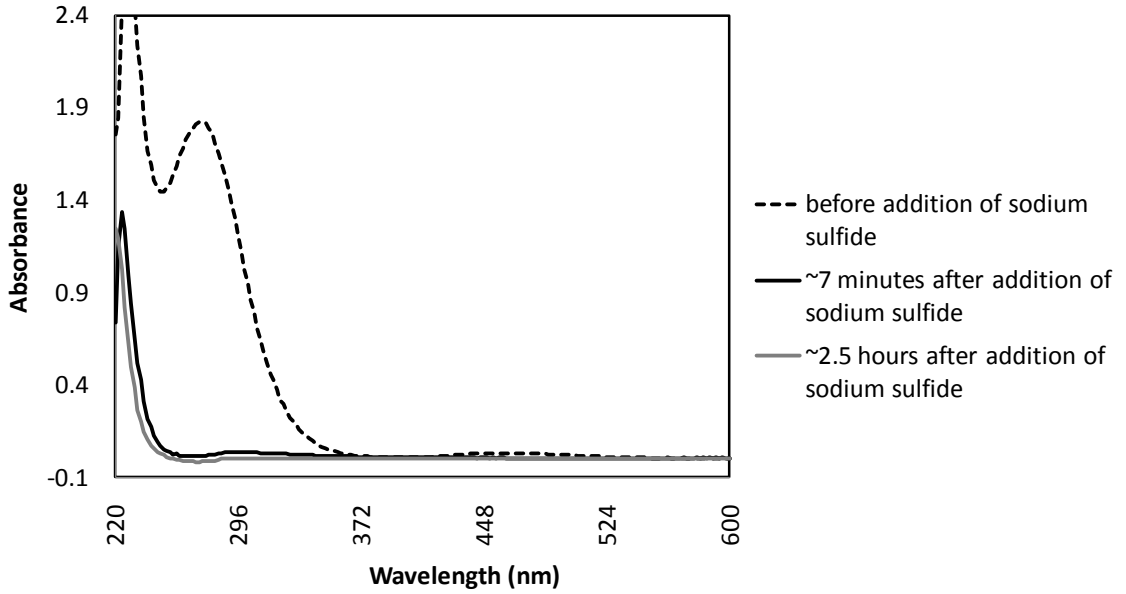

Figure 5-6: Addition of the reducing agent sodium sulfide resulted in removal of nearly all of the absorbance.

A volume (22.5 mL) of supernatant from each of the treatments active rMnP/0.1 mM hydrogen peroxide and inactive rMnP/0.1 mM hydrogen peroxide was filtered through a 10 kDa centrifugal filter (Millipore Centriplus) at 3,000 rcf for 90 minutes to collect retentate. The centrifugal filter was then inverted and centrifuged at 2,000 rcf for 4 minutes. The spectra of the supernatants before filtration (Figure 5-7) and after filtration (Figure 5-8) are shown below (the spectra of the supernatants before filtration are somewhat different from the spectra in Figure 5-3 due to differences in concentration, reaction replicate used, and degradation of supernatant components over time). The 10 kDa filter was able to retain most of the colored matter in the active rMnP retentate. Previously it was found that the colored matter was a Mn(III) malonate complex, so this complex apparently forms a large molecular weight structure.

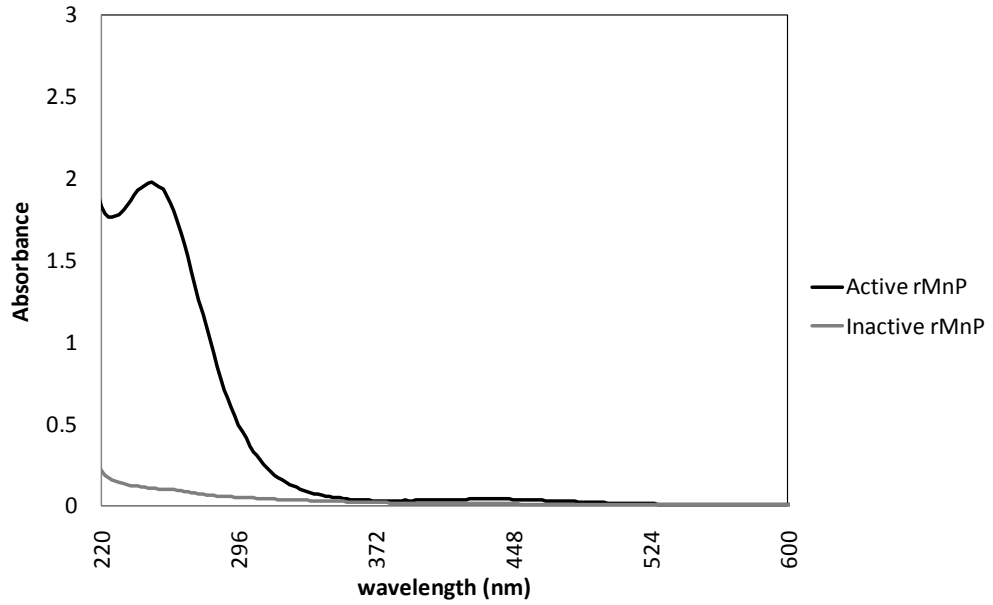

Figure 5-7: Spectra of reaction supernatants before centrifugal filtration.

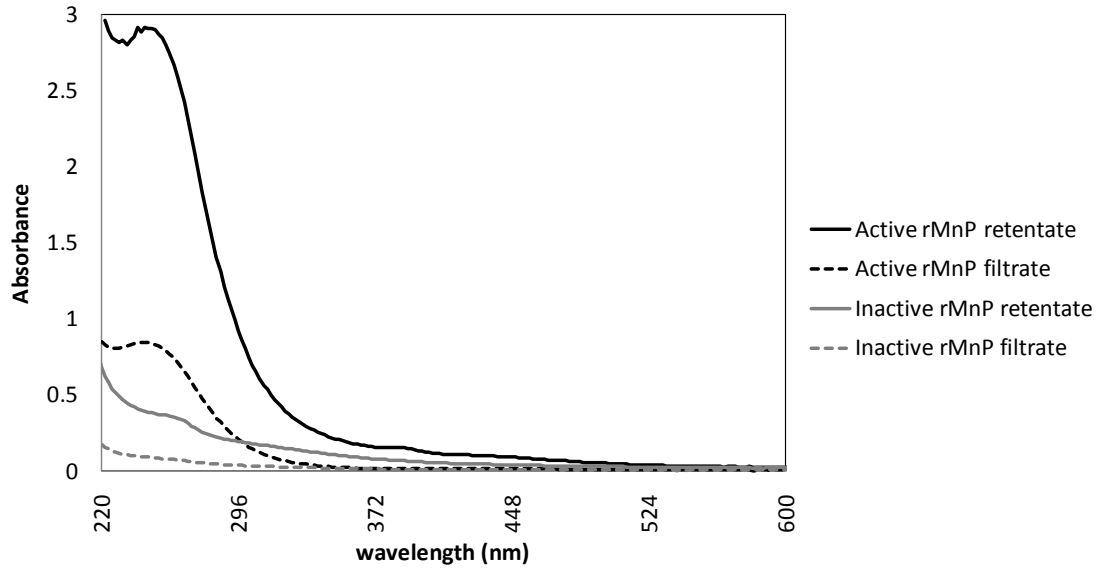

Figure 5-8: Spectra of filtered reaction supernatants (retentate and filtrate).

5.3.1.3.4 Lignin transformation system 2

Time course spectra (220-900 nm) were acquired for all treatments of the experiment using lignin transformation system 2. A time course for a base case replicate (Figure 5-9) exemplifies the typical patterns observed. One typical feature in treatments containing rMnP was a peak at 406 nm characteristic of the enzyme (Wariishi, Valli and Gold 1992) in only the initial sample taken ~20 minutes after enzyme addition. The peak at 406 nm was not apparent in the spectra of samples from lignin transformation system 1 because the active enzyme concentration was lower and the peak at 458 nm due to the Mn(III) malonate complex obscured it. Another typical feature in the spectra was the appearance of broad absorbance at one or more time points (16 hour time point in Figure 5-9), likely due to the presence of emulsified linoleic acid in the sample. The emulsion was mostly present towards the top of the reaction mixture, so the appearance of absorbance at a particular time point depended mostly on which part of the reaction liquid was sampled rather than the nature or rate of some reaction occurring in the mixture.

Besides the peak at 406 nm indicating the presence of rMnP, nothing in the time course spectra shed light on the composition or dynamics of the reaction mixtures.

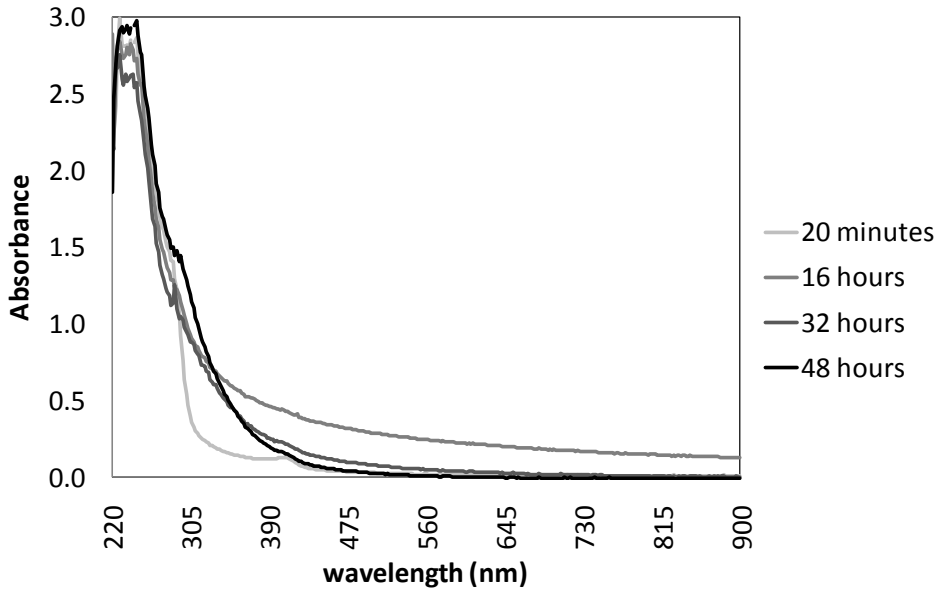

Figure 5-9: Time course spectra of base case of experiment using lignin transformation system 2.

5.3.2 Folin assay for soluble phenolics

5.3.2.1 Introduction

The Folin colorimetric assay is based on analytes reducing the Folin Ciocalteau reagent (FCR), a mixture of tungsten and molybdenum oxides, to give a blue color absorbing broadly around 765 nm (Waterhouse 2002); (Singleton, Orthofer and Lamuela-Raventos 1999). The intensity of absorption at that wavelength is proportional to the concentration of phenols or other reducing compounds present in the sample.

5.3.2.2 Folin assay methods

5.3.2.2.1 Standard method

The standard Folin assay method was used except where indicated. The assay was carried out in triplicate in 2 mL centrifuge tubes with samples and gallic acid standards. The standards were of concentrations 0 mg/L (distilled water) up to 500 mg/L. To each tube was added, in order, 13 µL sample or standard, 1000 µL distilled water, and 63 µL Folin-Ciocalteau reagent (Sigma F9252), then the mixture was agitated thoroughly. After one to eight minutes of incubation, 190 µL of 20% (w/v) sodium carbonate solution was added and the mixture agitated thoroughly. The end volume of the assay was 1,266 µL. The total assay volume was sometimes scaled up to 1,500 µL with all assay components added in proportionally higher volumes. The mixture was allowed to develop at room temperature for 2 hours ± 15 minutes, centrifuged to remove any white precipitate, and the absorbance measured at 765 nm. If the sample had an absorbance out of the range of the standards, the procedure was repeated. The absorbance of the 0 mg/L standard was subtracted from the absorbance of the other standards and samples. The net absorbance of the standards was plotted to form a standard curve from which the sample concentrations were inferred in units of gallic acid equivalents (GAE) per liter.

5.3.2.2.2 Method used in study of assay variables

Two different sodium carbonate solutions (20% and <20% w/v) were prepared for use in the study of assay variables. The <20% solution was made by adding 20 g sodium carbonate to 80 mL distilled water, boiling until dissolved, cooling, adding a few sodium carbonate crystals, and letting sit for more than a day, upon which large sodium carbonate crystals formed. The crystals were removed by filtration, and the filtrate was diluted to 100 mL with distilled water.

The other solution (20% w/v) solution was made simply by adding 20 g sodium carbonate to ~80 mL distilled water, heating until dissolved, then diluting to 100 mL with distilled water.

Assays were carried out in triplicate with the following discrepancies with the standard method: (1) the incubation times tested were 3, 5, 8, or 12 minutes, (2) the development times tested were 67 min, 125 min, 270 min, and 19.2 hrs, (3) the two sodium carbonate solutions described previously were used instead of just a 20% (w/v) solution, (4) only assay absorbance values uncorrected for the absorbance of the 0 mg/L gallic acid standard were reported, and (5) the assay volumes were centrifuged before all absorbance readings except the 19.2 hour reading.

5.3.2.2.3 Method used in study of assay interferences

Eight interference samples were mixed. The base case interference sample was mixed, in order, with gallic acid (500 mg/L), active rMnP (7.7 µL/mL), sodium malonate (21 mM), $MnSO_4$ (0.336 mM), hydrogen peroxide (42 µM), and enough distilled water to bring all components to concentration. The other interference samples consisted of the components listed previously but with inactive rMnP instead of active rMnP, or without hydrogen peroxide, or without gallic acid, or a combination missing active rMnP, hydrogen peroxide, and gallic acid. The interference samples were then centrifuged and assayed in triplicate. The inactive rMnP was obtained by boiling or autoclaving rMnP until zero activity was reached. The concentrations of hydrogen peroxide, $MnSO_4$, sodium malonate, and rMnP in the interference samples were the same as those in the diluted (42% concentration) supernatant samples from lignin transformation system 1. About 35 minutes elapsed between the time of hydrogen peroxide addition to the interference samples and the start of the Folin assay.

Assays were carried out with the following discrepancies with the standard method: (1) The assays were allowed to incubate for about 10 minutes, (2) allowed to develop for about 2.5 hours, and (3) only assay absorbance values uncorrected for the absorbance of the 0 mg/L gallic acid standard were reported.

5.3.2.2.4 Method used in assays of lignin treatment system 1

The Folin assay was performed in triplicate on acid insoluble lignin that had undergone 24 hours of reaction in lignin transformation system 1. The lignin from one replicate of the active rMnP/0.1 mM hydrogen peroxide treatment and from one replicate of the inactive rMnP/0.1 mM

hydrogen peroxide treatment were dried at 105 °C, washed with ~ 100 mL distilled water over a 0.20 um cellulose filter (Nalgene cat # 290-3320) under vacuum to rid of impurities, then air dried overnight before being assayed. Each assay replicate contained 10-11 mg of lignin. No liquid sample was added, so to maintain total assay volume of 1,500 µL, an extra 15 µL of distilled water was added.

The Folin assay was also performed on supernatant samples from the same treatments. The samples were at 42% concentration, and one replicate from each treatment was assayed.

Assays were carried out with the following discrepancies with the standard method: (1) The supernatant assays were allowed to incubate for about 10 minutes, and develop for about 2.5 hours, and (2) only assay absorbance values uncorrected for the absorbance of the 0 mg/L gallic acid standard were reported.

5.3.2.2.5 Methods used in assays of lignin transformation system 2

Each of the three replicates of the treatments “base case”, “no cellulases”, and “no cellulase, no rMnP” were assay once, and each replicate of the treatments “no rMnP” and “no cellulases at second enzyme addition” was assayed three times due to inconsistency in the first assay of replicates of those treatments. The assay differed from the standard method is several ways: (1) An amount of 300 mg/L gallic acid was added to each sample assay as a standard addition to bring the total phenol concentration to a level at which the assay was more sensitive, (2) a line of best fit was found for the 250-500 mg/L gallic acid standards which were approximately linearly related, and the line used to infer the phenolics concentrations (mg/L gallic acid equivalents [GAE]) of each sample. The difference in the concentration between the 48 hour and initial samples was calculated for each replicate.

5.3.2.3 Folin assay results and discussion

5.3.2.3.1 Study of assay variables

There were questions about the effects of several parameters within the Folin assay. Namely, there was concern over (1) the appropriate sodium carbonate concentration, (2) the effect of the incubation time between the addition of the Folin-Ciocalteau Reagent (FCR) and sodium

carbonate, and (3) the duration of the time between sodium carbonate addition and the absorbance reading. Thus, an experiment was completed to test the effect of these three variables.

The concern over sodium carbonate concentration arose over disparate recommendations by Waterhouse (2002), who recommends using a <20% (w/v) solution, and Singleton et al. (1999), who recommends using a 20% (w/v) solution. Waterhouse's recommendation of a <20% solution is due to the recommended solution preparation method. Both the Singleton et al. (1999) and Waterhouse (2002) procedures call for a 1-8 min incubation time between FCR and sodium carbonate addition, and about 2 hrs of development time between sodium carbonate addition and absorbance measurement. But there were questions whether the assay result was the same with different incubation times (e.g. three minute versus eight minute), and whether the development time could be shortened or varied to save time and increase convenience.

Figure 5-10 shows the Folin assay absorbance with variation in development time when the assays were allowed to incubate for 5 minutes before addition of 20% sodium carbonate. The result shows that varying the development time from 67 minutes to 19.2 hours does significantly affect the final absorbance reading. The trend is typical among the other assays performed with difference incubation times or with a <20% sodium carbonate solution. Therefore, approximate adherence to some standard development time (listed as 2 hours ± 15 minutes in the standard procedures) is recommended to facilitate comparison between assays completed at different times or by different people.

The later development times consistently gave higher absorbance values. Some of the elevated absorbance could be due to evaporation of the assay volume and/or precipitate formation. Absorbance measurements of a few assay volumes after 4.5 hours of development with and without centrifugation were compared and the difference was found to be negligible, so evaporation may be the cause of the increased absorbance after longer development times.

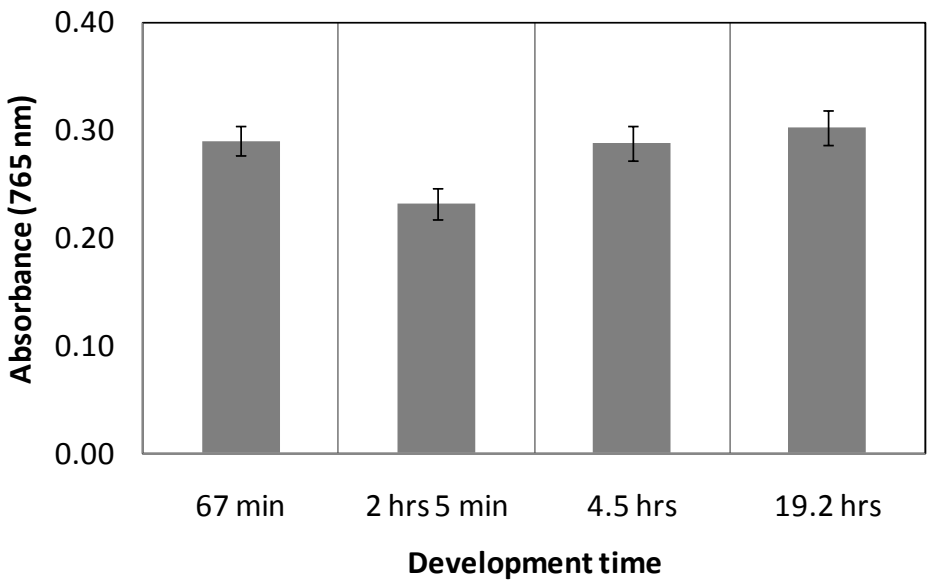

Figure 5-10: Folin assay absorbance with variation of development time for the assay completed with 5 minutes incubation and 20% sodium carbonate. Error bars are ±1 standard deviation of triplicate assays performed simultaneously.

Figure 5-11 shows that at a fixed development time of 2 hours 5 minutes, there were no significant differences in assay absorbance with variation in incubation time or concentration of sodium carbonate solution except perhaps between the 5 minute/<20% sodium carbonate treatment and either 8 minute treatment. Thus, if a <20% sodium carbonate solution is used in the assay, it appears that the assay result may vary if a five minute incubation time is used instead of an eight minute incubation time. To avoid the variable assay results that could arise from variation in incubation time when using the <20% solution, it is recommended that a 20% solution is used instead. Given that the pH values of the assay solutions using 20% sodium carbonate was nearly the desired value of 10 (Singleton, Orthofer and Lamuela-Raventos 1999), and the pH values of the solutions using the <20% solution were significantly less, the 20% solution is further recommended (pH data not shown).

Figure 5-11 also shows that variation of using any incubation time between 3 minutes and 12 minutes in the assay is acceptable since absorbance values did not vary significantly within this time range. This finding expands the recommended incubation interval of 1-8 minutes up to 3-12 minutes.

In conclusion, it is recommended to perform the Folin assay with a 20% (w/v) sodium carbonate solution, 3-12 minute incubation time, and 2 hour ± 15 minute development time to reduce unnecessary variability and facilitate inter-assay comparisons.

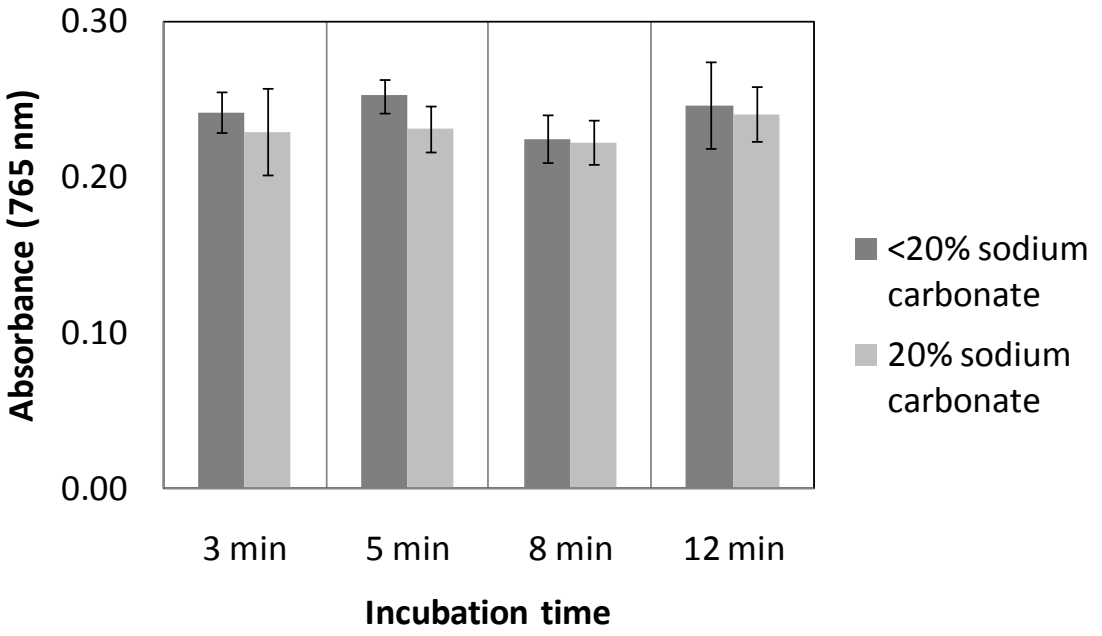

Figure 5-11: Folin assay absorbance with variation of incubation time and sodium carbonate solution. Development time was fixed at 2 hours 5 minutes. Error bars are ±1 standard deviation of triplicate assays performed simultaneously.

5.3.2.3.2 Study of assay interferences

There was the question whether the presence of hydrogen peroxide and active rMnP in the supernatant samples from lignin transformation system 1 would interfere with the Folin assay of those samples. Thus, mixtures were made and assayed that contained all reaction components of the lignin transformation system 1 but without hydrogen peroxide or active rMnP or both, and the samples assayed. The results are shown in Figure 5-12. The results show that hydrogen peroxide and active rMnP do not significantly affect the assay result.

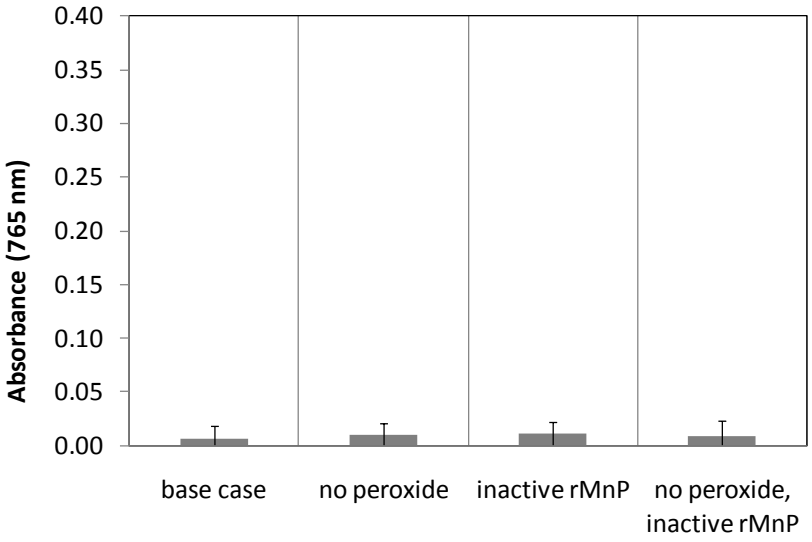

Figure 5-12: Effect of eliminating hydrogen peroxide and active rMnP from Folin assay sample. Error bars are ±1 standard deviation of triplicate assays performed simultaneously.

The effect of these two interferences could have depended on the presence of a phenolic compound, so a fixed amount of gallic acid was added to the same set of samples and the samples assayed (Figure 5-13). The same conclusion is reached that neither hydrogen peroxide nor active rMnP have an effect on the assay result.

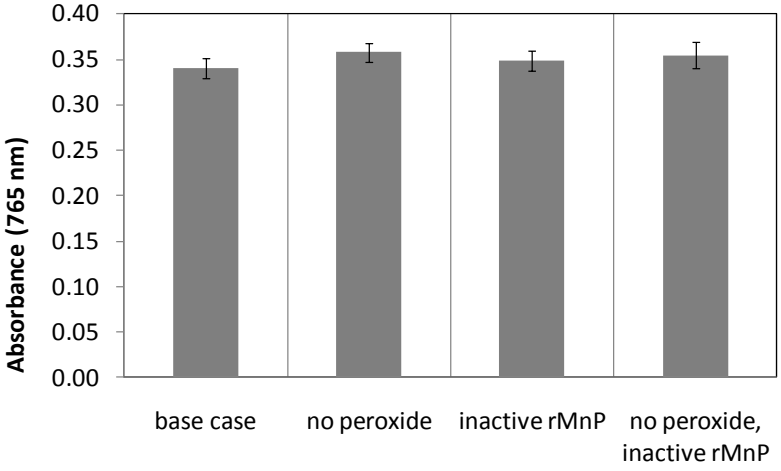

Figure 5-13: Effect of eliminating hydrogen peroxide and active rMnP from Folin assay sample in the presence of gallic acid. Error bars are ±1 standard deviation of triplicate assays performed simultaneously.

5.3.2.3.3 Standard curve

Gallic acid standards (0-500 mg/L) were measured with the Folin assay. A plot of the resulting absorbance values (Figure 5-14) is nonlinear. The nonlinearity indicates that the assay sensitivity is lower at smaller gallic acid concentrations (0-200 mg/L) than at higher concentrations (200-500 mg/L). It may be necessary to add a fixed amount of gallic acid to samples to raise the total phenolic concentration to a level where sensitivity is adequate to detect small differences in phenolics concentration.

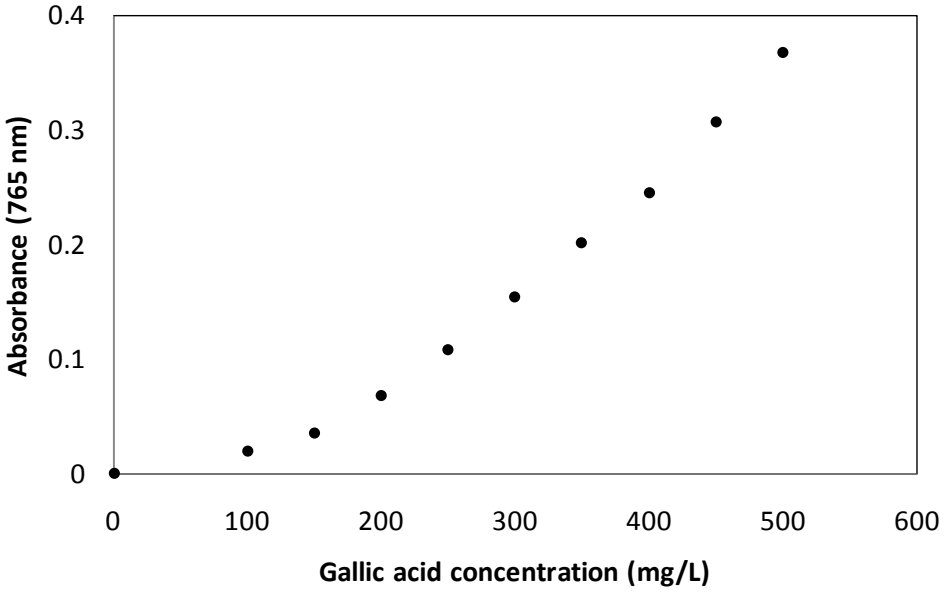

Figure 5-14: Gallic acid standard curve for the Folin total phenol assay.

5.3.2.3.4 Assay of lignin transformation system 1

The Folin assay was performed on the acid insoluble lignin remaining in the active rMnP/0.1 mM hydrogen peroxide and inactive rMnP/0.1 mM hydrogen peroxide treatments after 24 hours of reaction in lignin transformation system 1. The assay was performed on the solids to test the hypothesis that during the reaction active rMnP could have altered the surface chemical structure of the lignin solids, and oxidation of the solids by the tungsten and molybdenum oxides of the Folin-Ciocalteau reagent (FCR) could possibly detect this difference. Active rMnP induced alteration of the solids could have consisted of the formation of phenolic lignin subunits on the surface which could be more susceptible to oxidation by the FCR than non-phenolic units.

The assay was also performed on the supernatant samples, at 42% concentration, from the same treatments.

The results (Figure 5-15) show that there are no significant differences in the assay absorbance values for either supernatant or solids. Thus, the assay did not detect the presence of any soluble phenolics from lignin transformation or changes to the structure of the solid lignin. The Mn(III) malonate complex detected by absorbance in the active rMnP supernatant was also not detected. It is possible that there are more phenolics in the active rMnP supernatant than in the inactive rMnP supernatant, but the concentrations are low enough that the assay does not detect them due to the low sensitivity of the Folin assay at low phenolic concentrations as shown by the standard curve (Figure 5-14). As mentioned previously, in the future it may be necessary to add gallic acid to samples to raise the signal to a level where small concentration differences can be detected. A blue color was observed evolving from the solids into the assay volume upon addition of sodium carbonate. The high assay absorbance values are due to this factor, which may be caused by the solid lignin solubilizing in the basic solution and reacting with the Folin-Ciocalteau reagent. A lignin solids concentration (~2,000 mg/L) was added to the assay and was four times higher than the recommended upper limit of the assay (500 mg/L). Future assays of solid lignin substrates should account for the possibility of the lignin dissolving and add only an amount appropriate for the assay. An appropriate amount might assume that all solid lignin will dissolve in the assay volume, and so the amount of solid lignin added to the assay should be a quantity still within the linear range of the standards and less than the recommended upper limit of the assay (500 mg/L).

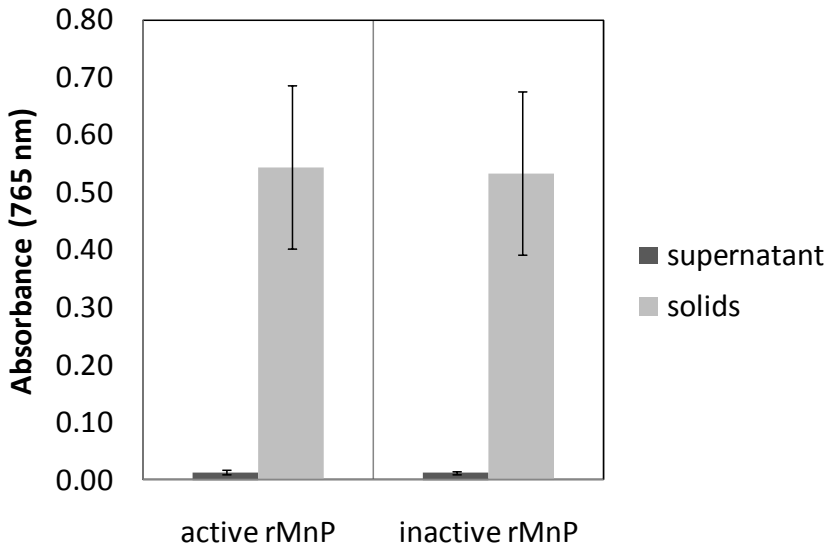

Figure 5-15: Folin assay absorbance of supernatant and solids of active and inactive rMnP treatments with 0.1 mM hydrogen peroxide in the lignin transformation system 1. Error bars are ±1 standard deviation of triplicate assays performed simultaneously.

5.3.2.3.5 Assay of lignin transformation system 2

Figure 5-16 shows the difference in phenolics concentration (mg/L gallic acid equivalents [GAE]) between the 48 hour and initial sample of each treatment, thus each bar is a measure of phenolics generated during the course of the experiment. If the phenolic measurements are accurate, then it appears that the combination of rMnP and cellulases generated more phenolics from the substrate than either enzyme alone or in the absence of both enzymes. The "no cellulases at second enzyme addition" treatment had less lignin substrate (Table 5-1), so the evolution of approximately an equal amount of phenolics as the "base case" perhaps indicates more thorough lignin degradation than in the "base case". Also, there is no significant difference between the "no cellulases" and "no cellulases, no rMnP" treatments, but a difference would be expected if rMnP alone was able to transform the substrate. Thus, the results of this assay possibly indicate synergy between rMnP and cellulases in evolving phenolics, but rMnP alone does not appear to have a significant effect.

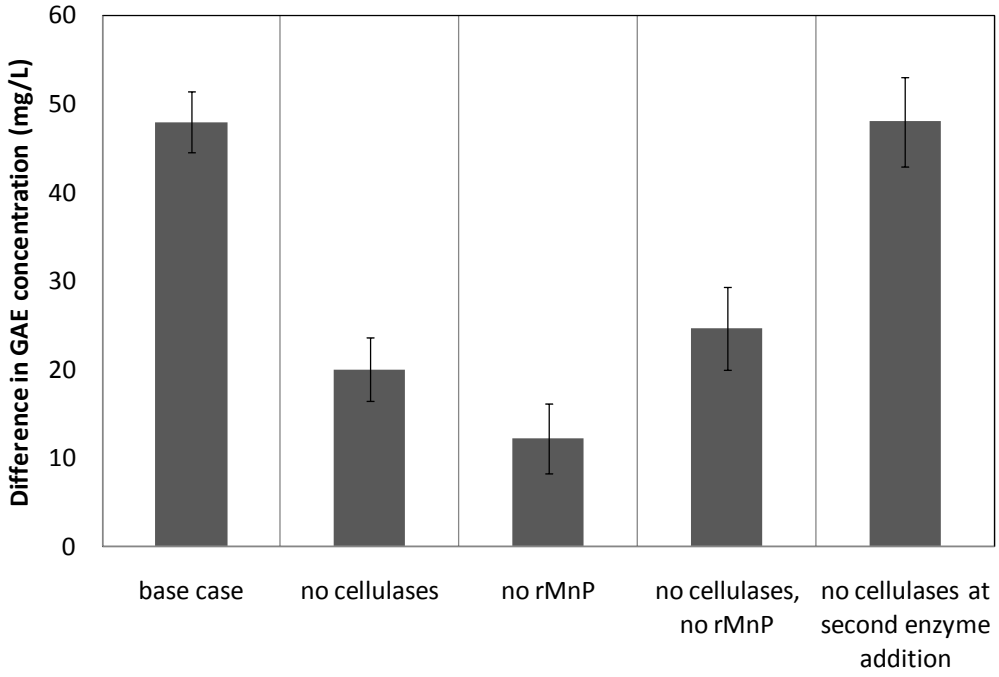

Figure 5-16: Difference between the final and initial phenolics concentrations in supernatant samples from lignin transformation system 2. Phenolics concentration is mg/L gallic acid equivalents (GAE). Error bars are ±1 standard deviation of the three assays performed on the samples of the three reaction replicates, except for the "no rMnP" and "no cellulases at second enzyme addition" treatments where the error bars are ±1 standard deviation of the averages of triplicate assays performed on each of the samples of the three reaction replicates.

Another possible interpretation is that active rMnP converts the cellulases to products that are detected as phenolics by the Folin assay.

A third possible interpretation relates to the phenolic amino acids present in cellulases and rMnP possibly tending to react more readily with the Folin reagent when those enzymes are active than when they are inactive. The difference in reactivity towards the Folin reagent could be due to a more open protein structure when active compared to the condensed structure of deactivated enzyme. If this phenomenon occurred during the Folin assay, the highest phenolic concentrations would be obtained for the treatments with the most active enzyme, namely the "base case" and "no cellulases as second enzyme addition" treatments, which is what is observed.

5.3.3 Pearl-Benson assay for phenolics

5.3.3.1 Introduction

The principle of the Pearl-Benson assay is the reaction of the phenolic units in lignin with nitrous acid (sodium nitrite acidified with acetic acid) to form nitrosophenols (Figure 5-17). These nitrosophenols, upon the addition of alkali, tautomerize to an intensely colored quinone mono-oxime that absorbs at 430 nm.

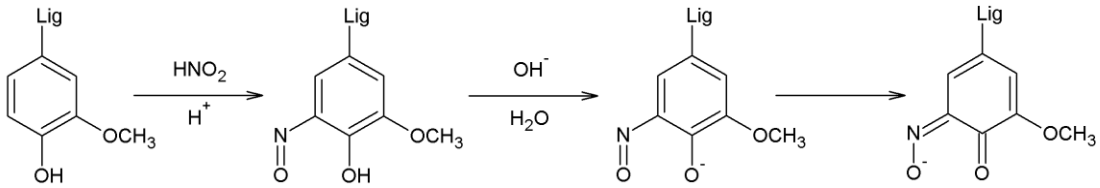

Figure 5-17: Nitrosation of a phenolic unit in lignin followed by deprotonation and tautomerization to a colored quinone mono-oxime.

The procedure calls for the addition of reagents to a sample in an order such that nitrosation occurs, and in an order such that nitrosation does not occur to obtain a blank absorbance value. The blank absorbance is due only to the absorbance of sample and reagents, and is subtracted from the sample absorbance.

5.3.3.2 Pearl-Benson assay methods

5.3.3.2.1 Standard method

The standard method was based on Dence (1992). The assay standards were made using alkali lignin (Aldrich 471003) as standard compound. A 1000 ppm alkali lignin stock solution was made by adding 100 mg (dry weight) to a 100 mL volumetric flask and filling to volume with distilled water. The first stock solution was diluted to make another 100 ppm stock solution in a 100 mL volumetric flask. The 100 ppm stock was then used to make standards spanning the lignin concentrations expected in the samples.

All samples and standards were assayed in triplicate. Into a 2 mL centrifuge tube were added 650 µL of sample or standard, 13 µL of 10% (v/v) acetic acid, and 13 µL of 10% (w/v) sodium nitrite solution. After mixing well, the solution was allowed to sit at room temperature for 15 minutes. Then 26 µL of 2 N ammonium hydroxide was added, the solution mixed well, and allowed to sit

at room temperature for 20-25 minutes. Thus, the total assay volume was 702 µL. The sample or standard was then centrifuged and the absorbance read at 430 nm.

Blank absorbance values were obtained by adding the same quantities of sample/standard and reagents but in the order: sample/standard, acetic acid, ammonium hydroxide (mix well), sodium nitrite solution (mix well) and allowed to sit at room temperature for 15-20 minutes. The assay volume was then centrifuged and the absorbance read at 430 nm. The nitrosation reaction does not occur in the basic mixture created by adding ammonium hydroxide before the sodium nitrite.

The blank absorbance was subtracted from the sample or standard absorbance to obtain the net absorbance. The net absorbance values of the standards were used to derive a standard curve from which sample concentrations could be inferred. If the standard curve was nonlinear or the sample absorbance values did not fall within the standard range, the assay was repeated.

5.3.3.2.2 Method used in assay supernatant and solids from lignin treatment system 1

The solids remaining after 24 hours of reaction in the active rMnP/0.1 mM hydrogen peroxide and inactive rMnP/0.1 mM hydrogen peroxide treatments of lignin transformation system 1 had been previously dried for several hours at 105 °C. To remove soluble contaminants before use in the Pearl-Benson assay, they were washed under vacuum with ~100 mL distilled water over a 0.20 µm cellulose filter (Nalgene cat # 290-3320) and air dried. A mass of 6 mg air dried solids was added to each assay.

No liquid sample was involved with the assay of solids, so the 1000 µL of distilled water was added in its place to maintain assay volume. The assay on the solids was conducted according to the standard method except that it was scaled up to a total volume of 1,080 µL, the reactive assay was incubated for 20-25 minutes instead of 10 minutes, the unreactive assay was incubated for 15-20 minutes instead of 10 minutes, and only the net absorbance values were reported without conversion to alkali lignin units.

Alkali lignin standards of concentration 30, 20, 10, 0 mg/L were prepared and assayed.

5.3.3.3 Pearl-Benson results and discussion

5.3.3.3.1 Pearl-Benson assay on supernatant and solids from lignin transformation system 1

The alkali lignin was chosen as standard for the Pearl-Benson assay because it was assumed that a standard curve developed from such a compound would infer a dissolved lignin concentration closer to the true concentration than if a standard such as gallic acid were used due to alkali lignin's similarity with the expected soluble lignin transformation products.

The Pearl-Benson nitrosation assay was completed in triplicate on the supernatant and solids remaining after 24 hours of reaction in the active rMnP/0.1 mM hydrogen peroxide and inactive rMnP/0.1 mM hydrogen peroxide treatments of lignin transformation system 1. The assay was performed on the solids to test a hypothesis consisting of several parts: (1) during the reaction active rMnP could have altered the surface structure of the severe acid pretreated lignin solids, (2) these surface changes may involve the conversion of non-phenolic lignin units to phenolic units that would be susceptible to nitrosation, and (3) some of these nitrosated phenolic units may dissolve into solution and become observable through absorbance at the 430 nm wavelength of the Pearl-Benson assay.

The curve from standards in the concentration range 0- 30 mg/L was linear (Figure 5-18).

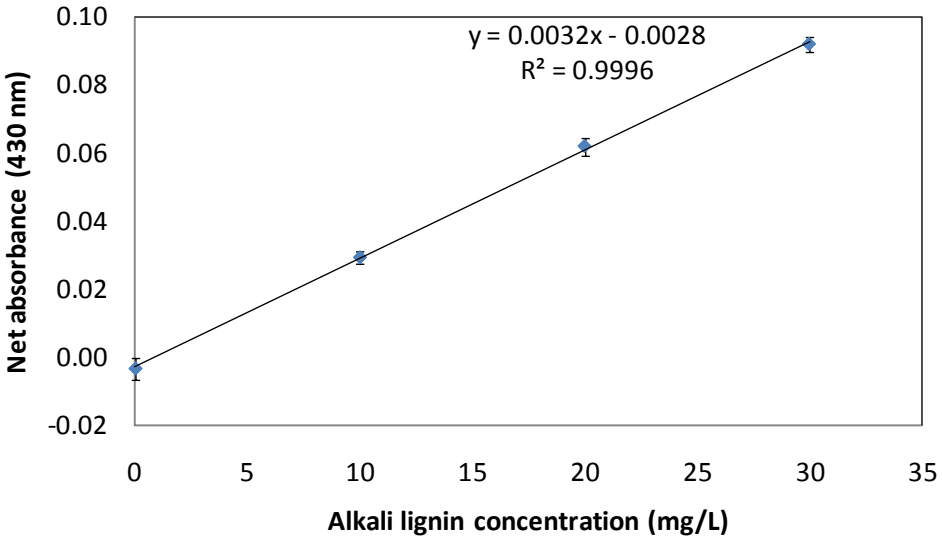

Figure 5-18: Standard curve for the Pearl-Benson phenolics assay using alkali lignin as standard compound.

If the assay responds to samples like it does to the alkali lignin, the standard curve shows that the assay is a sensitive assay. Both the greater linearity and sensitivity contrast with the standard curve of the Folin assay. Pearl-Benson absorbance of the 30 mg/L alkali lignin standard was 0.092, while the Folin absorbance of a 100 mg/L gallic acid standard was 0.020.

Figure 5-19 shows that the mean net absorbance of the supernatants and solids was negative, indicating that the mean blank absorbance was greater than the mean sample absorbance (net absorbance = sample absorbance – blank absorbance). Nitrosation of phenolics occurs in the reactive mixture because sodium nitrite is added to an acidic mixture. If sodium nitrite is added to an alkaline mixture, such as in the unreactive blank mixture, nitrosation does not occur (the unreactive mixture is alkaline because both 20 µL of 1.75 N acetic acid and 40 µL of 2 N ammonium hydroxide are added before sodium nitrite). Thus, a possible explanation for the negative absorbance of the active rMnP supernatant sample is that the acidic conditions of the reactive assay mixture allowed unknown chemical changes to occur to the sample that reduced absorbance, and the same changes did not occur in the alkaline environment of the unreactive assay mixture. The opposite could also have occurred: chemical changes occurred in the unreactive mixture to increase absorbance over the reactive mixture. This second possibility may

explain the negative net absorbance of the solid samples because the alkaline blank may have dissolved some of the solid lignin as appeared to occur during the Folin assay of the solids.

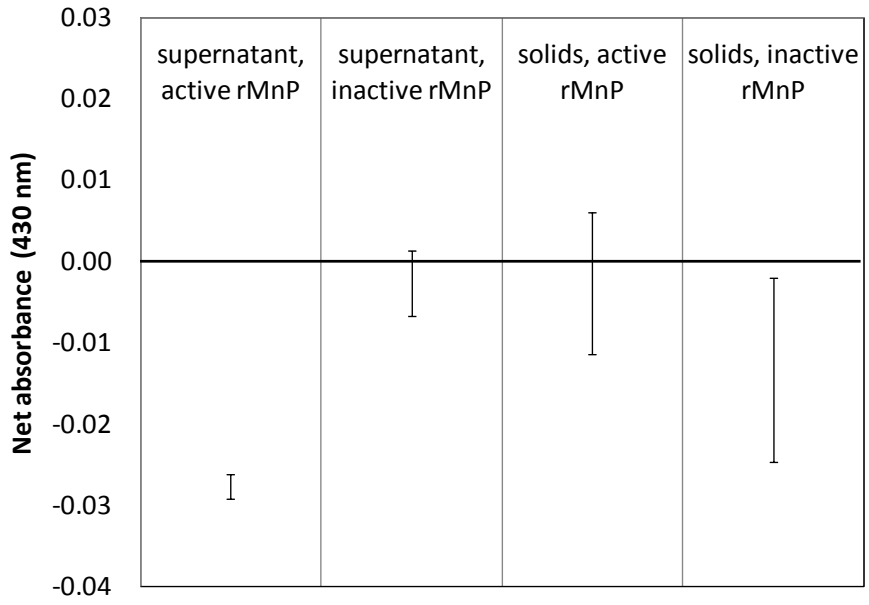

Figure 5-19: Net absorbance of supernatant and solids. Error bars are ±1 standard deviation of triplicate assays performed simultaneously.

Another important conclusion from Figure 5-19 is that there is a significant difference between the two supernatant samples, but not between the two solid samples, possibly indicating a difference between the two solid samples, but the nature of any such difference remains unknown.

5.3.4 Glucose assay

5.3.4.1 Introduction

It was necessary to know the glucose concentration during the enzymatic saccharification of wheat straw and the acid hydrolysis step of biomass compositional analysis. It was necessary to measure glucose also in the supernatant samples from the experiment using lignin transformation system 2 where cellulases were used. The glucose oxidase/horseradish peroxidase (GOP) assay was used due to its specificity for glucose, speed, and low cost. In the assay, glucose in a sample is oxidized to gluconic acid and hydrogen peroxide by glucose oxidase, then horseradish

peroxidase uses the hydrogen peroxide to oxidize added *o*-dianisidine to a product which exhibits an orange/brown color. In the presence of sulfuric acid, the oxidized *o*-dianisidine converts to a pink form, the concentration of which can be read by absorbance, and related to the original glucose concentration through a standard curve.

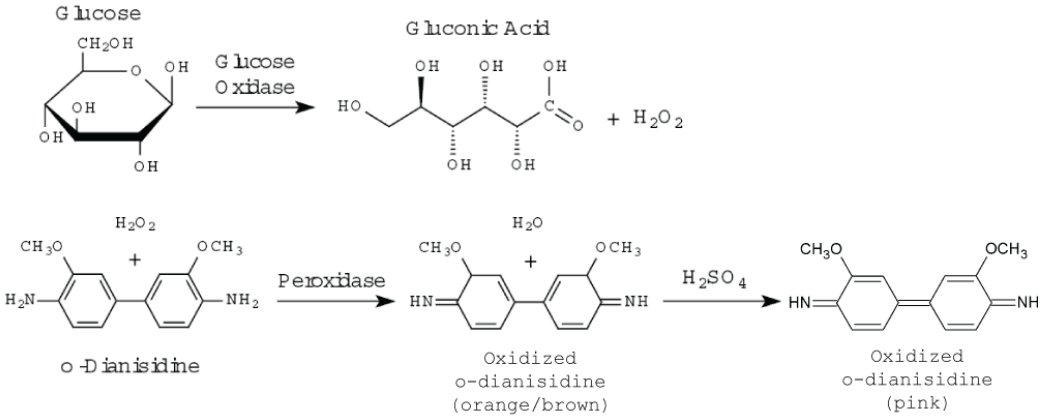

Figure 5-20: Reaction sequence for the glucose oxidase/horseradish peroxidase (GOP) assay for glucose. Adapted from Sigma-Aldrich (2006).

5.3.4.2 Glucose assay methods

5.3.4.2.1 Standard method

A glucose reagent was first made. It consisted of a solution of 500 units of crude glucose oxidase from *Aspergillus niger* (Sigma), 100 purpurogallin units of horseradish peroxidase (Sigma), and 800 µL of *o*-dianisidine solution. The *o*-dianiside solution was made by dissolving 5 mg *o*-dianisidine (Sigma) in 1 mL of 200 proof ethanol, then dissolving the ethanol mixture into 38.2 mL distilled water.

An aliquot of 50 µL of sample was added in triplicate to a 96-well polymerase chain reaction (PCR) plate. If a sample contained solids, it was first centrifuged to ensure that only solids-free sample was analyzed. Glucose standards made in the same medium as the samples were also added to the PCR plate. The plate was inserted into a thermal cycler (BioRad MyCycler), 100 µL of glucose reagent was added, and the mixtures were allowed to incubate at 37 °C for 20-25 minutes at which time samples containing glucose turned an orange/brown color.

After incubation, the mixtures were transferred to a clear 96 well polypropylene microplate. Each well of the microplate had been previously loaded with 100 µL of 6 M sulfuric acid. Upon addition to the acid, the samples turned pink. Air bubbles inside each well were removed with a hypodermic needle to avoid interfering with the absorbance reading, and the absorbance of each well read at 531 nm using a Perkin Elmer Victor 3 1420 plate reader. If the absorbance readings were outside the standards range, the assay was repeated with more dilute sample.

Hydrogen peroxide is typically added to reaction mixtures containing MnP enzyme since it is used to initiate the MnP enzymatic cycle. This hydrogen peroxide would interfere with the GOP assay applied to samples taken from these reaction mixtures, so it was necessary to rid of peroxide before conducting the assay. Thus, catalase solution (1 mg catalase (Sigma, from bovine liver) per mL distilled water) was added to each sample in a ratio of 102 µL catalase solution per 1 mL sample. A quantity of 50 µL of the catalase/sample mixture then served as the sample in the GOP assay. The catalase/sample mixtures were allowed to incubate at 37 °C in the thermal cycler before starting the GOP assay with the addition of glucose reagent.

5.3.4.3 Glucose assay results and discussion

5.3.4.3.1 Assay of lignin transformation system 2

The standard glucose assay was used to measure glucose generation in the supernatant samples from the reaction using lignin transformation system 2. Shown here are only the treatments that contained cellulases. The treatments without cellulases showed negligible glucose levels at all times.

The substrate used in the experiment was the wheat straw in which cellulose had already been partially removed by cellulases over 48 hours of enzymatic saccharification (Section 4.5.2), but subsequent desorption of cellulase and re-saccharification showed that the remaining cellulose was still accessible to cellulases (section 4.5.5). Thus, the evolution of glucose from the substrate is not unexpected.

The base case glucose levels (Figure 5-21) already were ~0.2 mg/mL in the first sample taken ~20 minutes after enzyme addition. The levels continued to increase, and upon the addition of more cellulases at 29 hours, the glucose production rate increased with subsequent decline. The

decline was likely due to microbial growth as confirmed by culturing the supernatant of one replicate on YPD media.

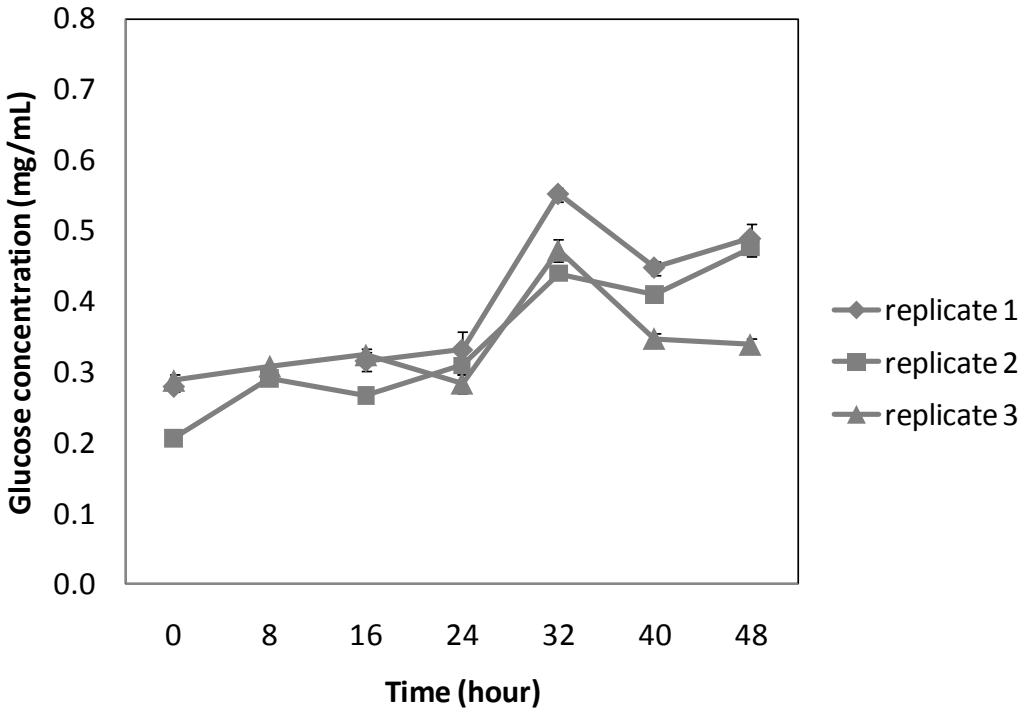

Figure 5-21: Glucose concentration over time in supernatant of base case. Error bars are ±1 standard deviation of triplicate assays performed simultaneously.

The "no rMnP" treatment (Figure 5-22) showed a similar initial glucose concentration as the base case, but a sharper and more sustained rise over time. The sharper rise could be due to less microbial contamination or the absence of rMnP inhibition of cellulase hydrolysis. Inhibition of cellulases by rMnP has not been demonstrated, but is proposed as a possibility since the Mn(III) chelates or reactive radical species generated during rMnP turnover could react with and inactivate cellulases. The inactivation of cellulases could occur by means of hydrogen abstraction of any acidic hydrogen on the polypeptide chain and the ensuing radical chain reactions. There is an abundance of acidic hydrogens, and the resulting radical reactions possibly could damage full enzyme function.

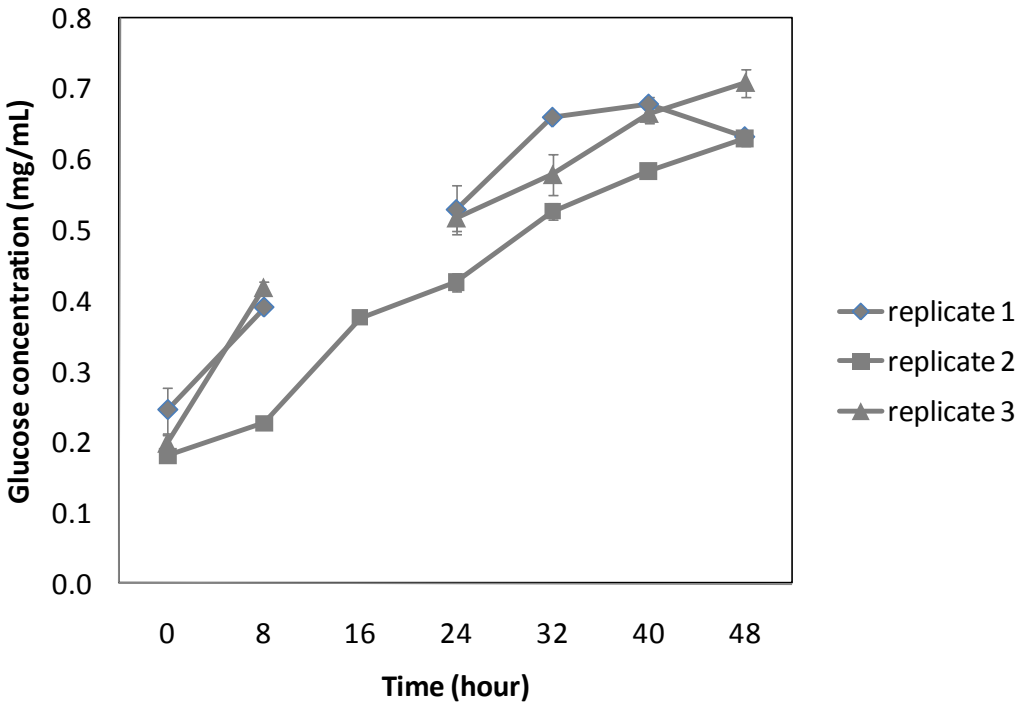

Figure 5-22: Glucose concentration over time in supernatant of "no rMnP" treatment. Error bars are ±1 standard deviation of triplicate assays performed simultaneously.

The "no cellulases at second enzyme addition" treatment (Figure 5-23) also shows a similar initial glucose concentration as the base case and "no rMnP" treatment, and some glucose decrease later in the reaction, but surprisingly low glucose generation throughout. This result is further evidence that rMnP may inhibit cellulase hydrolysis.

Previously it was found by the Folin assay that the base case and "no cellulases at second enzyme addition" treatments contained the highest levels of phenolics, thus suggesting a synergy between the rMnP and cellulases in solubilizing lignin. One may expect that the more lignin is degraded, the more cellulose is made accessible to cellulases and enzymatically hydrolyzed to glucose. This does not appear to occur here since less glucose was evolved in the two treatments with the most apparent evolved phenolics.

This association between low evolved glucose and high phenolics suggests the possibility that rMnP-induced oxidation of cellulases transformed the cellulases into a chemical species that would be detected as phenolics in the Folin assay.

One of the hypotheses of the experiment using lignin degradation system 2 was that rMnP would increase the rate of cellulase-mediated saccharification by degrading lignin which may sterically hinder cellulase access to cellulose. This dynamic would be detected by observing more glucose in cellulase treatments with rMnP than without, but the exact opposite was observed here: more glucose was evolved in treatments without rMnP.

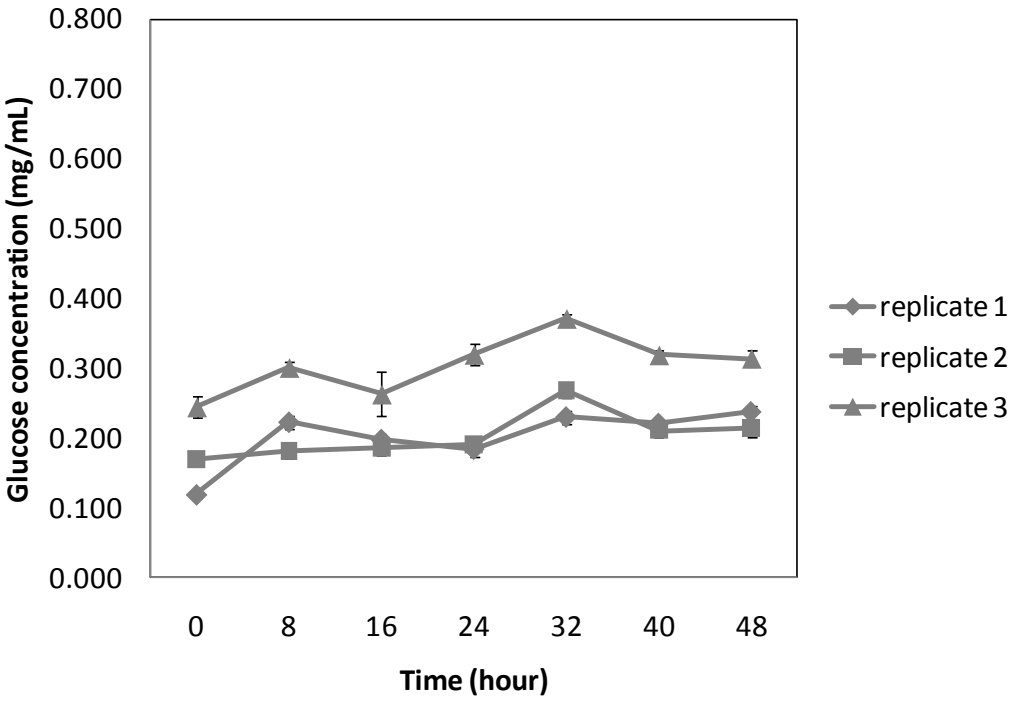

Figure 5-23: Glucose concentration over time in supernatant of "no cellulases at second enzyme addition" treatment. Error bars are ±1 standard deviation of triplicate assays performed simultaneously.

5.3.5 rMnP activity assay

5.3.5.1 Introduction

Knowing the activity of rMnP in reaction mixtures is important for ensuring sustained enzymatic transformation of substrates and for studying the kinetics of reactions. The MnP activity in a sample was measured by monitoring the quantity of 2,6-dimethoxyphenol (2,6-DMP) oxidized to the diquinone product (2,2',6,6'-tetramethoxydibenzo-1,1'-diquinone) by monitoring absorbance

at 469 nm (Figure 5-24) (Wariishi, Valli and Gold 1992). One unit of activity was defined as the production of 1 µmole of diquinone in 1 minute.

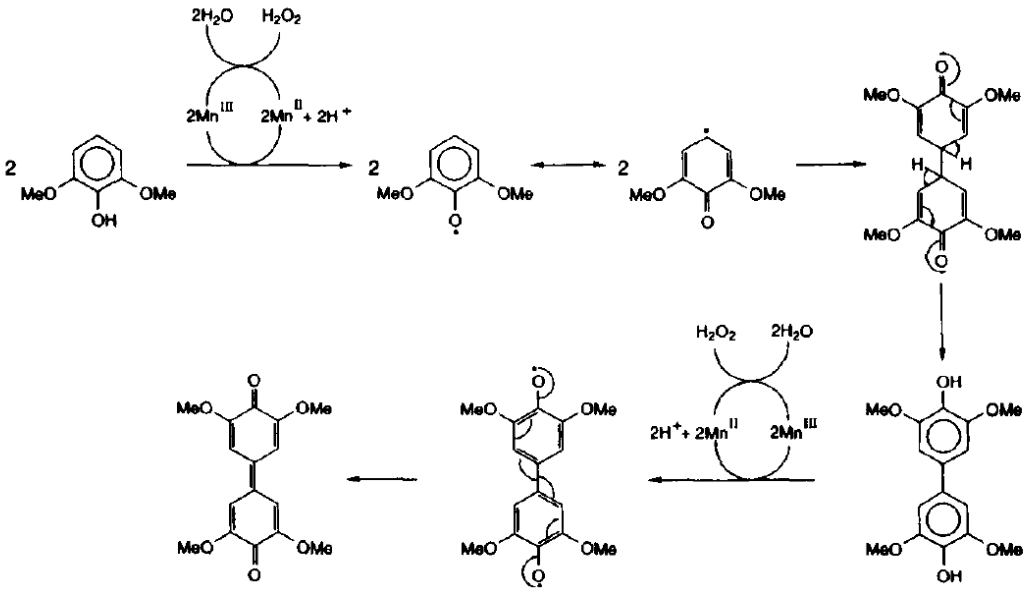

Figure 5-24: Oxidation of 2,6-dimethoxyphenol to the colored 2,2',6,6'-tetramethoxydibenzo-1,1'-diquinone by MnP (Wariishi, Valli and Gold 1992).

5.3.5.2 rMnP activity methods

5.3.5.2.1 Standard method

The assay was performed in cuvettes or in clear 96-well polypropylene microplates. In cuvettes, the assay was performed by combining, in order, 600 µL of sample, and 100 µL each of 4.0 mM $MnSO_4$, 502 mM disodium malonate, and 1.0 mM 2,6-DMP. The absorbance of the cuvette was then blanked. Exactly one minute after addition of 100 µL of 1.1 mM hydrogen peroxide, the absorbance was read at 469 nm. The sample was diluted to keep the absorbance reading in the linear range of 0.1-0.7 (Yee 2009). The absorbance was then used to determine the activity of the enzyme according to Equation 5-1.

$$A = \left(\frac{\text{Abs}}{\ell\varepsilon}\right)\left(\frac{10^6\ \mu\text{mole}}{\text{mole}}\right)\left(\frac{1\ \text{L}}{1000\ \text{mL}}\right)\text{Df}_{\text{enzyme}} \qquad \text{Equation 5-1}$$

Equation 5-1 has the following variables: A=activity (in U/mL); Abs=absorbance one minute after H_2O_2 addition, ℓ=path length (1 cm), ε=49,600 $M^{-1}cm^{-1}$ (molar absorptivity of 2,2',6,6'-tetramethoxydibenzo-1,1'-diquinone), and Df_{enzyme}=dilution factor of the sample in the assay volume of 1000 µL. The resulting activity from Equation 5-1 was then adjusted to account for any dilution of the sample that occurred before it was used in the assay.

When performed in microplates, the assay volume was 200 µL, so the volume of each component was reduced by a factor of five (120 µL sample, and 20 µL each of $MnSO_4$, disodium malonate, 2,6-DMP, and hydrogen peroxide). The Perkin Elmer Victor 3 1420 plate reader was used to add the last two components, then the absorbance was read one minute later at 465 nm. This wavelength was chosen because a filter emitting this wavelength was the closest available to the desired 469 nm.

When performing the microplate assay, the assay absorbance of several MnP standards in the wells was correlated against the assay absorbance of the same standards in the cuvettes so that well absorbance could be related to the enzyme activity of the standards calculated using Equation 5-1 and the cuvette absorbance values of those standards.

5.3.5.2.2 Methods used in rMnP stability study

Ten mixtures, 1.5 mL each, were made that contained rMnP (0.5 U/mL) and various other components. The base case mixture consisted of only rMnP (0.5 U/mL) in distilled water. Other mixtures contained the base case components plus one or more of the following: sodium malonate buffer (50 mM, pH 4.5), hydrogen peroxide (0.1 or 0.5 mM), $MnSO_4$ (0.4 mM), linoleic acid (9.0 mM), and glycerin (16.67 mM). The mixtures sat at 4 °C and 21 °C for ~28 hours before rMnP activity was measured in each using the microplate assay described previously.

Six rMnP standards spanning the enzyme concentration of the mixtures were made from a concentrated rMnP stock solution and their cuvette assay absorbance values measured. The standards were assayed to correlate with the microplate assay absorbance values and to test for linearity between enzyme concentration and assay response.

5.3.5.3 rMnP activity results and discussion

5.3.5.3.1 rMnP stability study

When rMnP reacts with a substrate over long periods, it is desirable to maintain rMnP activity to sustain substrate modification by the enzyme. There was a question whether the presence of certain components with rMnP would maintain or damage rMnP activity over time, so an experiment was completed to test the effect. The components added were sodium malonate, hydrogen peroxide, manganese, linoleic acid, or a combination thereof. Sodium malonate, hydrogen peroxide, and manganese were chosen since all are typically added to initiate rMnP degradation and buffer the reaction solution. Linoleic acid was chosen since it has been shown to be an effective redox mediator of rMnP oxidation of substrates, and glycerin was added to test the effect of a soluble short chain organic compound on rMnP activity. Malonate is also a soluble short chain organic, and testing glycerin would allow comparison with the effect of malonate.

Equation 5-1 assumes a linear relationship between enzyme concentration and the assay absorbance. To test this assumption, six rMnP standards made from a stock solution of rMnP concentrate were assayed. The absorbance of the standard with no rMnP was subtracted from the absorbance values of the other five standards, and the corrected absorbance values were plotted against the concentration of rMnP in the standards. The result is shown in Figure 5-25. The curve is slightly nonlinear at lower rMnP concentrations, leading to some inconsistency between rMnP activity values calculated from absorbance values <0.15 versus absorbance values >0.15.

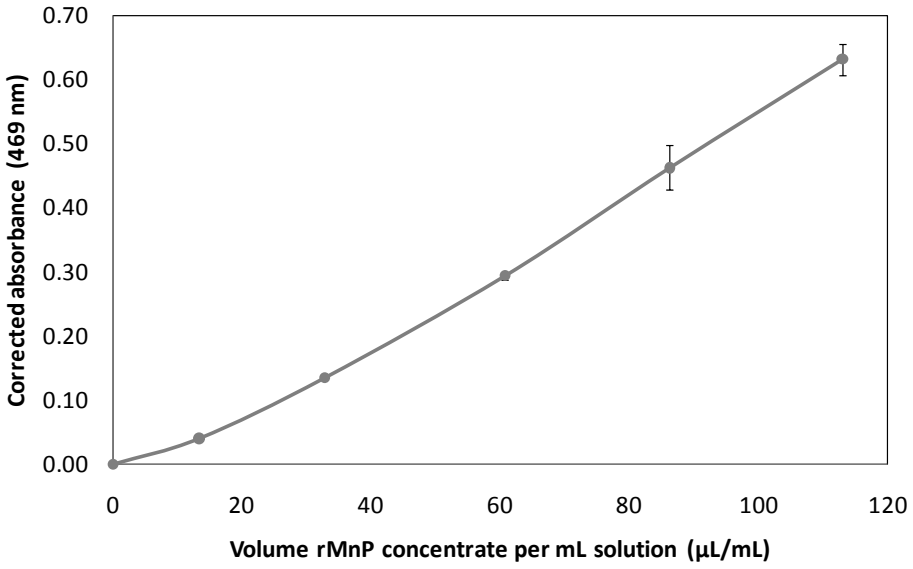

Figure 5-25: Corrected absorbance vs. concentration of rMnP standards.

The final rMnP activities of the base case (rMnP and distilled water) and the mixtures containing one extra component are shown in Figure 5-26. The addition of malonate and glycerin appears to have at least maintained rMnP activity at the initial activity level of 0.5 U/mL, while there was significant loss of activity in the base case and with linoleic acid. The fact that the activities of the malonate and glycerin mixtures are greater than 0.5 U/mL means either there was inaccuracy in the initial enzyme addition and more than 0.5 U/mL was added, or the malonate and glycerin enhance enzyme activity even after ~28 hours. The results cannot indicate which occurred. Malonate and glycerin are both short chain soluble organic compounds and may interact similarly with rMnP, whereas linoleic acid is an insoluble fatty acid. The enzyme possibly could have become sequestered inside micelles of linoleic acid thereby removing some of the enzyme from the activity assay. The decrease in the base case activity could have been due to denaturation and inactivation that is expected to occur over time.

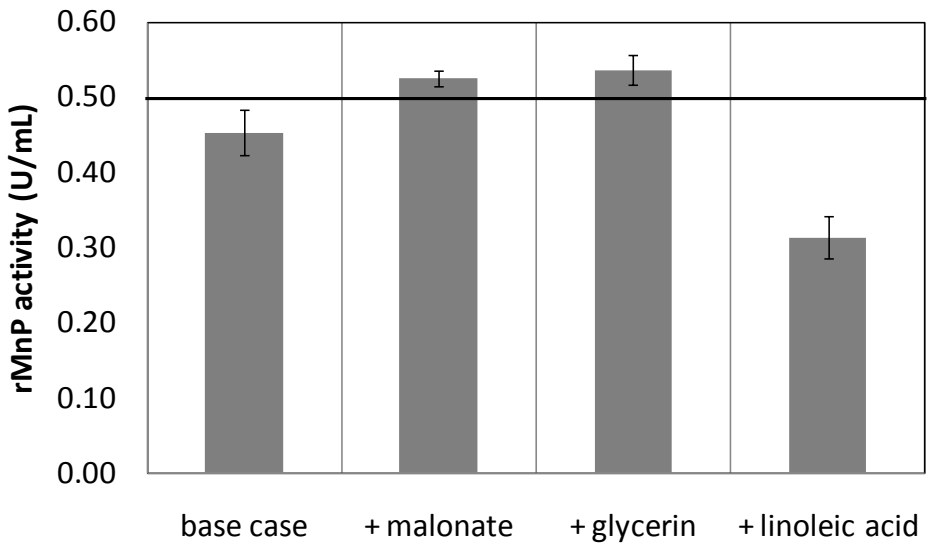

Figure 5-26: rMnP activities of mixtures with one extra component after ~28 hours. The horizontal line at 0.50 U/mL is shown to indicate the initial rMnP activity. An error bar is ±1 standard deviation of quadruplicate assays of one mixture performed simultaneously.

The final rMnP activities of the mixtures containing two or more extra component are shown in Figure 5-27. The addition of manganese or manganese and 0.5 mM peroxide to the malonate appears to have not harmed enzyme activity. The components possibly may have enhanced activity but the difference is not statistically significant because it is barely beyond the standard deviations. Addition of 0.1 mM peroxide and manganese also appears not to have harmed activity, but the addition of either 0.1 mM or 0.5 mM peroxide did harm activity. It appears that the presence of manganese was essential to prevent loss of activity if peroxide was present. The manganese could have bound to the active site of the enzyme and prevented inactivation by hydrogen peroxide.

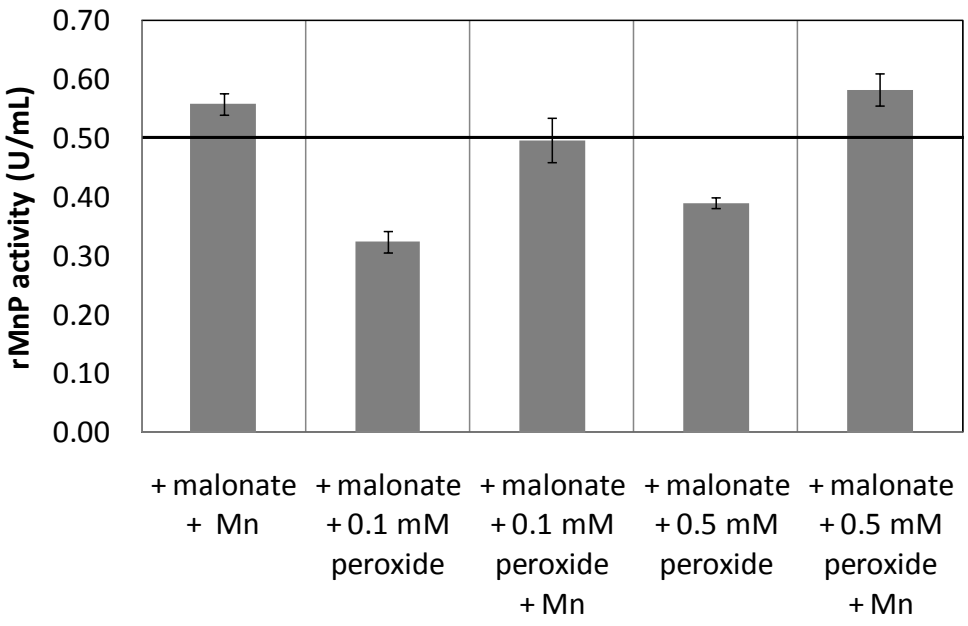

Figure 5-27: rMnP activities of mixtures with two or more extra components after ~28 hours. The horizontal line at 0.50 U/mL is shown to indicate the initial rMnP activity. An error bar is ±1 standard deviation of quadruplicate assays of one mixture performed simultaneously.

5.3.5.3.2 rMnP activity in lignin degradation system 2

rMnP activity was measured in the time course samples taken from the experiment using lignin degradation system 2. The microplate assay method was used. The results for only two treatments are shown here to demonstrate the challenges of the assay. The results for the base case treatment (Figure 5-28) showed inconsistency between replicates, and occasional high variation in individual activity measurements (e.g. 0 hour measurement of replicate (1).

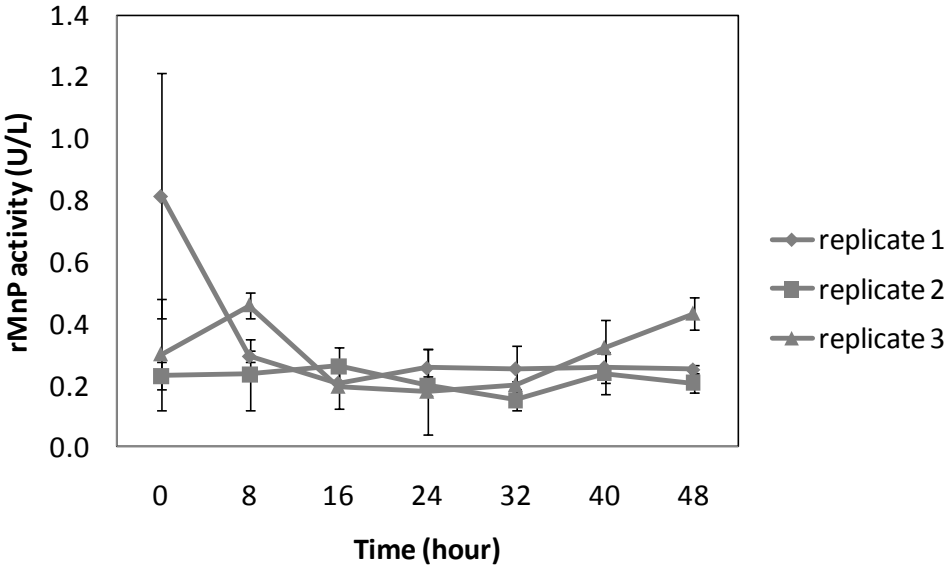

Figure 5-28: rMnP activity time course for the base case treatment of the experiment using lignin degradation system 2. Error bars are ±1 standard deviation of triplicate activity assays performed simultaneously.

The time course for the "no cellulases at the second enzyme addition" treatment (Figure 5-29) also showed inconsistency and variation among measurements, but to a lesser degree.

Some of the inconsistency between replicates is likely due to actual rMnP activity differences between those replicates, but the high variability in individual activity measurements is due to suboptimal assay results. Another trial of the microplate rMnP activity assay on samples from the lignin degradation system 1 experiment gave similarly inconsistent or variable results (data not shown).

Since activity measurements are often needed only for occasional time points, an appropriate strategy to reduce variability is to assay fewer samples in more replicates. The cuvette assay has tended to give results with lower variability, so performing the cuvette version of the assay is another option.

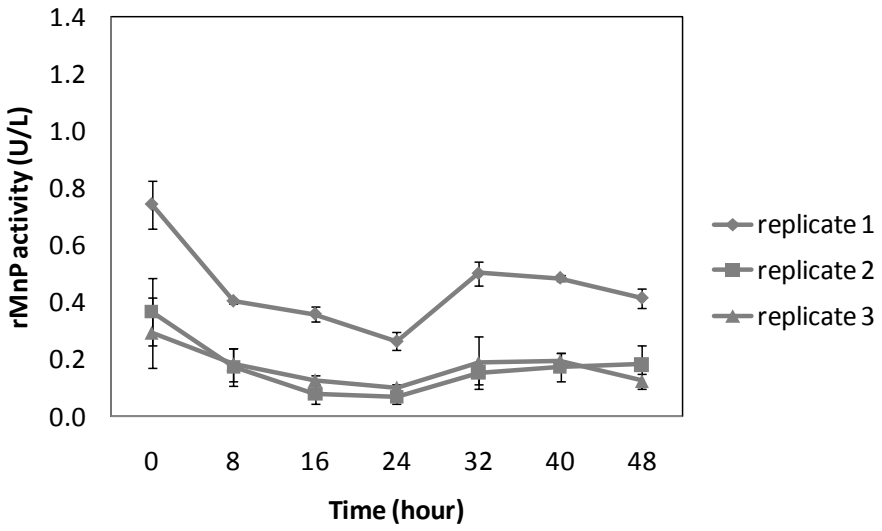

Figure 5-29: rMnP activity time course for the "no cellulases at the second enzyme addition" treatment of the experiment using lignin degradation system 2. Error bars are ±1 standard deviation of triplicate activity assays performed simultaneously.

5.3.6 pH

The pH of the reaction mixtures can affect enzyme stability, so it was measured at 0, 16, 32, and 48 hours in the treatments of lignin degradation system 2. The pH was fairly constant, staying between 6.2 and 6.0 for nearly all replicates throughout the 48 hours of the experiment. The reaction mixtures were initially buffered to pH 4.8 with 50 mM acetate, so the buffering capacity was overwhelmed with the alkalinity of added reaction components, probably the lignin substrate. Higher buffering capacity is recommended for future experiments with this lignin substrate.

5.3.7 Hypotheses tested

Among the assays completed during the tests of the two lignin transformation systems, there was not enough evidence to either confirm or deny the central hypotheses that (1) rMnP is capable of degrading solid lignin only in the presence of a polyunsaturated fatty acid, and that the degree of degradation will increase with increasing unsaturation, and (2) an rMnP system without a polyunsaturated fatty acid (i.e. a mildly oxidizing rMnP system) will degrade a solid lignin only after a Fenton pretreatment, and the ease by which the rMnP system degrades the lignin increases with increasing severity of the Fenton pretreatment as varied by the concentration of iron reducing agent. Experiments to confirm or deny these hypotheses are left to future studies.

6 CONCLUSIONS AND FUTURE WORK

6.1 Conclusions

6.1.1 Methylene blue studies

Treatment of methylene blue by a mixture of Fe(III), hydrogen peroxide, and iron reducing agent appears to degrade the dye chromophore by attack of hydroxyl radicals formed via the Fenton reaction. By analogy to the lipid/MnP degradation of phenanthrene, a tentatively proposed intermediate of methylene blue degradation by the Fenton system is a tetracarboxylic acid.

Dye degradation with wheat straw extracts occurred more rapidly than with DOPAC, possibly due to the degradation with extracts proceeding by means other than hydroxyl radical attack. For the concentrations of wheat straw extracts and DOPAC tested, the extent of degradation was directly related to the extract concentration, but higher DOPAC concentration eventually diminished the extent of degradation possibly due to DOPAC serving as a competitive substrate with the dye for attack by hydroxyl radicals.

Three unsaturated fatty acids (oleic, linoleic, and linolenic acids) were emulsified in Tween 20 and tested for their ability to degrade the dye when combined with the basic rMnP system consisting of rMnP, hydrogen peroxide, Mn(II), acetate buffer, dye, and distilled water. The magnitude of the degradation rates followed the order oleic acid<linoleic acid=linoleic acid. The addition of malonate or oxalate instead of an emulsified fatty acid resulted in degradation rates intermediate between oleic and linoleic acids. Thus, the first hypothesis of the methylene blue experiments was shown partly true: a polyunsaturated fatty acid was necessary in the rMnP system to significantly degrade the dye, and the greater the level of unsaturation of the fatty acid the greater the amount of degradation up until linolenic acid where the degradation amount was equal to that of linoleic acid.

Several components were then added to the rMnP system containing linoleic acid emulsified with Tween 20. Each iron reducing agent (vanillic acid, DOPAC, DOPAC + Fe(III), wheat straw extracts) inhibited dye degradation probably by the iron reducing agent serving as a radical scavenger or metal chelator (Kapich, Galkin and Hatakka 2007). The addition of oxalate did not have any significant effect, but malonate dramatically increased the rate. The system consisting of

rMnP, emulsified linoleic acid, and malonate was most quickly degraded the dye of all systems tested.

There are two likely reasons this system was optimal. The first reason is that malonate increases the rate of enzyme turnover by chelating and removing Mn(III) from rMnP more effectively than acetate or oxalate, the other two short chain organic acids tested. The second reason is that linoleic acid is easily converted to a peroxyl radical which is capable of oxidizing methylene blue through hydrogen or electron abstraction. Linoleic acid is more easily peroxidized because it contains a di-unsaturated functional group.

The same components were added to the rMnP system containing linolenic acid emulsified with Tween 20. But since the emulsion had been previously frozen, the results do not confidently indicate the effects of these components on the ability of the linolenic acid systems to degrade the dye.

The linoleic acid/Tween 20/rMnP system's ability to degrade the dye was greater in the presence of malonate than with oxalate, and the presence of oxalate had no significant effect. This result agrees with the ability of a previously reported Tween 80/rMnP system to depolymerize milled pine wood which showed that depolymerization occurred more with malonate than oxalate (Hofrichter, Lundell and Hatakka 2001). On the other hand, the ability of the linoleic acid/Tween 20/rMnP system's ability to degrade the dye was greater in the presence of malonate than without. This result does not agree with the ability of a linoleic acid/Tween 20/rMnP system to degrade a lignin model compound (Kapich, Steffen, et al. 2005) where the presence of malonate inhibited degradation over the absence of malonate. The result of the milled pine wood study could be due to malonate supporting greater Mn(III) production by MnP, or either the extractives in the pine or the Tween 80 surfactant interacting with malonate in some way. It remains unknown why the same effect as observed with the lignin model compound would not have been observed in the study presented here on methylene blue degradation since the reaction conditions are similar. Further research is needed here.

In the optimal linoleic acid/Tween 20/ rMnP/malonate dye degradation system, rMnP and Mn(II) were essential for dye degradation, while hydrogen peroxide was not, although dye degradation was slower without hydrogen peroxide. In the absence of hydrogen peroxide, enzyme turnover

may be induced by hydroperoxy acetic acid ($HOOCH_2COOH$) or hydrogen peroxide from malonate degradation, and by hydrogen peroxide from superoxide disproportionation or superoxide reduction by Mn(II). Enzyme turnover from these peroxides would produce sufficient Mn(III) and peroxyl radicals of linoleic acid or acetic acid to degrade the dye.

Removing acetate from the linoleic acid/Tween 20/malonate/rMnP system slightly increased the reaction rate probably because removal eliminated competition between the acetate and the other two species (malonate and linoleic acid) for coordination with Mn(III). Without competition with acetate, Mn(III) could oxidize malonate and linoleic acid and speed the formation of peroxyl radicals from both species that could oxidize the dye.

The presence of any of the three iron reducing agents vanillic acid, DOPAC, or wheat straw extracts consistently inhibited dye degradation by rMnP whether added together with the rMnP treatment, or as part of a Fenton treatment before the rMnP treatment. Also, the degree of inhibition depended entirely on their concentration. The three compounds could have acted as competitive substrates with the dye for rMnP oxidation, radical scavengers, or chelators of manganese, and therefore their presence should be avoided when one wishes to oxidize recalcitrant substrates with rMnP. The results were unable to confirm or deny the second hypothesis of the methylene blue experiments which was that an rMnP system not containing a polyunsaturated fatty acid (i.e. a mildly oxidative rMnP system) is capable of degrading the dye only when the dye is previously chemically altered with hydroxyl radicals generated by the Fenton reaction, and the rMnP degradability depends on the severity of the Fenton treatment gauged by the concentration of the iron reducing agent. The hypothesis could not be confirmed or denied because the presence of residual unoxidized iron reducing agent during the rMnP phase of dye degradation masked any chemical changes to the dye that could influence its degradability.

6.1.2 Lignin transformation systems studies

A Mn(III) malonate complex forms when rMnP is combined with 0.1 mM hydrogen peroxide, sodium malonate, and manganese. The complex absorbs maximally at 270 nm, and this absorbance peak likely would interfere with the detection of phenolics evolved from solid lignin since phenolics typically absorb ~270 nm (Silverstein, Bassler and Morrill 1991). Addition of sodium sulfide reduces the absorbance due to the Mn(III) malonate complex and thereby allows

detection of phenolics. Most of the Mn(III) malonate complex formed was unable to pass through a 10 kDa membrane, showing that the complex may have a polymeric structure.

More phenolics, as detected by the Folin assay, were evolved in the treatments with both active rMnP and active cellulases. This may be due to a genuine synergy between the two enzymes in degrading lignin, rMnP converting the cellulases to products that are detected as phenolics, or a higher concentrations of amino acids in the active enzymes are reducible by the Folin-Ciocalteau reagent compared to the inactive enzymes.

The presence of rMnP in a mixture of rMnP and cellulases appears to inhibit substrate saccharification compared to a mixture of just cellulases. A possible reason for this dynamic is rMnP-induced oxidation and inactivation of the cellulase enzymes.

In the trials of the two lignin transformation systems, there was not enough evidence to either confirm or deny the central hypotheses that (1) rMnP is capable of degrading solid lignin only in the presence of a polyunsaturated fatty acid, and that the degree of degradation will increase with increasing unsaturation, and (2) an rMnP system without a polyunsaturated fatty acid (i.e. a mildly oxidizing rMnP system) will degrade a solid lignin only after a Fenton pretreatment, and the ease by which the rMnP system degrades the lignin increases with increasing severity of the Fenton pretreatment as varied by the concentration of iron reducing agent. Experiments to confirm or deny these hypotheses are left to future studies.

6.1.3 Folin assay development

It is recommended to perform the Folin assay with a 20% (w/v) sodium carbonate solution, 3-12 minute incubation time, and 2 hour ± 15 minute development time to reduce unnecessary variability and facilitate inter-assay comparisons.

The result of the Folin assay is independent of the presence of 42 µM hydrogen peroxide or 7.7 µL/mL of rMnP concentrate in the active or inactive form. Other concentrations of hydrogen peroxide and rMnP concentrate may also not affect the assay, but further studies are necessary to confirm this.

6.1.4 rMnP stability

The presence of sodium malonate buffer (pH 4.5) and glycerin appeared to help maintain rMnP activity over time. When rMnP was combined with malonate, the presence of manganese prevented activity loss from hydrogen peroxide.

6.2 Future work

The studies that should be done first to extend the experiments completed here include applying the same rMnP systems used on methylene blue to a solid lignin substrate and monitoring at least absorbance of the reaction supernatant and weight of the solids before and after treatment. More advanced analytical technique such as electron microscopy, high performance liquid chromatography (HPLC), size exclusion chromatography (SEC), or Fourier transform infrared spectroscopy (FTIR) may also be necessary to better understand the effects of the rMnP systems on the solid lignin substrate. Information obtained from these techniques includes the number and hydrophobicity of products formed (HPLC), their molecular weight (SEC), and chemical changes to the surface of the lignin (FTIR). These first experiments would begin to test whether the ability of an rMnP system to degrade methylene blue correlates to its ability to degrade or otherwise transform a solid lignin substrate, and would help develop the analytical tools necessary to understand what is occurring to the solid substrate.

If a correlation is found, then further rMnP systems could be tested on both the methylene blue and solid lignin systems to gather more confidence in the predictive ability of using methylene blue as a lignin analog. If a correlation is not found, then a better soluble or insoluble lignin analog may exist. MnP will act differently towards soluble and insoluble solid substrates due to differences in enzymatic accessibility and diffusibility, so a solid lignin analog (e.g. a phenolic plastic) may better predict the ability of MnP to act upon solid lignin. Whichever surrogate is used, the goal is to simplify monitoring of the ability of an rMnP system to transform or degrade the lignin analog through a simple assay such as absorbance so that complicated analytical techniques can be avoided. The results of screenings and kinetic studies using a lignin analog will hopefully indicate which rMnP systems (made of rMnP, other enzymes, metals, organic acids, lipids, etc.) are most oxidative and the mechanisms of action.

The rMnP systems tested thus far have included simple additions of short chain organic acids, fatty acids, iron, iron reducing agents, and wheat straw extracts to the basic rMnP system (rMnP, Mn(II), hydrogen peroxide, distilled water) and observing their effects upon methylene blue, acid insoluble lignin, and the lignin remaining after dilute acid pretreatment and saccharification. Future research on the effects of isolated fungal enzymes on biomass should expand the studied conditions by using what is known about the processes white rot fungi use *in vivo* to degrade lignin. Such knowledge will help develop enzymatic treatment systems that mimic these natural processes. Consideration could be extended to all the other enzymes white rot fungi use, including the other lignin-degrading enzymes, cellulases, hemicellulases, and the enzymes that generate hydrogen peroxide to support MnP turnover. Other important considerations include Fenton chemistry, chelation of metals already present in biomass by oxalate or other organic acids, reduction/oxidation of metals by organics, the function of the polysaccharide matrix that fungal hyphae secrete over cell wall lumens, identifying the triggers for whether a white rot fungus acts as a selective or nonselective lignin degrader, and studying the importance of an increasing pH gradient from the fungal hyphae to the interior of a wood cell. Formation of peroxyl (Watanabe, Katayama, et al. 2000) or hydroxyl radicals (Goodell, Jellison, et al. 1997) inside the cell wall may depend on a higher pH inside the cell wall relative to near the hyphae.

White rot fungi may use alternating chemical or enzymatic cycles (e.g. Fenton chemistry, MnP peroxidation, cellulases, Fenton chemistry, MnP peroxidation, cellulases, etc.) to degrade biomass, and it may be important to mimic these cycles when applying enzymatic treatments to biomass in the laboratory. Before these cycles could be applied to substrates in the laboratory, the chemical changes occurring in any cycle element should be elucidated more thoroughly. The transient state of the radical species involved in some mechanisms may make the work challenging, but a detailed understanding is essential to controlling and optimizing an industrial system.

If isolated enzymes from white rot fungi are used in an industrial process, ultimately the cost of producing those isolated enzymes must be considered, as should be the stability of the enzymes, and how integrating them into an industrial step affects the cost of the entire process. If using isolated enzymes is costly, then one way to reduce cost may be to avoid biological enzyme production altogether, and use a synthetic enzyme, such as tetra-amido macrocyclic ligand

(TAML) that functions similarly to naturally occurring oxidative enzymes (Institute for Green Oxidation Chemistry 2008). Another way to avoid the costs of isolating enzymes is to grow the whole fungal organism and manipulate its environment to elicit the desired response, such as adding a signaling chemical to induce selective lignin degradation. Promising techniques for using whole fungal cultures to degrade lignin or other biomass components should borrow heavily from the decades of research on biopulping and biobleaching (Young and Akhtar 1998).

Immobilization of MnP using specific coupling techniques has already shown higher enzyme stability to temperature, pH, and organic solvents, thus giving biocatalysis an advantage as a potential application of MnP (Van Aken, et al. 2000); (Okazaka, et al. 2001). And the cost of enzyme production may not impact the degree to which biocatalysis is used as much as other applications (pulp bleaching) that use greater quantities of the enzyme.

BIBLIOGRAPHY

Adler, E. "Lignin chemistry--past, present and future." *Wood Sci Technol* 11 (1977): 169-218.

Adney, B, and J Baker. *Measurement of Cellulase Activities.* Golden, Colorado: National Renewable Energy Laboratory, 2008.

Aguiar, A, P Brazil de Souza-Cruz, and A Ferraz. "Oxalic acid, Fe3+-reduction activity and oxidative enzymes detected in culture extracts recovered from Pinus taeda wood chips biotreated by Ceriporiopsis subvermispora." *Enzyme and Microbial Technology* 38 (2006): 873-878.

Ahmad, S. *Oxidative Stress and Antioxidant Defenses in Biology.* NY: Chapman and Hall, 1995.

Antal, MJ Jr. "Water: a traditional solvent pregnant with new applications." Edited by HJ Jr. White. *Proceedings of the 12th International Conference on the Properties of Water and Steam.* New York: Begell House, 1996. 24-32.

Antongiovanni, M, and C Sargentini. "Variability in chemical composition of straws." *Options Méditerranéennes – Série Séminaires* 16 (1991): 49-53.

Arantes, V, and AMF Milagres. "Degradation of cellulosic and hemicellulosic substrates using a chelator-mediated Fenton reaction." *Journal of Chemical Technology and Biotechnology* 81 (2006): 413-419.

Arantes, V, and AMF Milagres. "The effect of a catecholate chelator as a redox agent in Fenton-based reactions on degradation of lignin-model substrates and on COD removal from effluent of an ECF kraft pulp mill." *Journal of Hazardous Materials* 141 (2007): 273-9.

Arantes, V, and AMF Milagres. "The synergistic action of ligninolytic enzymes (MnP and Laccase) and Fe3+-reducing activity from white-rot fungi for degradation of Azure B." *Enzyme and Microbial Technology* 42 (2007): 17-22.

Atalla, R. *Proceedings Eigth International Symposium Wood and Pulping Chemistry.* Helsinki: KCL, 1995. 77.

Bagby, M O, G H Nelson, E G Helman, and E F Clark. "Determination of lignin in non-wood plant fiber sources." *Tappi* 54 (1971): 1876-1878.

Bao, W, Y Fukushima, KA Jr. Jensen, MA Moen, and KE Hammel. "Oxidative degradation of non-phenolic lignin during lipid peroxidation by fungal manganese peroxidase." *FEBS Letters* 354 (1994): 297-300.

Blanchette, RA. *Microorganisms causing decay in trees and wood.* 2006. forestpathology.cfans.umn.edu/microbes.htm (accessed December 22, 2009).

Blanchette, RA, AR Abad, RL Farrell, and TD Leathers. "Detection of lignin peroxidase and xylanase by immunocytochemical labeling in wood decayed by basidiomycetes." *Appl. Environ. Microbiol.* 55 (1991): 1457-1465.

Blanchette, RA, EW Krueger, JE Haight, M Akhtar, and DE Akin. "Cell wall alterations in loblolly pine wood decayed by the white-rot fungus, Ceriporiopsis subvermispora." *Journal of Biotechnology* 53 (1997): 203-213.

Brownell, HH, EKC Yu, and JN Saddler. "Steam explosion pretreatment of wood: effect of chip size, acid, moisture content, and pressure drop." *Biotechnology and Bioengineering* 28 (1986): 792-801.

Buettner, GR. "The pecking order of free radicals and antioxidants: lipid peroxidation, α-tocopherol, and ascorbate." *Arch Biochem Biophys* 300 (1993): 535-43.

Burdsall, HH. "Taxonomy of Industrially Important White-Rot Fungi." In *Environmentally Friendly Technologies for the Pulp and Paper Industry*, edited by RA Young and M Akhtar, 259-272. New York: John Wiley & Sons, 1998.

Cadenas, E. "Mechanisms of oxygen activation and reactive oxygen species detoxification." In *Oxidative Stress and Antioxidant Defenses in Biology*, edited by S Ahmad, 1-61. NY: Chapman and Hall, 1995.

Carlsson, B. *Technological Systems in the Bio Industries: An International Study.* Norwell, Massachusetts: Kluwer Academic Publishers, 2002.

Chen, CL, and HM Chang. "Chemistry of lignin biodegradation." In *Biosynthesis and biodegradation of wood components*, edited by H Higuchi, 536-56. Orlando: Academic Press, 1985.

Chen, F, and RA Dixon. "Lignin modification improves fermentable sugar yields for biofuel production." *Nature Biotechnology* 25 (2007): 759-761.

Council, National Research. *Committee on Biobased Industrial Products, Biobased Industrial Products--Priorities for Research and Commercialization.* National Academy Press, 1999.

Demmer, H, I Hinz, H Keller-Rudek, K Koeber, H Kottelwesch, and D Schneider. Vol. 56, in *Coordination Compounds of Manganese*, edited by E Schleitzer-Rust, 1-185. New York: Springer-Verlag, 1980.

Dence, C W, and S Y Lin. "Introduction." In *Methods in Lignin Chemistry*, edited by C W Dence and S Y Lin, 3-19. Berlin Heidelberg: Springer-Verlag, 1992.

Dunford, HB. *Adv. Inorg. Biochem.* 4 (1982): 4-68.

Ege, S. *Organic Chemistry.* 2nd edition. Lexington, MA: D.C. Heath and Company, 1989.

Elissetche, JP, A Ferraz, J Freer, R Mendonca, and J Rodriguez. "Thiobarbituric acid reactive substances, Fe (III) reduction and enzymatic activities in cultures of Ganoderma australe growing on Drimys winteri wood." *FEMS Microbiol Lett* 260 (2006): 112-118.

Encyclopedia of Reagents for Organic Synthesis. 2006. http://www.mrw.interscience.wiley.com/eros/articles/rs102/frame.html (accessed November 26, 2009).

Enoki, M, et al. "Extracellular lipid peroxidation of selective white-rot fungus, Ceriporiopsis subvermispora." *FEMS Microbiology Letters* 180 (1999): 205-211.

Erickson, M, S Larsson, and G E Miksche. "Gas-chromatographische Analyse von Ligninoxydationsprodukten. VII. Zur Strukture des Lignins der Fichte." *Acta Chem Scand* 27 (1973): 903-904.

Erickson, O, DAI Goring, and BO Lindgren. "Structural studies on the chemical bonds between lignins and carbohydrates in spruce wood." *Wood Sci Technol* 14 (1980): 267-279.

Fengel, D. *Wood: chemistry, ultrastructure, reactions.* Berlin: Walter de Gruyter, 1989.

Ferreira-Leitão, VS, J Godinho da Silva, and EPS Bon. "Methylene blue and azure B oxidation by horseradish peroxidase: a comparative evaluation of class II and class III peroxidases." *Applied Catalysis B: Environmental* 42 (2003): 213-221.

Ferreira-Leitão, VS, ME Andrade de Carvalho, and EPS Bon. "Lignin peroxidase efficiency for methylene blue decolouration: Comparison to reported methods." *Dyes and Pigments* 74 (2007): 230-236.

Glasser, W G, R A Northey, and T P Schultz. "Preface." In *Lignin: Historical,Biological, and Materials Perspectives*, edited by W G Glasser, R A Northey and T P Schultz, xiii-xv. Oxford University Press, 2000.

Glenn, JK, L Akileswaran, and MH Gold. "Mn(II) oxidation is the principal function of the extracellular Mn-peroxidase from Phanerochaete chrysosporium." *Arch Biochem Biophys* 251, no. 2 (1986): 688-696.

Goodell, B. *Brown-rot fungal degradation of wood: our evolving view*. Vol. ACS Symp. Ser. 845, in *Wood deterioration and preservation--advances in our changing world*, edited by B Goodell, DD Nicholas and TP Schultz, 97-118. Washington DC: American Chemical Society, 2003.

Goodell, B, et al. "Low molecular weight chelators and phenolic compounds isolated fromwood decay fungi and their role in the fungal biodegradation of wood." *J Biotechnol* 53 (1997): 133-62.

Goring, DA. In *Cellulose chemistry and technology*, edited by JC Arthur, 273. Washington DC: American Chemical Society, 1977.

Graf, A, and T Koehler. "Oregon Cellulose-Ethanol Study." 2000.

Gray, KA, Z Lishan, and M Emptage. "Bioethanol." *Current Opinion in Chemical Biology* 10 (2006): 141-146.

Gutiérrez, A, Jose del Río, MJ Martínez-Íñigo, MJ Martínez, and AT Martínez. "Production of New Unsaturated Lipids during Wood Decay by Ligninolytic Basidiomycetes." *American Society for Microbiology* 68, no. 3 (2002): 1344-1350.

Halliwell, B, and JMC Gutteridge. *Free radicals in biology and medicine.* 3rd Edition. Oxford: Oxford University Press, 1999.

Hames, B, R Ruiz, C Scarlata, A Sluiter, J Sluiter, and D Templeton. "Preparation of Samples for Compositional Analysis." *Technical Report NREL/TP-510-42620.* National Renewable Energy Laboratory, January 2008.

Hammel, KE, AN Kapich, KA Jr. Jensen, and CR Zachary. "Reactive oxygen species as agents of wood decay by fungi." *Enzyme and Microbial Technology* 30 (2002): 445-453.

Hammel, KE, and MA Moen. *Enzyme Microb. Technol* 13 (1991): 15-18.

Harazono, K, R Kondo, and K Sakai. "Bleaching of Hardwood Kraft Pulp with Manganese Peroxidase from Phanerochaete sordida YK-624 without Addition of MnSO4." *Applied and Environmental Microbiology* 62, no. 3 (1996): 913-917.

Harazono, K, Y Watanabe, and K Nakamura. "Decolorization of Azo Dye by the White-Rot Basidiomycete Phanerochaete sordida and by Its Manganese Peroxidase." *Journal of Bioscience and Bioengineering* 95, no. 5 (2003): 455-459.

Hatfield, R, and RS Fukushima. "Can Lignin Be Accurately Measured?" *Crop Sci.* 45 (2005): 832-839.

Hildén, L, G Johansson, G Pettersson, J Li, P Ljungquist, and G Henriksson. "Do the extracellular enzymes cellobiose dehydrogenase and manganese peroxidase form a pathway in lignin biodegradation?" *FEBS Letters* 477 (2000): 79-83.

Hofrichter, M. "Review: lignin conversion by manganese peroxidase (MnP)." *Enzyme and Microbial Technology* 30 (2002): 454-466.

Hofrichter, M, et al. "Oxidative decomposition of malonic acid as bassis for the action of manganese peroxidase in the absence of hydrogen peroxide." *FEBS Letters* 434 (1998): 362-366.

Hofrichter, M, T Lundell, and A Hatakka. "Conversion of Milled Pine Wood by Manganese Peroxidase from Phlebia radiata." *Applied and Environmental Microbiology* 67, no. 10 (2001): 4588-4593.

Hsu, T.-A. "Pretreatment of biomass." Chap. 10 in *Handbook on Bioethanol Production and Utilization. Applied Energy Technology Series*, edited by CE Wyman. Washington DC: Taylor & Francis, 1996.

Institute for Green Oxidation Chemistry. 2008. http://www.chem.cmu.edu/groups/collins/about/about.html (accessed November 30, 2009).

Jain, RK, RM Mathur, VV Thakur, and AG Kulkarni. "Enzyme Prebleaching of Pulp: Perspectives in Indian Paper Industry." In *Lignocellulose Biotechnology*, edited by RC Kuhad and A Singh, 261-267. New Delhi: IK International Publishing House, 2007.

Jeffries, TW, S Choi, and TK Kirk. "Nutritional Regulation of Lignin Degradatio by Phanerochaete chrysosporium." *Appl. Environ. Microbiol.* 42, no. 2 (1981): 290-296.

Jensen, KA, CJ Houtman, ZC Ryan, and KE Hammel. "Pathways for extracellular Fenton chemistry in the brown rot basidiomycete Gloeophyllum trabeum." *Appl Environ Microbiol* 67 (2001): 2705-2711.

Jiang, F, et al. "Production and Separation of Manganese Peroxidase From Heme Amended Yeast Cultures." *Biotechnology and Bioengineering* 99 (2008): 540-549.

Kapich, AN, KA Jensen, and KE Hammel. "Peroxyl radicals are potential agents of lignin biodegradation." *FEBS Letters* 461 (1999): 115-119.

Kapich, AN, KT Steffen, M Hofrichter, and A Hatakka. "Involvement of lipid peroxidation in the degradation of a non-phenolic lignin model compound by manganese peroxidase of the litter-decomposing fungus Stropharia coronilla." *Biochemical and Biophysical Research Communications* 330 (2005): 371-377.

Kapich, AN, S Galkin, and A Hatakka. "Effect of phenolic acids on manganese peroxidase-dependent peroxidation of linoleic acid and degradation of a non-phenolic lignin model compound." *Biocatalysis and Biotransformatino* 25 (2007): 350-358.

Kawai, S, M Nakagawa, and H Ohashi. "Degradation mechanisms of a non-phenolic B-O-4 lignin model dimer by Trametes versicolor laccase in the presence of 1-hydroxybenzotriazole." *Enzyme Microbial Technol* 30 (2002): 482-9.

Keyser, P, TK Kirk, and JG Zeikus. "Ligninolytic enzyme system of Phanaerochaete chrysosporium: synthesized in the absence of lignin in response to nitrogen starvation." *J. Bacteriol.* 135, no. 3 (1978): 790-797.

Khindaria, A, TA Grover, and SD Aust. "Evidence for Formation of the Veratryl Alcohol Cation Radical by Lignin Peroxidase." *Biochemistry* 34 (1995): 6020-6025.

Kirk, TK, and D Cullen. "Enzymology and Molecular Genetics of Wood Degradation by White-Rot Fungi." In *Environmentally Friendly Technologies for the Pulp and Paper Industry*, edited by RA Young and M Akhtar, 273-307. New York: John Wiley & Sons, 1998.

Kirk, TK, and RL Farrell. "Enzymatic "combustion": the microbial degradation of lignin." *Annu Rev Microbiol* 41 (1987): 465-505.

Kishi, K, H Wariishi, L Marquez, HB Dunford, and MH Gold. "Mechanism of manganese peroxidase compound II reduction. Effect of organic acid chelators and pH." *Biochemistry* 33, no. 29 (1994): 8694-701.

Knapp, JS, PS Newby, and LP Reece. "Decolorization of dyes by wood-rotting basidiomycete fungi." *Enzyme and Microbial Technology* 17, no. 7 (1995): 664-668.

Koshijima, T, T Watanabe, and F Yaku. "Structure and properties of the lignin-carbohydrate complex polymer as an amphipathic substance. In: Glasser WG, Sarkanen S (eds) Lignin: properties and material." *ACS Symp Ser* 397 (1989): 11-28.

Kremer, SM, and PM Wood. "Evidence that cellobiose oxidase from Phanerochaete chrysosporium is primarily an Fe(III) oxidase." *Eur J Biochem* 205 (1992): 133-8.

Kuan, I-C, KA Johnson, and M Tien. "Kinetic Analysis of Manganese Peroxidase." *Journal of Biological Chemistry* 268, no. September 25 (1993): 20064-20070.

Lee, J. "Biological conversion of lignocellulosic biomass to ethanol." *Journal of Biotechnology* 56, no. 1 (1997): 1-24.

Leisola, MSA, B Kozulic, F Meussdoerffer, and A Fiechter. *J. Biol. Chem* 262 (1987): 419-424.

Lequart, C, B Kurek, P Debeire, and B Monties. "MnO2 and Oxalate: An Abiotic Route for the Oxidation of Aromatic Components in Wheat Straw." *J. Agric. Food Chem.* 46 (1998): 3868-3874.

Messner, K, and E Srebotnik. "Biopulping: An overview of developments in an environmentallly safe paper-making technology." *FEMS Microbiol. Rev.* 13 (1994): 351-364.

Meunier-Goddik, L, and MH Penner. "Enzyme-Catalyzed Saccharification of Model Celluloses in the Presence of Lignacious Residues." *J. Agric. Food Chem.* 47 (1999): 346-351.

Minor, J L. "Chemical linkage of polysaccharides to residual lignin in loblolly pien kraft pulp." *J Wood Chem Technol* 6 (1986): 185-201.

Moen, MA, and KE Hammel. "Lipid peroxidation by the manganese peroxidase of Phanerochaete chrysosporium is the basis for phenanthrene oxidation by the intact fungus." *Appl Environ Microbiol* 60 (1994): 1956-61.

Mosier, N, et al. "Features of promising technologies for pretreatment of lignocellulosic biomass." *Bioresource Technology* 96, no. 6 (2005): 673-686.

Nadarajah, N, J Van Hamme, J Pannu, A Singh, and O Ward. "Enhanced transformation of polycyclic aromatic hydrocarbons using a combined Fenton's reagent, microbial treatment and surfactants." *Appl Microbiol Biotechnol* 59 (2002): 540-544.

Nicole, M, et al. "Wood degradation by Phellinus noxius: Ultrastructure and cytochemistry." *Can. J. Microbiol.* 41 (1995): 253-265.

Nimz, H H. "Beech lignin--proposal of a constitutional scheme." *Angew Chem Int Ed* 13 (1974): 313-321.

Nutt, A, A Salumets, G Henriksson, V Sild, and G Johansson. "Conversion of O2 species by cellobiose dehydrogenase (cellobiose oxidase) and glucose oxidase--a comparison." *Biotechnology Letters* 19 (1997): 379-384.

Okazaka, S, M Goto, S Furusaki, H Wariishi, and H Tanaka. "Preparation and catalytic performance of surfactant-manganese peroxidase-MnII terneary complex in organic media." *Enyzme Microb Technol* 28 (2001): 329-32.

O'Neal, HE, and SW Benson. "Thermochemistry of free radicals." In *Free radicals*, edited by JK Kochi, 275-359. New York: Wiley-Interscience, 1973.

Ooshima, H, DS Burns, and AO Converse. "Adsorption of cellulase from Trichoderma reesei on cellulose and lignaceous residue in wood pretreated by dilute sulfuric acid with explosive decompression." *Biotechnology Bioengineering* 36 (1990): 446-452.

Paice, MG, ID Reid, R Bourbonnais, FS Archibald, and L Jurasek. "Manganese peroxidase, produced by Trametes versicolor during pulp bleaching, demthylates and delignifies kraft pulp." *Appl. Environ. Microbiol.* 59 (1993): 260-265.

Pettersen, R C. *The chemical composition of wood.* Vol. 207, in *The chemistry of solid wood. Adv Chem Ser*, edited by R M Rowell, 57-126. 1984.

Pointing, SB. "Feasibility of bioremediation by white-rot fungi." *Appl Microbiol Biotechnol* 57 (2001): 20-33.

Popp, JL, and TK Kirk. "Oxidation of methoxygenzene by manganese peroxidase and by Mn3+." *Arch Biochem Biophys* 288 (1991): 145-8.

Pueyo, C, and RR Ariza. "Role of reactive oxygen species in the mutagenicity of complex mixtures of plant origin." In *DNA and Free Radicals*, edited by B Halliwell and OI Aruoma, 275-291. Chichester: Ellis Horwood, 1993.

Reddy, CA. "The potential for white-rot fungi in the treatment of pollutants." *Current Opinion in Biotechnology* 6, no. 3 (1995): 320-328.

Reid, ID, GD Abrams, and JM Pepper. "Water-soluble products from the degradation of aspen lignin by Phanerochaete chrysosporium." *Can. J. Bot.* 60, no. 11 (1982): 2357-2364.

Roy, BP, MG Paice, FS Archibald, SK Misra, and LE Misiak. "Creation of metal-complexing agents, reducing of manganese dioxide, and promotion of manganese peroxidase-mediated Mn(III) production by cellobiose:quinone oxidoreductase from Trametes versicolor." *Journal of Biological Chemistry* 269 (1994): 19745-19750.

Sack, U, M Hofrichter, and W Fritsche. "Degradation of polycyclic aromatic hydrocarbons by manganese peroxidase of Nematoloma frowardii." *FEMS Microbiol Lett* 152 (1997): 227-34.

Sarkanen, K V, and CH Ludwig. *Lignin: Occurrence, Formation, Structure and Reactions.* Edited by K V Sarkanen and C H Ludwig. New York: John Wiley & Sons, 1971.

Selig, M, N Weiss, and Y Ji. *Enzymatic Saccharification of Lignocellulosic Biomass.* Golden, Colorado: National Renewable Energy Lab, 2008.

Selig, MJ, S Viamajala, SR Decker, MP Tucker, ME Himmel, and TB Vinzant. "Deposition of Lignin Droplets Produced During Dilute Acid Pretreatent of Maize Stems Retards Enzymatic Hydrolysis of Cellulose." *Biotechnol Prog* 23 (2007): 1333-1339.

Selig, MJ, TB Vinzant, ME Himmel, and SR Decker. "The Effect of Lignin Removal by Alkaline Peroxide Pretreatment on the Susceptibility of Corn Stover to Purified Cellulolytic and Xylanolytic Enzymes." *Appl Biochem Biotechnol* 155 (2009): 397-406.

Sharma, KK, S Kuhar, RC Kuhad, and PN Bhat. "Combinatorial Approaches to Improve Plant Cell Wall Digestion: Possible Solutions for Cattle Feed Problems." In *Lignocellulose Biotechnology*, edited by RC Kuhad and A Singh, 233-244. New Delhi: IK International Publishing House, 2007.

Sigma-Aldrich. 2009. http://www.sigmaaldrich.com/catalog/ProductDetail.do?lang=en&N4=M9140|SIAL&N5=SEARCH_CONCAT_PNO|BRAND_KEY&F=SPEC (accessed November 28, 2009).

Sigma-Aldrich. 2009. http://www.sigmaaldrich.com/catalog/ProductDetail.do?lang=en&N4=471003|ALDRICH&N5=SEARCH_CONCAT_PNO|BRAND_KEY&F=SPEC (accessed November 30, 2009).

Silverstein, RM, GC Bassler, and TC Morrill. *Spectrometric Identification of Organic Compounds.* Fifth Edition. New York: John Wiley & Sons, Inc., 1991.

Singh, D, and S Chen. "The white-rot fungus Phanerochaete chrysosporium: conditions for the production of lignin-degrading enzymes." *Applied Microbiology and Biotechnology* 81, no. 3 (2008): 399-417.

Singleton, VL, R Orthofer, and RM Lamuela-Raventos. "Analysis of Total Phenols and Other Oxidation Substrates and Antioxidants by Means of Folin-Ciocalteu Reagent." *Methods in Enzymology* 299 (1999): 152-178.

Sluiter, A, B Hames, D Hyman, C Payne, R Ruiz, and C Scarlata. "Determination of Total Solids in Biomass and Total Dissolved Solids in Liquid Process Samples." *Technical Report NREL/TP-510-42621.* National Renewable Energy Laboratory, March 2008.

Sluiter, A, B Hames, R Ruiz, C Scarlata, J Sluiter, and D Templeton. "Determination of Ash in Biomass." *Technical Report NREL/TP-510-42622.* National Renewable Energy Laboratory, January 2008.

Sluiter, A, et al. "Determination of Structural Carbohydrates and Lignin in Biomass." *Technical Report NREL/TP-510-42618.* National Renewable Energy Laboratory, April 2008.

Sluiter, A, R Ruiz, C Scarlata, J Sluiter, and D Templeton. "Determination of Extractives in Biomass." *Technical Report NREL/TP-510-42619.* National Renewable Energy Laboratory, January 2008.

StainsFile. September 2009. http://stainsfile.info/StainsFile/jindex.html (accessed November 22, 2009).

Sun, RC, D Salisbury, and J Tomkinson. "Chemical composition of lipophilic extractives released during the hot water treatment of wheat straw." *Bioresource Technology* 88 (2003): 95-101.

Sundaramoorthy, M, K Kishi, MH Gold, and TL Poulos. "Crystal Structure of Substrate Binding Site Mutants of Manganese Peroxidase." *The Journal of Biological Chemistry* 272, no. 28 (1997): 17574-17580.

Sutherland, GRJ, ZL Schick, M Tien, and SD Aust. "Role of calcium in maintaining the heme environment of manganese peroxidase." *Biochemistry* 36 (2000): 3654-62.

Tanaka, H, S Itakura, and A Enoki. "Hydroxyl Radical Generation by an Extracellular Low-Molecular-Weight Substance and Phenol Oxidase Activity During Wood Degradation by the White-Rot Basidiiomycete Phanerochaete chrysosporium." *Holzforschung* 53 (1999): 21-28.

Tanaka, H, S Itakura, and A Enoki. "Hydroxyl radical generation by an extracellular low-molecular-weight substance and phenol oxidase activity during wood degradation by the white-rot basidiomycete Trametes versicolor." *J Biotechnol* 75 (1999): 57-70.

Torget, R, C Hatzis, TK Hayward, T -A Hsu, and GP Philippidis. "Optimization of reverse-flow, two-temperature, dilute-acid pretreatment to enhance biomass conversion to ethanol." *Applied Biochemistry and Biotechnology* 57/58 (1996): 85-101.

Ueda, J, N Saito, and T Ozawa. "Detection of free radicals produced from reactions of lipid hydroperoxide model compounds with Cu(II) complexes by ESR spectroscopy." *Arch. Biochem. Biophys.* 325 (1996): 65-76.

Urzúa, U, LF Larrondo, S Lobos, J Larraín, and R Vicuña. "Oxidation reactions catalyzed by manganese peroxidase isoenzymes from Ceriporiopsis subvermispora." *FEBS Letters* 371 (1995): 132-136.

Urzúa, U, PL Kersten, and R Vicuna. "Manganese peroxidase-dependent oxidation of glyoxilic and oxalic acids synthesized by Ceriporiopsis subvermispora produces extracellular hydrogen peroxide." *Appl Environ Microbiol* 64 (1998): 68-73.

Van Aken, B, P Ledent, H Vaneau, and SN Agathos. "Co-immobilization of manganese peroxidase from Phlebia radiata, and glucose oxidase from Aspergillus niger on porous silica beads." *Biotechnol Lett* 22 (2000): 641-6.

Walling, C, and A Goosen. "Mechanism of the ferric ion catalysed decomposition of hydrogen peroxide: effects of organic substrate." *J Am Chem Soc* 95 (1973): 2987-2991.

Wardman, P. "Reduction Potentials of One-Electron Couples Involving Free Radicals in Aqueous Solution." *J. Phys. Chem. Ref. Data* 18, no. 4 (1989): 1637-1755.

Wariishi, H, HB Dunford, ID MacDonald, and MH Gold. "Manganese Peroxidase from the Lignin-degrading Basidiomycete Phanerochaete chrysosporium. Transient state kinetics and reaction mechanism." *Journal of Biological Chemistry* 264, no. 6 (1989): 3335-3340.

Wariishi, H, K Valli, and MH Gold. "Manganese (II) Oxidation by Manganese Peroxidase from the Basidiomycete Phanerochaete chrysosporium." *Journal of Biological Chemistry* 267, no. 33 (1992): 23688-23695.

Wariishi, H, K Valli, V Renganathan, and MH Gold. "Thiol-mediated oxidation of non-phenolic lignin model compounds by manganese peroxidase." *J. Biol. Chem.* 264 (1989): 14185-14191.

Wariishi, H, L Akileswaran, and MH Gold. "Manganese Peroxidase from the Basidiomycete Phanerochaete chrysosporium: Spectral Characterization of the Oxidized States and the Catalytic Cycle." *Biochemistry* 27 (1988): 5365-5370.

Watanabe, T, K Koller, and K Messner. "Copper-dependent depolymerization of lignin in the presence of fungal metabolite, pyridine." *J. Biotechnol.* 62 (1998): 221-230.

Watanabe, T, S Katayama, M Enoki, Y Honda, and M Kuwahara. "Formation of acyl radical in lipid peroxidation of linoleic acid by manganese-dependent peroxidase from Ceriporiopsis subvermispora and Bjerkandera ajusta." *Eur J Biochem* 267 (2000): 4222-31.

Waterhouse, AL. "Determination of Total Phenolics." In *Current Protocols in Food Analytical Chemistry*, edited by R Wrolstad, I1.1.1-I1.1.8. John Wiley & Sons, Inc., 2002.

Waters, WA, and JS Littler. *Oxidation by Vanadium(V), Cobalt(III), and Manganese(III).* Vols. 5-A, in *Organic Chemistry: A Series of Monographs*, edited by KB Wiberg, 185-241. New York: Academic Press, 1965.

Weil, JR, M Brewer, R Hendrickson, A Sarikaya, and MR Ladisch. "Continuous pH monitoring during pretreatment of yellow poplar wood sawdust by pressure cooking in water." *Applied Biochemistry and Biotechnology* 68 (1998): 99-111.

Wyman, CE. "Biomass ethanol: technical progress, opportunities, and commercial challenges." *Annual Review Energy Environment* 24 (1999): 189-226.

Wyman, CE, BE Dale, RT Elander, M Holzapple, MR Ladisch, and YY Lee. "Coordinated development of leading biomass pretreatment technologies." *Bioresource Technology* 96 (2005): 1959-2966.

Yang, B, and CE Wyman. "Effect of xylan and lignin removal by batch and flow through pretreatment on the enzymatic digestibility of corn stover cellulose." *Biotechnology and Bioengineering* 86, no. 1 (2004): 88-95.

Yee, K. "Personal communication." Corvallis, Oregon, Summer 2009.

Young, RA, and M Akhtar, . *Environmentally Friendly Technologies for the Pulp and Paper Industry.* New York: John Wiley & Sons, 1998.